ACS SYMPOSIUM SERIES 1038

Ionic Liquid Applications: Pharmaceuticals, Therapeutics, and Biotechnology

EDITED BY

Sanjay V. Malhotra

Downloaded by 89.163.35.42 on June 22, 2012 | http://pubs.acs.org
Publication Date (Web): April 28, 2010 | doi: 10.1021/bk-2010-1038.fw001

Ionic Liquid Applications: Pharmaceuticals, Therapeutics, and Biotechnology

Downloaded by 89.163.35.42 on June 22, 2012 | http://pubs.acs.org
Publication Date (Web): April 28, 2010 | doi: 10.1021/bk-2010-1038.fw001

ACS SYMPOSIUM SERIES **1038**

Ionic Liquid Applications: Pharmaceuticals, Therapeutics, and Biotechnology

Sanjay V. Malhotra, Editor

Laboratory of Synthetic Chemistry, SAIC-Frederick, Inc.
National Cancer Institute at Frederick

Downloaded by 89.163.35.42 on June 22, 2012 | http://pubs.acs.org
Publication Date (Web): April 28, 2010 | doi: 10.1021/bk-2010-1038.fw001

Sponsored by the
ACS Division of Organic Chemistry

American Chemical Society, Washington, DC

Downloaded by 89.163.35.42 on June 22, 2012 | http://pubs.acs.org
Publication Date (Web): April 28, 2010 | doi: 10.1021/bk-2010-1038.fw001

Library of Congress Cataloging-in-Publication Data

Ionic liquid applications : pharmaceuticals, therapeutics, and biotechnology / Sanjay V. Malhotra, editor ; sponsored by the ACS Division of Organic Chemistry.
p. cm. -- (ACS symposium series ; 1038)
Includes bibliographical references and index.
ISBN 978-0-8412-2547-3 (alk. paper)
1. Ionic solutions--Therapeutic use. I. Malhotra, Sanjay V. II. American Chemical Society. Division of Organic Chemistry.
RS201.S6I56 2010
615'.19--dc22
2010012936

The paper used in this publication meets the minimum requirements of American National Standard for Information Sciences—Permanence of Paper for Printed Library Materials, ANSI Z39.48n1984.

Copyright © 2010 American Chemical Society

Distributed by Oxford University Press

All Rights Reserved. Reprographic copying beyond that permitted by Sections 107 or 108 of the U.S. Copyright Act is allowed for internal use only, provided that a per-chapter fee of $40.25 plus $0.75 per page is paid to the Copyright Clearance Center, Inc., 222 Rosewood Drive, Danvers, MA 01923, USA. Republication or reproduction for sale of pages in this book is permitted only under license from ACS. Direct these and other permission requests to ACS Copyright Office, Publications Division, 1155 16th Street, N.W., Washington, DC 20036.

The citation of trade names and/or names of manufacturers in this publication is not to be construed as an endorsement or as approval by ACS of the commercial products or services referenced herein; nor should the mere reference herein to any drawing, specification, chemical process, or other data be regarded as a license or as a conveyance of any right or permission to the holder, reader, or any other person or corporation, to manufacture, reproduce, use, or sell any patented invention or copyrighted work that may in any way be related thereto. Registered names, trademarks, etc., used in this publication, even without specific indication thereof, are not to be considered unprotected by law.

PRINTED IN THE UNITED STATES OF AMERICA

Downloaded by 89.163.35.42 on June 22, 2012 | http://pubs.acs.org
Publication Date (Web): April 28, 2010 | doi: 10.1021/bk-2010-1038.fw001

Foreword

The ACS Symposium Series was first published in 1974 to provide a mechanism for publishing symposia quickly in book form. The purpose of the series is to publish timely, comprehensive books developed from the ACS sponsored symposia based on current scientific research. Occasionally, books are developed from symposia sponsored by other organizations when the topic is of keen interest to the chemistry audience.

Before agreeing to publish a book, the proposed table of contents is reviewed for appropriate and comprehensive coverage and for interest to the audience. Some papers may be excluded to better focus the book; others may be added to provide comprehensiveness. When appropriate, overview or introductory chapters are added. Drafts of chapters are peer-reviewed prior to final acceptance or rejection, and manuscripts are prepared in camera-ready format.

As a rule, only original research papers and original review papers are included in the volumes. Verbatim reproductions of previous published papers are not accepted.

ACS Books Department

Downloaded by 89.163.35.42 on June 22, 2012 | http://pubs.acs.org
Publication Date (Web): April 28, 2010 | doi: 10.1021/bk-2010-1038.pr001

Preface

In the late 1990s, there was an explosion of research on ionic liquids (ILs) and they are now a major topic of academic and industrial interest with numerous existing and potential applications. Since then, ionic liquids have certainly captured the imagination of chemists across the globe. The reasons for such phenomenal interest in this area are due to several factors, most notably however, is the ability to design an ionic liquid with desired physio-chemical properties facilitating a specific task to occur and the prospect of discovering new chemistry.

This book is derived from papers presented at the special symposium entitled, *"Ionic Liquid Applications: Pharmaceuticals, Therapeutics, and Biotechnology"*, held under the auspices of the Organic Division during the 236th national meeting of the American Chemical Society in Philadelphia, Pennsylvania, August 17-21, 2008. Chapter 1 gives a historical overview of "pharmaceutical salts having properties similar to materials now known as ionic liquids." The focus of Chapters 2-4, 6 and 7 is on pharmaceutical related applications on ionic liquids, i.e. as solvents for synthesis, separation and analysis. While Chapter 5 illustrates examples of biologically active molecules with ionic liquid like structures. Chapter 8 shows the therapeutic application of ionic liquids as potential anti-cancer drugs. Biomaterials obtained from ionic liquids are discussed in Chapters 9 & 10, and the toxicological evaluation of ILs is examined in Chapter 11. Ionic liquids have found many applications in biotechnology. Some of the latest examples in this area are presented in Chapters 12-16. It is my pleasure to acknowledge the contribution of all speakers to the symposium and to authors for their contributions to this book. I am also greatful the ACS organic Division for sponsoring this symposium and to CEM corporation and EMD chemicals for additional financial support.

Taken together, the collection of chapters in this book represents how the field is progressing and evolving. However, the research on finding many other applications of ILs would require interdisciplinary endeavor that brings together various disciplines such as synthetic, organic, bioorganic, medicinal and biological chemistry, chemical biology, pharmacology, biochemistry, toxicology, materials sciences etc. It is hoped that these communities will greatly benefit from this book. With publication of this book I wish to encourage and stimulate ongoing and new interdisciplinary research activities on the development of novel applications of ionic liquids in the biomedical fields.

This book is dedicated to all those who have contributed and participate in the advancement of the field of ionic liquids.

Sanjay V. Malhotra

Laboratory of Synthetic Chemistry-SAIC
National Cancer Institute at Frederick, U.S.A.

Downloaded by 89.163.35.42 on June 22, 2012 | http://pubs.acs.org
Publication Date (Web): April 28, 2010 | doi: 10.1021/bk-2010-1038.ch001

Chapter 1

Ionic Liquids as Pharmaceutical Salts: A Historical Perspective

Vineet Kumar and Sanjay V. Malhotra*

**Laboratory of Synthetic Chemistry, SAIC-Frederick, Inc.,
National Cancer Institute at Frederick, 1050 Boyles Street,
Frederick, MD 21702, USA
*malhotrasa@mail.nih.gov**

Design and synthesis of pharmaceutically acceptable salts is one of the prime aspect of drug development. An estimated half of all drugs used in medicine are administered as salts. The salt formation of drug candidates has been recognized as an essential preformulation task. Salt formation of APIs can improve their aqueous solubility, industrial processing, safety aspects and sometimes biological properties. These properties can be further enhanced by changing counterion of the active component. Though there is no concerned effort of finding applications of ionic liquids in the pharmaceutical arena in recent years, a detailed survey of the literature shows that pharmaceutical salts having properties now termed as 'ionic liquids' have existed for a long time. In this chapter a historical overview of 'ionic liquid like pharmaceutical salts', their importance and application in drug development has been described.

Pharmaceutical Salts: An Overview

The first nitrogen-containing bases (also known as 'vegetable alkalis') extracted from plant materials, and later termed as alkaloids were isolated and purified as well-crystallizing salts. These salts were found to be more stable and water-soluble in comparison to free bases which qualifies them as the preferred forms for use as therapeutic agents e.g. morphine hydrochloride, atropine sulfate, quinine sulfate, pilocarpine nitrate, codeine phosphate, etc. Among endogenous biological agents, most of the neutrotransmitters biologically derived from amino acids, are also nitrogenous bases able to form salts (*1*).

The salt formation of a drug substance is a critical step in drug development (*1*, *2*). An estimated 50% of all drug molecules are administered as salts. The suboptimal physicochemical or biopharmaceutical properties of a drug can be overcome by pairing a basic or acidic drug molecule with a counterion to create a salt version of the drug. Such salts may offer advantages over the corresponding free drug in terms of physical properties such as melting point (thermal stability), crystallinity, hygroscopicity, dissolution rate, or solubility (bioavailability). From a pharmaceutical viewpoint the melting enthalpy, melting temperature and solubility are of particular importance, both because of their routine measurement and due to their potential influence on processing and bioavailability (*3*). The process is a simple way to modify the properties of a drug with ionizable functional groups to overcome undesirable features of the parent drug (*4*). This fact underlines the importance of salt formation for drugs that are designed, developed, and marketed after a rigorous research and development program. Salt forms of drugs have a large effect on quality, safety, and performance of drug. The selected salt ion can significantly influence the pharmacokinetics of a drug candidate, especially the absorption or membrane-transfer process. As a result, the time course of its pharmacodynamic and toxicological effects may undergo a modification or modulation. This can significantly assist chemists and formulators in various aspects of drug discovery and development (*5*). This is also the reason why regulatory authorities have started to treat the new salt of a registered drug as a new chemical entity (*1*).

Downloaded by 89.163.35.42 on June 22, 2012 | http://pubs.acs.org
Publication Date (Web): April 28, 2010 | doi: 10.1021/bk-2010-1038.ch001

Ionic Liquids: Properties and Applications

Main advantages of ionic liquids (ILs) as compared to common molecular organic solvents are their negligible vapour pressure, resulting in reduced inhalatory exposure, absence of flammability, and their high variability concerning chemical structure of headgroups, substituents and anions. These variabilities and combinations thereof lead to an enormous number of theoretically accessible ionic liquids. The possibility to modify structural elements in order to optimise technological features like solvation properties, viscosity, conductivity and thermal as well as electrochemical stability is ideal in terms of technical applicability. Over the years, these neoteric salts have been reviewed extensively for their wide range of applications including organic synthesis, electrochemistry, chromatography, transition metal catalysis, biocatalytic transformations, asymmetric synthesis, polymers, biomaterials and material science, etc. Most of the new applications of ILs take advantage of the unique combinations of chemical and physical properties due to their dual-functional (two component) nature and their inherent design flexibility which allow targeted synthesis of ‘tuned’ material. ILs make a unique architectural platform on which, at least potentially, the properties of both cation and anion can be independentaly modified, enabling tunability in the design of new functional materials, while retaining the core desired features of an IL (*6*, *7*).

However, concerning the risk assessment for man and the environment this structural variability presents an almost insurmountable problem as it is impossible to generate profound knowledge of the effects on human health and the environment for every single compound in this heterogeneous substance group. Therefore, there is a growing attention towards the environmental and mammalian toxicity of these salts. There have been constant efforts in recent years for establishing the structure activity relationship between these vast variety of salts and their toxicity (*8*). On the subcellular toxicity level of ionic liquids, enzyme inhibition data have been published for the acetylcholinesterase (AChE)(*9*) and AMP deaminase (*10*). Other studies of biological effects of ionic liquids on microorganisms and cell cultures in different test systems including HeLa (*11*), IPC-81 (*12*), HT-29(*13*) and CaCo-2(*13*) cells have also been reported. The results so far show that the most important property of ILs, is their 'tunability' which also apply for their toxicity and one can design biodegradable ILs which are non-toxic for humans and environment.

Downloaded by 89.163.35.42 on June 22, 2012 | http://pubs.acs.org
Publication Date (Web): April 28, 2010 | doi: 10.1021/bk-2010-1038.ch001

Ionic Liquids as Pharmaceuticals

Ionic liquids have been extensively studied for the replacement of VOCs in organic chemistry for the synthesis of biologically active compounds including APIs. However, the pharmaceutical industry does not appear to take ILs seriously as solvents due to issues of their purity, toxicity, and regulatory approval. But the applications of ILs in pharmaceuticals are not limited only as reaction medium. Though there is no concerned effort of finding applications of ILs in the pharmaceutical arena in recent years, a detailed survey of the literature shows that pharmaceutical salts having properties now termed as 'ionic liquids' have existed for a long time.

There are numerous examples in literature where pharmaceutically active compounds are salts of an acitve ion in combination with a relatively simple and inert counterion. The combined ion pair possess properties that are similar to those compounds now termed as 'ionic liquids'. Table 1 shows examples of such 'ionic liquid like pharmaceutical salts', categorized by their biological activity where the active cation has been combined with an inert anion to give the final drug molecule. On the other hand a suitable drug can be combined with a second active substance by salt formation to give an ionic liquid like compound. Upon dissolution, such a molecular drug combination will dissociate in the body fluids, whereupon the cationic and anionic components follow their independent kinetic and metabolid pathways. This class of pharmaceutical salt pairs i.e. composed of both cation and anion as active ingredients and having ioinc liquid like properties are known in literature for a long time. Exchanging the inert counterion of an active drug with a pharmaceutically active counterion can change their phyisco-chemical properties e.g. melting point, solubility, etc.; and also pharmaceutical properties like bioavailability, stability, permeability. In principle each component of a drug salt i.e. the active entity and the counter ion (which itself can be an active component with simlar or different effects), can excert its own biological effects on a living organism. The counter-ion can be chosen to synergistically enhance the desired effects or to neutralize unwanted side effects of the active entity. The counter-ion can also be chosen to pharmacologically act independently, but therapeutically in a synergestic manner. Examples of these pharmacutical salts, their biologocal activities and literature references are given in Table 2.

Conclusion and Future Direction

Most of the active salts given in Tables 1 and 2 structurally resemble the class of compounds now known as ‘ionic liquids’. It is important to note that some of these salts were reported in literature over a century ago. However, its only during the last two decades that there have been significant efforts to develop an understanding of the physico-chemical of ILs which ahs lead to their wide range of applications. Obviously, much more research has to be done to explore their biomedical applications. Perhaps, we should revisit the ‘ionic liquid-like compounds with pharmaceutical and/or biological application’ already reported in the literature. A better undersating of their properties (especially their toxicity could help the IL community in designing biologically active and useful ILs. A modular IL starategy has the potential to transform the pharmaceutical intustry in ways never expected. This approach can provide a platform for improved activity with new treatment options or even personalized medication.

Downloaded by 89.163.35.42 on June 22, 2012 | http://pubs.acs.org
Publication Date (Web): April 28, 2010 | doi: 10.1021/bk-2010-1038.ch001

Downloaded by 89.163.35.42 on June 22, 2012 | http://pubs.acs.org
Publication Date (Web): April 28, 2010 | doi: 10.1021/bk-2010-1038.ch001

Table 1. Some examples of pharmaceutical salts having one component as active drug categorised by their biological activities

Name	Structure	First patent/report (year, originator)
Drugs for functional gastrointestinal disorders		
Methylscopolamine bromide	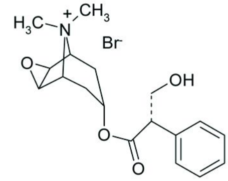	*DE 145,996* (**1902**, E. merck AG.)
Butylscopolamine bromide	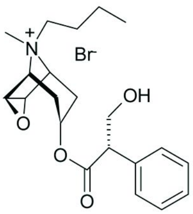	*DE 856890* (**1950**, Boehringer Inglheim)
Anti-dementia and other CNS drugs		
Neostigmine	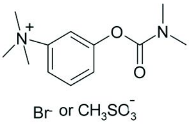	*US 1905990* (**1931**, Roche)
Pyridostigmine	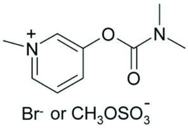	*US 2572579* (**1945**, Roche)
Antiseptic and disinfectant		
Cetylpyridinium chloride m.p = 77 °C	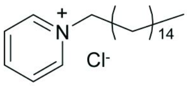	*FR 812360* (**1937**)
Domiphen bromide	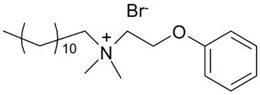	*CH 258715* (**1949**, CIBA Ltd.)
Antifbrillatory and antiarrhythmic agent		
Bretylium m.p = 85-86 °C	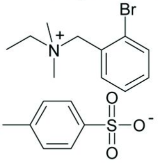	*GB 881265* (**1961**, Wellcome Foundation Ltd.)

Continued on next page.

Downloaded by 89.163.35.42 on June 22, 2012 | http://pubs.acs.org
Publication Date (Web): April 28, 2010 | doi: 10.1021/bk-2010-1038.ch001

Table 1. (Continued). Some examples of pharmaceutical salts having one component as active drug categorised by their biological activities

Herbicide		
Diquat Mp = >300 °C	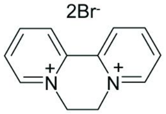	*GB785732* (**1957**, Imperial Chemical Ind. Ltd.)
Paraquat m.p = 175-180 °C	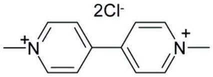	*J. General Physiology*, **1933**, *16*, 859.
Difenzoquat Mp = 146-148 °C	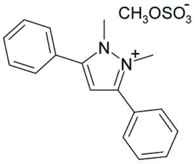	*DE 2260485* (**1973**, American Cyanamid Co.)
Acetylcholinesterase inhibitor		
Edrohonium m.p. = 162-163 °C (dec)	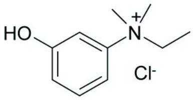	*Annals of the New York Academy of Sciences*, **1951**, *54*, 438.
Anticholinergic, antimuscarinic and antispasmodic drugs		
Tridihexethyl Chloride	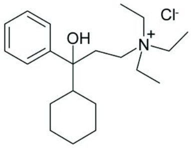	*BE 612357* (**1962**, Compagnie Francaise des Matieres Colorantes)
Oxyphenonium bromide m.p. = 184-194 °C	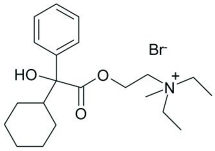	*CH 259958* (**1949**, CIBA Ltd.)
Pipenzolate m.p. = 179.5 °C	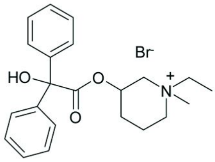	*J. Am. Pharm. Assoc.* **1954**, *43*, 616.
Methacholine m.p. = 200-201 °C	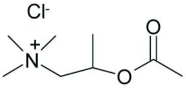	*J. Am. Chem. Soc.* **1935**, *57*, 2125.

Downloaded by 89.163.35.42 on June 22, 2012 | http://pubs.acs.org
Publication Date (Web): April 28, 2010 | doi: 10.1021/bk-2010-1038.ch001

Table 2. Some examples of ionic liquid like salt pairs having both cation and anion as active component

Cationic drug component	Anionic drug component	Salt Pair	Reference
Phenazone 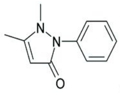 m.p. = 113 °C analgesic, antiinflammatory, antipyretic	*Salicylic acid* 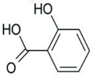 m.p. = 159 °C analgesic, antiinflammatory, antipyretic	*Phenazone salicylate* m.p. = 149-150 °C analgesic, antiinflammatory, antipyretic	*RU 23402* (**1931**)
Promethazine 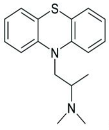 m.p. = 60 °C antihistaminic	*8-chlorotheophylline* 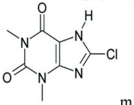 m.p. = 290 °C central stimulant	*Promethazine theoclate* m.p. = 152-153 °C antihistaminic	*US 2534237* (**1950**)
Pyrathiazine 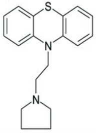 antihistaminic	*8-chlorotheophylline* 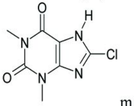 m.p. = 290 °C central stimulant	*Parathiazine theoclate* m.p. = 166-167 °C antihistaminic	*US 2534237* (**1950**)
Phenazone 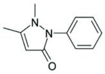 m.p. = 113 °C analgesic, antiinflammatory, antipyretic	*Gentisic acid* 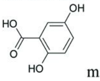 m.p. = 200-205 °C analgesic, antiinflammatory, antipyretic	*Phenazone gentisate* m.p. = 87-88 °C analgesic, antiinflammatory, antipyretic	*US 2541651* (**1951**)
Aminophenazone 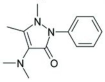 m.p. = 168-170 °C analgesic, antiinflammatory, antipyretic	*Gentisic acid* 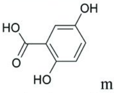 m.p. = 200-205 °C analgesic, antiinflammatory, antipyretic	*Aminophenazone gentisate* m.p. = 122.5 °C analgesic, antiinflammatory, antipyretic	*US 2541651* (**1951**)
Diphenhydramine 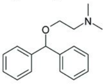 antihistaminic	*8-chlorotheophylline* 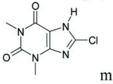 m.p. = 290 °C central stimulant	*Dimenhydrinate* m.p. = 102-107 °C antihistaminic	*GB 667113* (**1952**)
Nicotinamide 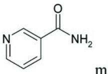 m.p. = 129 °C Vitamin	*Ascorbic acid* 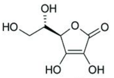 m.p. = 190 °C Vitamin	*Nicotinamide ascorbate or Niscoscrobine* m.p. = 141-145 °C Vitamin combinatin	*Bulletin de la Societe de Chimie Biologique* **1953**, *35*, 326.

Continued on next page.

Downloaded by 89.163.35.42 on June 22, 2012 | http://pubs.acs.org
Publication Date (Web): April 28, 2010 | doi: 10.1021/bk-2010-1038.ch001

Table 2. (Continued). Some examples of ionic liquid like salt pairs having both cation and anion as active component

Isoniazid 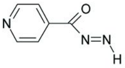 antitubercular	*4-Aminosalicylic acid* 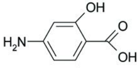 m.p. = 150 °C antitubercular	*Pasiniazide* m.p. = 142-144 °C antitubercular combination	*Therapie* **1954**, *9*, 273.
Choline 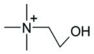 m.p. = 232-233 °C lipotropic, hepatoprotectant	*Theophylline* 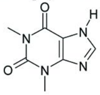 m.p. = 275 °C coronary dilator and analeptic	*Choline theophyllinate* m.p. = 185-189 °C broncholytic	*US 2670350* (**1954**)
Diphenylpyraline 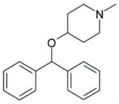 antihistaminic	*8-chlorotheophylline* 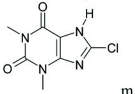 m.p. = 290 °C central stimulant	*Diprinhydrinate* m.p. = 174-176 °C antihistaminic	*Arch. Pharm.* **1955**, *288*, 400.
Sparteine 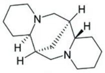 b.p. = 325 °C antiarrhythmic	*Theophylline* 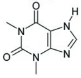 Cardiac-stimulant, bronchodilator	*Sparteine theophylline* antiarrhythmic	*Arch. ital. sci. farmacol.* [3] **1957**, 7, 314.
Clemizole 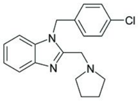 m.p. = 167 °C anti-histaminic	*Benzylpenicillin* 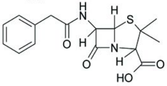 anti-biotic	*Benzylpenicillin clemizole* m.p. = 147-148.7 °C slow releasing antibiotic and antihistaminic	*US 2776279* (**1957**)
Etamiphylline 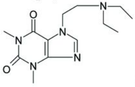 m.p. = 75 °C spasmolytic	*Camphorsulfonic acid* 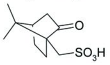 m.p. = 195 °C respiratory analeptic	*Camphophylline* m.p. = 174 °C bronchospasmolytic	*Therapie* **1959**, *14*, 844.
Chloroquine 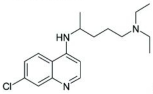 m.p. = 87 °C Anti-inflammatory	*Salicylic acid* 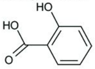 m.p. = 159 °C anti-inflammatory, antipyretic, analgesic	*Chloroquine salicylate* m.p. = 150 °C rheumatoid polyarthritis	*FR 1241135* (**1960**)
Phenmetrazine 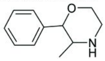 central stimulant, anorexic	*8-chlorotheophylline* 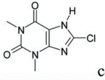 central stimulant	*Phenmetrazine theoclate* m.p. = 133 °C central stimulant, anorexic	*FR 1234842* (**1960**)

Continued on next page.

Downloaded by 89.163.35.42 on June 22, 2012 | http://pubs.acs.org
Publication Date (Web): April 28, 2010 | doi: 10.1021/bk-2010-1038.ch001

Table 2. (Continued). Some examples of ionic liquid like salt pairs having both cation and anion as active component

Chloroquine 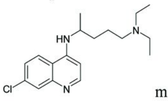 m.p. = 87 °C antiinflammatory	*Gentisic acid* 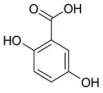 m.p. = 200-205 °C antiinflammatory, antipyretic,	*Chloroquine gentisate* m.p. = 165-170 °C rheumatoid polyarthritis	*FR 1241135* (**1960**)
Xanthinol 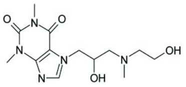 peripheral and cerebral vasodilator	*Nicotinic acid* 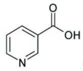 m.p. = 235 °C peripheral vasodilator	*Xanthinol nicotinate* m.p. = 180 °C peripheral and cerebral vasodilator	*US 2924598* (**1960**)
Etamiphylline 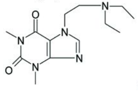 m.p. = 75 °C spasmolytic	*Methesculetol* 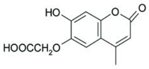 Vitamin *p* activity	*Metescufylline* m.p. = 124 °C capillary protectant	*FR M1234* (**1962**)
Propylhexedrine or levopropylhexedrin 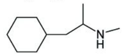 b.p. = 205 °C sympathomimetic	*Penobarbital* 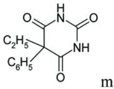 m.p. = 175 °C anticunvulsive, sedative, hypnotic	*Barbexaclone* anticunvulsive	*J. Pharmacol. Exp. Therap.* **1963**, *141*, 369.
Ornithin 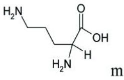 m.p. = 226-227 °C anticholesteremic	*Aspartic acid* 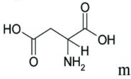 m.p. = 270 °C non-essential amino acid	*Ornithine aspartate* m.p. = 202 °C liver therapeutic	*FR M2677* (**1964**)
Papaverine 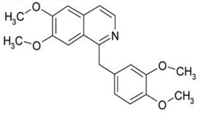 m.p. = 147 °C Spasmolytic	*Nicotinic acid* 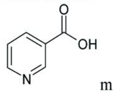 m.p. = 235 °C peripheral vasodilator	*Papaverine nicotinate* m.p. = 143-145 °C spasmolytic	*FR 1392510* (**1965**)
Heptaminol 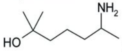 m.p. = <25 °C Cardiotonic	*Theophylline* 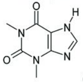 coronary dilator	*Heptaminol thephyllinate* m.p. = 170 °C cardiotonic	*GB 1136667* (**1968**)
Bamethan 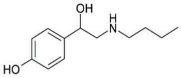 m.p. = 124 °C peripheral and cerebral vasodilator	*Nicotinic acid* 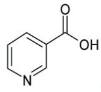 m.p. = 235 °C peripheral vasodilator	*Bamethan nicotinate* peripheral and cerebral vasodilator	*FR 2025133* (**1970**)

Continued on next page.

Table 2. (Continued). Some examples of ionic liquid like salt pairs having both cation and anion as active component

Papaverine 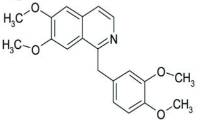 m.p. = 147 °C spasmolytic	*Camphorsulfonic acid* 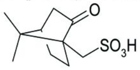 m.p. = 195 °C respiratory analeptic	*Papaverine camsylate* spasmolytic; cerebral vasodilator	*FR 6858* (**1969**)
Bromohexine 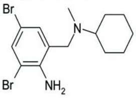 m.p. = 238 °C expectorant, mucolytic	*Camphorsulfonic acid* 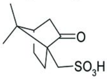 m.p. = 195 °C respiratory analeptic	*Bromhexine camsylate* antitussive, expectorant	*ES 392203* (**1971**)
Benzydamine 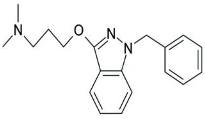 analgesic, antiinflammatory, antipyretic	*Salicylic acid* 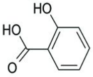 m.p. = 159 °C analgesic, antiinflammatory, antipyretic	*Benzydamine salicylate* analgesic, antiinflammatory, antipyretic	*ES 447306* (**1977**)
Codeine 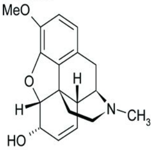 m.p. = 157.5 °C Analgesic	*Dichlofenac* 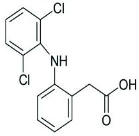 m.p. = 156-128 °C NSAID	*Codeine diclofenac* strong analgesic	*EP 472501* (**1992**)
Benzalkonium Chloride 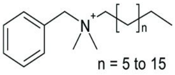 anti-bacterial	*Sodium ibuprofenate* 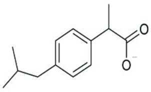 anti-inflammatory	*Benzalkonium ibuprofenate* m.p.: -41 °C	*Bull. Chem. Soc. Jpn.* **2007**, *80*, 2262.
Didecyldimethylammonium bromide 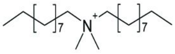 anti-bacterial	*Sodium ibuprofenate* 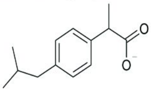 anit-inflammatory	*Didecyldimethylammonium ibuprofenate* m.p.: liquid at RT	*New J. Chem.* **2007**, *31*, 1429.

Continued on next page.

Downloaded by 89.163.35.42 on June 22, 2012 | http://pubs.acs.org
Publication Date (Web): April 28, 2010 | doi: 10.1021/bk-2010-1038.ch001

Downloaded by 89.163.35.42 on June 22, 2012 | http://pubs.acs.org
Publication Date (Web): April 28, 2010 | doi: 10.1021/bk-2010-1038.ch001

Table 2. (Continued). Some examples of ionic liquid like salt pairs having both cation and anion as active component

Benzalkonium Chloride 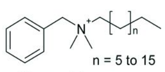 anti-bacterial	*Colawet MA-80* 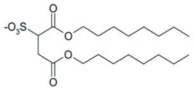 wetting agent	*Benzalkonium Colawet MA-80* m.p.: liquid at RT	*Bull. Chem. Soc. Jpn.* **2007**, *80*, 2262.
Benzalkonium Chloride 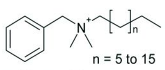 anti-bacterial	*Sodium sulfacetamide* 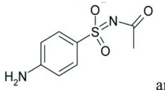 anti-acne	*Benzalkonium sulfacetamide* m.p.: liquid at RT	*Bull. Chem. Soc. Jpn.* **2007**, *80*, 2262.
Lidocaine hydrochloride 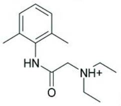 Pain reliever	*Sodiium docusate* 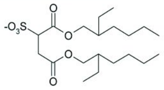 emollient	*Lidocaine docusate* m.p.: liquid at RT	*New J. Chem.* **2007**, *31*, 1429.
Ranitidine hydrochloride 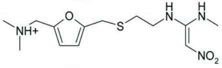 histamine H_2-receptor antagonist	*Sodiium docusate* 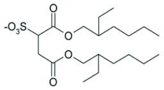 emollient	*Ranitidine docusate* m.p.: liquid at RT	*New J. Chem.* **2007**, *31*, 1429.

References

1. *Handbook of Pharmaceutical Salts: Properties, Selection, and Use*; Wermuth, C. G., Stahl, P. H., Eds.; Wiley-VCH: Weinheim, Germany, 2002.
2. Berge, S. M.; Bighley, L. M.; Monkhouse, D. C. *J. Pharm. Sci.* **1977**, *66*, 1.
3. Black, S. N.; Collier, E. A.; Davey, R. J.; Robert, R. J. *J. Pharm. Sci.* **2007**, *96*, 1053.
4. Anderson, B. D.; Conradi, R. A. *J. Pharm. Sci.* **1985**, *74*, 815.
5. Binghley, L. D.; Berge, S. M.; Monkhouse, D. C. *Encyclopedia of Pharmaceutical Technology*; Marcel Dekker: New York, 1966; p 453.
6. *Ionic Liqiuds in Synthesis*; Wasserscheid, P., Welton, T., Eds.; Wiley-VCH: Weinheim, Germany, 2003.
7. (a) Wasserscheid, W.; Kim, W. *Angew. Chem. Int. Ed.*, **2000**, *39*, 3772. (b) Lagrost, H. C. *Chem. Rev.* **2008**, *108*, 2238. (c) Martins, A. P. M.; Frizzo, C. P.; Moreira, D. N.; Zanatta, N.; Bonacorso, H. G. *Chem. Rev.* **2008**, *108*, 2015.
8. Ranke, J.; Stolte, S.; Stormann, R.; Arning, J.; Jastorff, B. *Chem. Rev.* **2007**, *107*, 2183.
9. Stock, F.; Hoffman, J.; Ranke, J.; Ondruschka, B.; Jastroff, B. *Green Chem.* **2004**, *6*, 286.
10. Skladanowski, A.C.; Stepnowski, P.; Kleszczynski, K.; Dmochowska, B. *Environ. Toxicol. Pharmacol.* **2005**, *19*, 291.
11. (a) Wang, X.; Ohlin, C. A.; Lu, Q.; Fei, Z.; Hu, J.; Dyson, P. J. *Green Chem.* **2007**, *9*, 1191. (b) Stepnowski, P.; Skladanowski, A.; Ludwiczak, A.; Laczynska, E. *Hum. Exp. Toxicol.* **2004**, *23*, 513.

12. (a) Stolte, S.; Arning, J.; Bottin-Weber, U.; Matzke, M.; Stock. F.; Thiele, K.; Uerdingen, M.; Welz-Biermann, U.; Jastorff, B.; Ranke, J. *Green Chem.* **2006**, *8*, 621. (b) Stolte, S.; Arning, J.; Bottin-Weber, U.; Muller, A.; Pitner, W.-R.; Welz-Biermann, U.; Jastorff, B.; Ranke, J. *Green Chem.* **2007**, *9*, 760.
13. Frade, R. F. M.; Matias, A.; Branco, L. C.; Afonso, C. A. M.; Dusrte, C. M. M. *Green Chem.* **2007**, *9*, 873.

Downloaded by 89.163.35.42 on June 22, 2012 | http://pubs.acs.org
Publication Date (Web): April 28, 2010 | doi: 10.1021/bk-2010-1038.ch001

Downloaded by PENNSYLVANIA STATE UNIV on June 22, 2012 | http://pubs.acs.org
Publication Date (Web): April 28, 2010 | doi: 10.1021/bk-2010-1038.ch002

Chapter 2

Ionic Liquids: New Opportunities for the Chemistry of Amino Acids, Peptides, and Pharmaceutical Compounds

**James Ternois,[2] Laurent Ferron,[2] Gérard Coquerel,[2]
Frédéric Guillen,[1] and Jean-Christophe Plaquevent[1,*]**

**[1]CNRS-UMR 5068, LSPCMIB, Université Paul Sabatier,
118 route de Narbonne, F-31062 Toulouse Cedex 9, France
[2]UPRES-EA 3233, SMS, IRCOF, Université de Rouen,
rue Tesnière, F-76821 Mont-Saint-Aignan Cedex, France
*plaquevent@chimie.ups-tlse.fr**

In this chapter are described two approaches involving ionic liquids as solvents for the synthesis of target molecules of real interest. First, peptide synthesis has been shown to be efficient in ionic media. Particular attention is paid to the construction of cyclopeptides in these conditions. Second, enantioselective oxidations leading to chiral sulfoxides were examined as a route to drugs such as modafinil. Unexpected observations incited us to propose different mechanistic pathways in ionic liquids with respect to molecular solvents. In both studies, we showed that ionic liquids can efficiently replace organic solvents.

Ionic liquids and their combination of unique properties have given rise to a growing interest among numerous chemists. Their negligible vapor pressure makes confinement and recycling easy, and renders them almost non-flammable. This, along with their ability to dissolve various organic and organometallic compounds, and the possibility to finely tune their physical and chemical properties, makes them credible alternative solvents in the context of green chemistry (*1*). Moreover it has been shown in the recent years that their use could lead to increases in yield and selectivity, or even to complete modification of reaction routes (*2*).

In the context of organic synthesis, two areas of investigation appealed to us as particularly interesting: "ionic liquids and chirality" (*3*) (including the synthesis (*4*) and the use of chiral ionic liquids), and "ionic liquids and biomolecules" (some impressive success have recently been disclosed in the chemistry of carbohydrates, proteins, lignins, etc.).

The aim of this account is to report our recent findings concerning the use of ionic liquids in the synthesis of target molecules of real interest, in the field of peptide synthesis and pharmaceutics.

Peptide Synthesis in Ionic Media

Peptide synthesis, despite its long history, still suffers from severe drawbacks such as low atom economy (protection/deprotection steps), high–cost coupling reagents, and tedious processes, especially for unnatural amino acids. These drawbacks have led to continuing research focusing on the use of simplified procedures, cheaper reagents, their recycling, and possibly the absence of protecting groups. In this context, ionic solvents are increasingly being tested in peptide chemistry, both for synthetic and analytical purposes (*5*). Some of these very recent studies highlight a real potential as well as new opportunities.

Enzymatic and chemical transformations of amino acid derivatives have recently benefited from the use of ionic liquids as reaction media in terms of improved yield, ee, or stability and recycling of the enzyme. For example, Malhotra investigated for the first time the use of ionic liquid [EtPy][TFA] as a catalyst for the esterification of amino acids, including unnatural compounds (*6*). After *N*-acetylation, the *N*-protected amino acid was dissolved in anhydrous ethyl or *i*-propyl alcohol, and the ionic liquid added to the solution. Yields were generally good, especially for ethyl esters. Much information is available now that clearly shows the greater stability and activity of enzymes when they are diluted in ionic solvents, inciting chemists to examine the construction of peptide bonds in ionic media by means of proteolytic enzymes. Aspartame (as the Z-protected derivative) was obtained from a thermolysin-catalyzed reaction of Z-aspartate and phenylalanine methyl ester hydrochloride in [bmim][PF_6]. The authors observed a competitive rate with respect to the same reaction in molecular solvents, as well as a remarkable stability of the enzyme (*7*). Recycling of the ionic liquid was successfully performed.

More recently, Malhotra *et al* reported the protease-catalyzed synthesis of peptides from natural amino acids in various ionic liquids. A comparative study with molecular solvents found the approach simple and more effective in ILs (*8*). In 2007, α-chymotrypsin-catalyzed peptide synthesis was examined in ILs. The model reaction was the synthesis of a fragment of Leu-enkephalin, *ie* ZTyrGlyGlyOEt. Six different ionic liquids were screened, and it was shown that the water content of the reaction medium has a great influence on the enzyme activity. Several di- and tri-peptides were also obtained with a 70-75% yield (*9*).

The field of chemical peptide synthesis in ILs has attracted much less interest than enzymatic peptide synthesis. Trulove et al, in a congress abstract, reported the

Downloaded by PENNSYLVANIA STATE UNIV on June 22, 2012 | http://pubs.acs.org
Publication Date (Web): April 28, 2010 | doi: 10.1021/bk-2010-1038.ch002

incubation of amino acid mixtures in [bmim][PF_6], in the absence of any coupling reagent giving, after aqueous extraction, peptides (as unidentified and unquantified mixtures) when the reaction temperature was greater than 100°C (*10*). However, no reports on controlled chemical peptide coupling in ionic liquids were available in the literature till 2004. This is rather surprising, as ILs are good solvents for amino acid derivatives and could favor coupling reactions by the stabilization of charged coupling reagents and reaction intermediates.

Modern coupling agents such as BOP and HATU are salts that present similarities with ionic liquids (Figure 1). We therefore considered some years ago their use for peptide coupling in ILs (*11*, *12*). We surmised that ionic liquids would be able to easily dissolve and stabilize these salts, and give rise to more selective reactions. Thus, we focused on quaternary amino acids such as α-methyl-α-*para*-tolylglycine (MPG) that are much more difficult to couple than proteinogenic ones. After optimization of reaction conditions and extraction process, good yields were obtained for dipeptides. In addition to a similar efficiency with respect to molecular solvents, the advantage of ionic liquids was the higher purity of the crude products: pure dipeptides were obtained by simple extraction, without any additional purification. Shortly after, two papers confirmed the interest of chemical peptide coupling in ionic liquids, and the main conclusions of our studies. First, diketopiperazines were efficiently obtained in [bdmim][PF_6], using low–power microwave irradiation (*13*). Second, Sega published an example of peptide bond construction in ionic liquid, with 90% yield (peptide obtained: Cbz-Phe-Ser-OMe) (*14*). A simple ether extraction afforded the desired product, and serine was coupled without protection of the side chain.

In a following study, we embarked on the synthesis of longer peptides. Indeed, it is well known that classical methods for peptide synthesis, although largely used and efficient, still suffer from low productivity in solid-phase methods, or from limited chain construction in homogeneous liquid synthesis. Thus, it was interesting to evaluate the construction of longer peptide sequences, including cyclopeptides that are not always easy to obtain.

Tetrapeptide Z-(Gly-(R)-MPG)$_2$-OMe was prepared using HATU as coupling reagent, according to the same protocol as for dipeptides (Figure 2).

We were delighted to obtain a very good conversion, slightly better than in a molecular solvent such as THF. This protected tetrapeptide was then deprotected on the *N*-terminal position using standard procedure (Figure 3), with a quantitative yield. Another sample was deprotected on the *C*-terminal function by alkaline hydrolysis with 85% yield (Figure 3).

In the following step, we coupled these two fragments in order to obtain the corresponding linear octapeptide. Again, we used HATU as coupling agent, and obtained the expected compound with 83% yield (Figure 4), very similar to that obtained when using THF as medium. We then deprotected both functions of the octapeptide to obtain the required precursor for cyclisation. We proceeded in a sequential manner, first by saponification of the *C*-terminal function, then by reductive cleavage of the Z protecting group (Figure 5). Both steps were efficient with ca 80% yields.

We then decided to go further by examination of the cyclisation reaction to yield the cyclooctapeptide, using [bmim][PF_6] as solvent. The reaction

Downloaded by PENNSYLVANIA STATE UNIV on June 22, 2012 | http://pubs.acs.org
Publication Date (Web): April 28, 2010 | doi: 10.1021/bk-2010-1038.ch002

Downloaded by PENNSYLVANIA STATE UNIV on June 22, 2012 | http://pubs.acs.org
Publication Date (Web): April 28, 2010 | doi: 10.1021/bk-2010-1038.ch002

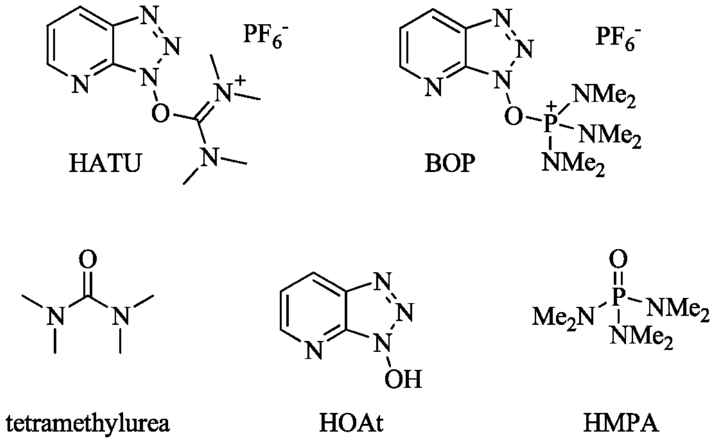

Figure 1. Coupling agents and their residual components

was monitored by reversed phase HPLC. A frequent issue in macrocyclisation reactions is the possibility of dimerisation, which is often circumvented by the use of high dilutions to slow down intermolecular reactions. Ionic liquids are highly viscous liquids, with very low diffusivity: we therefore hoped that the reaction could proceed at higher concentrations in ILs than in molecular solvents, the unwanted dimerisation being prevented by low diffusivity. The use of HATU yielded mainly impurities, and was discarded for the cyclisation step. However, BOP gave a very exciting result with a cyclopeptide yield of 85%. To the best of our knowledge, this is the first reported access to “long” peptide chains, with tetra-, octa- and cyclocta-peptide construction in excellent yields. Also, the cyclisation in classical dilutions was observed, avoiding the use of large amounts of ionic solvent. The complete data for the synthesis and structural aspects of this series of peptides will be published elsewhere (*15*). As mentioned before, one interesting aspect of this method is the high purity of the crude peptides. This could be due, at least in part, to the ability of ionic solvents to keep the residual components (HOAt and tetramethylurea or HMPA) of the coupling agents in solution (Figure 1). In addition to benefits for the purification procedure, this suggests that recycling the expensive activation agent could be feasible.

Having in hand a series of successful information about peptide coupling in ILs, we then wondered if it would be possible to prepare peptides possessing ionic liquid properties. We previously described the synthesis of chiral ILs bearing an imidazolium moiety from the natural amino acid histidine (*16–18*). Monoprotected “histidiniums” were reacted with *N*-Boc-alanine (respectively alanine *tert*-butylester) using HATU and DIEA, affording the novel dipeptides in good yields and without epimerization (Figure 6). Worthy of note is that peptide coupling under standard conditions leads to the desired targets in excellent yields, even starting from unprecedented ionic structures.

Downloaded by PENNSYLVANIA STATE UNIV on June 22, 2012 | http://pubs.acs.org
Publication Date (Web): April 28, 2010 | doi: 10.1021/bk-2010-1038.ch002

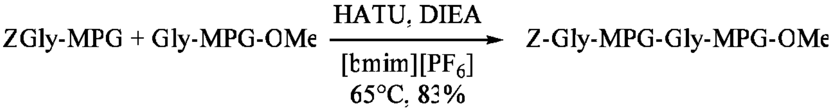

$$\text{ZGly-MPG} + \text{Gly-MPG-OMe} \xrightarrow[\substack{[\text{bmim}][\text{PF}_6] \\ 65^\circ\text{C},\ 83\%}]{\text{HATU, DIEA}} \text{Z-Gly-MPG-Gly-MPG-OMe}$$

Figure 2. Synthesis of tetrapeptide Z-(Gly-(R)-MPG)$_2$-OMe

Enantioselective Oxidation in Ionic Liquids

In the second part of this chapter, we will focus on the asymmetric synthesis of a series of chiral sulfoxides in the family of modafinil, an atypical psychostimulant recently approved in the United States as a treatment for excessive daytime sleepiness associated with narcolepsy and shift-work sleep disorder (Figure 7). Indeed, we chose as a key strategy the enantioselective oxidation of the corresponding prochiral sulfides (*19*). Our goals consisted of: *i*) deciding on a reliable and robust method, applicable to polyfunctional molecules rather than just to model compounds and *ii*) finding a method avoiding the classical use of halogenated solvents for oxidation systems.

After rather disappointing results obtained when using catalytic oxidation systems (*19*), we turned to the study of stoichiometric chiral oxidants (Figure 8).

In our hands, oxaziridine **1**, developed by Davis (*20*), gave particularly interesting results with e.e. of up to 90% for modafinic acid (*19*). This prompted us to evaluate this enantioselective oxidizing agent in a hydrophobic ionic liquid, [bmim][PF$_6$], to avoid the use of toxic CCl$_4$ which is the usual solvent for this reaction. Moreover, no examples of enantioselective oxidation of sulfoxides in ILs had been published at the time.

The results obtained for oxidation with oxaziridine **1** in CCl$_4$ and [bmim][PF$_6$] with the three functionalized substrates are summarized in Table I. As thioanisole (methylphenylthioether) is routinely used as substrate for enantioselective oxidation of thioether, we also tested it in these conditions.

In both solvents this enantioselective oxidative system appear much more robust than previously tested systems (*19*), giving significant enantiomeric excesses for each substrate. We were pleased to find that the reaction in ionic liquid gave only slightly diminished e.e., but comparable or higher yields, than in CCl$_4$.

However the most intriguing result was obtained with the model compound thioanisole: switching from the molecular apolar solvent CCl$_4$ to the polar ionic liquid [bmim][PF$_6$] induced a reversal of the absolute configuration of the sulfoxide obtained, along with a decrease in enantioselectivity. None of the modafinil-related substrates showed the same inversion.

This observation led us to examine the role of the solvent in this asymmetric reaction more precisely. We thus conducted the reaction in various solvents of increasing polarities: the results are presented in Figure 9, along with the dielectric constant of the solvent.

Downloaded by PENNSYLVANIA STATE UNIV on June 22, 2012 | http://pubs.acs.org
Publication Date (Web): April 28, 2010 | doi: 10.1021/bk-2010-1038.ch002

Table I. Enantioselective oxidations by oxaziridine 1[a]

Sulfoxide	*Solvent*	*Yield (%)*	*ee (%)*	*Conf.*
thioanisole	CCl_4	85	65	(S)
	[bmim][PF_6]	77	33	(R)
modafinil	CCl_4	66	60	(S)
	[bmim][PF_6]	73	55	(S)
modafinic acid	CCl_4	47	90	(S)
	[bmim][PF_6]	73	78	(S)
DMSAM	CCl_4	90	75	(S)
	[bmim][PF_6]	87	70	(S)

[a] Reaction conditions: 20°C, 24h.

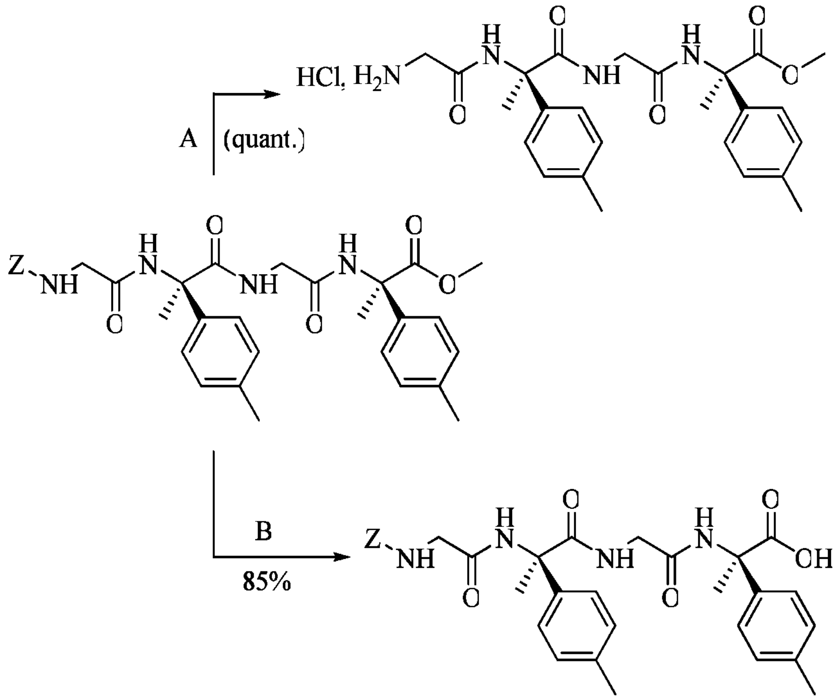

A: 1. H_2, Pd/C (11%), MeOH. 2. HCl 5-6M in *i*PrOH
B: 1. NaOH 2M (3 eq.), *i*PrOH. 2. HCl 1M

Figure 3. Deprotection of tetrapeptide Z-(Gly-(R)-MPG)$_2$-OMe

Downloaded by PENNSYLVANIA STATE UNIV on June 22, 2012 | http://pubs.acs.org
Publication Date (Web): April 28, 2010 | doi: 10.1021/bk-2010-1038.ch002

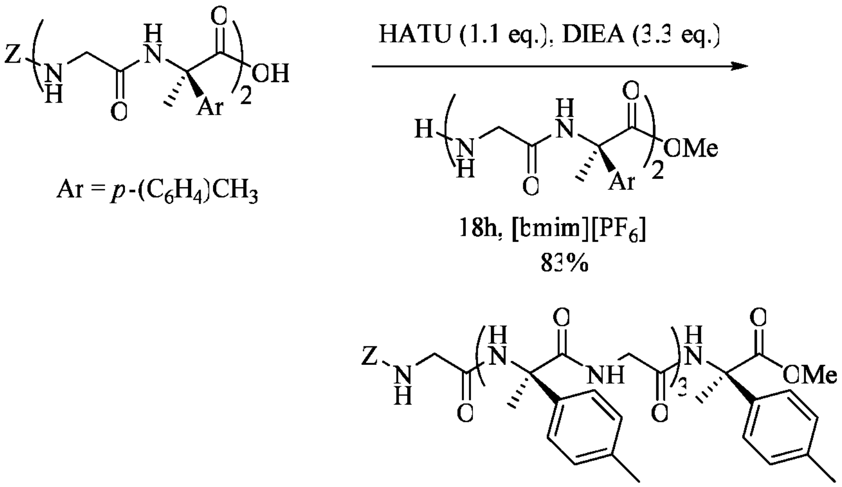
Ar = p-(C6H4)CH3
HATU (1.1 eq.), DIEA (3.3 eq.)
18h, [bmim][PF6]
83%
Z
OH
OMe
Ar

Figure 4. Synthesis of octapeptide Z-(Gly-(R)-MPG)₄-OMe

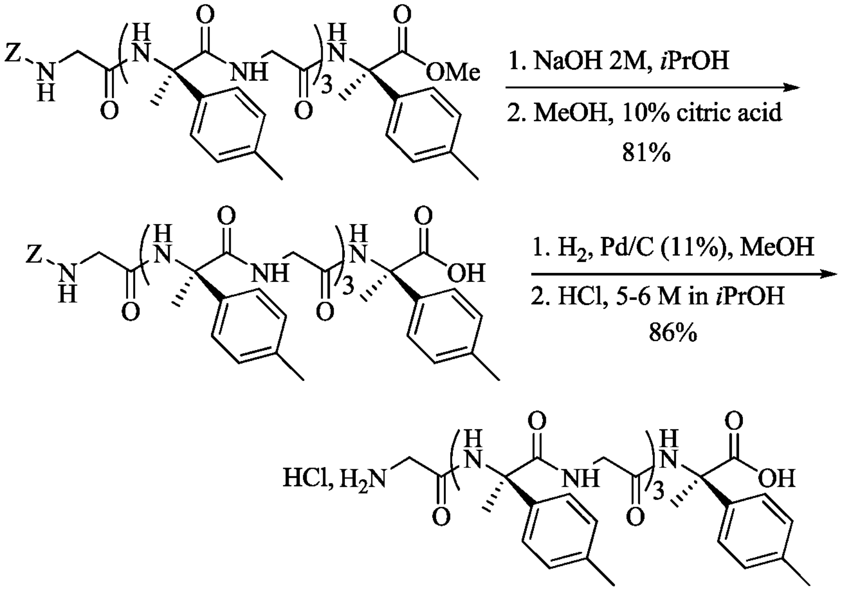
1. NaOH 2M, iPrOH
2. MeOH, 10% citric acid
81%
1. H2, Pd/C (11%), MeOH
2. HCl, 5-6 M in iPrOH
86%
HCl, H2N
Z
OMe
OH

Figure 5. Deprotection of octapeptide Z-(Gly-(R)-MPG)₄-OMe

Downloaded by PENNSYLVANIA STATE UNIV on June 22, 2012 | http://pubs.acs.org
Publication Date (Web): April 28, 2010 | doi: 10.1021/bk-2010-1038.ch002

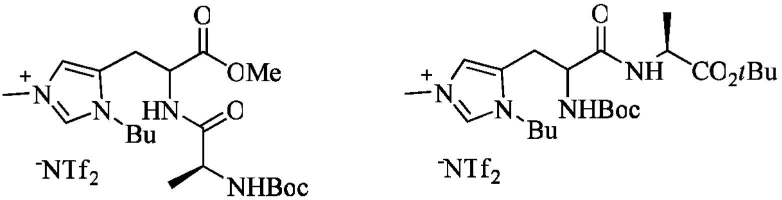

Figure 6. Chiral peptidic ionic liquids

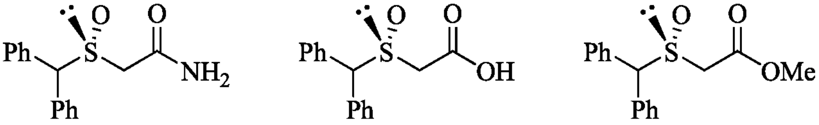

(*R*)-modafinil (*R*)-modafinic acid (*R*)-DMSAM

Figure 7. Chiral functional sulfoxides in the modafinil series

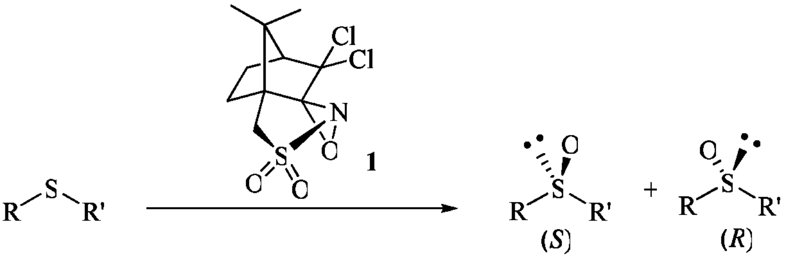

*Figure 8. Enantioselective oxidation with chiral oxaziridine **1***

Table II. Enantioselective oxidation of thioanisole in ionic liquids

Solvent	*Yield (%)*	*ee (%)*	*Conf.*
[bmim][PF_6]	77	33	(R)
[bmim][BF_4]	40	37	(R)
[bmim][NTf_2]	95	27	(R)
[bmim][Cl][a]	63	22	(R)
[bmmim][PF_6][b]	77	19	(R)
[bmmim][BF_4]	73	31	(R)

[a] Reaction at 40°C. [b] Reaction at 30°C.

Downloaded by PENNSYLVANIA STATE UNIV on June 22, 2012 | http://pubs.acs.org
Publication Date (Web): April 28, 2010 | doi: 10.1021/bk-2010-1038.ch002

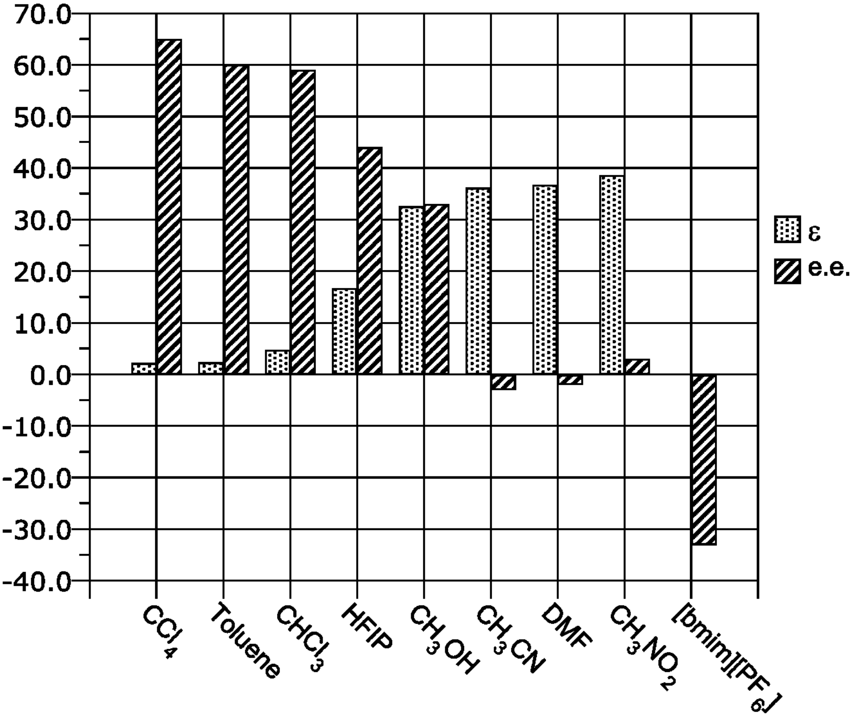

Figure 9. Enantiomeric excess of methylphenylsulfoxide. Positive values of e.e. arbitrarily refer to (S) configuration, and negative to (R).

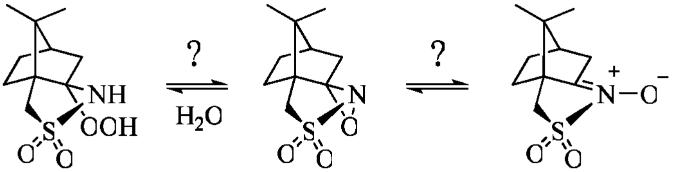

3 **2** **4**

Figure 10. Oxaziridine vs hydroperoxyamine or nitrone?

In view of these results, two conclusions emerge. First, the enantioselective oxidation of thioanisole with oxaziridine **1** is highly dependent on the polarity of the solvent, and is best conducted in apolar solvents like CCl_4 and toluene. Polar protic solvents like methanol and hexafluoroisopropanol give notably reduced enantioselectivities, and polar aprotic solvents give almost no enantioselectivity. Second, complete inversion of absolute configuration does not seem to occur in any molecular solvent, regardless of its polarity (the values obtained in DMF and

CH_3CN are indeed inverted, but too low to be significant). Moreover, conducting the reaction in other ionic liquids always afforded the (*R*) enantiomer of the sulfoxide (Table II).

As the reactions are routinely run at higher concentrations in ionic liquid than in molecular solvents, we also checked that the concentration was not responsible for the inversion: apart from a slight decrease in yield and e.e., no inversion phenomena were observed when running the reaction at the same concentrations in molecular solvents as in ionic liquids.

In the literature, Page reported a related inversion phenomenon using oxaziridine **2** (Figure 10) for the oxidation of *tert*-butylmethylthioether. The oxidation using either preformed oxaziridine or the corresponding imine and hydrogen peroxide led to (*S*) and (*R*) enantiomers of the sulfoxide, respectively (*21*). It should be noted that, as in our case, this inversion phenomenon is very specific and does not occur when using another oxaziridine or another thioether. Page tentatively proposed a different reaction pathway in the case of oxidation with the imine – hydrogen peroxide system, involving the corresponding α-hydroperoxyamine **3** (which is an intermediate in the synthesis of oxaziridine (*22*)) as oxidizing agent.

In our case, only preformed oxaziridine was used, and formation of α-hydroxyperoxyamine would require the presence of water in the reaction medium. However, the use of carefully dried or, on the contrary, water-equilibrated ionic liquids led to the same (*R*) enantiomer with very similar ee values. Involvement of an α-hydroxyperoxyamine similar to **3** seems therefore unlikely in our system. Nitrone **4**, which is a charged isomer of oxaziridine **2**, could also be involved in this process. We are currently investigating the mechanistic implications of this reversal of configuration.

Conclusion and Prospects

Ionic liquids are now generally recognized as powerful media for organic synthesis (*2*), and we think that it is time to take advantage of their unique properties to address real synthetic issues. In this context, we designed new experiments and methods using ionic liquids instead of molecular solvents for reactions of real importance in organic synthesis, *ie* peptide coupling of crowded amino acids (including access to long peptidic chains and cyclo peptides) and asymmetric synthesis of functionalized sulfoxides of pharmaceutical interest. We wanted to assess the real potential of ionic liquids for these purposes, with the aim of replacing organic solvents such as THF or halogenated solvents. This has been shown in both studies with success. In addition to this aspect, we were delighted by new findings, sometimes unexpected, which open the door to new processes and new insights in the field of organic synthesis in ionic liquids. For example, we believe that peptide synthesis could benefit from ionic liquid chemistry with the possibility of discovering simpler and cheaper methods. Regarding sulfoxide chemistry, an observation led us to postulate different mechanistic pathways in ionic liquids with respect to molecular solvents, leading to the hypothesis that,

Downloaded by PENNSYLVANIA STATE UNIV on June 22, 2012 | http://pubs.acs.org
Publication Date (Web): April 28, 2010 | doi: 10.1021/bk-2010-1038.ch002

among current progress in organic synthesis, this chemistry will afford new information about chemical reactivity.

Acknowledgments

The authors wish to thank Rhodia and Cephalon for financial support and research grants given to LF and JT, as well as for stimulating scientific discussions. We also thank Professor P. Winterton for his help in preparing the final version of the manuscript.

Downloaded by PENNSYLVANIA STATE UNIV on June 22, 2012 | http://pubs.acs.org
Publication Date (Web): April 28, 2010 | doi: 10.1021/bk-2010-1038.ch002

References

1. Welton, T. *Green Chem.* **2008**, *10*, 483.
2. *Ionic Liquids in Synthesis*, 2nd ed.; Wasserscheid, R., Welton, T., Eds.; Wiley-VCH: Weinheim, Germany, 2008.
3. For a review about ILs and chirality see: Baudequin, C.; Baudoux, J.; Levillain, J.; Cahard, D.; Gaumont, A.-C.; Plaquevent, J.-C. *Tetrahedron: Asymmetry* **2003**, *14*, 3081−3093.
4. For a review about chiral ILs see: Baudequin, C.; Brégeon, D.; Levillain, J.; Guillen, F.; Plaquevent, J.-C.; Gaumont, A.-C. *Tetrahedron: Asymmetry* **2005**, *16*, 3921−3945.
5. Plaquevent, J.-C.; Levillain, J.; Guillen, F.; Malhiac, C.; Gaumont, A.-C. *Chem. Rev.*, in press.
6. Zhao, H.; Malhotra, S. V. In *Catalysis of Organic Reactions*; Morrell, D. G., Ed.; Marcel Dekker, Inc.: New York, 2003; pp 667−673.
7. Erbeldinger, M.; Mesiano, A. J.; Russel, A. J. *Biotechnol. Prog.* **2000**, *16*, 1129–1131.
8. Zhang, C.; Malhotra, S. V. *Abstracts of Papers*, 228th ACS National Meeting, Philadelphia, PA, August 22−26, 2004.
9. Xing, G.-W.; Li, F.-Y.; Ming, C.; Ran, L.-N. *Tetrahedron Lett.* **2007**, *48*, 4271–4274.
10. Smith, V. F.; De Long, H. C.; Trulove, P. C.; Sutto, T. E. AG1-13th International Symposium on Molten Salts, Philadelphia, PA, May 12−17, 2002; *Proc. Electrochem. Soc.* **2002**, 2002-19 (Molten Salts XIII), 268.
11. Vallette, H.; Ferron, L.; Coquerel, G.; Gaumont, A.-C.; Plaquevent, J.-C. *Tetrahedron Lett.* **2004**, *45*, 1617–1619.
12. Vallette, H.; Ferron, L.; Coquerel, G.; Guillen, F.; Plaquevent, J.-C. *Arkivoc* **2006**, *4*, 200–211.
13. Yen, Y.-H.; Chu, Y. H. *Tetrahedron Lett.* **2004**, *45*, 8137–8137.
14. Lampariello, L. R.; Peruzzi, D.; Sega, A.; Taddei, M. *Lett. Org. Chem.* **2005**, *2*, 265–270.
15. Ferron, L.; Guillen, F.; Coste, S.; Coquerel, G.; Cardinaël, P.; Schwartz, J.; Paris, J.-M.; Plaquevent J.-C. Manuscript in preparation.

16. Brégeon, D.; Levillain, J.; Guillen, F.; Plaquevent, J.-C.; Gaumont, A.-C. In *Ionic Liquids in Organic Synthesis*; Malhotra, S. V., Ed.; ACS Symposium Series, N°950, Oxford University Press: Washington, DC, 2007; pp 246−258.
17. Guillen, F.; Brégeon, D.; Plaquevent, J.-C. *Tetrahedron Lett.* **2006**, *47*, 1245–1248.
18. Brégeon, D.; Levillain, J.; Guillen, F.; Plaquevent, J.-C.; Gaumont, A.-C. *Amino Acids* **2008**, *35*, 175–184.
19. Ternois, J.; Guillen, F.; Plaquevent, J.-C.; Coquerel, G. *Tetrahedron: Asymmetry* **2007**, *18*, 2959–2964.
20. Davis, F. A.; Weismiller, M. C.; Murphy, C. K.; Thimma Reddy, R.; Chen, B.-C. *J. Org. Chem.* **1992**, *57*, 7274–7285.
21. Page, P. C. B.; Heer, J. P.; Bethell, D.; Lund, B. A. *Phosphorus, Sulfur Silicon Relat. Elem.* **1999**, *153-154*, 247–258.
22. Rebek, J., Jr.; McCready, R. *J. Am. Chem. Soc.* **1980**, *102*, 5602–5605.

Downloaded by PENNSYLVANIA STATE UNIV on June 22, 2012 | http://pubs.acs.org
Publication Date (Web): April 28, 2010 | doi: 10.1021/bk-2010-1038.ch002

Chapter 3

Enzymatic Membrane Reactor for Resolution of Ketoprofen in Ionic Liquids and Supercritical Carbon Dioxide

**Pedro Lozano,*,[1] Teresa De Diego,[1] Arturo Manjón,[1]
Miguel A. Abad,[1] Michel Vaultier,[2] and José L. Iborra[1]**

**[1]Departamento de Bioquímica y Biología Molecular B e Inmunología,
Facultad de Química, Universidad de Murcia, P.O. Box 4021,
E-30100 Murcia, Spain
[2]UMR CNRS 6510, Université de Rennes Campus de Beaulieu. Av.
Général Leclerc, 35042 Rennes, France
*plozanor@um.es**

Ionic liquids (ILs) have attracted growing interest as alternative reaction media for enzyme-catalyzed transformations because of their unique properties as green solvents, opening up news opportunities in the field of pharmaceutical synthesis. Additionally, enzymatic transformations in ILs/scCO$_2$ biphasic systems have been described as an interesting way of carrying out clean synthetic processes whereby enzyme molecules are "immobilized" into the IL phase, while substrates/products are transported by the scCO$_2$ phase.

Several ILs based on alkyl-imidazolium cations and associated with different anions, ([PF$_6$], [BF$_4$] and [NTf$_2$]), have been assayed for the *Candida antarctica* lipase B (CALB)-catalyzed resolution of the analgesic *rac*-ketoprofen by esterification with different 1-alkanols. A membrane reactor working with both IL and supercritical carbon dioxide (scCO$_2$) phases has been applied for separation of R-ketoprofen ester products.

Downloaded by OHIO STATE UNIV LIBRARIES on June 22, 2012 | http://pubs.acs.org
Publication Date (Web): April 28, 2010 | doi: 10.1021/bk-2010-1038.ch003

In Ionic Liquid Applications: Pharmaceuticals, Therapeutics, and Biotechnology; Malhotra, S.;
ACS Symposium Series; American Chemical Society: Washington, DC, 0.

Introduction

The preparation of chiral drugs as single enantiomers is one of the main goals of pharmaceutical science because of the distinct biological activity exhibited by each enantiomers. In some cases only one of the enantiomer contributes to its pharmacological behavior, while the other shows no effect or side-effects, or even toxicity (*1*). Enzymes are the most efficient tools for the resolution of racemic mixtures in aqueous media, although their practical applications to produce enantiopure fine chemicals is limited because most chemicals of interest are insoluble in water. Furthermore, switching from water to non-aqueous solvents, as reaction medium for enzyme-catalyzed reactions, is not always a simple answer, because the native structure of the enzyme can easily be destroyed, resulting in deactivation. Water is the key component of all non-conventional media, because of the importance that enzyme-water interactions have in maintaining the active conformation of the enzyme (*2*).

Enzymatic reactions based on neoteric solvents, such as ionic liquids (ILs) and supercritical fluids (SCFs), are promising alternative media for developing integral green chemical processes in non-aqueous conditions (*3*). Free and immobilized enzymes (*e.g.* lipases, proteases, etc.) have been shown as suitable for catalyzing chemical transformations (*e.g.* esterification, alcoholysis, asymmetric synthesis, etc.) in supercritical carbon dioxide ($scCO_2$) (*4*). In such enzymatic processes, the classical advantages of $scCO_2$ to extract, dissolve and transport chemicals are tarnished by the denaturative effect has on enzymes (*5*, *6*). On the other hand, ILs, especially water-immiscible ILs, have shown themselves to be excellent non-aqueous environments for enzyme catalysis, because of the high level of activity and stereoselectivity for synthesizing many different compounds, *e.g.* aspartame, aliphatic and aromatic esters, chiral esters, polymers, etc. (*7*). Furthermore, the excellent stability of enzymes in water-immiscible ILs for reuse has been widely described (*8*, *9*), and spectroscopic techniques have demonstrated the ability of these neoteric solvents to maintain the secondary structure and the native conformation of the protein towards the usual unfolding that occurs in non-aqueous environments (*10*). Biphasic systems based on ILs and supercritical carbon dioxide have been proposed as the first approach to integral green bioprocesses in non-aqueous media, whereby both the biocatalytic and extraction steps are coupled in an environmentally benign and efficient reaction/separation process (*3*, *4*, *11*).

Ketoprofen is an active anti-inflammatory compound usually employed as racemate in pharmaceuticals formulations, the S-enantiomer being the active compound. Several enzymatic strategies, based on the stereoselective hydrolysis of rac-ketoprofen esters in aqueous media (*12*) or on the stereoselective synthesis of ketoprofen alkyl esters in chlorinated solvents (*13*, *14*), have been applied to separate the *S*-enantiomer. For the first time, this work shows the ability of CALB to catalyze the resolution of *rac*-ketoprofen in ILs by esterification with different 1-alkanols Figure 1. The influence of both concentration and chain-length of the 1-alkanols have also been studied. Furthermore, a membrane reactor, based on both IL and $scCO_2$ neoteric solvents, has been applied to separate the *R* and *S*-enantiomers.

Downloaded by OHIO STATE UNIV LIBRARIES on June 22, 2012 | http://pubs.acs.org
Publication Date (Web): April 28, 2010 | doi: 10.1021/bk-2010-1038.ch003

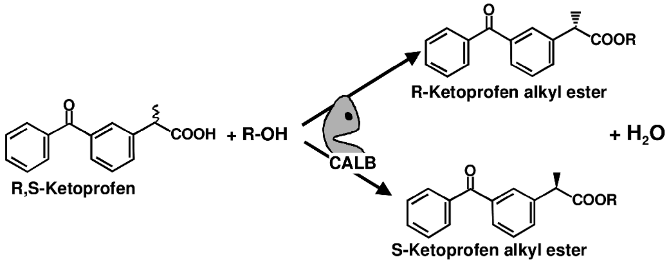

Figure 1. Schema of the C. antarctica lipase B (CALB)-catalyzed esterification of rac-ketoprofen with 1-alkanols.

Downloaded by OHIO STATE UNIV LIBRARIES on June 22, 2012 | http://pubs.acs.org
Publication Date (Web): April 28, 2010 | doi: 10.1021/bk-2010-1038.ch003

Materials and Methods

Materials

Immobilized CALB (Novozym 435®, EC 3.1.1.3) was a gift from Novozymes S.A. (Madrid, Spain). 1-butyl-3-methylimidazolium hexafluoro phosphate ([Bmim][PF_6]), 1-octyl-3-methylimidazolium hexafluorophosphate ([Omim][PF_6]), 1-butyl-3-methylimidazolium tetrafluoroborate ([Bmim][BF_4]), 1-butyl-2,3-dimethylimidazolium hexafluorophosphate ([Bdmim][PF_6] were obtained from Solvent Innovation GmbH (Germany) at a purity of 99 %. The 1-octadecyl-3-methylimidazolium bistriflymide ([Ocdmim][NTf_2]) were from Merck GMbH (Germany), while the N,N,N-trioctylmethylammonium bistriflymide ([Toma][NTf_2]) was prepared as previously described in detail (*8*). Substrates, solvents and other chemicals were purchased from Sigma-Aldrich-Fluka Chemical Co, and were of the highest purity available.

Enzymatic Resolution of *rac*-Ketoprofen in ILs

Four milligrams (15.4 μmol) of rac-ketoprofen and 30 μL (325 μmol) of 1-butanol were added to different screw-capped vials of 1 mL total capacity containing 470 μL of ILs ([Bmim][PF_6], [Omim][PF_6], [Bmim][BF_4], or [Bdmim][PF_6], [Toma][NTf_2] or [Ocdmim][NTf_2]. The reaction was started by adding 5 mg Novozym 435®, and run at 60 °C in an oil bath, shaking for 24 h. At regular time intervals, 20 μl aliquots were taken and suspended in 1 mL of toluene. The biphasic mixture was strongly shaken for 3 min to extract all substrates and product into the toluene phase. Samples were analyzed by HPLC.

Enzymatic Reactions in ILs-$scCO_2$

A high-pressure enzymatic membrane reactor was developed in our laboratory, and was placed in an oven for temperature control (see Figure 2). The system is based in two different stainless-steel circuits for both IL and $scCO_2$ neoteric solvents, which are connected through a polymeric membrane (nylon membrane, 47 mm diameter, 0.45mm pore size), placed into the filtration unit (60-mL total volume) which was also made of stainless-steel. The IL circuit has a reservoir tank and runs in recirculation mode by using an HPLC pump at the entry of the filtration cell and a back-pressure needle valve at the exit to maintain a desired constant pressure into the system. The $scCO_2$ circuit runs in continuous mode by using an ISCO DX100 syringe pump to introduce the CO_2 at the desired pressure, and placing a double needle valve to control the $scCO_2$ flow at the outlet. For operation, one hundred milligrams (385.4 μmol) of *rac*-ketoprofen and 90 μL (964 μmol) of 1-butanol were dissolved in 20 mL [Bmim][PF_6], and then placed in the reservoir tank of IL circuit at 40 °C. Then, the IL recirculation pump was started at a 10 mL/min total flow to fill the circuit with the reaction mixture. The racemic resolution was started by adding Novozym 435® (1 g) to the reservoir tank. The presence of an on-line filter avoids any damage of immobilized enzyme particles in the pump. At the same time, the syringe pump pressurizes the $scCO_2$ circuit and then the double-needle valve placed at the exit was carefully closed by hand reach the desired pressure and $scCO_2$ flow (100 bar, 0.8-1.0 mL/min) are reached. Samples were collected from the $scCO_2$ flow by continuous depressurizing through a heated restrictor (60 °C) for 30-minute steps by bubbling into a test-tube containing toluene (3 mL) placed in an ice bath. Furthermore, at given reaction times, 20 μl aliquots were taken from the IL reservoir tank and suspended in 1 mL of toluene. The resulting biphasic mixture was strongly shaken for 3 min to extract all substrates and products into the toluene phase. All samples were analyzed by HPLC.

Analytical Methods

Analyses were performed with a Shimadzu HPLC instrument equipped with a multi-channel pump (mod LC-20AD) and a DAD detector (260 nm, mod. SPD-M20A), by using a chiral stationary phase column (Chiralpack AD column, 0.46 x 25 cm, Diacel Chemical Industries Ltd.), and hexane:2-propanol:trifluoroacetic acid (80:19.9:0.1 v/v/v) as isocratic mobile phase at 0.8 mL/min total flow. One unit of activity was defined as the amount of enzyme that produces 1 μmol of ketoprofen alkyl ester per min.

The conversion of ketoprofen ester was calculated using the following equations:

$$\mathbf{X\ (\%) = [(C_0\text{-}C_i)/C_0] \times 100} \qquad (1)$$

where X is the overall conversion (%), C_0 the initial amount of racemic ketoprofen (mM), C_i the amount of racemic ketoprofen (mM) at reaction time i.

The enantiomeric excess of substrate (ee_s) and product (ee_p) and the enantiomeric ratio or enantioselectivity (Eval) were calculated using the following equations (*12*):

Downloaded by OHIO STATE UNIV LIBRARIES on June 22, 2012 | http://pubs.acs.org
Publication Date (Web): April 28, 2010 | doi: 10.1021/bk-2010-1038.ch003

$$ee_s\,(\%) = 100 \times ([S]_{acid} - [R]_{acid}) / ([S]_{acid} + [R]_{acid}) \quad (2)$$

$$ee_p\,(\%) = 100 \times ([R]_{ester} - [S]_{ester}) / ([S]_{ester} + [R]_{ester}) \quad (3)$$

$$Eval = \ln[1-(X/100)(1+(ee_p/100))] / \ln[1-(X/100)(1-ee_p/100))] \quad (4)$$

where $[R]_{acid}$ and $[S]_{acid}$ represent the concentration of the *R*- and *S*- enantiomers of ketoprofen acid, while $[R]_{ester}$ and $[S]_{ester}$ represent the concentration of the *R*- and *S*- enantiomers of ketoprofen ester.

Downloaded by OHIO STATE UNIV LIBRARIES on June 22, 2012 | http://pubs.acs.org
Publication Date (Web): April 28, 2010 | doi: 10.1021/bk-2010-1038.ch003

Results and Discussion

CALB-Catalyzed Resolution of *rac*-Ketoprofen in ILs

The catalytic efficiency of Novozym, as commercial CALB immobilized derivative, was tested in several ILs for the resolution of *rac*-ketoprofen by esterification with 1-butanol. Figure 3 shows the time course profiles of conversion of *R*- and *S*-ketoprofen into their respective *R*- and *S*-ketoprofen butyl ester. As can be seen in Figure 3, the enzyme was able to accept both *R*- and *S*- enantiomers as acyl-donor substrates although at different reaction rates: the *R*-substrate was practically consumed after 24 h of reaction, while 30 % of the initial *S*-substrate remained unreacted, resulting in a reaction mixture with a 40 % ee_p.

However, it is noticeable how the enantioselectivity fell during the first hour of the reaction and then remained practically unchanged at a relatively low level (Eval = 5). The preferential esterification of *R*-enantiomer by CALB has also been described by using hexane:1,2-dichloropropane (80:20 v/v) as reaction medium, being obtained Eval values ranged from 2 to 10 (*13*).

Figure 4 shows the influence of different ILs on the esterification reaction rate of Novozym for both *R*- and *S*-ketoprofen with 1-butanol from a racemic mixture at 60 °C. As can be seen, all ILs were suitable reaction media for the proposed biotransformation, although the enzyme shows a moderate enantioselectivity at 24 h (ranged from 4 to 7.8) for the *R*-substrate in all cases.

Several authors have reported the relatively low enantioselectivity (Eval ranged from 5 to 10) displayed by different lipases (*e.g. C. antarctica*, *M. miehei*, *P. cepacia*, etc.) during the enantioselective esterification of ketoprofen in many organic solvents, which can not be greatly improved by reaction medium engineering (*13–15*). The activity level shown by Novozym in $[Bmim][PF_6]$, $[Omim][PF_6]$ and $[Ocdmim][NTf_2]$ was practically the same, while $[Bmim][BF_4]$ and $[Bdmim][PF_6]$ showed the lowest values. It is also noticeable how the highest Eval of the enzyme was obtained for $[Toma][NTf_2]$, although its high viscosity was a clear limitation for further application in a membrane reactor.

Downloaded by OHIO STATE UNIV LIBRARIES on June 22, 2012 | http://pubs.acs.org
Publication Date (Web): April 28, 2010 | doi: 10.1021/bk-2010-1038.ch003

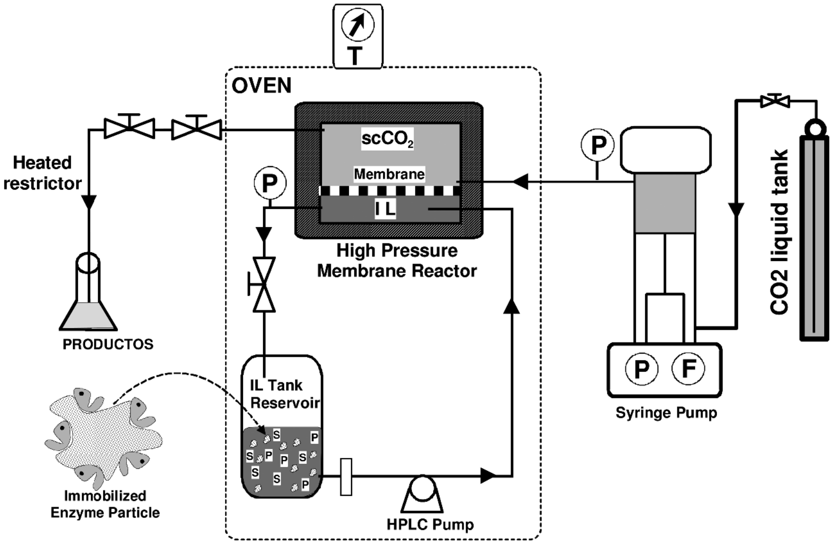
T
OVEN
$scCO_2$
Membrane
I L
P
High Pressure
Membrane Reactor
Heated
restrictor
PRODUCTOS
IL Tank
Reservoir
S
P
Immobilized
Enzyme Particle
HPLC Pump
P
P
F
Syringe Pump
CO2 liquid tank

Figure 2. Experimental set-up of the continuous enzymatic membrane reactor working with IL and $scCO_2$.

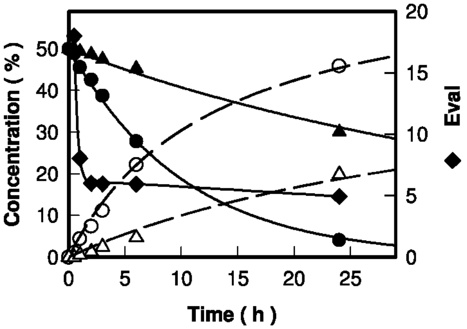

Figure 3. Time-course of (●) R-ketoprofen, (▲) S-ketoprofen, (○) R-ketoprofen butyl ester, (△) S-ketoprofen butyl ester and (◆) Eval for the esterification reaction catalyzed by Novozym in [Omim][PF_6] at 60 °C.

Downloaded by OHIO STATE UNIV LIBRARIES on June 22, 2012 | http://pubs.acs.org
Publication Date (Web): April 28, 2010 | doi: 10.1021/bk-2010-1038.ch003

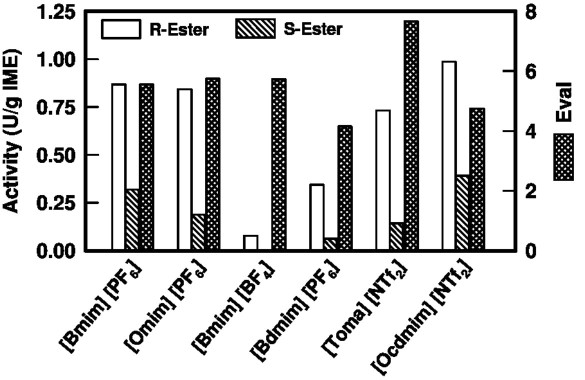

Figure 4. Influence of different ILs on the Novozym-catalyzed esterification of rac-ketoprofen.

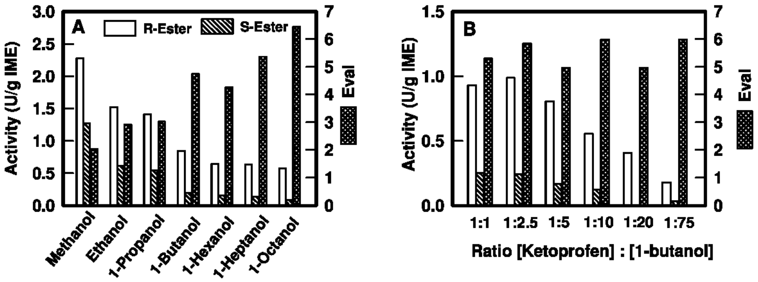

Figure 5. Influence of (A) the alkyl chain length of the alcohol, and (B) the ratio [ketoprofen]:[1-butanol] on the Novozym-catalyzed enantioselective esterification of rac-ketoprofen in [Omim][PF$_6$] at 60 °C.

In order to improve the activity and enantioselectivity displayed by Novozym for the esterification of ketoprofen in ILs, the influence of both the alkyl chain length of the alcohol, and the alcohol/ketoprofen concentration ratio were also studied in [Omim][PF$_6$] at 60 °C (Figure 5). As can be seen in Figure 5A, the esterification rate for both *R*- and *S*-enantiomers was exponentially reduced with the increase in the alkyl chain length of the alcohol, in agreement with results observed by other authors (*13–15*). This behavior also resulted in a concomitant enhancement of the enantioselectivity at 24 h, in agreement with the Eval profile in Figure 3, where the lower conversion level provided the highest Eval value.

Figure 5B shows the influence of the ketoprofen:1-butanol concentration ratio on the enantioselective esterification of ketoprofen catalyzed by Novozym in [Omim][PF$_6$] at 60 °C. As can be seen, the esterification rate of the R-enantiomer shows a bell-shape profile, the best result being obtained at a 1:2.5 [ketoprofen]:[1-butanol] ratio. However, the Eval profile was practically unchanged for all the conditions assayed. Ong *et al* (*13*) reported how the highest conversion was obtained when the molar ratio of 1-butanol to *rac*-ketoprofen was 1:1, and how conversion then fell as alcohol concentration increased, because of its role as inhibitor and/or enzyme deactivating agent.

Enzymatic Membrane Reactor for Resolution of *rac*-Ketoprofen in IL/scCO$_2$

Downloaded by OHIO STATE UNIV LIBRARIES on June 22, 2012 | http://pubs.acs.org
Publication Date (Web): April 28, 2010 | doi: 10.1021/bk-2010-1038.ch003

Membrane systems based on supported ILs have been described as an excellent way of performing selective transport of organic compounds separation of racemic mixtures (*16*). We used the enzymatic membrane reactor depicted in Figure 2 for the enantioselective esterification of ketoprofen catalyzed by Novozym in [Bmim[[PF$_6$] at 40 °C. This process was coupled with a continuous extraction of substrate/products mixture through the nylon membrane with scCO$_2$ at 200 bar and 40 °C. In spite of previous results, the [Omim][PF$_6$] IL can not be used because the HPLC pump was unable to recirculate this IL, as a consequence of its high viscosity (0.682 Pa.s). In the same way, the temperature was reduced from 60 to 40 °C to avoid damage to the pump. The selection of the supercritical pressure was established as a function of the ability of CO$_2$ to extract ketoprofen compounds from [Bmim][[PF$_6$]. Preliminary studies (data not reported) showed that no extraction was observed at 100 bar, being improved the extraction of the ketoprofen esters by the increase in pressure up 200 bar (higher pressures were not assayed because of the safety limits of the reactor).

As can be seen in Figure 6A, the enzyme action that occurred in the IL circuit was able to produce the R-ketoprofen butyl ester at an initial rate three times higher than that observed for the S-ketoprofen ester, in agreement with the result depicted in Figure 3. This fact involves a continuous decay in the ee$_p$ profile from 57 to 25 % during the 24 h of the reaction. The coupling of the IL reaction medium with the scCO$_2$ flow (200 bar, 40 °C) by means of a polymeric membrane allowed the continuous extraction of ketoprofen ester products, as a results of their higher hydrophobicity with respect to ketoprofen. In this context, Figure 6B depicts the time-course profiles for all ketoprofen compounds extracted by the scCO$_2$ from the IL reaction medium. As can be seen, a mixture of ketoprofen butyl esters enriched in the *R*-isomer (ee$_{R\text{-ester}}$ ranged from 100 to 60 %), and free of ketoprofen substrates, was obtained.

The weak enantioselectivity of the enzyme in the IL phase avoid the possibility of obtaining the pure *R*-ester product at the scCO$_2$ exit valve. The use of membranes with supported IL to facilitate the selective transport of hydrophobic compounds (*e.g.* ibuprofen, organic acids) from aqueous phases after enzymatic esterification has been described (*17*, *18*). In all cases, the selectivity of the transport was attributed to both the enzyme efficiency towards the desired product and the solubility of the reaction product in the receiving phase. In the same context, the use of enantioselective membranes based on chiral polymers or achiral polymer containing chiral selectors has been described as an excellent way to perform membrane processes for chiral separations (*19*), and its application in the IL/scCO$_2$ reactor could improves the results obtained.

Downloaded by OHIO STATE UNIV LIBRARIES on June 22, 2012 | http://pubs.acs.org
Publication Date (Web): April 28, 2010 | doi: 10.1021/bk-2010-1038.ch003

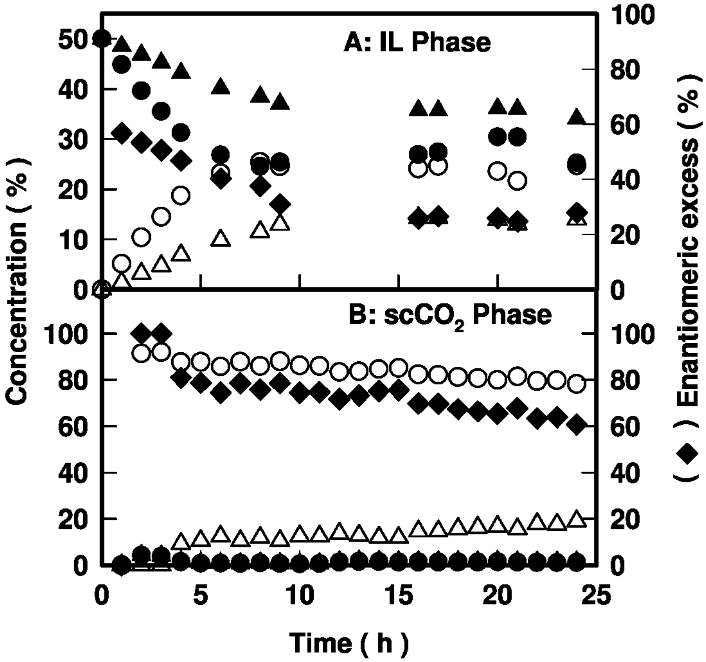

Figure 6. Time-course profiles of (●) R-ketoprofen, (▲) S-ketoprofen, (○) R-ketoprofen butyl ester, (△) S-ketoprofen butyl ester and (◆) ee$_p$ for the esterification reaction catalyzed by Novozym in both the IL tank ([Bmim][PF$_6$]) (A), and at the scCO$_2$ exit of the membrane reactor(B) working at 200 bar and 40 °C.

Conclusions

ILs have been shown to act as excellent reaction media for the immobilized CALB-catalyzed synthesis of ketoprofen esters by esterification with 1-alkanols. Both the activity (ranging from 0.6 to 1 U/g IME) and enantioselectivity (ranging from 4 to 7.8 for the *R*-substrate at 24 h) were practically independent of the nature of the assayed IL. However, other reaction parameters, such as the alkyl chain length of the alcohol and the ketoprofen: alcohol molar ratio, had an strong influence on the reaction rate. An enzymatic membrane reactor, based on [Bmim][PF6] and scCO$_2$ (200 bar, 40 °C) was applied to perform the chiral resolution of *rac*-ketoprofen by esterification with 1-butanol. The scCO$_2$ flow was able to extract continuously the R-ketoprofen butyl ester (ee ranging from 100 to 60 % for 24 h) from the IL reaction medium through a nylon membrane. The limited enantioselectivity shown by the enzyme in the proposed biotransformation was the weak point for reaching the full chiral separation of ketoprofen isomers. The enzymatic membrane reactor developed in this work can be regarded as a simple green chemistry tool to easily carry out the separation of ketoprofen isomers, which are obtained as pure compounds at the depressurization valve. Appropriate selection of the enzyme and/or the membrane will improve results. Another step toward the green chemical industry of the near future has been taken.

Acknowledgments

This work was partially supported by the CICYT (CTQ2005-01571-PPQ), SENECA Foundation (02910/PI/05), and CARM (BIO-BMC 06/01-0002) grants We like to thanks Mr. R. Martínez from Novo España, S.A. the gift of Novozym.

Downloaded by OHIO STATE UNIV LIBRARIES on June 22, 2012 | http://pubs.acs.org
Publication Date (Web): April 28, 2010 | doi: 10.1021/bk-2010-1038.ch003

References

1. Xie, R.; Chu, L. Y.; Deng, J. G. *Chem. Soc. Rev.* **2008**, *37*, 1243–1263.
2. Klibanov, A. M. *Nature* **2001**, *409*, 241–246.
3. Lozano, P.; De Diego, T.; Iborra, J. L. *Chem. Today* **2007**, *25*, 76–79.
4. Hobbs, H. R.; Thomas, N. R. *Chem. Rev.* **2007**, *107*, 2786–2820.
5. Lozano, P.; Avellaneda, A.; Pascual, R.; Iborra, J.L. *Biotechnol. Lett.* **1996**, *18*, 1345–1350.
6. Giessauf, A.; Magor, W.; Steinberger, D. J.; Marr, R. *Enzyme Microb. Technol.* **1999**, *24*, 577–583.
7. van Rantwijk, F.; Sheldon, R. A. *Chem. Rev.* **2007**, *107*, 2757–2785.
8. Lozano, P.; De Diego, T.; Carrié, D.; Vaultier, M.; Iborra, J. L. *Biotechnol. Lett.* **2001**, *23*, 1529–1533.
9. Ulbert, O.; Belafi-Bako, K.; Tonova, K.; Gubicza, L. *Biocatal. Biotransform.* **2005**, *23*, 177–183.
10. De Diego, T.; Lozano, P.; Gmouh, S.; Vaultier, M; Iborra, J. L. *Biomacromolecules* **2005**, *6*, 1457–1464.
11. Lozano, P.; De Diego, T.; Carrié, D.; Vaultier, M.; Iborra, J. L. *Chem. Commun.* **2002**, 692–693.
12. Jin, J. N.; Lee, S. H.; Lee, S. B. *J. Mol. Catal. B: Enzym.* **2003**, *26*, 209–216.
13. Ong, A. L.; Kamaruddin, A. H.; Bhatia, S.; Long, W. S.; Lim, S. T.; Kumari, R. *Enzyme Microb. Technol.* **2006**, *39*, 924–929.
14. Crescenzo, G.; Ducret, A.; Trani, M.; Lortie, R. *J. Mol. Catal B: Enzym.* **2000**, *9*, 49–56.
15. Ong, A. L.; Kamaruddin, A. H.; Bhatia, S. *Process Biochem.* **2005**, *40*, 3526–3535.
16. Afonso, C. A. M.; Crespo, J. G. *Angew Chem., Int. Ed.* **2004**, *43*, 5293–5295.
17. Miyako, E.; Maruyama, T.; Kamiya, N.; Goto, M. *Chem. Commun.* **2003**, 2926–2927.
18. Miyako, E.; Maruyama, T.; Kamiya, N.; Goto, M. *Chem. Eur. J.* **2005**, *11*, 1193–1170.
19. Xie, R.; Chu, L. Y.; Deng, J. G. *Chem. Soc. Rev.* **2008**, *37*, 1243–1263.

Downloaded by PENNSYLVANIA STATE UNIV on June 22, 2012 | http://pubs.acs.org
Publication Date (Web): April 28, 2010 | doi: 10.1021/bk-2010-1038.ch004

Chapter 4

Development of a Universal Method Based on Ionic Liquids for Determination of Enantiomeric Compositions of Pharmaceutical Products

Chieu D. Tran*

Department of Chemistry, Marquette University, P. O. Box 1881,
Milwaukee, Wisconsin 53201-1881
***chieu.tran@marquette.edu**

In this paper we describe the work which exploits unique features of ILs to develop novel spectroscopic methods which otherwise is not possible. Specifically, we have successfully developed a novel, highly sensitive and accurate method for the determination of enantiomeric compositions of chiral compounds with different sizes, shape and functional groups This method is based on the use of a chiral IL which serves both as a solvent and also as a chiral selector.

Ionic liquids (ILs) are a group of organic salts that are liquid at room temperature. They have unique chemical and physical properties, including being air and moisture stable, a high solubility power, and virtually no vapor pressure (*1–9*). Because of these properties, they can serve as a "green" recyclable alternative to the volatile organic compounds that are traditionally used as industrial solvents (*1–9*). The ILs have, in fact, been successfully used in many applications, including replacing traditional organic solvents in (1) organic and inorganic syntheses (*2*), (2) solvent extractions (*10*), (3) liquid-liquid extractions (*11–13*), (4) electrochemical reactions (*14*) and (5) as a medium for enzymatic reaction (*15*).

A large number of scientists from many disciplines have been engaged on study of ILs. However, to date, majority of research on ILs has focused on synthesizing novel ILs with either new anions and/or cations and determining

In Ionic Liquid Applications: Pharmaceuticals, Therapeutics, and Biotechnology; Malhotra, S.;
ACS Symposium Series; American Chemical Society: Washington, DC, 0.

Downloaded by PENNSYLVANIA STATE UNIV on June 22, 2012 | http://pubs.acs.org
Publication Date (Web): April 28, 2010 | doi: 10.1021/bk-2010-1038.ch004

their chemical properties. Because of the efforts, substantial advances have been made, and it has been estimated that the number of novel and task-specific ILs which can be readily synthesized can be as large as 10^6. In spite of availability of a rather large number of newly synthesized ILs, information on their spectroscopic and thermal properties is not widely available. This is rather unfortunate because with their superior spectroscopic and physical properties, the ILs can potentially be used not only as a green but also as superior solvent in term of enhancing sensitivity and selectivity of spectroscopic measurements, as well as high performance fluids for use of a wide range of engineering and materials science applications, such as high pressure and high temperature lubricants. It is probable that laboratory and industrial applications of ILs in spectroscopy, engineering and material processing are limited because of lack of studies and the paucity of data on their spectroscopic and physical properties.

This overview addresses these shortcomings. Specifically, its focus is not on the synthesis of novel ILs or the investigations of their chemical properties but rather on what ILs can uniquely do. Specifically, we will focus on the exploitation of unique properties of ILs to develop novel method which is not possible otherwise.

Chiral analysis is an important subject in science as well as in technology. Enantiomeric forms of many compounds are known to have different physiological and therapeutic effects (*16–19*). Very often, only one form of enantiomeric pair is pharmacologically active (*16–19*). The other or others can reverse or otherwise limit the effect of the desired enantiomer. Recognizing the importance of chiral effects, the FDA in 1992 has issued a mandate requiring pharmaceutical companies to verify the enantiomeric purity of chiral drugs that are produced (*16–19*). It is thus hardy surprising that pharmaceutical industry needs effective methods to determine enantiomeric purity.

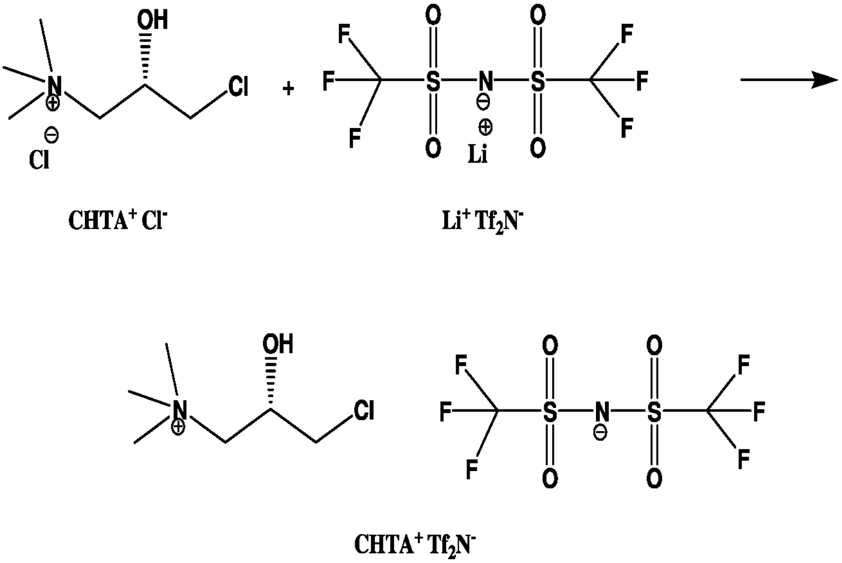

Downloaded by PENNSYLVANIA STATE UNIV on June 22, 2012 | http://pubs.acs.org
Publication Date (Web): April 28, 2010 | doi: 10.1021/bk-2010-1038.ch004

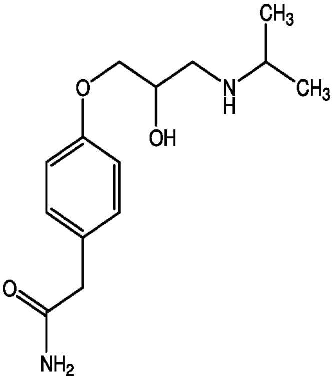

4-[2-hydroxy-3-(1-methylethyl)-amino) propoxy]benzenacetramide or Atenolol

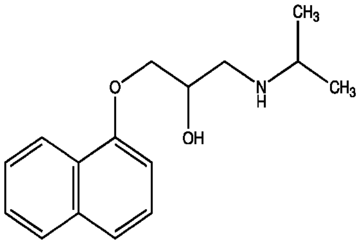

1-(isopropylamino)-3-(1-naphthyloxy)-2-propranolol or Propranolol

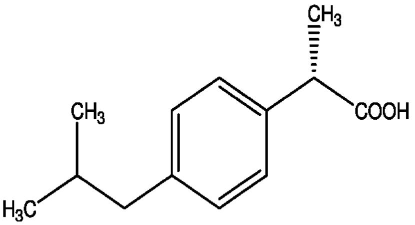

(S)-(+)-2-(4-isobutylphenul)-propionic acid or (S)-Ibuprogen

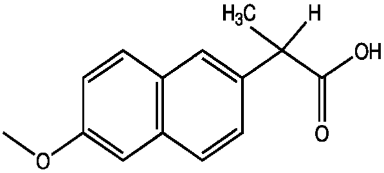

2-(6-methoxy-2-naphthyl) propionic acid or Naproxen

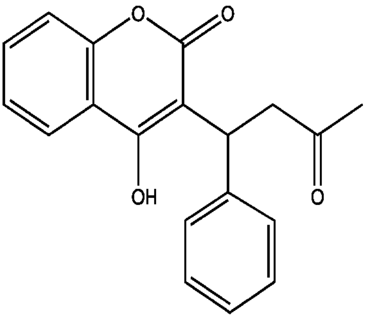

4-hydroxy-3-(3-oxo-1-phenylbutyl)-2-benzopyrone or Warfarin

Scheme 1. Structures of pharmaceutical products analyzed in this study.

Downloaded by PENNSYLVANIA STATE UNIV on June 22, 2012 | http://pubs.acs.org
Publication Date (Web): April 28, 2010 | doi: 10.1021/bk-2010-1038.ch004

Table 1. Compositions of Atenolol Solutions Used for Calibration

sample	*R-atenolol (mole fraction)*	*S-atenolol (mole fraction)*
1	0.30	0.70
2	0.40	0.60
3	0.45	0.55
4	0.50	0.50
5	0.55	0.45
6	0.60	0.40
7	0.65	0.35
8	0.70	0.30
9	0.75	0.25
10	0.85	0.15

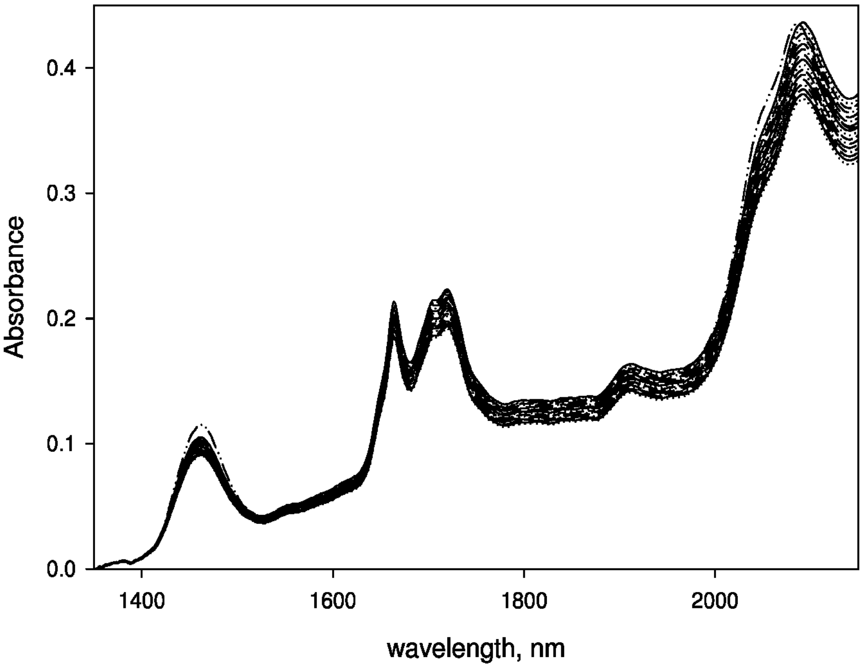

Figure 1. NIR spectra of the pure S-CHTA$^+$ Tf$_2$N$^-$ and of 17 solutions of atenolol with the same total concentration of 60 mM but different enantiomeric compositions.

Downloaded by PENNSYLVANIA STATE UNIV on June 22, 2012 | http://pubs.acs.org
Publication Date (Web): April 28, 2010 | doi: 10.1021/bk-2010-1038.ch004

Methods currently available for the determination of enantiomeric purity are based either on separation (HPLC, GC, CE) or spectroscopy (CD, NMR, MS) (*20–25*). While these methods have proven to be effective, they all have some drawbacks including time consuming, low sensitivity and destructive (*20–25*). More importantly, none of them is truly universal; namely, they cannot be used for all types of compounds. Contrary to the general belief, we have demonstrated recently that it is possible to develop a novel method which is not only universal but also has relatively higher sensitivity and accuracy (*26*, *27*). The method is based on the use of the NIR technique to measure diastereomeric interactions between an added carbohydrate compounds (e.g., α-, β-, γ-cyclodextrin or sucrose) with both enantiomeric forms of an analyte followed by partial least square analysis of the data (*26*, *27*). Compared to other existing methods this method not only has relatively higher sensitivity and accuracy but also is universal (*26*, *27*). Specifically, it can be used to determine enantiomeric compositions of all types of compounds including amino acids and pharmaceutical products (propranolol, atenolol, ibuprofen) with only microgram concentration and enantiomeric excess as low as 1.5% (*26*, *27*). It is noteworthy to add that while this method has proven to be very effective, it still has some limitations such as the need to add a carbohydrate compound (to induce the diastereomeric interactions) and the fact that the analysis must be performed in a solvent which can dissolve both analyte and the carbohydrate compound. Because of the latter requirement (and because of the different solubility of various types of analytes), it may be necessary to perform the analysis in a variety of solvents including water or a mixture of water and organic solvents. As a consequence, a separated calibration curve must be constructed for each set of carbohydrate - analyte in each specific solvent system. This cumbersome and time consuming task somewhat limits the application of the method. It is, therefore, desirable to modify this method by eliminating the added carbohydrate and using only one solvent system for the analysis of all types of compounds. Chiral ionic liquid with its unique properties offers a solution for this problem.

Advances in ILs have made synthesis of chiral ILs a subject of intense study in recent years (*28–43*). The popularity stems from the fact that it is possible to use chiral ILs as chiral solvents for optical resolutions, for asymmetric induction in synthesis and as chiral stationary phase in chromatography (*28–43*). It may also be possible to use chiral IL to replace the solvent as well as the added carbohydrate compound for the enantiomeric purity determination method. Specifically, the chiral IL with its high solubility power, should dissolve many different types of analytes. Its chirality may produce the needed diastereomeric interactions with both enantiomeric forms of an analyte. Unfortunately, in spite of their potentials, chiral ILs are not commercially available. Only a few chiral ILs have been synthesized, and the synthesis of reported chiral ILs required rather expensive reagents and elaborated synthetic schemes (*28–43*). Because of these limitations, in spite of extensive efforts made by various groups, to date, the study and applications of chiral ILs have been severely hindered. Therefore, it is of particular importance to develop a novel synthesis method by which chiral ILs can be simply and easily prepared from commercially available reagents by chemists from various disciplines, not just by those with expertise in synthesis.

Downloaded by PENNSYLVANIA STATE UNIV on June 22, 2012 | http://pubs.acs.org
Publication Date (Web): April 28, 2010 | doi: 10.1021/bk-2010-1038.ch004

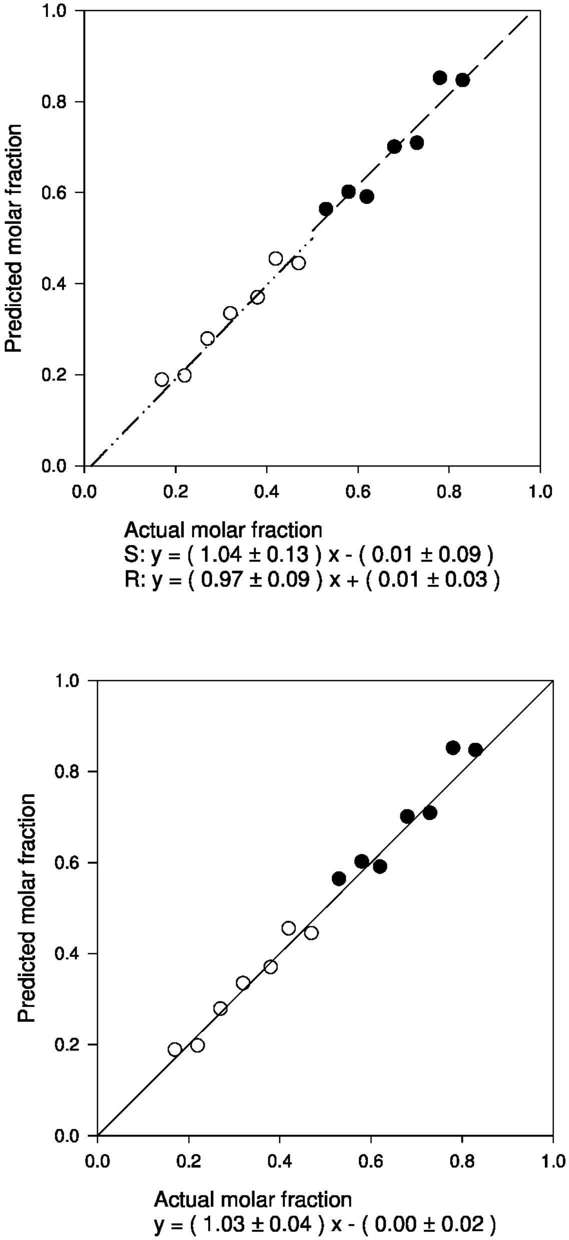

Figure 2. Predicted enantiomeric composition versus actual composition for 60 mM Atenolol in S-CHTA^{+} Tf$_2$N^{-} ionic liquid. Filled circles, S-atenolol; open circles, R-atenolol. ***Top****: Predicted R-atenolol values were plotted separately from S-atenolol;* ***Bottom****: R-atenolol and S-atenolol were plotted together*

Downloaded by PENNSYLVANIA STATE UNIV on June 22, 2012 | http://pubs.acs.org
Publication Date (Web): April 28, 2010 | doi: 10.1021/bk-2010-1038.ch004

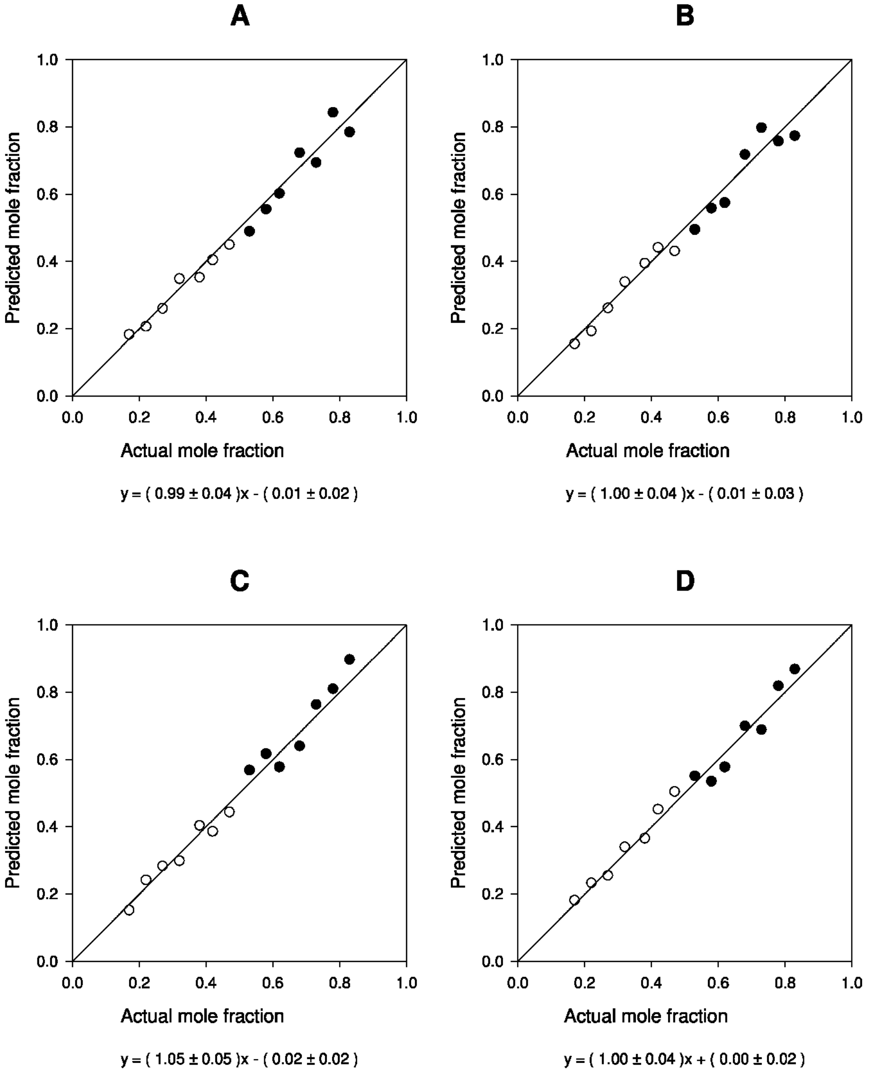

Figure 3. Predicted enantiomeric composition versus actual composition for 60 mM of: (A) ibuprofen; (B) atenolol; (C) phenylalanine and (D) alanine in S-CHTA$^+$ Tf$_2$N$^-$ ionic liquid. Filled circles, S-enantiomers for ibuprofen and propranolol and L-enantiomers for phenylalanine and alanine; Open circles, R-enantiomers for propranolol and D-enantiomers for phenylalanine and alanine

We have demonstrated recently (*43*) that both enantiomeric forms of a novel chiral ionic liquid, R- and S-(3-chloro-2-hydroxypropyl)trimethylammonium Tf2N- ((R)- and S-[CHTA]+ [Tf2N]-) can be readily synthesized in enantiomerically pure form by a simple ion exchange reaction from corresponding (R)- and (S)-chloro-2-hydroxypropyl)trimethylammonium chloride salts which are commercially available (Scheme 1) (*43*).

Downloaded by PENNSYLVANIA STATE UNIV on June 22, 2012 | http://pubs.acs.org
Publication Date (Web): April 28, 2010 | doi: 10.1021/bk-2010-1038.ch004

Table 2. Actual and Calculated Enantiomeric Excess of Solution of 10 mM Atenolol in (S) $CHTA_+$ Tf_2N^- Ionic Liquid

sample	*R-atenolol (mole fraction)*	*S-atenolol (mole fraction)*	*actual ee (%)*[a]	*calculated ee (%)*[a]	*relative error (%)*[b]
1	0.050	0.950	-90.00	-82.17	8.70
2	0.150	0.850	-70.00	-72.95	4.21
3	0.300	0.700	-40.00	-39.34	1.65
4	0.365	0.350	-27.00	-27.69	2.55
5	0.480	0.520	-4.00	-4.25	6.25
6	0.496	0.504	-0.80	-0.74	7.50
7	0.503	0.497	0.60	0.58	3.33
8	0.510	0.490	2.00	2.10	5.00
9	0.800	0.200	60.00	61.86	3.10
10	0.985	0.015	97.00	101.06	4.19

[a] Defined as ee (%) = [(R-atenolol – S-atenolol)/(R-atenolol + S-atenolol)] X 100. [b] Defined as relative error = [(actual value – calculated value) / (actual value)] 100.

Table 3. Actual and Calculated Enantiomeric Excess (ee) of Solution of 10 µM of Propranolol in S-$CHTA^+$ Tf_2N^- Ionic Liquid

sample	*R-propranolol (mole fraction)*	*S-propranolol (mole fraction)*	*actual ee (%)*[a]	*calculated ee (%)*[a]	*relative error (%)*[b]
1	0.0500	0.9500	-90.00	94.19	4.66
2	0.2500	0.7500	-50.00	47.85	4.31
3	0.4400	0.5600	-12.00	12.77	6.42
4	0.5015	0.4985	0.30	0.32	5.88
5	0.5030	0.4970	0.60	0.64	7.13
6	0.5100	0.4900	2.00	2.14	7.09
7	0.5350	0.4650	7.00	6.37	8.94
8	0.7250	0.2750	45.00	47.95	6.56
9	0.9000	0.1000	80.00	75.30	5.87
10	0.9850	0.0150	97.00	93.18	3.94

[a] Defined as ee (%) = [(R-propranolol – S-propranolol)/(R-propranolol + S-propranolol)] X 100. [b] Defined as relative error = (actual value – calculated value) X 100.

Downloaded by PENNSYLVANIA STATE UNIV on June 22, 2012 | http://pubs.acs.org
Publication Date (Web): April 28, 2010 | doi: 10.1021/bk-2010-1038.ch004

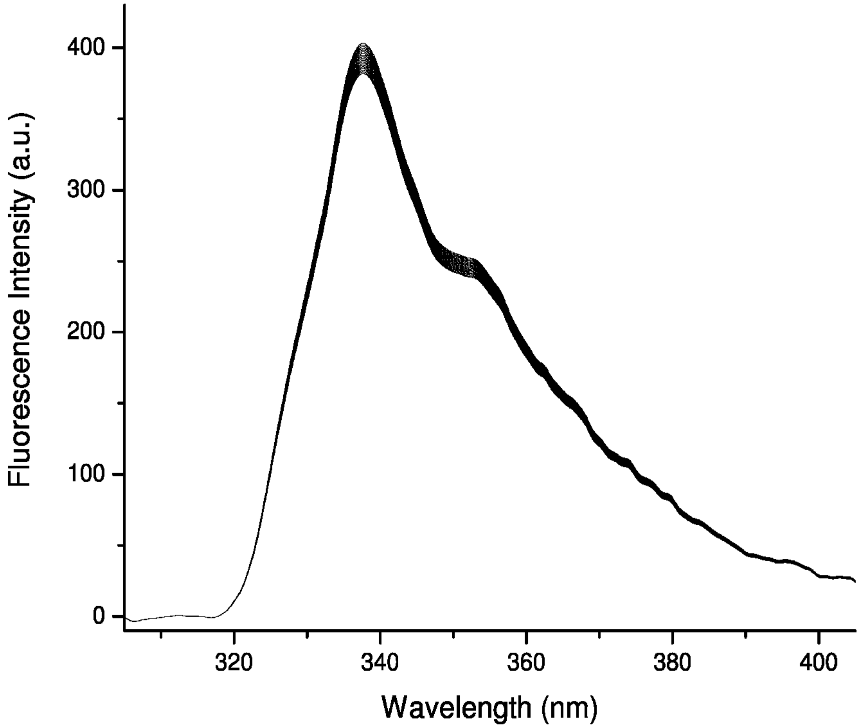

Figure 4. Fluorescence spectra of 22 solutions of propranolol in S-CHTA with total concentration of 10 µM but different enantiomeric compositions. Each spectrum was an average of 20 spectra taken with 280 nm excitation wavelength.

(R)- and S-[CHTA]+ [Tf2N]- are liquid at room temperature, and results from differential scanning calorimetric (DSC) measurements indicate that they have glass transition temperature of –58.4°C. Thermal gravimetric analysis (TGA) results show that this chiral IL has high thermal stability, namely it remains stable at 300°C and loses only 1% of its weight at 326 °C38. Even at temperature as high as 437 °C, it still retains 50% of its mass. More important are the results of ^{19}F NMR study of the interactions between optically active S- CHTA+ Tf2N- ionic liquid and racemic Mosher's salt. It seems that chiral S- CHTA+ Tf2N- readily differentiates R-Mosher salt from S-Mosher's salt, and this disastereomeric interaction resulted in the shift of the Mosher's salt fluorine signal. The difference in the chemical shifts was found to be 24.6 Hz (*43*). These results clearly indicate that optically active R- and S- CHTA+ Tf2N- ionic liquid do exhibit relatively strong enantiomeric recognition and that their chiral recognition is relatively stronger than those for other reported chiral ILs (*29*, *30*). Taken together, the combined high solubility power and enantiomeric recognition ability of the IL clearly indicate that it is possible to use this chiral IL to solubilize an analyte and to induce diastereomeric interactions for the determination of enantiomeric purity.

Downloaded by PENNSYLVANIA STATE UNIV on June 22, 2012 | http://pubs.acs.org
Publication Date (Web): April 28, 2010 | doi: 10.1021/bk-2010-1038.ch004

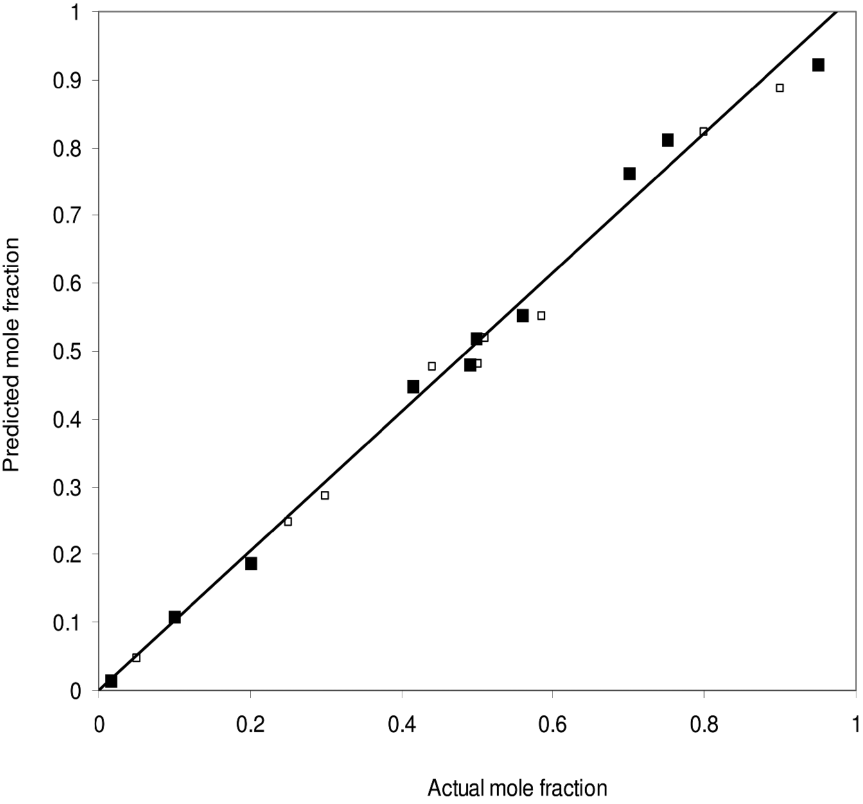

Figure 5. Predicted enantiomeric composition versus actual composition for 10 µM of propranolol in (S)-CHTA$^+$ Tf$_2$N$^-$ ionic liquid. Filled circles, (S)-propranolol; open circles, (R)-propranolol.

Initially, atenolol, a beta blocker drug, was used to evaluate chiral recognition of S-CHTA+ Tf$_2$N$^-$- ionic liquid. Ten solutions of atenolol in S- CHTA+ Tf$_2$N$^-$ ionic liquid having the same total concentration of 60 mM with relatively different enantiomeric compositions (see Table 1for their enantiomeric compositions) were prepared, and their NIR spectra were taken. If the chiral ionic liquid has enantiomeric recognition toward R- and S-atenolol, the distereomeric interactions will lead to changes in the NIR spectra. Figure 1 shows eighteen NIR spectra: a spectrum of the pure S-CHTA+ Tf2N-, spectra of the ten standard solutions of atenolol and spectra of seven solutions of atenolol whose compositions are to be calculated. It is evident from the figure that adding atenolol to the S-CHTA+ Tf2N- solution leads to changes in the spectra. Of interest are the differences among the spectra of atenolol solutions. Since these atenolol solutions have the same total concentration (60 mM) but different enantiomeric compositions, the observed differences clearly indicate that, similar to cyclodextrins and sucrose (*26*, *27*), the chiral S-CHTA+ Tf2N- ionic liquid can differentiate R-atenolol from S-atenolol, and, as expected, the diastereomeric interactions lead to changes

Downloaded by PENNSYLVANIA STATE UNIV on June 22, 2012 | http://pubs.acs.org
Publication Date (Web): April 28, 2010 | doi: 10.1021/bk-2010-1038.ch004

in the NIR spectra. Similar to the procedures used in our previous studies (*26*, *27*, *44–47*), multivariate method of analysis (i.e., partial least squares method (PLS)) was used to develop calibration models for subsequent determination of enantiomeric purity of unknown samples. Results from the PLS cross-validation show that calibration for 10 models require a relatively small number of factors for optimal performance (12 for R- atenolol and 9 for S-atenolol). The root mean standard error of prediction (RMSEP) values are 0.122 and 0.109 for R- and S-atenolol, while the standard error of prediction (SEP) values are 0.120 and 0.110 for R- and S-atenolol, respectively.

To evaluate the effectiveness of this method, seven samples of atenolol with the same total concentration of 60 mM but different enantiomeric compositions were prepared, and the concentrations of R- and S-atenolol in each sample were calculated using the calibration models developed above. Results obtained are shown in Figure 2A and B, where the calculated concentrations of R- and S-atenolol in seven samples were plotted against actual concentrations. To illustrate the accuracy of the method, calculated concentrations of R-atenolol (in seven samples) were plotted separately from those of S-atenolol (of the same sample) (Fig 2A). As expected, the calculated concentrations for both R-and S-atenolol are linearly related to actual concentrations. Furthermore, the linear relationship obtained for R-atenolol (y = (0.97±0.09)x + (0.01±0.03)) is, within experimental error, the same as that for S-atenolol (y = (1.04±0.13)x + (0.01±0.09)). In fact, both concentrations of R- and S-propranolol fit well into a single equation with y = (1.03±0.04)x + (0.00±0.02) with correlation coefficient of 0.99999 (Fig 2B).

Table 4. Actual and Calculated Enantiomeric Excess (ee) of Solution of 10 μM of Naproxen in S-CHTA$^+$ Tf$_2$N$^-$ Ionic Liquid

sample	*R-naproxen (mole fraction)*	*S-naproxen (mole fraction)*	*actual ee (%)*[a]	*calculated ee (%)*[a]	*relative error (%)*[b]
1	0.0500	0.9500	-90.00	-94.05	4.5
2	0.2500	0.7500	-50.00	-51.70	3.4
3	0.3000	0.7000	-40.00	-42.04	5.1
4	0.4400	0.5600	-12.00	-12.48	4.0
5	0.5015	0.4985	0.30	0.29	3.9
6	0.5100	0.4900	2.00	2.09	4.3
7	0.5850	0.4150	17.00	15.98	6.0
8	0.8000	0.2000	60.00	56.94	5.1
9	0.9000	0.1000	80.00	82.96	3.7
10	0.9850	0.0150	97.00	91.57	5.6

[a] Defined as ee (%) = [(R-naproxen – S-naproxen)/(R-naproxen + S-naproxen)] X 100. [b] Defined as relative error = (actual value – calculated value) X 100.

Downloaded by PENNSYLVANIA STATE UNIV on June 22, 2012 | http://pubs.acs.org
Publication Date (Web): April 28, 2010 | doi: 10.1021/bk-2010-1038.ch004

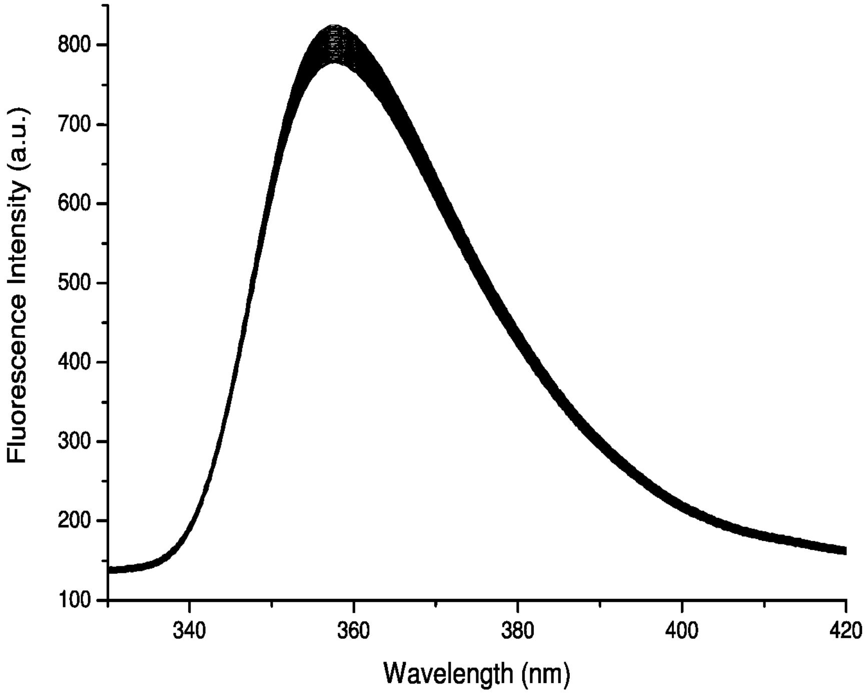

Figure 6. Fluorescence spectra of 22 solutions of naproxen in S-CHTA with total concentration of 10 μM but different enantiomeric compositions. Each spectrum was an average of 20 spectra taken with 280 nm excitation wavelength.

It is expected that the method is not specific to atenolol but is effective for other compounds as well. This possibility was investigated by studying its effectiveness on other types of compounds including two drugs (ibuprofen and propranolol) and two amino acids (alanine and phenylalanine). Figure 3A-D show the results obtained where the calculated concentrations are plotted against actual concentrations. As illustrated, enantiomeric compositions for ibuprofen, propranolol, alanine and phenylalanine can be accurately determined by this method. It is important to add that the three pharmaceutical products studied here (atenolol, ibuprofen and propranolol) are different not only on their structures but also on their sizes, shapes and solubility as well (see Scheme 1 for their structures). Specifically, propranolol is probably the largest among them as it has a naphthalene ring. Atenolol and ibuprofen both have a phenol ring but ibuprofen is relatively smaller than atenolol. Except ibuprofen, other two drugs are soluble in water. The solubility of ibuprofen in water is so poor that in our previous work (with cyclodextrins and sucrose as chiral selector12), instead of water we had to use a mixture of 30:70 ethanol:water mixture. It was not necessary to change the solvent in this case because CHTA+ Tf2N- ionic liquid has so high solubility power that it dissolves ibuprofen as well as it does for propranolol and atenolol.

It is expected that similar to method reported previously based on the use of cyclodextrins and sucrose (*23*, *24*), the present method should have high sensitivity. Its sensitivity can be evaluated from two values: the lowest enantiomeric excess (EE % which is defined as EE% = [(R-enantiomer – S-enantiomer)/(R-enantiomer + S-enantiomer)]) that can be determined at the lowest concentration of a sample. It should be noted that these two terms are interdependent to each other, namely, the limit of detection (LOD) on ee% can be improved by increasing sample concentration or vice versa. In an attempt to estimate the sensitivity of the method, we performed measurements on 10 samples of 10.0 mM or 2.66 mg/mL of atenolol with different ee%'s in S- CHTA+ Tf2N-. Results obtained are listed in Table 2 . It is evident from the table that the method is not only effective but also very sensitive. It can accurately determine samples with concentration as low as micrograms having ee value as high as –90.00% (or +97.00%) and as low as 0.6%. Furthermore, even at ee as low as 0.6%, the relative error was only 3.33%.

It is noteworthy to add that the enantiomeric composition determination method based on chiral IL is not specific to near-infrared spectroscopic technique but is rather general as it can be used with other spectroscopic techniques as well. It may be possible to use fluorescence rather than the NIR as the detection for the enantiomeric determination of drugs which are fluorescent. Since propranolol is known to be fluorescent, this possibility was investigated by preparing ten solutions of propranolol in S-CHTA$^+$ Tf$_2$N$^-$ ionic liquid having the same total concentration of 10 μM with relatively different enantiomeric compositions, and their fluorescence spectra were measured (Fig 4). It is evident from the spectra that adding propranolol to the S-CHTA$^+$ Tf$_2$N$^-$ solution leads to changes in the spectra. Since these propranolol solutions have the same total concentration (10 μM) but different enantiomeric compositions, the observed differences clearly indicate that the chiral S-CHTA$^+$ Tf$_2$N$^-$ ionic liquid can differentiate R-propranolol from S-propranolol, and, as expected, the diastereomeric interactions lead to changes in the fluorescence spectra. Similar to the procedures used in the NIR based method described above (*11*, *12*), PLS method was used to develop calibration models for subsequent determination of enantiomeric purity of unknown samples. Results from the PLS cross-validation show that calibration for 10 models require a relatively small number of factors for optimal performance (10 for R-propranolol and 6 for S-propranolol). The root mean standard error of prediction (RMSEP) values are 0.097 and 0.096 for R- and S-propranolol, while the standard error of prediction (SEP) values are 0.094 and 0.092 for R- and S-propranolol, respectively.

To evaluate the effectiveness of this method, twelve samples of propranolol with the same total concentration of 10 μM but different enantiomeric compositions were prepared, and the concentrations of R- and S-propranolol in each sample were calculated using the calibration models. Results obtained are shown in Figure 5, where the calculated concentrations of R- and S-propranolol in seven samples were plotted against actual concentrations. To illustrate the accuracy of the method, calculated concentrations of R-propranolol (in seven samples) were plotted separately from those of S-propranolol (of the same sample) (Figure 5). As expected, the calculated concentrations for both R-and S-propranolol are linearly related to actual concentrations. Furthermore, the linear relationship obtained for R-propranolol (y = (1.02±0.04)x + (0.00±0.02))

Downloaded by PENNSYLVANIA STATE UNIV on June 22, 2012 | http://pubs.acs.org
Publication Date (Web): April 28, 2010 | doi: 10.1021/bk-2010-1038.ch004

Downloaded by PENNSYLVANIA STATE UNIV on June 22, 2012 | http://pubs.acs.org
Publication Date (Web): April 28, 2010 | doi: 10.1021/bk-2010-1038.ch004

is, within experimental error, the same as that for S-propranolol (y = (1.06±0.04)x + (0.02±0.02)). In fact, both concentrations of R- and S-propranolol fit well into a single equation with y = (1.04±0.03)x + (0.01±0.01) with correlation coefficient of 0.99999.

The chiral recognition ability of S-CHTA$^+$ Tf$_2$N$^-$ was found not to be specific to propranolol but also is effective to other fluorescent chiral compounds as well. Shown in Figure 6 and 7 are spectra of 22 solutions of naproxen with the same total concentration of 10 μM and different enentiomeric compositions (Fig 6) and of 22 solutions of 10 μM warfarin with different enantiomeric compositions (Fig 7). As in the case of propranolol, the chiral IL S-CHTA$^+$ Tf$_2$N$^-$ exhibits chiral recognition toward R- and S-naproxen, and R-and S-warfarin, and the diastereomeric interactions lead to changes in the fluorescence spectra of these solutions. These chiral discriminations can, therefore, be used to determine enantiomeric compositions of naproxen and warfarin. Shown in figure 8A and 8B are plots of calculated versus actual concentrations of R and S-naproxen (8A) and R- and S-warfarin (8B). As illustrated, the calculated concentrations for all ten solutions of naproxen and 15 solutions of warfarin agree well with actual concentrations.

Table 5. Actual and Calculated Enantiomeric Excess (ee) of solution of 10 μM of warfarin in S-CHTA$^+$ Tf$_2$N$^-$ ionic liquid

sample	*R-warfarin (mole fraction*	*S-warfarin (mole fraction)*	*actual ee (%)*[a]	*calculated ee (%)*[a]	*relative error (%)*[b]
1	0.0500	0.9500	-90.00	-94.48	4.98
2	0.2500	0.7500	-50.00	-46.52	6.97
3	0.3000	0.7000	-40.00	-37.74	5.65
4	0.4800	0.5200	-4.00	-3.66	8.48
5	0.5015	0.4985	0.30	0.32	6.79
6	0.5100	0.4900	2.00	2.12	6.06
7	0.5850	0.4150	17.00	16.03	5.70
8	0.7250	0.2750	45.00	41.64	7.46
9	0.9000	0.1000	80.00	75.60	5.12
10	0.9850	0.0150	97.00	92.17	4.98

[a] Defined as ee (%) = [(R-warfarin – S-warfarin)/(R-warfarin + S-warfarin)] X 100. [b] Defined as relative error = (actual value – calculated value) X 100.

Downloaded by PENNSYLVANIA STATE UNIV on June 22, 2012 | http://pubs.acs.org
Publication Date (Web): April 28, 2010 | doi: 10.1021/bk-2010-1038.ch004

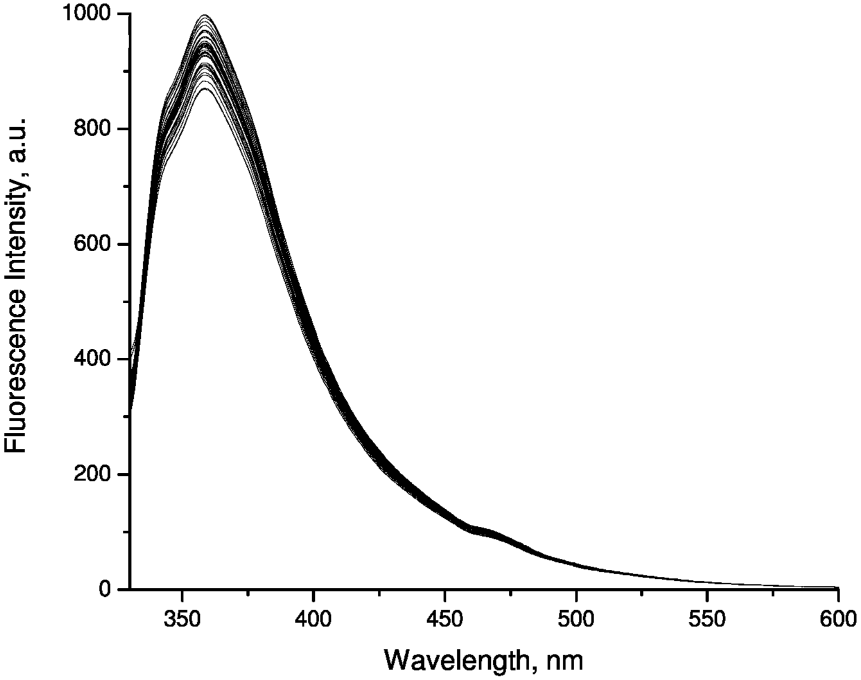

Figure 7. Fluorescence spectra of 22 solutions of warfarin in S-CHTA with total concentration of 10 μM but different enantiomeric compositions. Each spectrum was an average of 20 spectra taken with 320 nm excitation wavelength.

It is expected that method should have high sensitivity. Its sensitivity can be evaluated from three values: the lowest ee% (as described above for NIR based method) and the lowest % enantiomeric impurity (ei% is defined as ei% =([minor enantiomer]/[both enantiomer]) 100) that can be determined at the lowest concentration of a sample. It should be noted that both ee% and ei% values are dependent on the sample concentration, namely, the limits of detection (LOD) on ee% and ei% can be improved by increasing sample concentration or vice versa. Results for propranolol, naproxen and warfarin are listed in Table 3, 4 and 5. It is evident from the table that the method is very sensitive for all three drugs. It can accurately determine samples with concentration as low as micrograms having ee value as high as 99.90% and as low as 0.30%. Furthermore, even at ee as low as 0.30%, the relative error was only 5.88% (for propranolo), 3.90% for naproxen and 6.79% for warfarin. Table 6A and 6B list ei% values for warfarin. As listed, even at concentration as low as 10 μm, this method is capable of detecting 0.60 % of S-warfarin impurity in the presence of 99.40 of R-warfarin. More importantly, even at this low ei% level, the relative error was only 5.98%. Much lower ei% can, in fact, be determined by this method (e.g., 0.08%) but at relatively higher error (12.05%).

Downloaded by PENNSYLVANIA STATE UNIV on June 22, 2012 | http://pubs.acs.org
Publication Date (Web): April 28, 2010 | doi: 10.1021/bk-2010-1038.ch004

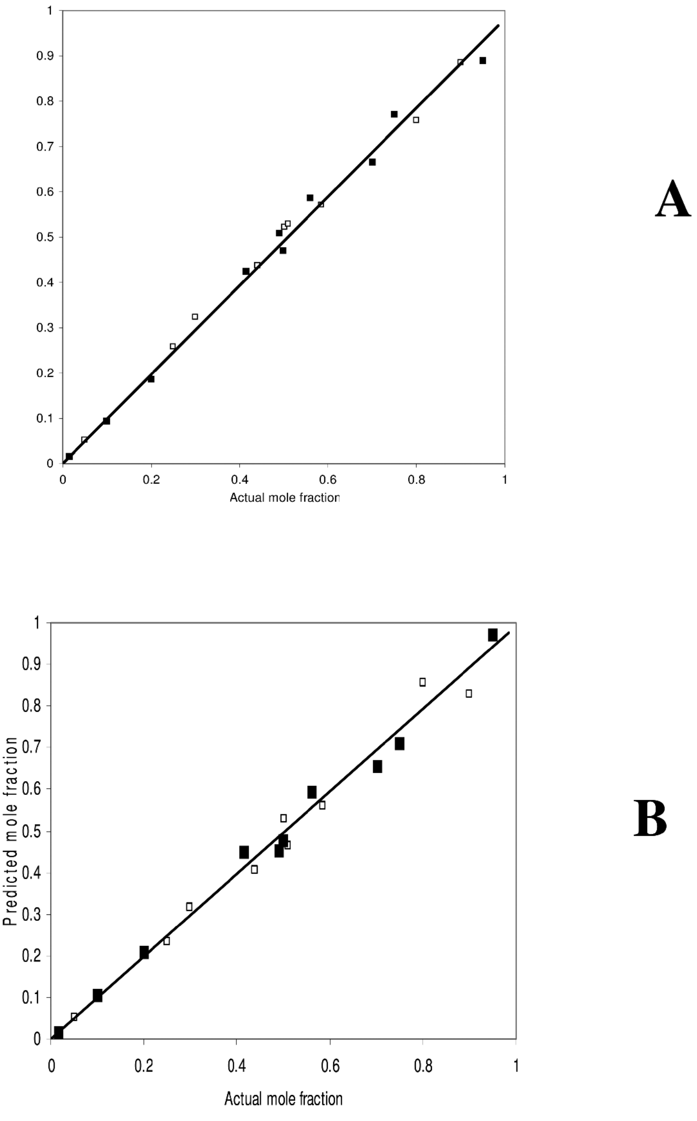

Figure 8. Predicted enantiomeric composition versus actual composition for 10 µM of (A) naproxen and (B) warfarin in (S)-CHTA$^+$ Tf$_2$N$^-$ ionic liquid. Filled circles, S enantiomers; open circles, R enantiomers.

Table 6A. Actual and Calculated Relative Concentration of S-warfarin and in 5 solutions of 10 μM warfarin in S-CHTA$^+$ Tf$_2$N$^-$

S-Warfarin (actual mole fraction)	*S-Warfarin (calculated mole fraction)*	*relative error (%)*
0.0010	0.0008	12.05
0.0060	0.0064	5.98
0.0080	0.0087	8.84
0.0100	0.0093	7.14
0.0200	0.018	7.76
0.0500	0.053	5.48
0.2500	0.235	6.12
0.3000	0.315	4.97
0.4400	0.404	8.17
0.5015	0.529	5.54
0.5100	0.464	9.06
0.5850	0.561	4.09
0.8000	0.854	6.78
0.9000	0.829	7.89
0.9850	1.021	3.62

Collectively, the results presented clearly demonstrate that a novel chiral ionic liquid S-[CHTA]$^+$ [Tf$_2$N]$^-$ exhibits high solubility power and strong enantiomeric recognition. Because of these features, it is possible to use this chiral IL to solubilize an analyte and to induce diastereomeric interactions for the determination of enantiomeric purity. We have, in fact, successfully developed a new method based on either the NIR or the fluorescence technique with this chiral IL where the IL serves both as a solvent and also as a chiral selector for the determination of enantiomeric purity. Enantiomeric compositions of a variety of drugs including propranolol, naproxen and warfarin, can be sensitivily (microgram concentration) and accurately (enantiomeric excess as low as 0.30 % and enantiomeric impurity as low as 0.08%) determined by use of this method. As stated in the previous paragraph, both ee% and ei% values are dependent on the sample concentration, namely the ee% and the ei% (and their associated errors) can be improved by increasing sample concentration and *vice versa*. To our knowledge, the method reported here has the highest sensitivity (sample concentrations in the μM or μg range) and highest accuracy (ee% as high as 97% and as low as 0.30% and ei% as low as 0.08%). To date, other reported methods based on a variety of techniques including HPLC, GC, FTIR, MS, NMR, have either lower sensitivity and/or lower accuracy (*24*, *25*, *48–53*). For example, all of these methods can only detect samples in the millimolar concentration range which is about 1000 times higher than the LOD values obtained with the methods

Downloaded by PENNSYLVANIA STATE UNIV on June 22, 2012 | http://pubs.acs.org
Publication Date (Web): April 28, 2010 | doi: 10.1021/bk-2010-1038.ch004

reported here (*24*, *25*, *48–53*). Furthermore, even at these high LOD's, the lowest ee% and ei% values that these method can determine are in the 1% and 0.1% range, respectively, but with associated error as high as 5% (*24*, *25*, *48–53*). Even at concentration as low as micrograms level, the ee% and ei% values obtained by the methods reported here for all the drugs are much lower than all other reported methods. More importantly, because in this method, the chiral IL serves both as solvent and chiral selector, it is not necessary to add either a chiral selector or chiral column to perform the analysis. Relatively fewer and simpler calibration models are needed. As a consequence, the method will have wider applications and universal utility as it can be used for the analysis of all type of compounds with relatively shorter analysis time and easier procedure. The three drugs used in this study were selected because they are commercially available in both enantiomeric forms. It does not mean that the method reported here is limited to these three drugs. In fact, the method is rather general as we have recently used this method for the ee and ei determination of other compounds including tryptophan and dansyl-amino acids which absorb and emit in relatively different spectral region. Experiments are now in progress in our laboratory to extend the use of this method for the ee and ei determination of multicomponent pharmaceutical compounds.

Downloaded by PENNSYLVANIA STATE UNIV on June 22, 2012 | http://pubs.acs.org
Publication Date (Web): April 28, 2010 | doi: 10.1021/bk-2010-1038.ch004

Table 6B. Actual and Calculated Relative Concentration of R-warfarin and in 5 solutions of 10 μM warfarin in S-CHTA$^+$ Tf$_2$N$^-$

R-warfarin (actual mole fraction)	*R-warfarin (calculated mole fraction)*	*relative error (%)*
0.9990	0.868	13.08
0.9940	1.104	11.05
0.9920	0.934	5.84
0.9900	1.069	8.07
0.9800	0.919	6.22
0.9500	0.971	2.19
0.7500	0.712	5.04
0.7000	0.655	6.48
0.5600	0.596	6.50
0.4985	0.477	4.22
0.4900	0.452	7.81
0.4150	0.451	8.64
0.200	0.208	4.14

Continued on next page.

Table 6B. (Continued). Actual and Calculated Relative Concentration of R-warfarin and in 5 solutions of 10 μM warfarin in S-CHTA$^+$ Tf$_2$N$^-$

R-warfarin (actual mole fraction)	*R-warfarin (calculated mole fraction)*	*relative error (%)*
0.1000	0.108	7.98
0.0150	0.016	6.67

Acknowledgments

The author wishes to thank his present and former coworkers and collaborators whose work is cited in the references.

References

1. Welton, T. *Chem. Rev.* **1999**, *99*, 2071–2083.
2. *Ionic Liquids in Synthesis*; Wasserscheid, P., Welton, T. Eds.; Wiley-VCH: Weinheim, Germany, 2003.
3. Tran, C. D.; Lacerda, S. H. P. *Anal. Chem.* **2002**, *74*, 5337–5341.
4. Tran, C. D.; Lacerda, S. H. P.; Oliveira, D. *Appl. Spectrosc.* **2003**, *57*, 152–157.
5. Mele, A.; Tran, C. D.; Lacerda, S. H. P. *Angew. Chem., Int. Ed.* **2003**, *42*, 4364–4366.
6. Frez, C.; Diebold, G. J.; Tran, C. D.; Yu, S. *J. Chem. Eng. Data* **2006**, *51*, 1250–1255.
7. Tran, C. D.; Challa, S.; Franko, M. *Anal. Chem.* **2005**, *77*, 7442–2447.
8. Tran, C. D.; Challa, S. *Analyst* **2008**, *132*, 455–464.
9. Tran, C. D.; Mejac, I. *J. Chromatogr., A.* **2008**, *1204*, 204–209.
10. Dietz, M. L.; Dzielawa, J. A. *Chem. Commun.* **2001**, 2124–2125.
11. Blanchard, L. A.; Brennecke, J. F. *Ind. Eng. Chem. Res.* **2001**, *40*, 287–292.
12. Kazarian, S. G.; Briscoe, B. J.; Welton, T. *Chem. Commun.* **2000**, 2047–2048.
13. Compton, D. L.; Laszlo, J. A. *J. Electroanal. Chem.* **2002**, *520*, 71–78.
14. Quinn, B. M.; Ding, Z.; Moulton, R.; Bard, A. J. *Langmuir* **2002**, *18*, 1734–1742.
15. Laszlo, J. A.; Compton, D. L. *Biotech. Bioeng.* **2001**, *75*, 181–186.
16. *Chem. Eng. News*, **1990**, *68* (19), 38−44; **1992**, *70* (28) 46−79; **2001**, *79*, 45−56, 79−97.
17. Armstrong, D. W.; Han, S. H. *CRC Crit. Rev. Anal. Chem.* **1988**, *19*, 175.
18. Hinze, W. H. *Sep. Purif. Methods* **1981**, *10*, 159.
19. Armstrong, D. W. *Anal. Chem.* **1987**, *59*, 84A.
20. Hinze, W. L.; Armstrong, D. W. *Ordered Media in Chemical Separations*; American Chemical Society: Washington, DC, 1987.
21. Tran, C. D.; Dotlich, M. *J. Chem. Ed.* **1995**, *72*, 71–73.

Downloaded by PENNSYLVANIA STATE UNIV on June 22, 2012 | http://pubs.acs.org
Publication Date (Web): April 28, 2010 | doi: 10.1021/bk-2010-1038.ch004

22. Tran, C. D.; Kang, J. *J. Chromatogr, A* **2002**, *978*, 221–230.
23. Tran, C. D.; Kang, J. *Chromatographia* **2003**, *57*, 81–86.
24. Tao, W. A.; Cooks, R. G. *Anal. Chem.* **2003**, *75*, 25A–31A.
25. Rothchild, R. *Enantiomer* **2000**, *5*, 457–471.
26. Tran, C. D.; Grishko, V. I.; Oliveira, D. *Anal. Chem.* **2003**, *75*, 6455–6462.
27. Tran, C. D.; Oliveira, D.; Grishko, V. I. *Anal. Biochem.* **2004**, *325*, 206–214.
28. Earle, M. J.; McCormac, P. B.; Seddon, K. R. *Green Chem.* **1999**, *1*, 23–28.
29. Wasserscheid, P.; Bosmann, A.; Bolm, C. *Chem. Commun.* **2002**, 200–201.
30. Levillain, J.; Dubant, G.; Abrunhosa, I.; Gulea, M.; Gaumont, A. C. *Chem. Commun.* **2003**, 2914–2915.
31. Fukumoto, K.; Yoshizawa, M.; Ohno, H. J. *J. Am. Chem. Soc.* **2005**, *127*, 2398–2399.
32. Ding, J.; Desikan, V.; Han, X.; Xiao, T. L.; Ding, R.; Jenks, W. S.; Armstrong, D. W. *Org. Lett.* **2005**, *7*, 335–337.
33. Ding, J.; Welton, T.; Armstrong, D. W. *Anal. Chem.* **2004**, 6819–6822.
34. Baudequin, C.; Baudoux, J.; Levillain, J.; Cahard, D.; Gaumont, A.; Plaquevent, J. *Tetrahedron: Asymmetry* **2003**, *14*, 3081.
35. Bao, W.; Wang, Z.; Li, Y. *J. Org. Chem.* **2003**, *68*, 591.
36. Ishida, Y.; Miyauchi, H.; Saigo, K. *Chem. Commun.* **2002**, 2240.
37. Vo-Thanh, G.; Pegot, B.; Loupy, A. *Eur. J. Org. Chem.* **2004**, *5*, 1112.
38. Pegot, B.; Vo-Thanh, G.; Gori, D.; Loupy, A. *Tetrahedron Lett.* **2004**, *45*, 6425.
39. Howarth, J.; Hanlon, K.; Fayne, D.; McCormac, P. *Tetrahedron Lett.* **1997**, *38*, 3097.
40. Kumar, V.; Pei, C.; Olsen, C. E.; Schaeffer, S. J. C.; Parmar, V. S.; Malhotra, S. V. *Tetrahedron: Asymmetry* **2008**, *19*, 664–671.
41. Poletti, L.; Chiappe, C.; Lay, L.; Pieraccini, D.; Polito, L.; Russo, G. *Green Chem.* **2007**, *9*, 337–341.
42. Yu, S.; Lindeman, S.; Tran, C. D. *J. Org. Chem.* **2008**, *73*, 2576–2591.
43. Tran, C. D.; Oliveira, D.; Yu, S. *Anal. Chem.* **2006**, *78*, 1349–1356.
44. Tran, C. D.; Kong, X. *Anal. Biochem.*, **2000**, *286*, 67−74.
45. Alexander, T.; Tran, C. D. *Anal. Chem.* **2001**, *73*, 1062–1067.
46. Alexander, T.; Tran, C. D. *Appl. Spectrosc.* **2001**, *55*, 939–945.
47. Tran, C. D.; Challa, S. *Spectrochim. Acta, Part A* **2005**, *62*, 38–41.
48. Jackson, P.; Kim, T.; Carr, P. *Anal. Chem.* **1997**, *69*, 5011–5017.
49. Baumann, M.; Sturmer, R.; Bornscheurer, U. A. *Angew. Chem., Int. Ed.* **2001**, *40*, 4201–4204.
50. Tielmann, P.; Boese, W.; Luft; Reetz, M. A. *Chem. Eur. J.* **2003**, *9*, 3882–3887.
51. Tao, W.; Gozzo, F.; Cooks, R. *Anal. Chem.* **2001**, *73*, 1692–1698.
52. Reetz, M.; Tielmann, P.; Eipper, A.; Ross, A.; Schlotterbeck, G. A. *Chem. Commun.* **2004**, 1366–1367.
53. Reetz, M.; Becker, M.; Klein, H.; Stockigt, D. A. *Angew. Chem., Int. Ed.* **1999**, *38*, 1758–1761.

Downloaded by PENNSYLVANIA STATE UNIV on June 22, 2012 | http://pubs.acs.org
Publication Date (Web): April 28, 2010 | doi: 10.1021/bk-2010-1038.ch004

Downloaded by PENNSYLVANIA STATE UNIV on June 22, 2012 | http://pubs.acs.org
Publication Date (Web): April 28, 2010 | doi: 10.1021/bk-2010-1038.ch005

Chapter 5

New Method for Installation of the Imidazole Ring and Synthesis of Biologically Active Molecules with Ionic Liquid-Like Structures

Yuichi Kobayashi,* Yohei Kiyotsuka, Hukum P. Acharya, and Key Miyoshi

**Department of Biomolecular Engineering, Tokyo Institute of Technology,
Nagatsuta-cho 4259, Midori-ku, Yokohama 226-8501, Japan
*ykobayas@bio.titech.ac.jp**

In relation to ionic liquids, we have accomplished synthesis of epoxyisoprostane A_2 phosphorylcholine, which possesses zwitter ion structure. We also developed a method to attach an imidazole ring to a chiral carbon by using allylic substitution reaction.

We have several projects concerning synthesis of ionic liquids. One of which is the synthesis of isoprostane phosphorylcholines and phoslactomycins both of which are biologically important natural products possessing ionic liquid structures. Another project is the development of methods to obtain new types of imidazolium salts. Herein, we report synthesis of 2-(5-epoxyisoprostane A_2)phosphoryl-choline and anti S_N2' selective allylation reaction with imidazolyl anions to furnish chiral imidazoles, which were converted to the imidazolium salts successfully.

Synthesis of Epoxyisoprostane Phosphorylcholine

Zwitter ion structure is seen in several classes of biologically active compounds, and the structure plays a key role in their functions and activities. For example, phospholipids are components of low-density lipoprotein (LDL) and major carrier of cholesterol in human blood. Under oxidative stress,

In Ionic Liquid Applications: Pharmaceuticals, Therapeutics, and Biotechnology; Malhotra, S.;
ACS Symposium Series; American Chemical Society: Washington, DC, 0.

Downloaded by PENNSYLVANIA STATE UNIV on June 22, 2012 | http://pubs.acs.org
Publication Date (Web): April 28, 2010 | doi: 10.1021/bk-2010-1038.ch005

the unsaturated part of a fatty acid, especially arachidonic acid, undergoes oxidation, and deposition of the oxidized LDL in vascular tissues is believed to be responsible for atherosclerosis. Recently, Berliner isolated 2-(5-epoxyisoprostane A_2)phosphorylcholine as one of such compounds from atherosclerotic lesions and determined the planer structure for 5-epoxyisoprostane A_2 (*1*). Since the structural information is insufficient for further investigation, we started a research to elucidate the stereochemistry by comparing stereoisomers, and envisioned a strategy shown in Scheme 1, in which aldol condensation between stereodefined enone **1** and epoxy aldehyde **2** is a key step (*2*).

The key enone **1** was prepared by a sequence shown in Scheme 2. (1*R*)- Monoacetate **9** was converted to (*S*)-pivaloyl ester **10**, which upon CuCN-catalayzed reaction with propargylic Grignard reagent **11** in the presence of $MgCl_2$ (*3*) afforded **12** regioselectively (ca 93:7). The propargylic reagent **11** used herein was prepared from propargyl bromide and Mg in the presence of $ZnBr_2$ according to the Hg-free procedure developed recently by us (*4*). The remaining C_5H_{11} chain was installed to **12** by alkylation and the resulting compound **14** was oxidized to the key enone **1** in good yield.

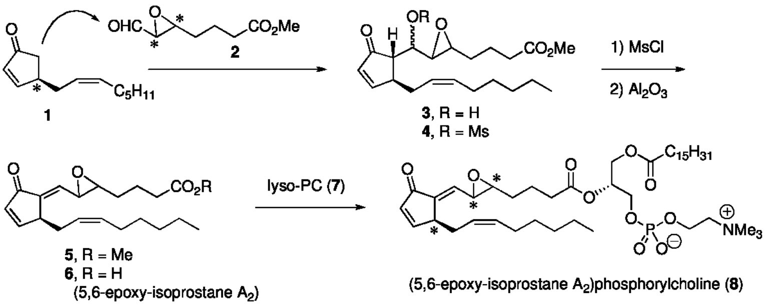
1
2
3, R = H
4, R = Ms
1) MsCl
2) Al_2O_3
5, R = Me
6, R = H
(5,6-epoxy-isoprostane A_2)
lyso-PC (7)
(5,6-epoxy-isoprostane A_2)phosphorylcholine (8)

Scheme 1. Our approach to 5,6-epoxyisoprostane A_2 phosphorylcholine

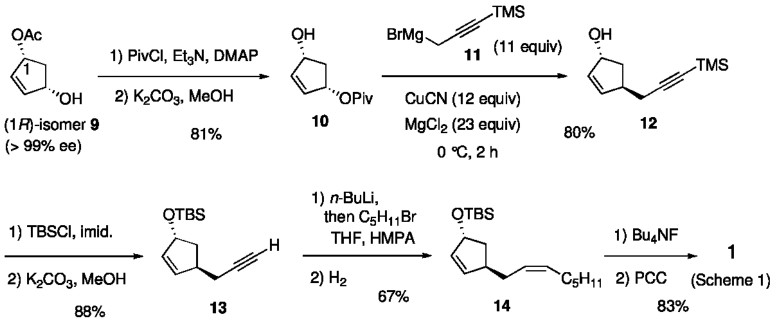
(1*R*)-isomer 9
(> 99% ee)
1) PivCl, Et_3N, DMAP
2) K_2CO_3, MeOH
81%
10
11 (11 equiv)
CuCN (12 equiv)
$MgCl_2$ (23 equiv)
0 °C, 2 h
80%
12
1) TBSCl, imid.
2) K_2CO_3, MeOH
88%
13
1) *n*-BuLi, then $C_5H_{11}Br$ THF, HMPA
2) H_2
67%
14
1) Bu_4NF
2) PCC
83%
1 (Scheme 1)

*Scheme 2. Preparation of the key enone **1**.*

Downloaded by PENNSYLVANIA STATE UNIV on June 22, 2012 | http://pubs.acs.org
Publication Date (Web): April 28, 2010 | doi: 10.1021/bk-2010-1038.ch005

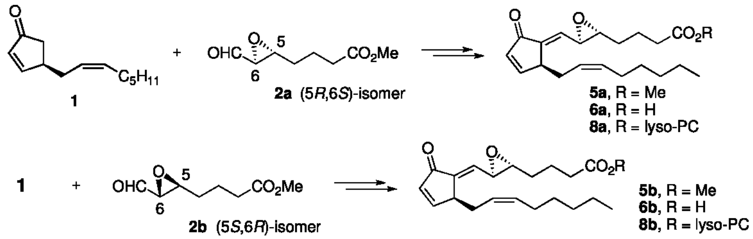

Scheme 3. Synthesis of ***8a*** *and its diastereoisome* ***8b****.*

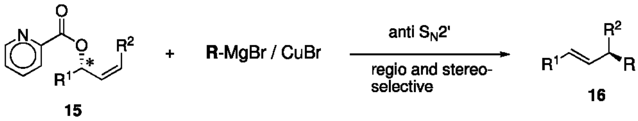

Scheme 4. Anti S_N2' *allylation of picolinoates with RMgBr·CuBr complexes.*

The enone **1** was treated with LDA at –78 °C in THF and the resulting enolate was subjected to aldol reaction with (5*R*,6*S*)-isomer **2a** to give a mixture of anti/syn aldols (Scheme 3). Without separation the mixture was converted to mesylate, which was exposed to Al_2O_3 to furnish **5a** stereoselectively. Methyl ester was hydrolyzed using pig pancreatic lipase (PPL) to afford acid **6a**. Similarly, enone **1** was condensed with (5*S*,6*R*)-epoxide **2b** to furnish acid **6b**. Among **6a** and **6b**, the ^{1}H NMR spectra of the former was coincident with the data reported by Berliner, thus establishing the relative stereochemistry of the epoxyisoprosatne A_2. Attempted condensation of **6a** with lyso-PC (7) with DCC, the standard reagent, even at higher temperatures resulted in recovery of the starting acid. After examination of other reagents, we found that Yamaguchi reagent afforded **8a** in 53% yield. Likewise, diastereomer **8b** was synthesized.

Synthesis of Chiral Imidazolium Salts

Another project started last year in our laboratory is allylation of secondary allylic alcohol derivatives with hard nucleophiles. We found high regio- and stereoselectivities in the reaction of allyic picolinoates **15** and RMgBr/CuBr complexes, affording anti S_N2' products **16** (Scheme 4) (*5*). Aryl, alkenyl and alkyl Grignard reagents are good reagent sources. In this reaction system, the picolinoxy group is much activated by the electron-withdrawing pyridyl group and by chelation to Mg cation to allow aryl and alkenyl Grignard reagents to be involved in the reaction.

With the above reaction in mind, we were attracted by a possibility that use of imidazolyl and pyridyl anions in place of RMgBr would furnish imidazoles and pyridines possessing a chiral side chain at the α-carbon. Scheme 5 illustrates the

Downloaded by PENNSYLVANIA STATE UNIV on June 22, 2012 | http://pubs.acs.org
Publication Date (Web): April 28, 2010 | doi: 10.1021/bk-2010-1038.ch005

reaction and further conversion to imidazolium salts by *N*-alkylation. However, reactivity and selectivity of such lithium anions toward the allylation with the picolinoates were uncertain.

Consequently, reaction with PhLi (2 equiv) was preliminary investigated to establish suitable conditions. Results are summarized in Table 1. For comparison, those for PhMgBr/CuBr·Me_2S complexes are shown in entries 1–3. First, phenylcopper reagents derived from salt free PhLi (2 equiv) and different concentrations of CuBr·Me_2S (2, 1, and 0.5 equiv) (defined as 2/2, 2/1, and 2/0.5 Ph/Cu reagents, respectively) were subjected to reaction with racemic picolinoate *rac*-**15a** at 0 °C for 1 h in THF to afford a mixture of anti S_N2' product *rac*-**16a**, alcohol **22** (byproduct), and unreacted substrate **15a** (entries 4, 6, and 10), indicating competition with an attack to the carbonyl carbon of the picolinoxy group. However, we were delighted by the fact that the S_N2 product (**21**) was *not* detected by ^1H NMR spectroscopy. To improve the product selectivity, reactions with the 2/1 Ph/Cu reagent were reinvestigated in the presence of $MgBr_2$ (2–4 equiv). Among these quantities, *rac*-**16a** was produced almost exclusively with 3 and 4 equiv of $MgBr_2$ (entries 8 and 9, cf. entry 7 for 2 equiv., Table 1) Furthermore, $MgBr_2$ was found to accelerate the reaction to be completed within 1 h. No retardation was observed even at –60 ~ –50 °C (data not shown). Addition of $MgBr_2$ was also effective on the reactions with the 2/2 and 2/0.5 Ph/Cu reagents (entries 5 and 11, Table 1).

We then applied the PhLi/CuBr/$MgBr_2$ reagent to the enantiomerically enriched (*S*)-**15a** (95–98% e.e.). Reactions of (*S*)-**15a** with 2/2, 2/1, and 2/0.5 Ph/Cu reagents were carried out in the presence of $MgBr_2$ (3 equiv) at two temperature ranges (0 °C and at –60 ~ –50 °C) for 1 h, and chirality transfer (C.T.), defined as % ratio of enantiomeric excesses of product over substrate, were calculated from the chiral HPLC data. Excellent C.T.s were obtained with the 2/2 and 2/1 Ph/Cu reagents (Table 2, entry 2, Method B for 2/1 Ph/Cu reagent) and are almost same efficiency as one obtained with PhMgBr/Cu (entry 1). The C.T.s were independent from the reaction temperatures (data not shown), indicating that a narrow range of temperature control is not necessary for efficient C.T. and reaction rate. On the other hand, the 2/0.5 reagent gave somewhat low C.T. (71–84%).

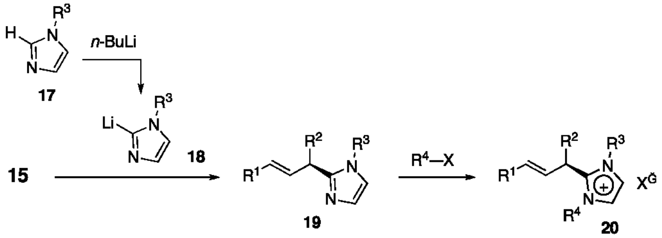

Scheme 5. A method to obtain chiral imidazolium salts.

Next, PhLi prepared in situ by lithium-halogen exchange was investigated to clarify any effect by the residue(s) coproduced with PhLi. Lithiation of PhX (X = Br, 2 equiv) was carried out using *t*-BuLi (4 equiv) at 0 °C for 30 min in Et_2O, and PhLi (2 equiv) produced with LiBr (2 equiv), $Me_2C=CH_2$ (2 equiv), and *t*-BuH (2 equiv) was converted to the 2/1 Ph/Cu reagent, which upon reaction with (*S*)-**15a** in the presence of $MgBr_2$ (5 equiv) produced (*R*)-**16a** with excellent product selectivity and reactivity as presented in entry 3. A similar efficiency was also recorded with PhI (entry 4). In contrast to *t*-BuLi, preparation of PhLi from PhX (X = Br, I; each 2 equiv) and *n*-BuLi (2 equiv) was not compatible with the allylation.

Downloaded by PENNSYLVANIA STATE UNIV on June 22, 2012 | http://pubs.acs.org
Publication Date (Web): April 28, 2010 | doi: 10.1021/bk-2010-1038.ch005

Table 1. Preliminary Study Using *rac*-15a and PhLi/CuBr·Me₂S

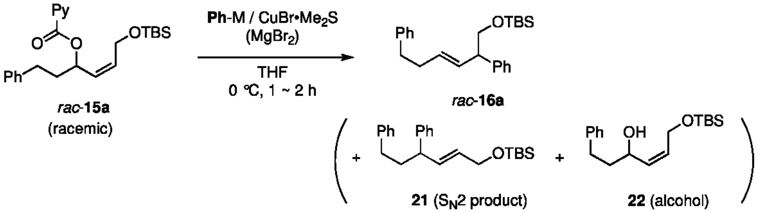

Entry	*Ph-M (equiv)*	*CuBr·Me₂S (equiv)*	*MgBr₂ (equiv)*	*Ratio of* ***16a*** *:* ***21*** *:* ***22*** *:* ***15a***	*Yield (%)*
1	PhMgBr (2)	2	–	98 : 2 : 0 : 0	84
2	PhMgBr (2)	1	–	99 : 1 : 0 : 0	91
3	PhMgBr (2)	0.5	–	99 : 1 : 0 : 0	85
4	PhLi (2)	2	–	9 : 0 : 69 : 22	nd
5	PhLi (2)	2	3	99 : 1 : 0 : 0	97
6	PhLi (2)	1	–	11 : 0 : 47 : 42	nd
7	PhLi (2)	1	2	84 : 0 : 15 : 1	nd
8	PhLi (2)	1	3	99 : 1 : 0 : 0	94
9	PhLi (2)	1	4	98 : 0 : 2 : 0	92
10	PhLi (2)	0.5	–	48 : 0 : 44 : 8	nd
11	PhLi (2)	0.5	3	94 : 0 : 6 : 0	nd

Table 2. Chirality Transfer (C.T.) with "Ph-M/CuBr"

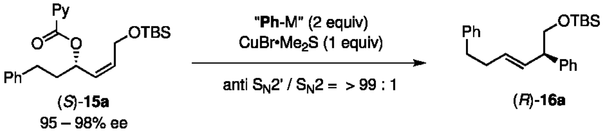
Py
OTBS
Ph
(S)-15a
95 – 98% ee
"Ph-M" (2 equiv)
CuBr•Me2S (1 equiv)
anti SN2' / SN2 = > 99 : 1
Ph
OTBS
Ph
(R)-16a

Entry	*Method*	*Reagents for Ph-M (equiv)*	*Yield (%)*	*C.T. (%)*
1	A	PhMgBr (2)	93	99
2	B	PhLi (2), $MgBr_2$ (3)	92	98
3	C	PhBr (2), *t*-BuLi (4), $MgBr_2$ (5)	93	98
4	C	PhI (2), *t*-BuLi (4), $MgBr_2$ (5)	90	98

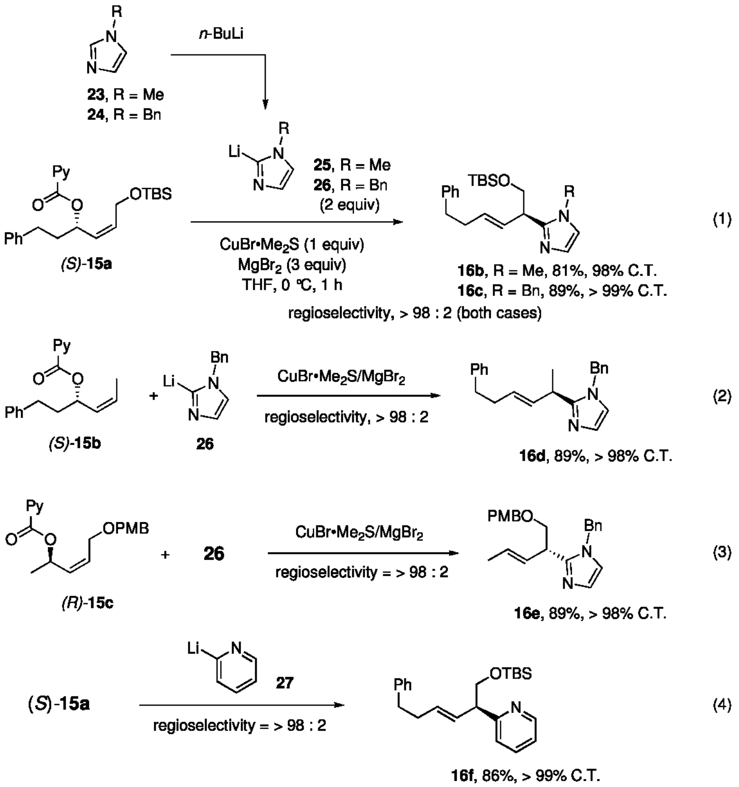
R
23, R = Me
24, R = Bn
n-BuLi
Li
25, R = Me
26, R = Bn
(2 equiv)
Py
OTBS
Ph
(S)-15a
CuBr•Me2S (1 equiv)
MgBr2 (3 equiv)
THF, 0 °C, 1 h
TBSO
Ph
16b, R = Me, 81%, 98% C.T.
16c, R = Bn, 89%, > 99% C.T.
regioselectivity, > 98 : 2 (both cases)
(1)
(S)-15b
26
CuBr•Me2S/MgBr2
regioselectivity, > 98 : 2
Bn
16d, 89%, > 98% C.T.
(2)
OPMB
(R)-15c
26
CuBr•Me2S/MgBr2
regioselectivity = > 98 : 2
PMBO
16e, 89%, > 98% C.T.
(3)
(S)-15a
27
regioselectivity = > 98 : 2
16f, 86%, > 99% C.T.
(4)

Scheme 6. Anti S_N2' selective allylation with heteroaromatic coppers.

Downloaded by PENNSYLVANIA STATE UNIV on June 22, 2012 | http://pubs.acs.org
Publication Date (Web): April 28, 2010 | doi: 10.1021/bk-2010-1038.ch005

Downloaded by PENNSYLVANIA STATE UNIV on June 22, 2012 | http://pubs.acs.org
Publication Date (Web): April 28, 2010 | doi: 10.1021/bk-2010-1038.ch005

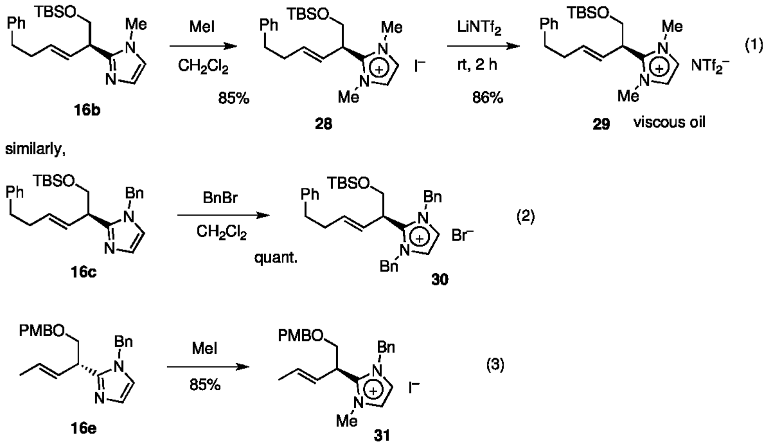

Scheme 7. Conversion of the imidazoles to imidazolium salts.

The reaction conditions established above was applied to *N*-alkyl imidazoles and pyridine. First, the lithium anion **25** was prepared from *N*-Me imidazole (**23**) by direct lithiation with *n*-BuLi and subjected to allylation with (*S*)-**15a** in the presence of $MgBr_2$. The reaction proceeded at 0 °C as expected to produce **16b** with excellent selectivity (Scheme 6, eq 1). Anion **26** derived from Bn imidazole **24** gave **16c** as well. The regio- and stereoselectivities were not affected by substituents around the allylic moiety (eqs 2 and 3). Pyridyl lithium **27** was prepared from bromopyridine and *t*-BuLi and converted to copper reagent, which led to successful allylation with (*S*)-**15a** to afford **16f** efficiently (eq 4, Scheme 6).

The imidazoles **16b**,**c**,**e** thus synthesized were converted to imidazolium salts **28**, **30**, **31** by *N*-alkylation in good yield. Although **28** was solids, TFSI salt **29** synthesized by anion exchange was viscose oil (Scheme 7).

In summary, we have succeeded in synthesis of epoxyisoprostane A_2 phosphorylcholine, with which biological research would be spurred. We have also developed a method to obtain optically active imidazoles by using allylic substitution of allylic picolinoates. Since allylic alcohols in optically active forms are available from natural sources and by asymmetric reactions, the method would produce architecturally and/or biologically attractive imidazolium salts. We believe the method would produce key compounds in organic synthesis and in material science.

References

1. Watson, A. D.; Subbanagounder, G.; Welsbie, D. S.; Faull, K. F.; Navab, M.; Jung, M. E.; Fogelman, A. M.; Berliner, J. A. *J. Biol. Chem.* **1999**, *274*, 24787.
2. Acharya, H. P.; Kobayashi, Y. *Angew. Chem., Int. Ed.* **2005**, *44*, 3481.

3. (a) Kobayashi, Y.; Nakata, K.; Ainai, T. *Org. Lett.* **2005**, *7*, 183. (b) Nakata, K.; Kobayashi, Y. *Org. Lett.* **2005**, *7*, 1319.
4. Acharya, H. P.; Miyoshi, K.; Kobayashi, Y. *Org. Lett.* **2007**, *9*, 3535.
5. Kiyotsuka, Y.; Acharya, H. P.; Katayama, Y.; Hyodo, T.; Kobayashi, Y. *Org. Lett.* **2008**, *10*, 1719.

Downloaded by PENNSYLVANIA STATE UNIV on June 22, 2012 | http://pubs.acs.org
Publication Date (Web): April 28, 2010 | doi: 10.1021/bk-2010-1038.ch005

Downloaded by UNIV OF GUELPH LIBRARY on June 22, 2012 | http://pubs.acs.org
Publication Date (Web): April 28, 2010 | doi: 10.1021/bk-2010-1038.ch006

Chapter 6

Separation and Recovery of Penicillin in an Integrated System Containing Ionic Liquids

Yangyang Jiang,[1,2] Chen Guo,[1] Hansong Xia,[1] and Huizhou Liu*,[1]

[1]Laboratory of Separation Science and Engineering, Key Laboratory of Green Process and Engineering, State Key Laboratory of Biochemical Engineering, Institute of Process Engineering, Chinese Academy of Sciences, Beijing 100190, China
[2]Graduate School of the Chinese Academy of Science, Beijing 100039, China
***To whom correspondence should be addressed.**
Tel. & Fax: (8610) 62554264. E-mail: hzliu@home.ipe.ac.cn.

An integrated process based on hydrophilic and hydrophobic ionic liquids is proposed to extract penicillin G from its fermentation broth and recover it into fresh water. With the aid of buffer salt, hydrophilic ionic liquid [C_4mim]BF_4 (1-butyl-3-methylimidazolium tetrafluoroborate) could form an ionic liquid aqueous two-phase system (ILATPS) and extract penicillin into the ionic liquid-rich phase of ILATPS, while leaving miscellaneous proteins in the ionic liquid-poor phase. Subsequently, hydrophobic [C_4mim]PF_6 (1-butyl-3-methylimidazolium hexafluorophosphate) is introduced into the ionic liquid-rich phase of ILATPS, which transfers the system into a hydrophobic ionic liquid phase in equilibrium with a water phase system (MILWS). The majority of hydrophilic [C_4mim]BF_4 is transferred into the ionic liquid-rich phase of MILWS, leaving most of the penicillin in the conjugated water phase. The integrated ionic liquids system shows several advantages: (1) Penicillin is efficiently extracted into the ionic liquid-rich phase at neutral pH, so the protein emulsification met in the organic solvent system is avoided. (2) Hydrophobic ionic liquids could separate hydrophilic ionic liquids away from the penicillin–containing aqueous phase. Consequently, the trouble for recovering the phase-forming material is overcome. Ionic liquids aggregate into cylindrical

In Ionic Liquid Applications: Pharmaceuticals, Therapeutics, and Biotechnology; Malhotra, S.;
ACS Symposium Series; American Chemical Society: Washington, DC, 0.

Downloaded by UNIV OF GUELPH LIBRARY on June 22, 2012 | http://pubs.acs.org
Publication Date (Web): April 28, 2010 | doi: 10.1021/bk-2010-1038.ch006

micelle in ILATPS, which leave sufficient room for transferring the substrate into the ionic liquid-rich phase. The micelles grow rapidly in MILWS. As a result, low water activity in hydrophobic ionic liquids phase leads to a low affinity with the polar penicillin and brings it back into water.

Introduction

Penicillin is an important antibiotic in clinical medicine, which can be used as raw material to produce 6-APA (6-aminopenicillanic acid) (*1–3*). The traditional way to obtain penicillin includes the extraction with organic solvent at low pH, back-extraction into aqueous phase at high pH, and crystallization for pure product (*4*). Several problems exits in this process. (1) Miscellaneous proteins in the fermentation broth cause serious emulsification at low pH. (2) Volatile organic solvent pollutes the environment. (3) Low pH leads to decomposition of penicillin.

Aqueous two-phase (ATP) is another choice for penicillin separation. It is made of two polymers or one polymer and one inorganic salt (*5*). Because of the >70% water in each phase and a low interfacial tension between them, ATP facilitates the separation of polar solutes without the troubles of pH adjustment and volatile organic solvent (*6*). Several articles dealt with the extractions of amino acids, protein and antibiotics in polymer ATP (*7–13*). However, the bottleneck for recycling the phase-forming polymers from the aqueous phase containing substrate precludes its further industrial utilization (*14*).

Another method for separating penicillin is ILATPS. Ionic liquids are novel liquids salts with negative volatile pressure, tunable structure, and interesting properties (Figure 1) (*15*, *16*), which are widely employed in the fields of catalysis, extraction and material science (*17–19*). With the aid of buffer salt, ionic liquids could form ILATPS and extract various solutes into the ionic liquid-rich phase efficiently (*20*). For example, Liu and co-workers used a $[C_4mim]BF_4/Na_2HPO_4$ ILATPS to extract penicillin and got a satisfying yield of 94% without protein emulsification (*21*). The main drawback of ILATPS route is its difficulty in recycling ionic liquids from aqueous phase.

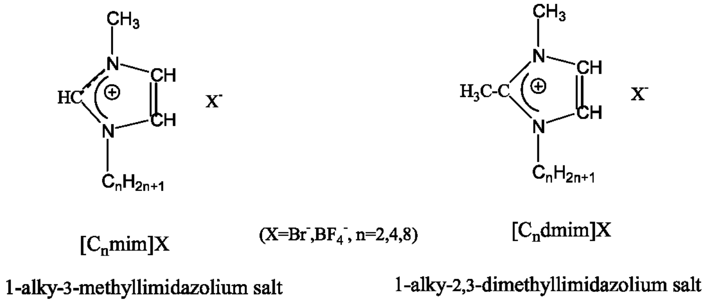

Figure 1. The structure of ionic liquids [C$_n$mim]X and [C$_n$dmim]X.

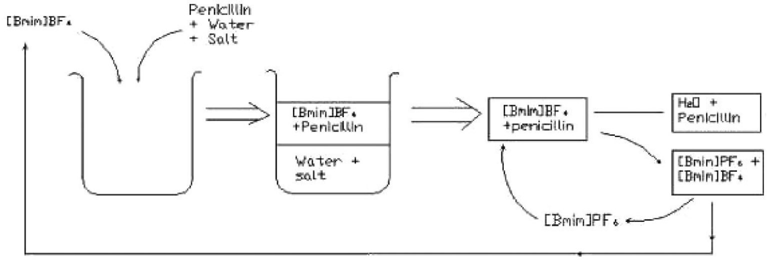

Figure 2. Strategy for recovering penicillin in ionic liquids aqueous solution.

Downloaded by UNIV OF GUELPH LIBRARY on June 22, 2012 | http://pubs.acs.org
Publication Date (Web): April 28, 2010 | doi: 10.1021/bk-2010-1038.ch006

In this work, we propose an integrated process derived from ILATPS (Figure 2), which could not only separate penicillin from the fermentation broth but also recover ionic liquids from penicillin-containing aqueous solution. The novel work is based on the idea that ionic liquids are the unique materials that combined with the nature of surfactants and solvent. The advantages make ionic liquids act as a good extractant for penicillin in ILATPS and a good reservoir for the extractant in MILWS.

Experimental Section

Preparation of Ionic Liquids

A 1:1.15 mol ratio of *N*-methylimidazole and bromobutane was added into a flask and the solution was agitated at 70 °C for 24 h. After cooling down, an equal volume of ethyl acetate was mixed with the sample and extracted twice. The sample was evaporated, and the product [C_4mim]Br (1-butyl-3-methylimidazolium bromide) was obtained. [C_4mim]Br was subjected to a metathesis with the intended anion, such as BF_4^- or PF_6^-, at room temperature for 24 h. The aqueous solution, so obtained was extracted with CH_2Cl_2 and washed with water until no Br^- ion was found. After evaporation for 8 h, the product [C_4mim]BF_4 or [C_4mim]PF_6 was obtained.

Phase Diagram of Ionic Liquids Aqueous Solution

The phase diagrams of ILATPS and MILWS were prepared using the "cloud point" method (*22*, *23*). Simply, a certain amount of hydrophobic [C_4mim]PF_6 was introduced into the aqueous solution containing preweighed hydrophilic [C_4mim]BF_4 and buffer salt. The turbidity of the solution was inspected by UV spectrometer (Lambda bio 40, Perkin Elmer company) at 600 nm until full phase separation was reached. The weight of [C_4mim]PF_6 was recorded, and the procedure was repeated until a sufficient number of points for the construction of the binodal curve were obtained.

Characteristic of Ionic Liquids Micelle Aggregate

The 40% NaH_2PO_4 and 30% [C_4mim]BF_4 were mixed into water to form ILATPS. The mixture was centrifuged at 4000 rpm for 5 min. The ionic liquids-rich phase was taken out for the freezing-fracture TEM experiment: 2 μl sample was added into the sample seat and cooled down to -130 °C with liquid nitrogen. The solid sample was sent into a HUS-SGB vacuum sprayer to cover a layer of platinum at horizontal 45 and a layer of carbon powder with 20 nm member to support the surface. Finally, the micelle structure was checked under Philip GAINAI G2 TEM electronic monitor.

Downloaded by UNIV OF GUELPH LIBRARY on June 22, 2012 | http://pubs.acs.org
Publication Date (Web): April 28, 2010 | doi: 10.1021/bk-2010-1038.ch006

Partitioning Behaviors of Penicillin in ILATPS and MILWS

Preweighed hydrophilic ionic liquid [C_4mim]BF_4 and NaH_2PO_4 were added into 5 ml of fermentation broth containing 3.4%(w/w) penicillin. The system was stirred and centrifuged at 4000 rpm for 5 min. The concentrations of ionic liquids in the ionic liquid-rich and ionic liquid-poor phases were checked with UV spectrometer at 235 nm after dilution 50 times with water. The concentrations of penicillin in the two phases were measured with HPLC (HP1100 HPLC system, Agilent corporation, 250 mm×4 mm Zorbax SB-C18 column; the mobile phase was methanol:0.05 M phosphate at pH 3 (36:64 v/v), flow rate at 1 ml/min, inspected at 254 nm with a diode array detector (DAD)). The concentration of protein was checked with Coomassie blue method at 595 nm (*24*). The distribution ratios *K* of solutes in ionic liquids system were calculated from eq 1.

$$K = \frac{\text{solute's concentration in the ionic liquids-rich phase}}{\text{solute's concentration in the ionic liquids-poor phase}} \qquad (1)$$

After the phase equilibrium, the ionic liquids-rich phase was taken out from ILATPS and a certain amount of [C_4mim]PF_6 was introduced. The mixture was stirred and centrifuged at 4000 rpm for 5 min. The concentrations of ionic liquids and penicillin in the ionic liquids-rich and ionic liquids-poor phases of MILWS were checked with UV and HPLC. To decrease the errors for measuring the ionic liquids concentration in MILWS when it was sufficiently large, Karl-Fisher titration was employed to determine the water concentration in the ionic liquids-rich phase (*25*).

Results

Whole Process in Ionic Liquids Aqueous Solution

First of all, ILATPS is constructed with hydrophilic [C_4mim]BF_4 and phosphate salt (Figure 2, Figure 3A), in which penicillin is partitioned into the ionic liquid-rich phase (bottom phase in Figure 3A) (*26*), leaving miscellaneous proteins in the ionic liquids-poor phase (top phase in Figure 3A). Second, a certain amount of hydrophobic ionic liquid [C_4mim]PF_6 is introduced into the ionic liquids-rich phase of ILATPS (yellow-colored phase in Figure C). After phase equilibrium, a hydrophobic ionic liquid mixture is separated from the residual water phase (Mixed ionic liquids/water two phase system, MILWS, Figure 2, bottom phase in Figure 3D), and most of the penicillin remains in water. [C_4mim]PF_6 and [C_4mim]BF_4 in the ionic liquids mixture can be further separated from each other with an increase in the temperature.

Phase Diagram of Ionic Liquids Aqueous Solution

Figure 4 gives the phase diagram of ionic liquids aqueous solution. It was found that in the absence of buffer salt, a phase diagram includes two zones. Below the borderline (line a) is an isotropic solution, which comprises [C_4mim]BF_4, water, and a small amount of hydrophobic [C_4mim]PF_6. Above the borderline, the solution is separated into a two-phase system, which comprises ionic liquids mixture [C_4mim]PF_6/[C_4mim]BF_4 in equilibrium with a residual aqueous phase containing little amount of ionic liquids. While in the presence of 1 mol/L NaH_2PO_4, the ionic liquids system is divided into four portions. Zone I in the left corner refers to an aqueous single phase containing little ionic liquids but most of the salt; zone II in the right corner is a hydrophilic single phase that comprised hydrophilic ionic liquid [C_4mim]BF_4 and a little [C_4mim]PF_6. The middle zone between zones I and II refers to the ionic liquids two-phase district. Zone III represents ILAPTS with low [C_4mim]PF_6 concentration, while zone IV represents MILWS, which comprises an aqueous phase in equilibrium with a hydrophobic ionic liquid phase. The line between zones III and IV corresponds to the critical phase borderline between ILATPS and MILWS. When the [C_4mim]PF_6/[C_4mim]BF_4 ratio is beyond 0.4, ILATPS (Figure 3B) is transferred into MILWS (Figure 3C), and the tie-line length and Δ[ionic liquids] increase rapidly. As a result, most of the hydrophilic ionic liquid in ILATPS has been recovered into the hydrophobic phase of MILWS.

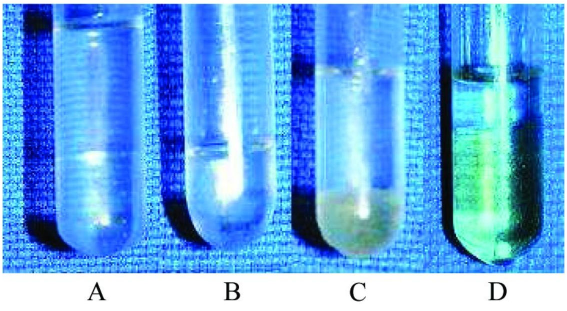

Figure 3. Separation of penicillin from the fermentation broth.

Downloaded by UNIV OF GUELPH LIBRARY on June 22, 2012 | http://pubs.acs.org
Publication Date (Web): April 28, 2010 | doi: 10.1021/bk-2010-1038.ch006

Downloaded by UNIV OF GUELPH LIBRARY on June 22, 2012 | http://pubs.acs.org
Publication Date (Web): April 28, 2010 | doi: 10.1021/bk-2010-1038.ch006

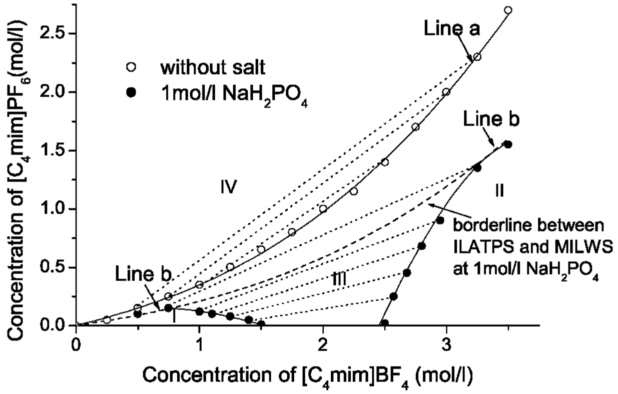

Figure 4. Phase diagram of [C$_4$mim]BF$_4$/[C$_4$mim]PF$_6$/water system.

Microscopic Architecture of Ionic Liquids Aggregates

Figure 5 illustrates the pictures of ionic liquids aggregates in ILATPS and MILWS. It is found that ionic liquids aggregated into cylindrical micelles in the ionic liquids-rich phase of ILATPS; its contour length is 150 nm, and axial ratio is 40 nm (Figure 5A, B). The micelle distributes evenly in a parallel way. The thickness between the surfaces of micelles reduced evidently with increasing the concentration difference of [C$_4$mim]BF$_4$ ($\Delta\{[C_4mim]BF_4\}$). At 1 mol/L $\Delta\{[C_4mim]BF_4\}$, the thickness is 130 nm, while it decreases to 70 nm at 2 mol/L $\Delta\{[C_4mim]BF_4\}$. The decrease could be attributed to the increasing osmotic pressure in ILATPS at high $\Delta\{[C_4mim]BF_4\}$. When hydrophobic [C$_4$mim]PF$_6$ is introduced, ILATPS is transferred into MILWS. The appearance and thickness between ionic liquids aggregates changes evidently. Parts C and D illustrate 10-fold increases in the counter length and axial ratio of cylindrical micelles when the [C$_4$mim]PF$_6$/[C$_4$mim]BF$_4$ ratio rises up from 0.3 to 1 in MILWS. But the thickness decreases with [C$_4$mim]PF$_6$ concentration. The inner structure of gigantic micelles in MILWS (Figure 5E) is similar to that in ILATPS (Figure 5A and B). The intrinsic relationship of the architectures in the two systems suggests that the big aggregate in MILWS is the assemblance from small micelles in ILATPS. The reason may be that the increased hydrophobicity on the surface of ionic liquids aggregates in MILWS might improve the hydrophobic attraction between ionic liquids aggregates (*27*) and results in the multilayer structure in Figure 5E. On the other hand, Figure 5F shows that the length and axial ratio of the ionic liquids micelle is analogous to that in the ionic liquids-rich phase of ILATPS, but the number density of micelles reduces. The phenomena suggests that the ionic liquids concentration in the residual water of MILWS is lower than that in the ionic liquids rich phase of ILATPS, i.e., most of the hydrophilic ionic liquids has been transferred from ILATPS into the ionic liquids mixture of MILWS.

Downloaded by UNIV OF GUELPH LIBRARY on June 22, 2012 | http://pubs.acs.org
Publication Date (Web): April 28, 2010 | doi: 10.1021/bk-2010-1038.ch006

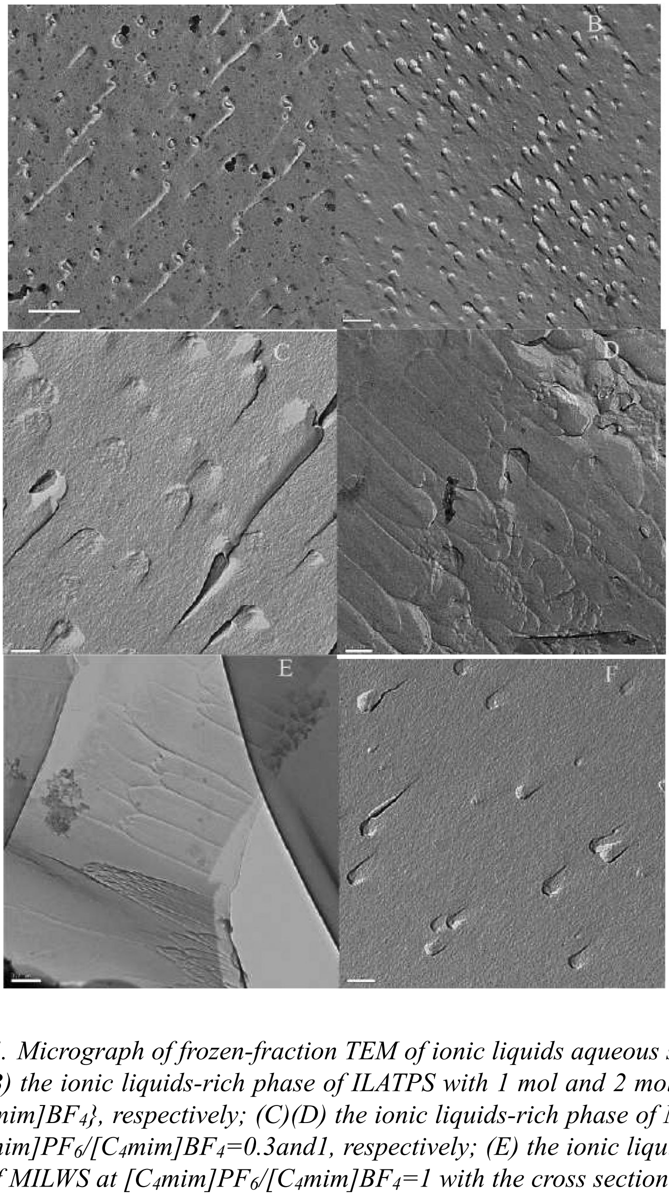

Figure 5. Micrograph of frozen-fraction TEM of ionic liquids aqueous solution: (A)(B) the ionic liquids-rich phase of ILATPS with 1 mol and 2 mol/L /L Δ{[C$_4$mim]BF$_4$}, respectively; (C)(D) the ionic liquids-rich phase of MILWS at [C$_4$mim]PF$_6$/[C$_4$mim]BF$_4$=0.3and1, respectively; (E) the ionic liquids-rich phase of MILWS at [C$_4$mim]PF$_6$/[C$_4$mim]BF$_4$=1 with the cross section; (F) the residual aqueous phase of MILWS at [C$_4$mim]PF$_6$/[C$_4$mim]BF$_4$=1 (the bars in parts A-F are 100 nm, 50 nm, 1 μm, 1 μm, 1 μm, and 200 nm, respectively).

Although the thickness between ionic liquids aggregates decreases both in ILATPS and MILWS, the phase-transition mechanisms in the two systems are different. In ILATPS, phase transition is induced by the increased osmotic pressure at high concentrations of salt or ionic liquids, which enhances the driving force between ionic liquids aggregates and pushes them together until an “energy barrier” is encountered (*28*). The energy barrier is yield from the

Downloaded by UNIV OF GUELPH LIBRARY on June 22, 2012 | http://pubs.acs.org
Publication Date (Web): April 28, 2010 | doi: 10.1021/bk-2010-1038.ch006

hydration repulsion between solute and hydrophilic surfaces of ionic liquids micelles in ILATPS (*29*), and it is strong enough to prevent the over approach of ionic liquids micelles. As a result, the phase transition from ILATPS to MILWS would never happen no matter how high the concentration of salt or ionic liquids employed (Figure 4) (*30*). On the contrary, when a small amount of hydrophobic ionic liquids is introduced, the phase transition from ILATPS to MILWS happens immediately. This may be due to the increased hydrophobicity on the micellar surfaces in the presence of $[C_4mim]PF_6$, which reduces the density of water film adjacent to micellar surfaces and decreases the hydration repulsion. For this reason, the energy barrier between two aggregates could be overcome, and two conjugated aggregates might approach together in the presence of "net" attractive force between ionic liquids micelles (*31*, *32*).

Extractive Behaviors of Penicillin in ILATPS

Effect of Salt Species

The variation of appearance and distance between ionic liquids aggregate at various Δ[ionic liquids] may lead to different partitioning behaviors of penicillin in ILATPS. Figure 6 shows the relationship between ln *K* and $\Delta\{[C_4mim]BF_4\}$ in ILATPS. It is found that ln *K* increases proportionally with $\Delta\{[C_4mim]BF_4\}$ until a critical concentration of 2.5 mol/L is reached. The maximum value of *K* in ILATPS might exceed over 1000 at this critical $\Delta\{[C_4mim]BF_4\}$, which is superior to the outcome in the organic solvent/water system or the PEG/salt ATP system (*33*). Moreover, the slope of ln $K/\Delta\{[C_4mim]BF_4\}$ shows little dependence on the salt species, no matter what NaH_2PO_4, Na_2SO_4, or Na_2HPO_4 is employed. The result is in line with Yaminsky's observation (*34*), which suggests that partitioning in ILATPS is primarily governed by a hydrophobic force, not an electrostatic origin.

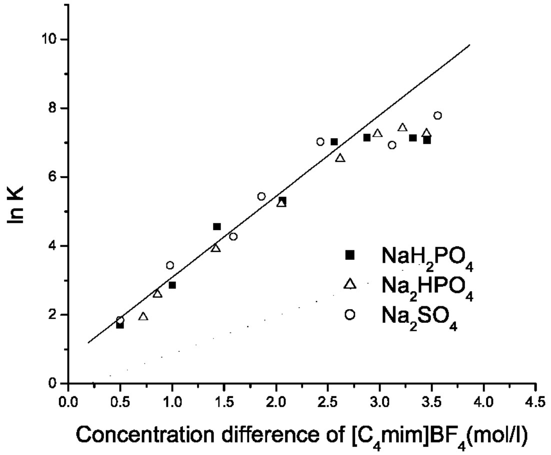

Figure 6. Effect of salt on relationship between ln K and Δ[ionic liquids].

In Ionic Liquid Applications: Pharmaceuticals, Therapeutics, and Biotechnology; Malhotra, S.;
ACS Symposium Series; American Chemical Society: Washington, DC, 0.

Downloaded by UNIV OF GUELPH LIBRARY on June 22, 2012 | http://pubs.acs.org
Publication Date (Web): April 28, 2010 | doi: 10.1021/bk-2010-1038.ch006

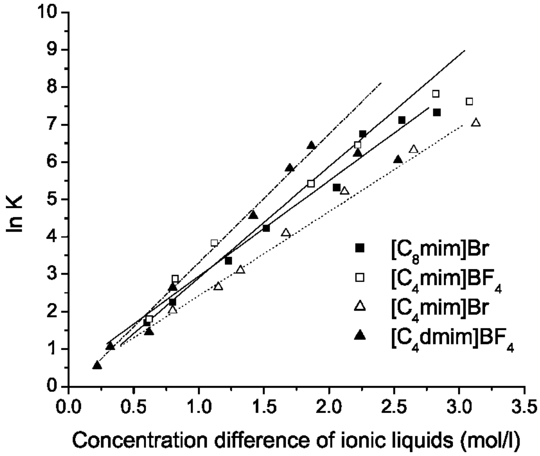

Figure 7. Relationship between ln K and Δ[ionic liquids] in ILATPS containing different ionic liquids species.

It is well-known that the microscopic characters of micelles change greatly with the structure and charges of surfactants (*35*). Hence, it is important to explore the influence of ionic liquids structure on the partitioning behaviors in ILATPS. Figure 7 compares the partition behaviors of penicillin in four ILATPS systems, in which ln *K* increases proportionally with Δ[ionic liquids] when Δ[ionic liquids] is below one critical value. When Δ[ionic liquids] exceeds the critical value, ln *K* maintains a constant value. The critical value of Δ[ionic liquids] with respect to the turnover of ln *K* decreases with ionic liquids hydrophobicity, i.e., in the order of $[C_4mim]Br$ < $[C_4mim]BF_4$ lt; $[C_4dmim]BF_4$ <$[C_8mim]Br$, while the slope of ln *K*/Δ[ionic liquids] increases with the hydrophobicity. However, in the relatively hydrophobic $[C_8mim]Br$ system, the slope of ln K/Δ{$[C_8mim]Br$} rises up to 3.435, and the critical value of Δ{$[C_8mim]Br$} decreases to 1.8 mol/L. This may be due to the intrinsic relationship between the slope of ln K/Δ[ionic liquids] and the hydrophobic attraction between ionic liquids aggregates. The higher the hydrophobicity of ionic liquids, the more positive is the contribution of the hydrophobic attraction and the larger is the slope of ln K/Δ[ionic liquids].

Downloaded by UNIV OF GUELPH LIBRARY on June 22, 2012 | http://pubs.acs.org
Publication Date (Web): April 28, 2010 | doi: 10.1021/bk-2010-1038.ch006

Flory-Huggins Expression in ILATPS

The mathematical expression of the relationship between ln *K* and Δ[ionic liquids] in ILATPS is given in eq 2.

$$\begin{aligned}
&\ln K([C_4mim]BF_4) = 0.399 + 2.548 * \Delta[IonicLiquids] \\
&\ln K([C_4dmim]BF_4) = -0.081 + 2.979 * \Delta[IonicLiquids] \\
&\ln K([C_4mim]Br) = 0.178 + 2.246 * \Delta[IonicLiquids] \\
&\ln K([C_8mim]Br) = -0.124 + 3.435 * \Delta[IonicLiquids]
\end{aligned} \quad (2)$$

The first term on the right-hand side of eq 2 represents the effect of Donnan-type electrostatic potentials, which is originated from the uneven distribution of inorganic salt and the dissociated anion from ionic liquids in ILATPS (*36*, *37*). The second term is the slope of ln *K*-Δ[ionic liquids], which represents the sum of energy contributions from the conformational entropy and "self-energy" to create a "cavity" in ionic liquids solution, as well as the enthalpic effect to accommodate a same-sized solute into the cavity.

Extractive Behavior of Penicillin in MILWS

Effect of Salt Species

After being extracted into the ionic liquids-rich phase of ILATPS, penicillin is required to be transferred back into fresh water by introduction of hydrophobic [C_4mim]PF_6 into the ionic liquids-rich phase containing penicillin. As a result, the phase transition happens from ILATPS to MILWS, and a residual aqueous phase is yielded as a reservoir for penicillin. Figure 8 shows ln K in MILWS as a function of [C_4mim]PF_6/[C_4mim]BF_4 ratio ([C_4mim]BF_4 concentration is kept at 2.8 mol/L). When [C_4mim]PF_6/[C_4mim]BF_4 ratio is below 0.4-0.5, ln *K* decreases monotonically with [C_4mim]PF_6/[C_4mim]BF_4. While at sufficiently large [C_4mim]PF_6/[C_4mim]BF_4 ratio, ln *K* keeps constant. The critical ratio with respect to the turnover of ln *K* in MILWS into a constant value is consistent with the value for phase borderline (line b in Figure 4). The consistency implies that the physical structure of ionic liquids aggregates has an intrinsic relationship with the partitioning behaviors of penicillin in MILWS. It is found from Figure 8 that the partitioning ratios of penicillin in MILWS are independent of the salt species and show little dependence on the salt concentration when [C_4mim]PF_6/[C_4mim]BF_4 is <0.4. Beyond this value, the partitioning ratio *K* increases proportionally with the salt concentration. The correlation between ln *K* and salt concentration in MILWS is in line with that in the butyl acetate/water system. The phenomena suggest that the primary role of salt in MILWS is to increase the osmotic pressure in the water phase (when [C_4mim]PF_6/[C_4mim]BF_4 ratio > 0.4), and not to effect the physical characters of ionic liquids aggregates in MILWS. In other word, the electrostatic effect is not the primary reason for recovering ionic liquids from the penicillin-containing aqueous phase in MILWS.

Effect of Ionic Liquids Species

Figure 9 compares the partitioning behaviors of penicillin in MILWS containing various ionic liquids species. It is found that ln *K* keeps nearly constant at sufficiently large $[C_4mim]PF_6/[C_4mim]BF_4$ ratios in different MILWS. The observation implies that the hydrophobic force is not the primary driving force for recovery of penicillin in MILWS. There should be another force besides the hydrophobic or electrostatic effect to dominate the partitioning behaviors of penicillin in MILWS.

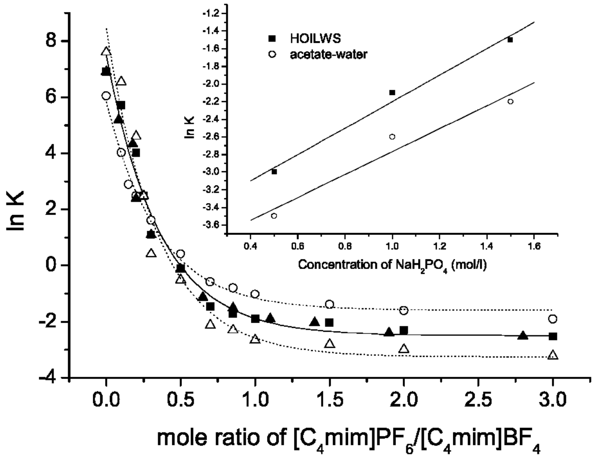

Figure 8. Effect of salt concentration and species on the characteristics of lnK-$[C_4mim]PF_6/[C_4mim]BF_4$ ratio in MILWS (■, 0.5 mol/L NaH_2PO_4; △, 1 mol/L NaH_2PO_4; O, 1.5 mol/L NaH_2PO_4; ▲, 0.5 mol/L Na_2HPO_4).

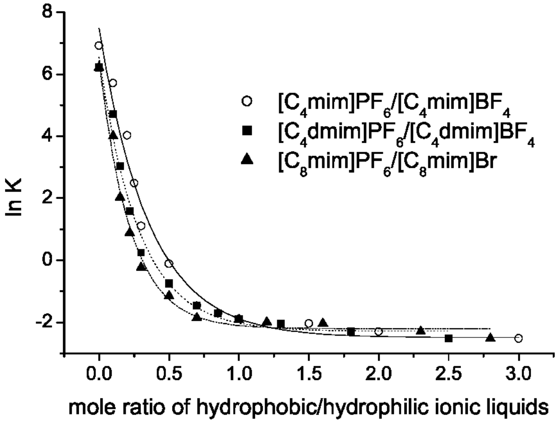

Figure 9. Effect of ionic liquids structures on the characteristics of ln K-hydrophobic/hydrophilic ionic liquids ratio in MILWS.

Downloaded by UNIV OF GUELPH LIBRARY on June 22, 2012 | http://pubs.acs.org
Publication Date (Web): April 28, 2010 | doi: 10.1021/bk-2010-1038.ch006

Downloaded by UNIV OF GUELPH LIBRARY on June 22, 2012 | http://pubs.acs.org
Publication Date (Web): April 28, 2010 | doi: 10.1021/bk-2010-1038.ch006

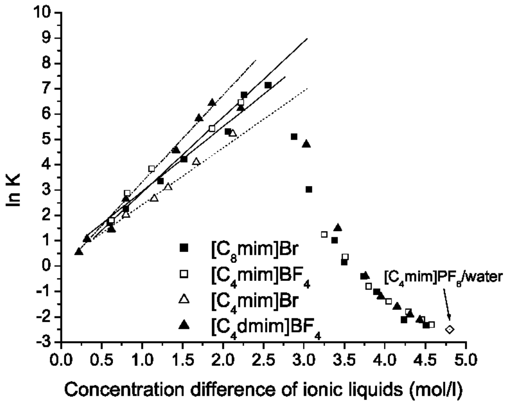

Figure 10. Uniform formulation of ln K-Δ[ionic liquids] over the range from ILATPS to MILWS.

Uniform Formulation of ln *K*-Δ[ionic liquids] in ILATPS and MILWS

The ln *K*-[C$_4$mim]PF$_6$/[C$_4$mim]BF$_4$ relationship could be further collaborated into the formulation between ln *K* and Δ[ionic liquids]. Figure 10 shows the uniform pictures of ln *K*-Δ[ionic liquids] in the whole ranges of ILATPS and MILWS. It is found that ln *K* increases proportionally with Δ[ionic liquids] in ILATPS until a maximum value is reached. After that value, ln *K* decreases monotonically with Δ[ionic liquids] in MILWS until a conventional [C$_4$mim]PF$_6$/water two-phase system is reached (diamond points in Figure 10). Figure 10 suggests that the different partitioning behaviors in the three ionic liquids aqueous systems, including ILATPS, MILWS, and the [C$_4$mim]PF$_6$/water system, could be correlated into a uniform picture. The observation is consistent with Angel et al.'s research, which suggests that the phase structure could be transferred from small micelles to concentrated liquid crystals with increasing concentration of surfactants (*38*). It is noteworthy that the effects of additives on the partitioning behaviors of penicillin are different in ILATPS and MILWS. In MILWS, ln *K* shows little dependence on the salt concentration or species, as well as the ionic liquids species, while in ILATPS, evident dependence of ln *K* on these factors is noticed. The phenomena suggest that the mechanisms for partitioning in ILATPS and MILWS are different.

Conclusions

In this work, an integrated process based on ionic liquids aqueous solution is proposed for the separation and enzymatic hydrolysis of penicillin G. The substrate is extracted into the ionic liquids-rich phase of ILATPS and back-extracted into the residual water after ILATPS is phase transferred into MILWS with the introduction of hydrophobic ionic liquids. A Flory-Huggins model is employed to elucidate the different partitioning behaviors in ILATPS and MILWS. It suggests that a uniform ln K-Δ[ionic liquids] relationship could be established in the two systems, and the formulation is governed by the energy equilibrium among conformational entropy, self-energy, and the hydration repulsion in the ionic liquids aqueous system. When Δ[ionic liquids] is relatively small in ILATPS, the long-range self-energy dominates the partitioning behaviors of penicillin, which leads to a proportional increase in ln K with Δ[ionic liquids]. On the contrary, when Δ[ionic liquids] is sufficiently large in MILWS, the effect of self-energy is overwhelmed by the short-range entropy loss. Moreover, the low water polarity in MILWS might increase hydration repulsion between ionic liquids micelle and solute, which leads to a low partitioning ratio of penicillin as that in [C_4mim]PF_6/water system when Δ[ionic liquids] is sufficiently large.

Downloaded by UNIV OF GUELPH LIBRARY on June 22, 2012 | http://pubs.acs.org
Publication Date (Web): April 28, 2010 | doi: 10.1021/bk-2010-1038.ch006

Acknowledgments

This work is financially supported by National High Technology Research and Development Program of China (863 Program) (No. 2006AA02Z215), 2006 key project of advanced industrial biotechnology innovation foundation of Chinese Academy of Sciences (No. KSCX2-YW-G-019), Advanced Research Project of Institute of Processing Engineering, CAS (2007-072701), and National Natural Science Foundation of China (No. 90610007).

References

1. Barenschee, T.; Scheper, T.; Schogerl, K. *J. Biotechnol.* **1992**, *26*, 143–154.
2. Arroyo, M.; De la Mata, I.; Acebal, C.; Castillon, M. P. *Appl. Microb. Biotechnol.* **1993**, *60*, L507–514.
3. Abian, O.; Mateo, C.; Fernandez-Lorente, G.; Guisan, J. M.; Fernandez-Lafuentz, R. *Biotechnol. Prog.* **2003**, *19*, 1639–1642.
4. Shewale, J. G.; Sivaraman, H. *Proc. Biochem.* **1989**, *24*, 146–157.
5. Chen, J.; Spear, S. K.; Huddleston, J. G.; Rogers, R. D. *Green Chem.* **2005**, *7*, 64–82.
6. Walter, H.; Johansson, G.; Brooks, D. E. *Anal. Biochem.* **1991**, *197*, 1–18.
7. Rogers, R. D.; Willauer, H. D.; Griffin, S. T.; Huddleston, J. G. *J. Chromatogr., B* **1998**, *711*, 255–263.
8. Liu, C.-l.; Kamei, D. T.; King, J. A.; Wang, D. I. C.; Blankschtein, D. *J. Chromatogr., B* **1998**, *711*, 127–138.
9. Eiteman, M. A.; Gainer, J. L. *Sep. Sci. Technol.* **1992**, *27*, 313–324.
10. Kaul R. *Aqueous Two-Phase Systems*; Humnan Press: Totowa, N. J., 1998.
11. Gulyaeva, N.; Zaslavsky, A.; Lechner, P.; Chait, P.; Zaslavsky, B. *J. Chromatogr., B* **2002**, *743*, 187–191.
12. Abbott, N. J.; Blankschtein, D.; Hatton, T. A. *Macromolecules* **1991**, *24*, 4334–4348.
13. Baskir, J. N.; Hatton, T. A.; Sweeu, U. *J. Phys. Chem.* **1989**, *93*, 2111–2123.

14. Walter, H.; Brooks, D. E.; Fisher, D. *Partitioning in Two-Phase Aqueous Systems*; Academic Press: Orlando, FL, 1985.
15. Visser, A. E. S.; Swatloski, S.; Reichert, W. M.; Mayton, R.; Sheff, W.; Wierzbichi, A.; Davis, J. H., Jr.; Rogers, R. D. *Chem. Commun.* **2001**, *56*, 135–137.
16. Dai, S.; Ju, Y. H.; Barnes, C. F. *J. Chem. Soc., Dalton. Trans. I.* **1999**, 1201–1202.
17. Wasserscheid, P.; Keim, W. *Angew. Chem., Int. Ed.* **2000**, *39*, 3773–3789.
18. Rogers, R. D.; Seddon, K. R. *Science* **2003**, *302*, 792–793.
19. Blanchard, L. A.; Hancu, D.; Backman, E. J. *Nature* **1999**, *399*, 28–29.
20. Gutowski, K. E.; Rogers, R. D. *J. Am. Chem. Soc.* **2003**, *125*, 6632–6633.
21. Liu; , Q. FYu, J.; Li, W. L.; Hu, X. S.; Xia, H. S.; Liu, H. Z. *Sep. Sci. Technol.* **2006**, *41*, 2849–2857.
22. Willaure, H. D.; Huddleston, J. G.; Rogers, R. D. *Ind. Eng. Chem. Res.* **2002**, *41*, 1892–1904.
23. Galaev, I. Y.; Mattiasson, B. *Enzyme Microb. Technol.* **1993**, *15*, 354–366.
24. Lü, X. Y.; Li, D. J.; Huang, Y.; Zhang, Y. Y. *Surf. Coat. Technol.* **2007**, *201*, 6843–6846.
25. Scholz, E. *Karl Fisher Titration*; Spriger Verlag Press: Berlin, 1983; pp 24−35.
26. Liu, Q. F.; Hu, X. S.; Wang, Y. H.; Yang, P.; Xia, H. S.; Yu, J.; Liu, H. Z. *Chinese Sci. Bull.* **2005**, *50*, 1582–1588.
27. Fieldenm, M. L.; Hayes, R. A.; Ralston, J. *Langmuir* **1996**, *12*, 3721–3727.
28. Leneveu, D. M.; Rand, R. P.; Parsegian, V. A.; Gingell, D. *Biophys. J.* **1997**, *18*, 209–230.
29. Israelachvili, J. N.; Wennerstrom, H. *J. Phys. Chem.* **1992**, *96*, 520–531.
30. Kokkoli, E.; Zukoski, F. *Langmuir* **1998**, *14*, 1189–1195.
31. Forsman, J.; Jonsson, B.; Woodward, C. E.; Wennerstrom, H. *J. Phys. Chem.* **1997**, *101*, 4253–4259.
32. Parker, J. L.; Claesson, P. M. *J. Phys. Chem.* **1994**, *98*, 8468–8480.
33. Guan, Y. X.; Zhu, Z. Q.; Mei, L. H. *Sep. Sci. Technol.* **1996**, *131*, 2589–2594.
34. Yaminsky, V. V.; Ninham, B.W. *Langmuir* **1993**, *9*, 3618–3624.
35. de Gennes, P. G.; Taupin, C. *J. Phys. Chem.* **1982**, *86*, 2294–2304.
36. Flory, J. *Principles of Polymer Chemistry*; Connell University Press: New York, 1953.
37. Pfennig, A.; Schwerin, A.; Gaube, J. *J . Chromatogr., B* **1998**, *711*, 45–52.
38. Angel, M.; Hoffmann, H.; Lobl, M.; Reizlein, K.; Thurn, H.; Wunderlich, A. *Prog. Colloid Polym. Sci.* **1984**, *69*, 12–28.

Downloaded by UNIV OF GUELPH LIBRARY on June 22, 2012 | http://pubs.acs.org
Publication Date (Web): April 28, 2010 | doi: 10.1021/bk-2010-1038.ch006

Downloaded by CORNELL UNIV on June 22, 2012 | http://pubs.acs.org
Publication Date (Web): April 28, 2010 | doi: 10.1021/bk-2010-1038.ch007

Chapter 7

Enzymatic Hydrolysis of Penicillin in an Integrated System Containing Ionic Liquids

Yangyang Jiang,[1,2] Chen Guo,[1] Hansong Xia,[1] and Huizhou Liu*,[1]

[1]Laboratory of Separation Science and Engineering, Key Laboratory of Green Process and Engineering, State Key Laboratory of Biochemical Engineering, Institute of Process Engineering, Chinese Academy of Sciences, Beijing 100190, China
[2] Graduate School of the Chinese Academy of Science, Beijing 100039, China
***To whom correspondence should be addressed.**
Tel. & Fax: (8610) 62554264. E-mail: hzliu@home.ipe.ac.cn.

Ionic liquids were employed as novel green solvents to develop an integrated process involving ionic liquids aqueous two-phase system (ILATPS) and mixed ionic liquids/water two-phase system (MILWS) for separation and enzymatic catalysis of penicillin. First, hydrophilic [C_4mim]BF_4 (1-butyl-3-methylimidazolium tetrafluoroborate) and NaH_2PO_4 salt form an ionic liquid aqueous two-phase system (ILATPS), which could extract penicillin from its fermentation broth efficiently. Second, hydrophobic [C_4mim]PF_6 (1-butyl-3-methylimidazolium hexafluorophosphate) is introduced into the ionic liquid-rich phase of ILATPS containing penicillin and converses it into MILWS. Penicillin is hydrolyzed by penicillin acylase in the water phase of MILWS at pH 5. The byproduct phenylacetic acid (PAA) is partitioned into the ionic liquids mixture phase, while the intended product 6-aminopenicillanic acid (6-APA) is precipitated at this pH. In comparison with a similar butyl acetate/water system (BAWS) at pH 4, MILWS exhibits two advantages: (1) The selectivity between PAA and penicillin is greatly optimized at pH 5 by varying the mole ratio of [C_4mim]PF_6/[C_4mim]BF_4 in MILWS, whereas in BAWS the unalterable nature of the organic solvent restricts the optimized pH for maximum selectivity between PAA and penicillin at pH 4. (2) The pH for 6-APA precipitation

In Ionic Liquid Applications: Pharmaceuticals, Therapeutics, and Biotechnology; Malhotra, S.;
ACS Symposium Series; American Chemical Society: Washington, DC, 0.

in BAWS is 4, whereas it shifts to pH 5 in MILWS due to the complexation between negatively charged 6-APA and the cationic surface of the ionic liquids micelle. As a result, the removal of the two products from the enzyme sphere at relatively high pH is permitted in MILWS, which is beneficial for enzymatic activity and stability in comparison with the acidic pH 4 environment in BAWS.

Introduction

6-APA is an important biomaterial for manufacturing semi-synthetic antibiotics (*1–3*). It is the intended product of penicillin hydrolysis by penicillin acylase in water at pH 7.5-8 (*4*) (Figure 1). To recover the product, the pH in a 6-APA solution is lowered to 2 for extraction with MIBK (methyl isobutyl ketone), increased to pH 7 for concentration, and finally adjusted to pH 4 for precipitation of the 6-APA (the isoelectric point, IEP) (*5*). The aqueous route exhibits several shortcomings: (1) The acidic byproduct PAA is produced continuously, which lowers the pH in water and decreases the enzymatic activity and stability. If pH adjustment is employed to maintain the pH within 7-8, waste salt starts forming. (2) Penicillin, PAA, and 6-APA all are inhibitors for penicillin acylase (*6*).

To reduce the inhibitive effects, various methods integrated with the in situ separation of product onto the hydrolysis of penicillin were proposed. Andersson and Hahn-Hägerdal (*7*, *8*) developed an integrated process to separate two products from the enzyme solution in a PEG20M/KH_2PO_4 aqueous two-phase (ATP) system. He found that two products, 6-APA and PAA, were transferred into the polymer-rich phase, while enzyme remained in the salt-rich phase, which greatly reduced the product inhibition. However, the polymer ATP system had three drawbacks: (1) Penicillin resides in the polymer-rich phase, so the efficient contact between catalyst and substrate is limited. (2) Due to the high water content in ATP, the H^+ ion dissociated from PAA cannot be neutralized by phosphate-buffered salt, so pH adjustment is still required. (3) The 6-APA and PAA in the polymer-rich phase need further separation after the reaction.

To overcome these shortcomings, Diender et al. (*9*) and Ferreira et al. (*10*) developed an integrated process based on a butyl acetate/water system (BAWS), in which penicillin was hydrolyzed by penicillin acylase in the aqueous phase, while the byproduct PAA was transferred into the butyl acetate phase. Chilov and Svedas (*11*) had given a thermodynamic and kinetic description for the novel system. The major merit of this process was its low operational pH around 3.5-4.4, which protonated the acidic product PAA into the organic phase and kept a constant pH in water (*9*). Another merit was its excellent ability to separate 6-APA from the aqueous phase in situ at pH close to the IEP of 6-APA (*12*). Third, the product inhibition of enzyme was reduced in BAWS due to the spontaneous separation of PAA from the catalyst (*11*).

Downloaded by CORNELL UNIV on June 22, 2012 | http://pubs.acs.org
Publication Date (Web): April 28, 2010 | doi: 10.1021/bk-2010-1038.ch007

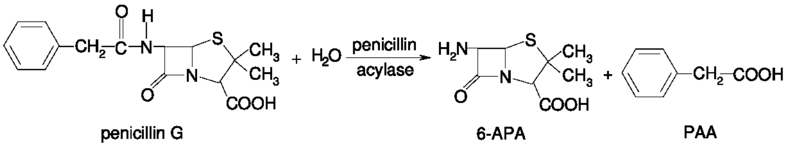
penicillin
acylase
penicillin G
6-APA
PAA

Figure 1. Process for enzymatic hydrolysis of penicillin.

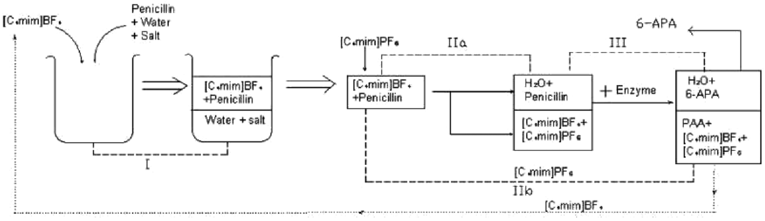
[C₄mim]BF₄
Penicillin
+ Water
+ Salt
[C₄mim]BF₄
+Penicillin
Water + salt
I
[C₄mim]PF₆
IIa
[C₄mim]BF₄
+Penicillin
H₂O+
Penicillin
[C₄mim]BF₄+
[C₄mim]PF₆
+ Enzyme
III
6-APA
H₂O+
6-APA
PAA+
[C₄mim]BF₄+
[C₄mim]PF₆
[C₄mim]PF₆
IIb
[C₄mim]BF₄

Figure 2. Integrated process for separation, recovery, and hydrolysis of penicillin in ionic liquids aqueous solution. Step I: Extraction of penicillin into the ionic liquids-rich phase of ILATPS. Step IIa: Recovery of penicillin into the residual water of MILWS. Step IIb: Thermal separation of hydrophilic [C_4mim]BF_4 from [C_4mim]PF_6 and recycling of it into formation of ILATPS and MILWS. Step III: Enzymatic hydrolysis of penicillin to product 6-APA in MILWS.

Despite these merits, BAWS shows several shortcomings: (1) Enzymatic activity and stability were seriously inhibited at low pH (*13*). (2) From a practical point of view, the task to maintain total PAA in the organic phase of BAWS was infeasible (due to 30% PAA remaining in water), so the pH could not maintain a constant value in BAWS during the hydrolytic process. For this reason, the pH deviated from the IEP of 6-APA, which led to a low efficiency for 6-APA precipitation (*9*). (3) In order to slow down the rate of penicillin decomposition, low temperature of 25 °C has to be employed in BAWS (*9*), which decreases the enzymatic activity and the final yield of 6-APA (*14*). (4) The volatile organic solvent pollutes the environment.

Ionic liquids are novel liquid salts with negative volatile pressure, tunable structure, and interesting properties (*15*, *16*), which are widely utilized in catalysis, extraction, and material science (*17–23*). In this study, ionic liquids are employed to develop a novel integrated process involving ionic liquid aqueous two-phase system (ILATPS) and mixed ionic liquids/water two-phase system (MILWS) for separation and enzymatic catalysis of penicillin (Figure 2).

Downloaded by CORNELL UNIV on June 22, 2012 | http://pubs.acs.org
Publication Date (Web): April 28, 2010 | doi: 10.1021/bk-2010-1038.ch007

Experimental Section

Preparation of Ionic Liquids

A 1:1.15 mol ratio of *N*-methylimidazole and bromobutane was added into a flask and the solution was agitated at 70 °C for 24 h. After cooling down, an equal volume of ethyl acetate was mixed with the sample and extracted twice. The sample was evaporated, and the product [C_4mim]Br (1-butyl-3-methylimidazolium bromide) was obtained. [C_4mim]Br was subjected to a metathesis with the intended anion, such as BF_4^- or PF_6^-, at room temperature for 24 h. The aqueous solution, so obtained was extracted with CH_2Cl_2 and washed with water until no Br^- ion was found. After evaporation for 8 h, the product [C_4mim]BF_4 or [C_4mim]PF_6 was obtained.

Downloaded by CORNELL UNIV on June 22, 2012 | http://pubs.acs.org
Publication Date (Web): April 28, 2010 | doi: 10.1021/bk-2010-1038.ch007

Formation of MILWS

A 15 ml ILATPS was formed with 35% [C_4mim]BF_4 and 15% NaH_2PO_4 salt, in which penicillin was extracted into the ionic liquid-rich phase from its fermentation broth. A 5ml sample of the ionic liquid-rich phase was removed from ILATPS, and its [C_4mim]BF_4 concentration was measured with HPLC. Then, 0.5 or 2 times of mole concentration of [C_4mim]PF_6 with respect to [C_4mim]BF_4 was introduced into the ionic liquid-rich phase. The two–phase system was centrifuged at 4000 rpm for 5 min.

Partitioning of Penicillin and PAA in MILWS

First, 0.1 g penicillin and 0.07 g PAA were introduced into 10 ml of MILWS with a predefined [C_4mim]PF_6/[C_4mim]BF_4 ratio. The mixture was stirred and centrifuged at 4000 rpm for 10 min. The penicillin and PAA concentrations in the hydrophobic ionic liquids mixture and water phase were measured with HPLC (HP1100 system, Agilent corporation, equipped with 250 mm×4 mm Zorbax SB-C18 column and DAO detector at 254 nm, the mobile phase was methanol:0.05 M phosphate at pH 3 at 36:64 v/v, flow rate at 1 ml/min). The partitioning ratio *K* of PAA and penicillin, as well as the selectivity *S* between them were obtained from eq 1:

$$K = \frac{\text{solute concentration in the ionic liquids phase}}{\text{solute concentration in the aqueous phase}}$$
$$S = \frac{\text{partitioning ratio of PAA in MILWS}}{\text{partitioning ratio of penicillin in MILWS}} \qquad (1)$$

Downloaded by CORNELL UNIV on June 22, 2012 | http://pubs.acs.org
Publication Date (Web): April 28, 2010 | doi: 10.1021/bk-2010-1038.ch007

IEP of 6-APA in MILWS

First, 0.1 g of 6-APA was added into a 20 ml MILWS containing a predefined [C_4mim]PF_6/[C_4mim]BF_4 ratio and 2% phosphate buffer. The system was stirred with a magnetic stirrer for 5 min. The pH in MILWS was adjusted by phosphate acid at room temperature under the inspection of pH indicator, which was inserted into the water layer of MILWS. After full phase equilibrium was reached, the final pH in the water phase was recorded with the pH indicator. Then a 3 ml sample was taken out carefully from the aqueous phase of MILWS, and its absorbance at 430 nm was checked with UV-Vis spectrometer (Perkin Elmer Corporation, Lambda Bio 40). The procedure was repeated at different pH levels until the optimized pH corresponding to the maximum absorbance of the aqueous sample was reached, which was the IEP of 6-APA in MILWS.

Enzymatic Activity and Stability in MILWS

A 30 ml MILWS containing equal volumes of ionic liquids and water was prewarmed at 37 °C, into which 0.01 g penicillin and 50 µl enzyme solution were introduced. Every 1.5 min, 0.6 ml samples were taken out from the ionic liquids and water phases, respectively, and the concentrations of PAA and penicillin in the two samples were measured with HPLC. The enzymatic activity was calculated from the average PAA concentration in the ionic liquids and water phases of MILWS (eq 2) after the initial 5 min (*4*).

$$\overline{C}_{PAA} = \frac{V^{IL}C^{IL}_{PAA} + V^{w}C^{w}_{PAA}}{V^{IL} + V^{w}} \qquad (2)$$

Where C_{PAA} is the average concentration of PAA in MILWS; C^{IL}_{PAA} and C^{W}_{PAA} are the PAA concentrations in the ionic liquids phase and water phase, respectively; V^{IL} and V^{W} are the volumes of ionic liquids and water phases in MILWS.

To measure the enzymatic stability in MILWS, 50 µl enzyme solution was prewarmed in 30 ml MILWS at a certain temperature for 30 min, and the enzymatic activity was measured by the method described above (*4*). The half-life of the enzyme was obtained from the kinetics model in eq 3 (*24*).

$$t_0 = -\ln 2 * 0.5 \Big/ \ln\left(\frac{A_{30}}{A_0}\right) \qquad (3)$$

where A_0 and A_{30} represent the enzymatic activity at 0 time and after 30 min, respectively, being prewarmed at one certain temperature. The t_0 term refers to the half-life (hours) of enzyme in MIILWS.

Ionic Liquids Concentration in the Residual Water of MILWS

A 0.5 ml sample was taken out from the residual water of MILWS. After being diluted 50 times by water, the absorbance at 235 nm of the residual water was inspected by UV-Vis spectrometer.

Results

Partitioning Ratios of Penicillin and PAA in MILWS

Effect of Mole Ratio of [C_4mim]PF_6 to [C_4mim]BF_4

It is well known that the reaction equilibrium in any two-phase system depends on the partitioning ratios between substrates and products. The selectivity between PAA and penicillin is adjustable with varying the [C_4mim]PF_6/[C_4mim]BF_4 ratio in MILWS. Figure 3 shows the partitioning ratios of penicillin, PAA and 6-APA in MILWS as functions of [C_4mim]PF_6/[C_4mim]BF_4 ratio. 6-APA primarily resides in water due to its zwitterionic nature, which facilitates its separation from penicillin and PAA after the reaction (*11*). In contrast, penicillin and PAA prefer to reside in ionic liquids phase, and their partitioning ratios increase from 0.08 (ln *K*=-2.5) to 12.5 (ln *K*=2.5) when the [C_4mim]PF_6/[C_4mim]BF_4 ratio decreases from 2.5 to 0.25. It is noteworthy that the relationships between ln *K* and [C_4mim]PF_6/[C_4mim]BF_4 ratio are quite different for PAA and penicillin. PAA begins to increase its ln *K* after [C_4mm]PF_6/[C_4mim]BF_4 ratio below 2.5, whereas the ln *K* of penicillin rises up only when [C_4mm]PF_6/[C_4mim]BF_4 ratio is below 1.5.

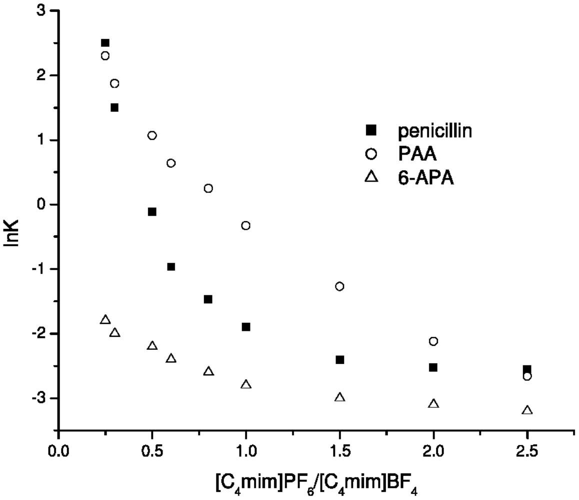

Figure 3. Partitioning ratios of penicillin, PAA and 6-APA in MILWS at pH 4.5 (containing 2% potassium phosphate).

Downloaded by CORNELL UNIV on June 22, 2012 | http://pubs.acs.org
Publication Date (Web): April 28, 2010 | doi: 10.1021/bk-2010-1038.ch007

Downloaded by CORNELL UNIV on June 22, 2012 | http://pubs.acs.org
Publication Date (Web): April 28, 2010 | doi: 10.1021/bk-2010-1038.ch007

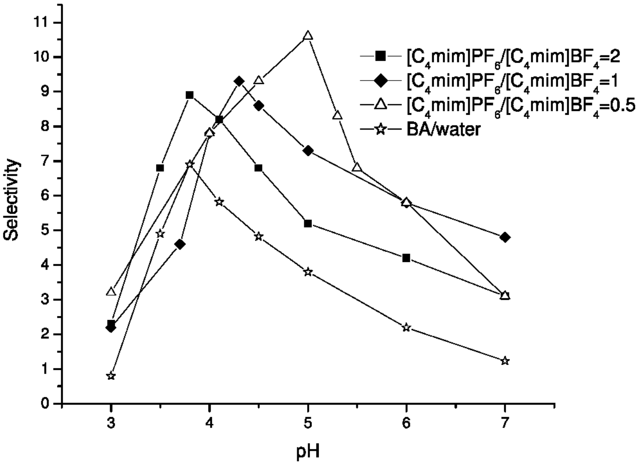

Figure 4. Selectivity between PAA and penicillin versus pH in MILWS at various [C_4mim]PF_6/[C_4mim]BF_4 ratio (with 2% potassium phosphate).

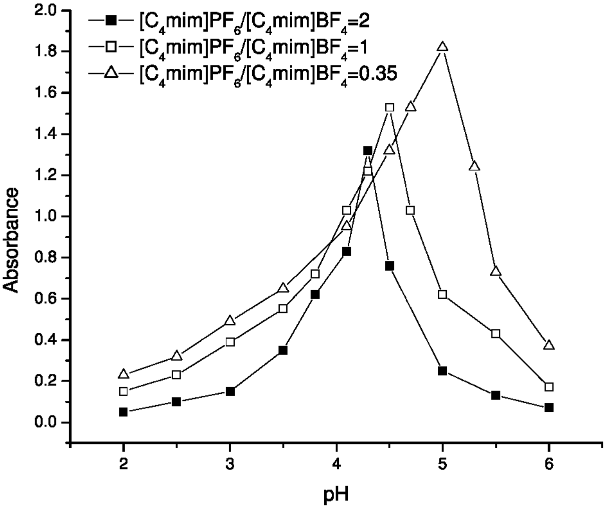

Figure 5. Absorbance of the water phase containing 6-APA in MILWS at various pH and different [C_4mim]PF_6/[C_4mim]BF_4 ratios (with 2% potassium phosphate).

Downloaded by CORNELL UNIV on June 22, 2012 | http://pubs.acs.org
Publication Date (Web): April 28, 2010 | doi: 10.1021/bk-2010-1038.ch007

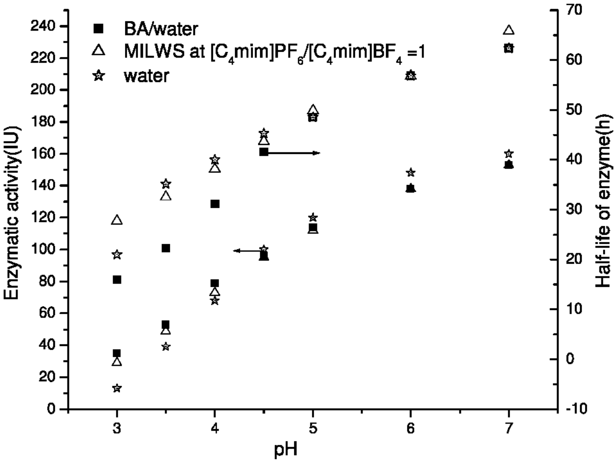

Figure 6. Enzymatic activity and stability as a function of pH in water, BAWS and MILWS with 0.5 molar ratio of [C_4mim]PF_6/[C_4mim]BF_4 (with 2% phosphate concentration).

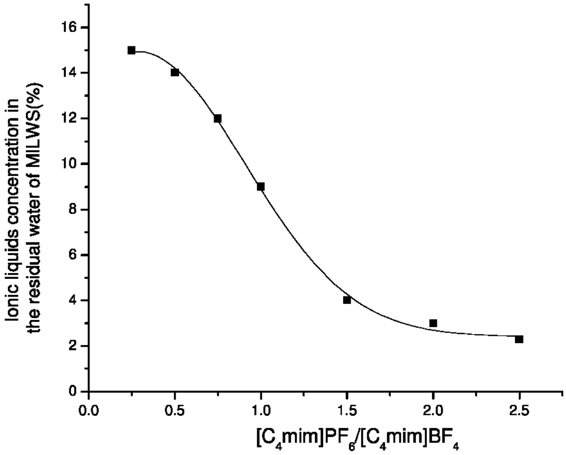

Figure 7. Ionic liquids concentration in the residual aqueous phase as a function of [C_4mim]PF_6/[C_4mim]BF_4 ratio in MILWS (with 2% potassium phosphate).

Influence of pH

In addition to the [C_4mim]PF_6/[C_4mim]BF_4 ratio, pH is another vital parameter for optimization of the selectivity. Figure 4 shows that the selectivity between PAA and penicillin reaches its maximum at a certain pH and then falls when the pH reduces further. The optimized pH with respect to the maximum selectivity in MILWS increases inversely with the [C_4mm]PF_6/[C_4mim]BF_4 ratio. When the [C_4mm]PF_6/[C_4mim]BF_4 ratio decreases from 2 to 0.5, the optimized pH in MILWS shifts from pH 3.8 to 5.

IEP of 6-APA

In addition to the selectivity between PAA and penicillin, the in situ precipitation of 6-APA is another driving force for the reaction equilibrium in MILWS (*25*). Generally, the IEP of 6-APA is pH 4.3 in an aqueous system (*4*), which means that enzymatic hydrolysis of penicillin has to be carried out at the extreme low pH if an optimized reaction equilibrium is desirable.

The situation is quite different in MILWS. Figure 5 shows the IEP of 6-APA in MILWS as a function of the [C_4mim]PF_6/[C_4mim]BF_4 ratio. When the mole ratio of [C_4mim]PF_6/[C_4mim]BF_4 decreases from 2 to 0.35, the apparent IEP of 6-APA shifts from pH 4.3 to 5. The increasing pH in MILWS made it more appealing for the enzymatic hydrolysis in comparison with that in BAWS at pH 4. The increase in IEP of 6-APA at a small [C_4mim]PF_6/[C_4mim]BF_4 ratio may be attributed to the complex formation between 6-APA and the cationic surface of ionic liquids micelle in MILWS. The 6-APA molecule is negatively charged at pH 5, which is preferable to form a complex with the positively charged micellar surface. As a result, the supramolecule with small charges prefers to be precipitated at higher IEP in comparison with the 6-APA molecule alone (*26*).

Enzymatic Activity and Stability in MILWS

Influence of pH

Although the reaction equilibrium in MILWS could be optimized at pH 5 (Figure 4 and 5), is it doubtful whether the enzymatic activity and stability could be well preserved at this acidic pH? Figure 6 compares the enzymatic activity and stability in MILWS and BAWS at different pH. It is found that the enzymatic activity in BAWS drops from 118 IU to 63 IU when the pH shifts from 5 to 4, while the enzymatic half-life decreases from 43 to 31 h (*27*). The results suggest that although pH 4 is favorable environment for the reaction equilibrium in BAWS, it is not satisfactory for enzyme performance.

The inherent conflict between enzyme performance and reaction equilibrium in BAWS may be partially overcome in MILWS. It is found in Figure 6 that the enzymatic performance changes much more slowly with decreasing pH in MILWS than in BAWS. Although similar enzymatic performances are found at pH 5 in MILWS and in BAWS, obvious advantage is found in MILWS at pH 4 in comparison with that in BAWS at pH 4. Moreover, it has been suggested that the reaction equilibrium is well optimized in MILWS at pH 5 (Figure 4 and 5). Therefore, pH 5 is a favorable condition not only for the reaction equilibrium, but also for the enzymatic performance in MILWS, whereas the reaction equilibrium and enzymatic performance in BAWS could not be optimized at the same pH.

Downloaded by CORNELL UNIV on June 22, 2012 | http://pubs.acs.org
Publication Date (Web): April 28, 2010 | doi: 10.1021/bk-2010-1038.ch007

Downloaded by CORNELL UNIV on June 22, 2012 | http://pubs.acs.org
Publication Date (Web): April 28, 2010 | doi: 10.1021/bk-2010-1038.ch007

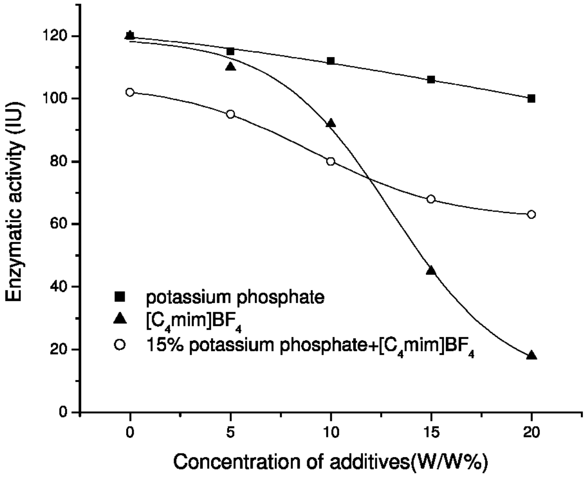

Figure 8. Effect of the concentrations of ionic liquids and inorganic salts on the enzymatic activity in aqueous solution at pH 5.

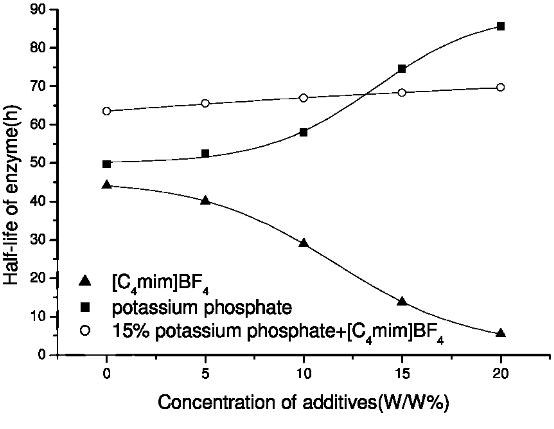

Figure 9. Half-life of enzyme as a function of the concentration of ionic liquids or salt in aqueous solution at pH 5.

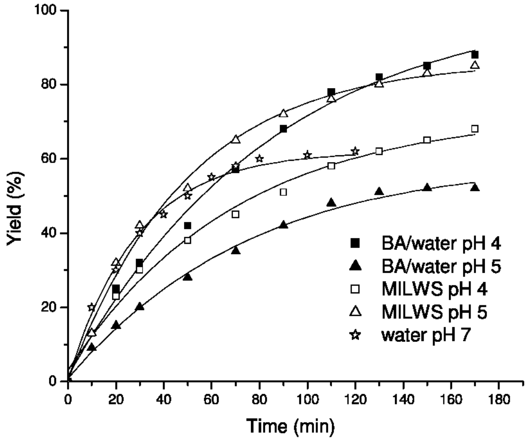

Figure 10. Comparison of the 6-APA yield in MILWS and BAWS (with 2% potassium phosphate, $[C_4mim]PF_6/[C_4mim]BF_4=0.5$).

Influence of the Ionic Liquids Concentration

Although the reaction equilibrium and enzymatic efficiency could be optimized at pH 5 in MILWS, it is necessary to employ a small $[C_4mim]PF_6/[C_4mim]BF_4$ ratio, which increases the residual concentration of ionic liquids in the aqueous phase of MILWS (Figure 7). It was suggested by Kim and Lee (*28*) that a high concentration of additives in water will decrease the enzyme activity seriously. Would the relatively high ionic liquids concentration suppress the enzyme activity in MILWS?

Figure 8 gives the enzymatic activity as a function of the additives' concentration in MILWS at pH 5. It is shown that when the concentration of phosphate salt increases from 0 to 20%, the enzymatic activity decreases slowly from 120 to 105 IU, which suggests that phosphate salt is a "safe" additive for the enzymatic performance. In the absence of buffer salt, the enzymatic activity drops dramatically from 120 IU to 18 IU with increase of the $[C_4mim]BF_4$ concentration from 0 to 20%, i.e. 85% enzyme lost its activity during the course. In sharp contrast, when 15% phosphate salt is employed in ionic liquids aqueous solution, the enzymatic activity shows only a small dependence on the ionic liquids concentration.

Similar effects of pH exist in regard to the enzymatic half-life (Figure 9). With increase in the concentration of potassium phosphate to 20%, the enzymatic stability rises up from 52 to 80 h. In the absence of buffer salt, the enzyme stability decreases from 44 h to 3.7 h when the $[C_4mim]BF_4$ concentration increases to 20%. When 15% potassium phosphate is employed, the half-life of enzyme remains almost constant in the entire concentration range of $[C_4mim]BF_4$. These observations suggested that ionic liquids facilitate the enzymatic catalysis in the presence of buffer salt (*29*), despite its negative role for the enzymatic activity when it is alone.

Downloaded by CORNELL UNIV on June 22, 2012 | http://pubs.acs.org
Publication Date (Web): April 28, 2010 | doi: 10.1021/bk-2010-1038.ch007

Downloaded by CORNELL UNIV on June 22, 2012 | http://pubs.acs.org
Publication Date (Web): April 28, 2010 | doi: 10.1021/bk-2010-1038.ch007

Dynamics of Enzymatic Catalysis

Figure 10 compares the overall 6-APA yields in MILWS, BAWS and water during the catalytic course. It is found that the final yield of 6-APA is 88% at pH 4 in BAWS, and it decreases to 52% at pH 5, in line with Hollander's observation (*30*). On the contrary, the final yield of 6-APA in MILWS increases from 63% to 85% when pH increases from 4 to 5. The better performance in MILWS at pH 5 may be due to the higher selectivity between PAA and penicillin and favorable 6-APA precipitation, as well as the improved enzymatic activity at pH 5 as compared to that in BAWS at pH 4 (Figure 4 and 5). In contrast, the 6-APA yield in the aqueous phase system at pH 7 increased evidently at the initial time and soon reached its equilibrium after 80 min. But the overall 6-APA yield was only 60%, which is smaller than that in MILWS and BAWS. The reason may be due to the coexistence of two products with the enzyme solution, which leads to a strong product inhibition and lower enzymatic activity at acidic pH in water.

Conclusions

The enzymatic hydrolysis of penicillin in a mixed ionic liquids/water two-phase system is explored. It is found that the $[C_4mim]PF_6/[C_4mim]BF_4$ ratio plays an essential role in optimizing the reaction equilibrium and enzymatic performance in MILWS. A small $[C_4mim]PF_6/[C_4mim]BF_4$ ratio favors the removal of two products from the aqueous solution (including the extraction of PAA and precipitation of 6-APA) at relatively high pH. As a result, not only is the reaction equilibrium in MILWS optimized, but also the enzymatic activity and stability are improved as a result of the favorable acidic environment in comparison with the extreme acidic condition in BA/water system at pH 4.

Acknowledgments

This work is financially supported by National High Technology Research and Development Program of China (863 Program) (No. 2006AA02Z215), 2006 key project of advanced industrial biotechnology innovation foundation of Chinese Academy of Sciences (No. KSCX2-YW-G-019), Advanced Research Project of Institute of Processing Engineering, CAS (2007-072701), and National Natural Science Foundation of China (No. 90610007).

References

1. Barenschee, T.; Scheper, T.; Schügerl, K. *J. Biotechnol.* **1992**, *26*, 143–154.
2. Van de Sandt, E. J. A. X.; van de Vroom, E. *Chim. Oggi.* **2000**, *18*, 72–75.
3. Arroyo, M.; De la Mata, I.; Acebal, C.; Castillon, M. P. *Appl. Microb. Biotechnol.* **2003**, *60*, 507–514.

4. Abian, O.; Mateo, C.; Fernandez-Lorente, G.; Guisan, J. M.; Fernandez-Lafuentz, G. *Biotechnol. Prog.* **2003**, *19*, 1639–1642.
5. Bora, M. M.; Ghosh, A. C.; Dutta, N. N.; Mathur, R. K. *Can. J. Chem. Eng.* **1997**, *75*, 520–526.
6. Harrison, F. G.; Gibson, E. D. *Process Biochem.* **1984**, *19*, 33–36.
7. Andersson, E.; Hahn-Hägerdal, B. *Biochim. Biophys. Acta* **1987**, *912*, 317–324.
8. Andersson, E.; Hahn-Hägerdal, B. *Biochim. Biophys. Acta* **1987**, *912*, 325–328.
9. Diender, M. B.; Straathof, A. J. J.; van der Does, T.; Ras, C.; Heijnen, J. J. *Biotechnol. Bioeng.* **2002**, *78*, 395–402.
10. Ferreira, J. S.; Straathof, A. J. J.; Tranco, T. T.; Van der Wielen, L. A. M. *J. Mol. Catal. B: Enzym.* **2004**, *27*, 29–35.
11. Chilov, G. G.; Svedas, V. K. *Can. J. Chem.* **2002**, *80*, 699–707.
12. Mwangi, S. M. Reactive Precipitation of 6-Amimopenicillanic Acid: Application of a Crystallization Methodology; Ph.D. Thesis, University of Manchester, U.K., 1994.
13. Schroen, C. G. P. H.; Nierstraze, V. A.; Kroon, P. J.; Bosma, R.; Janssen, A. E. M.; Beeftink, H. H.; Tramper, J. *Enzyme Microb. Technol.* **1999**, *24*, 498–507.
14. Illanes, A.; Fajardo, A. *J. Mol. Catal. B: Enzym.* **2001**, *11*, 587–593.
15. Visser, A. E. S.; Swatloski, S.; Reichert, W. M.; Mayton, R.; Sheff, W.; Wierzbichi, A.; Davis, J. H., Jr.; Rogers, R. D. *Chem. Commun.* **2001**, *56*, 135–137.
16. Dai, S.; Ju, Y. H.; Barnes, C. F. *J. Chem. Soc. Dalton. Trans.* **1999**, 1201–1202.
17. Dupon, J.; Suarez, P. A. Z.; de Souza, R. F. *Chem. Eur. J.* **2000**, *6*, 2377–2381.
18. Wasserscheid, P.; Keim, W. *Angew. Chem., Int. Ed.* **2000**, *39*, 3773–3789.
19. Seddon, K. R. *J. Chem. Technol. Biotechnol.* **1997**, *68*, 351–356.
20. Rogers, R. D.; Seddon, K. R. *Science* **2003**, *302*, 792–793.
21. Blanchard, L. A.; Hancu, D.; Backman, E. J. *Nature* **1999**, *399*, 28–29.
22. Welton, T. *Coord. Chem. Rev.* **2004**, *248*, 2459–2477.
23. Holbery, J. D.; Reichert, W. M.; Swatloski, R. P. *Green Chem.* **2002**, *4*, 407–413.
24. Walsh, C. *Enzymatic Reaction Mechanism*; W.H. Freeman: San Francisco, 1979.
25. Youshko, M. I.; van Langen, L. M.; de Vroom, E.; van Rantwjk, F.; Sheldon, R. A.; Svedas, V. K. *J. Mol. Catal. B: Enzym.* **2000**, *10*, 509–515.
26. Steed, J. W.; Atwood, J. L. *Supramolecular Chemistry*; Wiley: Chichester, U.K., 2000.
27. Masarova, J.; Mislovicova, D.; Geneiner, P.; Michalkova, E. *Biotechonol. Appl. Biochem.* **2001**, *34*, 127–133.
28. Kim, M. G.; Lee, S. B. *J. Mole. Catal. B: Enzym.* **1996**, *1*, 71–80.
29. Fernandez-Lafuentz, R.; Rosell, C. M.; Guisan, J. M. *Enzyme Microb. Technol.* **1998**, *23*, 305–310.
30. Hollander, J. L.; Zomerdijk, M.; Straathof, J. J.; vander Wielen, L. A. M. *Chem. Eng. Sci.* **2002**, *57*, 15–22.

Downloaded by CORNELL UNIV on June 22, 2012 | http://pubs.acs.org
Publication Date (Web): April 28, 2010 | doi: 10.1021/bk-2010-1038.ch007

Downloaded by DUKE UNIV on June 22, 2012 | http://pubs.acs.org
Publication Date (Web): April 28, 2010 | doi: 10.1021/bk-2010-1038.ch008

Chapter 8

Antitumor Activity of Ionic Liquids on Human Tumor Cell Lines

Vineet Kumar and Sanjay V. Malhotra*

**Laboratory of Synthetic Chemistry, SAIC-Frederick, Inc.,
National Cancer Institute at Frederick, 1050 Boyles Street,
Frederick, MD 21702, USA
*malhotrasa@mail.nih.gov**

Ionic liquids (ILs) have emerged as new class of compounds with unique properties and potential to tailor their physiochemical properties. However, very limited studies have been reported on their toxicity and safety causing concern for their use for biomedical applications, specifically as therapeutic agents and drugs. Our studies towards finding therapeutic applications of ILs for the first time demonstrated the anti-cancer activity and cytotoxicity of three different classes of ionic liquids (imidazolium, phosphonium and ammonium) on National Cancer Institute's 60 human tumor cell lines. In this chapter an overview of these results is presented through representative examples. The preleminary structure-activity relationship (SAR) showed that the chain length of alkyl substitution on the cations plays crucial role towards anti-tumor activity and cytotoxicity of ionic liquids. In general, phosphonium-based ILs were found to be more active and less cytotoxic as compared to their ammonium amd imidazolium conterparts. In-vitro cell line data and hollow fiber study has demonstrated the potential of ILs to be developed as therapeutic agent.

In Ionic Liquid Applications: Pharmaceuticals, Therapeutics, and Biotechnology; Malhotra, S.;
ACS Symposium Series; American Chemical Society: Washington, DC, 0.

Downloaded by DUKE UNIV on June 22, 2012 | http://pubs.acs.org
Publication Date (Web): April 28, 2010 | doi: 10.1021/bk-2010-1038.ch008

Introduction

Ionic liquids are rapidly growing as tunable materials with unique properties and the potential to have limitless applications in a wide variety of disciplines, making ionic liquid as new and broad area of scientific research (*1*). There has been a phenomenal growth in past two decades, resulting in few thousands of publications on ionic liquids covering different research fields e.g. synthesis, materials, speciality chemicals, etc. However, there has been only limited effort of finding their toxicity and safety (*2*). Therefore, even though ILs have found numerous applications in different areas of science and technology, the attempts of finding their usefulness in biomedical field has sofar been almost negligible.

"The poison is in the dose" has been quoted by Paracelsus, famous physician and occultist of 14th century (*3*). As such, toxicity could be a desirable property. Many toxins originally used as poisons later found to be medically important. Toxins can affect the funtioning of victim's body due to their biodynamic nature suggesting that they could potentially become vital source of medicines (*4*). Thus, understanding and managing the toxicity of small molecules is a major challenge in the discovery and development of new drugs (*5*). The development of new anti-cancer agents that reduce the toxicity associated with existing chemotherapies and those targeted at circumventing tumor resistance mechanism is a major focus of drug discovery efforts (*5*).

Once a compound is found to have desirable drug like property, its bioavalability also could become a challenge which can directly effect the efficacy. Therefore, as literature show one attractive and commonly used approach to overcome the problems of solubility and stability of 'Active Pharmaceutical Ingredients (APIs)' is their salt formation. Several acids and bases with different physico-chemical properties are utilized for this purpose with an estimated 50% of all APIs administered as salts (*6*). There are well known examples where pharmaceutically active cations and anions combine together and the resulted salt exhibits therapeutic effects of both of its components (*7*). Similar type of synergistic effect has been observed in some of the ionic liquids reported recently (*8*). Therefore, it is logical to think that ionic liquids with their tunable properties and toxicities could potentially be designed as anti-cancer, anti-viral and other therapeutic agents. These "Therapeutic Ionic Liquids" expectantly offer distinctly different properties. If therapeutic response is seen then the major advantage of ionic liquids would be in managing/tuning their toxicity while tailoring the physio-chemical and pharmacological properties necessary for desired therapeutic application. This possibility motivated us to explore the anti-cancer activity of representative imaidazolium, phosphonium and ammonium-based ionic liquids (Table 1).

Experimental

All the ionic liquids used in these study were purchased from Merck KgaA (EMD Chemicals), Darmstadt, Germany except

Downloaded by DUKE UNIV on June 22, 2012 | http://pubs.acs.org
Publication Date (Web): April 28, 2010 | doi: 10.1021/bk-2010-1038.ch008

1-methyl-3-methoxyethylimdazolium bistriflicimide ([MoemIm][Tf2N], entry 16, Table 1), which was synthesized and charactarized as reported previously (*9*).

In-Vitro Anti-Cancer Activity Evaluation Using NCI 60 Screening

Details of the methodology for NCI 60 cell line screening are described at http://dtp.nci.nih.gov/branches/btb/ivclsp.html. Briefly, the panel is organized into nine subpanels representing diverse histologies: leukemia, melanoma, and cancers of lung, colon, kidney, ovary, breast, prostate, and central nervous system (Table 2). The cells are grown in supplemented RPM1 1640 medium for 24 h. The test compounds **1–7** were dissolved in DMSO and incubated with cells at five concentrations with 10-fold dilutions, the highest being 10^{-4} M and the others being 10^{-5}, 10^{-6}, 10^{-7}, and 10^{-8} M. The assay is terminated by addition of cold trichloroacetic acid, and the cells are fixed and stained with sulforhodamine B. Bound stain is solubilized, and the absorbance is read on an automated plate reader. The cytostatic parameter i.e. 50% growth inhibition (GI_{50}) was calculated from time zero, control growth, and the five concentration level absorbance. The cytotoxic parameter i.e. inhibitory concentrations (LC_{50}) represent the average of two independent experiments. Prior of the five dose screening, all compounds were evaluated by a 10.0 μM single dose against all 60 human tumor cell, which is done by following same protocol as for five dose (*10*).

In-Vivo Anti-Cancer Activity Evaluation Using Hollow Fiber Assay

These experiments were carried out at the National Cancer Institute. The detailed protocol can be obtained from http://dtp.nci.nih.gov/branches/btb/hfa.html. In summary, a panel consisting of breast (MDA-MB-231), non-small cell lung (NCI-H23 and NCI-H522), colon (SW-620 and COLO 205), melanoma (UACC-62, MDA-MB-435 and LOXIMVI), ovarian (OVCAR-5 and OVCAR-3) and CNS (U251 and SF-295) cell lines was used to screen in vivo activity. The cell lines were cultivated in RPMI-1640, containing 10% FBS and 2mM glutamine and the suspension is flushed into 1 mm (internal diameter) polyvinylidene fluoride hollow fiber. A total of 3 different tumor lines were prepared for each experiment so that each mouse would receive 3 intraperitoneal (IP) implants (1 of each tumor line) and 3 subcutaneous (SC) implants (1 of each tumor line). The compounds were solubilized in 10% DMSO in saline/Tween 80R and mice are treated with either a high or a low dose (at 37.5 and 15mg/kg/dose) using a QD X 4 schedule (four daily treatments) administered intraperitoneally. The day after the last dose, the fibers were collected and assessed for viable cell mass using an MTT dye conversion assay. Altogether, 12 cell lines are studied resulting in 48 possible test combinations (12 cell lines x 2 sites x 2 doses). A score of 2 is assigned for each compound dose, which results in a 50% or greater reduction in viable cell mass. Compounds with a combined IP+SC score 20, a SC score 8 or a net cell kill of one or more cell lines are referred for further studies (*11*).

Downloaded by DUKE UNIV on June 22, 2012 | http://pubs.acs.org
Publication Date (Web): April 28, 2010 | doi: 10.1021/bk-2010-1038.ch008

Table 1. Ils Screened for NCI 60 Human Tumor Cell Lines

Compd #	*NSC#*	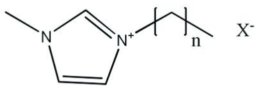		*Activity (one dose)**
		n	*X*	
1	747124	3	$(CF_3SO_2)_2N$	not active
2	747261	5	$(CF_3SO_2)_2N$	not active
3	747262	5	$(C_2F_5)_3F_3P$	not active
4	747266	7	BF_4	not active
5	747263	7	$C_8H_{17}SO_4$	not active
6	747264	7	Cl	not active
7	747265	7	PF_6	not active
8	747267	11	Cl	active
9	747268	11	BF_4	active
10	747260	15	Cl	active
11	747269	17	Cl	active
12	747270	17	PF_6	active
13	747271	17	$(CF_3SO_2)_2N$	active
14	747272	17	$(C_2F_5)_3F_3P$	active
15	747122	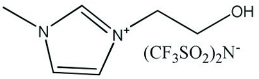		not active
16	747123	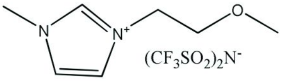		not active
18	747251	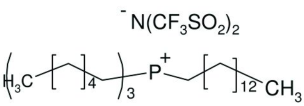		active
19	747252	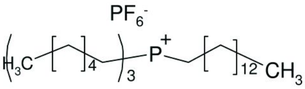		active
20	747253	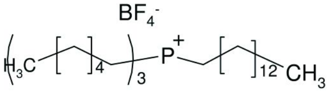		active

Continued on next page.

Table 1. (Continued). Ils Screened for NCI 60 Human Tumor Cell Lines

21	747273	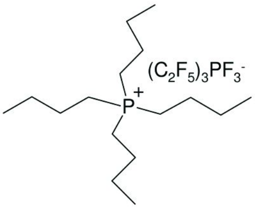	active
22	747259	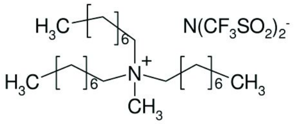	active
23	747120	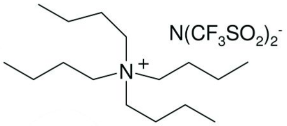	inactive
24	747121	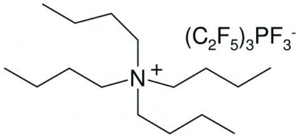	inactive
17	747125	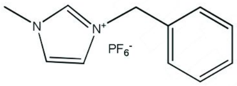	not active

* Compounds showing 60% tumor growth inhibition in 8 or more cell lines were considered to be acitve.

Downloaded by DUKE UNIV on June 22, 2012 | http://pubs.acs.org
Publication Date (Web): April 28, 2010 | doi: 10.1021/bk-2010-1038.ch008

Results and Discussion

Screening a compound in the NCI 60 cell line panel at the National Cancer Institute can potentially produce several results. The two-stage in-vitro screening process started with the evaluation of all the ionic liquids against the 60 human tumor cell lines at a single dose of 10.0 µM. The output from the single dose screen was reported as a mean graph. The number reported for the one-dose assay is growth relative to the no-drug control, and relative to the time zero number of cells. This allows detection of both growth inhibition (values between 0 and 100) and lethality (values less than 0). For example, a value of 100 means no growth inhibition. A value of 40 would mean 60% growth inhibition. A value of 0 means no net growth over the course of the experiment. A value of -40 would mean 40% lethality and a value of -100 means all cells are dead. Only the compounds which showed more then 60% of growth inhibition in atleast 8 tumor cell lines were selected for further testing and the others were assumed as inactive. A typical one dose mean graph of **18**, which was selected for five dose studies and further hollow fiber studies is given in figure 1. This primary one dose screening

Downloaded by DUKE UNIV on June 22, 2012 | http://pubs.acs.org
Publication Date (Web): April 28, 2010 | doi: 10.1021/bk-2010-1038.ch008

showed that imidazolium ILs **1**-**7** and **15**-**17** were essentially inactive, while ILs **8-14** were declared active. Similarly, all the phosponium ILs **18**-**21** and only one ammonium IL **21** were found to be active (Table 1). These prelimenary results show that the chain length of alkyl substitution on the cation is very crucial for the anticancer activity of these compounds. Compounds **1**-**7** with imidazolium cation having alkyl chain length upto C-8 were inactive, irrespective of the anions. Also, it is worth to mention that the aryl substitution or functionalization with methoxyether or hydroxy group on the short alkyl side chain of imidazolium cation does not show any improvement in the anticancer activity as observed in case of compounds **15**-**17**. When the chain length of alkyl substituents of imidazolium cation was increased to 12 or more, significant enhancement in the growth inhibition of tumor was observed in multiple cell lines. Similar results were observed in case of ammonium ILs where compounds **23** and **24** having C-4 alkyl chains were found to be inactive while **22** having C-8 alkyl chains was highly active (Table 1). Interestingly, all four phosphonium ILs **18**-**21** were found to be active in the preliminary screening even that with the short C-4 alkyl chain substitution (**21**) (*12*). This shows the importance of heteroatom of the cation in the bioactivity of ionic liquids. Once the primary screening was completed, the selected active compounds underwent for secondary five dose screening. The compounds were evaluated at five concentration levels (100, 10, 1.0, 0.1 and 0.01 μM) to generate the drug response curves and the cytostatitc (GI_{50}) and cytotoxic parameters (LC_{50}) were obtained. Typical drug response curves of compound **18** for all the 60 tumor cell lines and for individual renel cancer panel are presented in figures 2 and 3, respectively as example.

Compounds **8** (with Cl- anion) and **9** (with BF_4^- anion), both having 1-methy-3-undecylimidazolium cation showed remarkable activity against all 60 cell lines with overall potency in terms of GI_{50} values ranging from 0.109-22.60μM for **8** and 0.312-24.60μM for **9**. Also, the LC_{50} values were >100μM in most of the cases, which gives a very high therapeutic window for both of these compounds. In general, Compound **8** and **9** were found to be most sensitive to growth inhibition of leukemia cell lines indicated by GI_{50} <1μM in most of the cases with relatively higher LC_{50} values. Compound **8** was also highly active against non-small cell lung cancer cell lines EKVX and NCI-H23 and prostate cancer cell line DU-145 with GI_{50} 0.873, 0.885 and 0.688μM, respectively (cytotoxicity expressed in LC_{50} was >100μM for these cell lines).

Compound **9** exhibited GI_{50} of 0.792μM (LC_{50} >100μM) for EKVX (non-small cell lung cancer) and 0.533μM (LC_{50} >100μM) for IGROV1 (ovarian cance). As the chain length of N-3 alkyl substitution increased to C-16 and then to C-18, the compounds become more sensitive towards tumor cell lines. Compound **10** with C-16 alkyl chain length was highly active against all the tumor cell lines with overall potency of GI_{50} in the range of 0.092-2.10μM while **11** showed the GI_{50} 0.027-1.660μM for all cell lines, both having chloride as anion. However, with the increased alkyl chain length cytotoxicity also increased as seen by low LC_{50} values in most of the cases for compound **10** (LC_{50} 0.764 to >100μM) and **11** (LC_{50} 0.720 to >100μM). Similar results were observed with **12** (having PF_6^- anion), **13** (having $(CF_3SO_2)_2N^-$ anion) and **14** (having $(C_2F_5)_3F_3P^-$ anion) all having 1-methyl-3-octadecylimidazolium cation showing overall potency with

GI$_{50}$ 0.017-1.850μM (LC$_{50}$ 0.811 to >100μM), 0.062-2.090μM (LC$_{50}$ 3.970 to >100μM) and 0.086-3.370μM (LC$_{50}$ 0.778 to >100μM), respectively for all the tumor cell lines. These results also show that in the ionic liquid pair cation plays important role on the activity (compound **11-14**) while anion does not have similar effects, however more studies and screening should to be done to certain this fact. Interestingly, active compounds **8-14** were highly sensitive against leukemia cell lines, especially compounds **13** and **14** where the cytotoxicity was also very low with LC$_{50}$ >100μM in all six leukiemia cell lines.

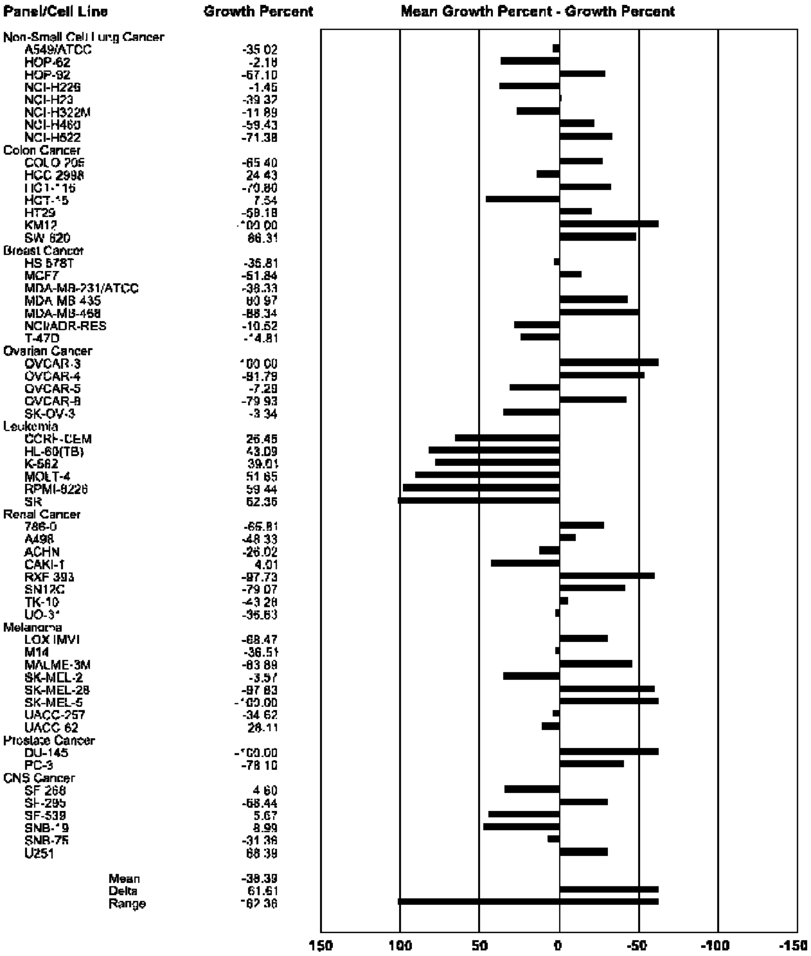

*Figure 1. One dose mean graph for **18** (NSC# 747251).*

Downloaded by DUKE UNIV on June 22, 2012 | http://pubs.acs.org
Publication Date (Web): April 28, 2010 | doi: 10.1021/bk-2010-1038.ch008

Downloaded by DUKE UNIV on June 22, 2012 | http://pubs.acs.org
Publication Date (Web): April 28, 2010 | doi: 10.1021/bk-2010-1038.ch008

Table 2. Different Panels and Corresponding Cell Lines Used for Screening

Panel	*Cell lines*
Leukemia	CCRF-CEM, HL-60(TB), K-562, MOLT-4, RPMI-8226, SR
Melanoma	LOX IMVI, MALME-3M, M14, SK-MEL-28, SK-MEL-5, UACC-257, UACC-62
Lung cancer	A549/ATCC, EKVX, HOP-62, HOP-92, NCI-H226, NCI-H23, NCI-H322M, NCI-H460, NCI-H522
Colon cancer	COLO 205, HCC-2998, HCT-116, HCT-15, HT29, KM12, SW-620
Renal cancer	786-0, A498, ACHN, CAK-1, RXF 393, SN12C, TK-10, UO-31
Ovarian cancer	IGROV1, OVCAR-3, OVCAR-4, OVCAR-5, OVCAR-8, SK-OV-3
Breast cancer	MCF7, NCI/ADR-RES, MDA-MB-231ATCC, HS 578T, MDA-MB-435, BT-549, T-47D, MDA-MB-468
Prostate cancer	PC-3, DU-145
Central nervous system cancer	COLO 205, HCC-2998, HCT-116, HCT-15, HT29, KM12, SW-620

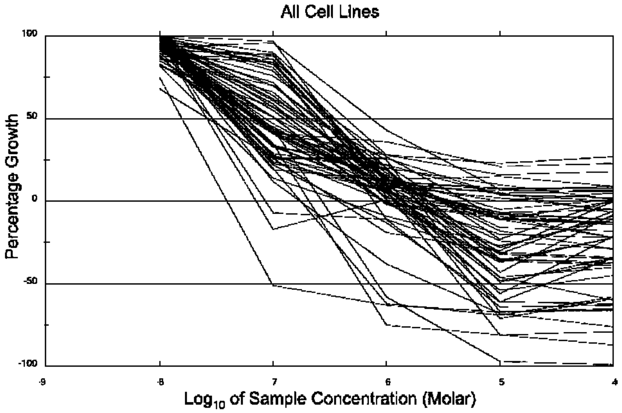

*Figure 2. Drug response curve of **18** for all 60 tumor cell lines.*

Downloaded by DUKE UNIV on June 22, 2012 | http://pubs.acs.org
Publication Date (Web): April 28, 2010 | doi: 10.1021/bk-2010-1038.ch008

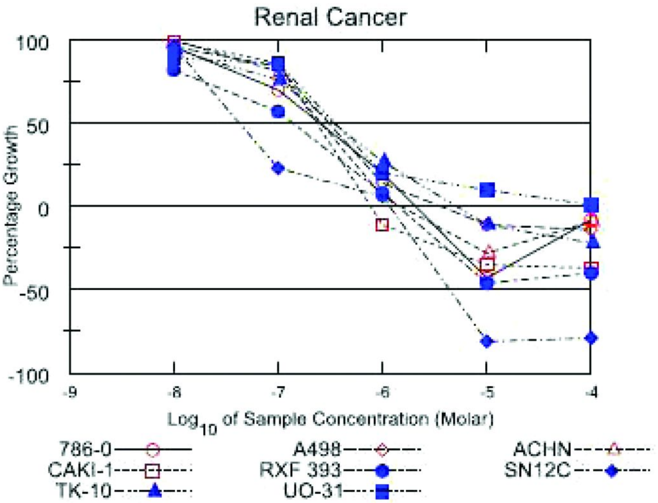

*Figure 3. Drug response curve of **18** for Renal caner panel.*

Increase in alkyl chain length contributed towards anticancer activity for ammonium ILs also, as can be seen in case of **22** (having C-8 alkyl substitution) which was highly sensitive towards all 60 tumor cell lines (unlike **23** and **24**, which were completely inactive) showing overall potency with GI_{50} values ranging from 0.046 to 1.900μM. However, with increase in activity, cytotoxicity was also found to be increased with LC_{50} values <10μM in more than 90% of cell lines. Similar trend was observed with phosphonium based ionic liquids, however, these were found to be more active as compared to their ammonium counter part. Compound **21** with C-6 alkyl substitution was the least active phosphonium IL showing overall potency towards all cell lines with GI_{50} values in range of 1.150 to 10.70μM, while it was completely non-toxic to all the cell lines with LC_{50} >100μM in all cases, except for COLO 205 (a colon cancer cell line) having LC_{50} 9.10μM. Interestingly, **21** and **24** both have similar anion but **21** found to be significantly active and completely non-toxic for all 60 cell lines, while **21** was completely inactive. Although **21** and **24** both have similar alkyl substitution on the cations but changing from ammonium to phosphonium made huge difference in the activity. Based on single dose data, compounds **18**, **19** and **20** having same cation were found to be active even though they have different anion. These three compounds were found to be highly sensitive against all 60 tumor cell lines showing overall potency with GI_{50} values ranging from 0.016 to 2.610 μM for **18**, 0.025 to 1.730μM for **19** and 0.016 to 0.947μM for **20**. Despite having same cation the cytotoxicity profiles of **18**-**20** were quite different. Compound **19** having hexafluorophosphate (PF_6^-) anion was found to be most toxic of all the phosphonium ILs toxic with LC_{50} <10μM for 95% of cell lines. In contrast, compound **18** with bis(triflic)imide ($(CF_3SO_2)_2N^-$) anion was non-toxic having LC_{50} >100μM for more than 75% of the cell lines. These results indicate that anions have significant effect on the cytotoxicity of ionic liquids and the cations seem to play a major role towards cytostatic activity. Ofcourse, it would require more studies and extensive screening to establish this fact.

The log mean values for GI_{50} and LC_{50} in 60 cell lines for all the active compounds except **20** are provided in Table 3 along with the log delta value (the maximum sensitivity in excess of the mean) and the log range (the maximum difference between the least sensitive and the most sensitive cell lines). These parameters provided insights into selectivity and potency of antitumor agents and gives an overall comparison of the anti-tumor activity and cytotoxicity of the tested compounds. Large values of the delta and range indicate high selectivity for some histological cancers over others. The drug response curves of **20** (not shown here) for all the cell lines showed further growth of the cells after their complete death and hence the results were not conclusive. This may be due to the precipitation of the compound at higher concentration because of its low solubility in the media and hence low bioavailability.

In case of imidazolium ILs (**8**-**14**) the median $\log GI_{50}$ and $\log LC_{50}$ increased as the chain length of alkyl substitution at N-3 increased from C-11 (**8** and **9**) to C-17 (**12**-**14**) (Table 3). This shows that with larger alkyl chain length, the overall anti-cancer activity as well as cytotoxicity of ionic liquids increases. The high GI_{50} range values were observed for **8** and **9** due to higher sensitivity of these compounds for leukemia and breast cancer cell lines as compared to others. The ILs **10**-**14** showed higher LC_{50} range values because of their less toxicity towards leukemia cell lines.

In case of phosphonium and ammonium ILs, lower median $\log GI_{50}$ of **18** and **19** show that these two compounds are most active followed by **22** and **21**. Also, the lower delta and range values indicated that all these compounds **18**, **19**, **21** and **22** are highly sensitive towards all 60 cell lines showing no selectivity for any particular case (Table 3). The high median $\log LC_{50}$ value of **21**, along with the low delta and range values, indicates the complete absence of cytotoxicity against all cell lines. Compound **18** is comparatively more cytotoxic with large delta and range values due to the high specificity for some of the Leukemia, melanoma and breast cancer cell lines. In contrast, compound **19** and **22** were found to be most cytotoxic as indicated by lower median $\log LC_{50}$ values (Table 3).

In all the ILs, **18** was found to be the best and was selected for in-vivo studies using hollow fiber assay. It showed the IP score of 12 (out of 24) and SC score of 4 (out of 24), with a total of 16 (out of 48) with no net cell kill. Although these results were not sufficient for NCI criteria of further xenograft testing, the overall study has clearly established the potential of these new class of compounds i.e. ionic liquids to be developed as anticancer drugs.

Downloaded by DUKE UNIV on June 22, 2012 | http://pubs.acs.org
Publication Date (Web): April 28, 2010 | doi: 10.1021/bk-2010-1038.ch008

Downloaded by DUKE UNIV on June 22, 2012 | http://pubs.acs.org
Publication Date (Web): April 28, 2010 | doi: 10.1021/bk-2010-1038.ch008

Table 3. Cytostatic (GT_{50}) and Cytotoxic (LC_{50}) Parameters of Active Compounds

Compd#	*GI_{50}*			*LC_{50}*		
	Median	*Delta*	*Range*	*Median*	*Delta*	*Range*
8	-5.57	1.39	2.7	-4.13	1.08	1.21
9	-5.46	1.05	2.11	-4.11	0.91	1.02
10	-6.3	1.32	1.94	-5.11	1.01	2.12
11	-6.36	1.21	1.79	-4.99	1.15	2.14
12	-6.17	1.61	2.04	-4.72	1.29	2.01
13	-6.17	1.04	1.53	-4.54	0.86	1.4
14	-6.47	0.59	1.59	-4.9	1.27	2.17
18	-7.01	0.79	1.66	-4.34	2.69	3.01
19	-7.04	0.56	1.48	-5.28	1.10	2.38
21	-5.46	0.48	1.48	-4.02	1.02	1.04
22	-6.42	0.91	1.61	-5.22	0.95	2.17

In summary, for the first time anti-tumor activity of phosphonium and ammonium-based ionic liquids has been determined using NCI 60 human tumor cell lines. With increase in alkyl chain length significant improvement in activity has been noticed. In general, phosphonium-based ILs were found to be more active then ammonium and imidazolium ILs. These results clearly demonstrate that the ‘tunability’ of ionic liquids (changing the cation/anion combination and modifying the cation with different substituents) could help to change their biological activity and cytotoxicity. Of course, more extensive screening and further studies into the mechanism of action of ILs in the biological environment are required to develop full understanding which could lead to multiple therapeutic applications.

Acknowledgments

This project has been funded in whole or in part with federal funds from the National Cancer Institute, National Institutes of Health, under Contract No. HHSN261200800001E. The content of this publication does not necessarily reflect the views or policies of the Department of Health and Human Services, nor does mention of trade names, commercial products, or organizations imply endorsement by the U.S. Government.

References

1. (a) Plaquevent, J.-C.; Levillain, J.; Guillen, F.; Malhiac, C.; Gaumont, A.-C. *Chem. Rev.* **2008**, *108*, 5035. (b) Dominguez de Maria, P. *Angew. Chem., Int. Ed.* **2008**, *47*, 6960. (c) Martins, M. A. P.; Frizzo, C. P.; Moreira, D. N.; Zanatta, N.; Bonacorso, H. G. *Chem. Rev.* **2008**, *108*, 2015. (d) Kumar, V.; Olsen, C. E.; Schaffer, S. J. C.; Parmar, V. S.; Malhotra, S. V. *Org. Lett.* **2007**, *9*, 3905. (e) Malhotra, S. V.; Kumar, V.; Parmar, V. S. *Curr. Org. Synth.* **2007**, *4*, 370. (f) Zhao, H.; Malhotra, S. V. *Aldrichimica Acta* **2002**, *35*, 75. (g) Wasserscheid, W.; Keim, W. *Angew. Chem.* **2000**, *39*, 3772.
2. (a) Ranke, J.; Stolte, S.; Stormann, R.; Arning, J.; Jastorff, B. *Chem. Rev.* **2007**, *107*, 2183. (b) Stepnowski, P.; Skladanowski, A. C.; Ludwiczak, A.; Laczynska, E. *Hum. Exper. Toxicol.* **2004**, *23*, 513. (c) Frade, R. F. M.; Matias, A.; Branco, L. C.; Afonso, C. A. M.; Duarte, C. M. M. *Green Chem.* **2007**, *9*, 873. (d) Wang, X.; Ohlin, C. A.; Lu, Q.; Fei, Z.; Hu, J.; Dyson, P. J. *Green Chem.* **2007**, *9*, 1191. (e) Ranke, J.; Muller, A.; Bottin-Weber, U.; Stock, F.; Stolte, S.; Arning, J.; Stormann, R.; Jastorff, B. *Ecotoxicol. Env. Saf.* **2007**, *67*, 430.
3. Paracelsus. http://en.wikipedia.org/wiki/Paracelsus (accessed April 28, 2009).
4. Ross, I. A. *Medicinal Plants of the World*; 2005; Vol. 3, Preface.
5. (a) *Anticancer Drug Toxicity: Prevention, Management, and Clinical Pharmacokinetics*, 1st ed.; Lipp, H.-P., Ed.; Informa HealthCare: London, 2009. (b) *Chemistry and Pharmacology of Anticancer Drugs*, 1st ed.; Thurston, D. E., Ed.; CRS Press, Taylor & Francis Group: Boca Raton, FL, 2006.
6. *Handbook of Pharmaceutical Salts: Properties, Selection, and Use*; Wermuth, C. G., Stahl, P. H., Eds.; Wiley-VCH: Weinheim, Germany, 2002; p 1.
7. Pfannkuch, F.; Rettig, H.; Stahl, P. H. In *Handbook of Pharmaceutical Salts: Properties, Selection, and Use*; Wermuth, C. G., Stahl, P. H., Eds.; Wiley-VCH: Weinheim, Germany, 2002; p 130.
8. (a) Hough, W. L.; Smiglak, M.; Rodriguez, H.; Swatloski, R. P.; Spear, S. K.; Daly, D. T.; Pernak, J.; Grisel, J. E.; Carliss, R. D.; Soutullo, M. D.; Davis, J. H., Jr.; Rogers, R. D. *New J. Chem.* **2007**, *31*, 1429. (b) Hough, W. L.; Rogers, R. D. *Bull. Chem. Soc. Jpn.* **2007**, *80*, 2262.
9. Liu, Q.; Janssen, M. H. A.; Van Rantwijk, F.; Sheldon, R. A. *Green Chem.* **2005**, *7*, 39.
10. (a) Alley, M. C.; Scudiero, D. A.; Monks, P. A.; Hursey, M. L.; Czerwinski, M. J.; Fine, D. L.; Abbott, B. J.; Mayo, J. G.; Shoemaker, R. H.; Boyd, M. R. *Cancer Res.* **1988**, *48*, 589. (b) Boyd, M. R.; Paull, K. D. *Drug Dev. Res.* **1995**, *34*, 91. (c) Shoemaker, R. H. *Nature Rev.* **2006**, *6*, 813.
11. (a) Decker, S.; Hollingshead, M.; Bonomi, C. A.; Certer, J. P.; Sausville, E. A. *Eur. J. Cancer* **2004**, *40*, 821. (b) Hollingshead, M. D.; Alley, M. C.; Camalier, R. F.; Abott, B. J.; Mayo, J. G.; Malspeir, L.; Grever, M. R. *Life Sci.* **1995**, *57*, 131.
12. Kumar, V.; Malhotra, S. V. *Bioorg. Med. Chem. Lett.* **2009**, *19* (16), 4643.

Downloaded by DUKE UNIV on June 22, 2012 | http://pubs.acs.org
Publication Date (Web): April 28, 2010 | doi: 10.1021/bk-2010-1038.ch008

Downloaded by DUKE UNIV on June 22, 2012 | http://pubs.acs.org
Publication Date (Web): April 28, 2010 | doi: 10.1021/bk-2010-1038.ch009

Chapter 9

Preparation of Ionic Liquid-Modified Inorganic Nanoparticles and Their Biomedical Application

Asako Narita,*[,1,3] Kensuke Naka,[2] and Yoshiki Chujo[1]

[1]Department of Polymer Chemistry, Graduate School of Engineering, Kyoto University, Katsura, Nishikyo-ku, Kyoto 615-8510, Japan
[2]Department of Chemistry and Materials Technology, Kyoto Institute of Technology, Matsugasaki, Sakyo-ku, Kyoto 606-8585, Japan
[3]Advanced Software Technology & Mechatronics Research Institute of Kyoto (ASTEM), Shimogyo-ku, Kyoto 600-8813, Japan
***nariasa@chujo.synchem.kyoto-u.ac.jp**

Ionic liquid-modified inorganic nanoparticles were prepared, and their biomedical applications were discussed. The N-methylimidazolium cation-modified hydrophilic gold nanoparticles became hydrophobic one when the counter anion was exchanged with hydrophobic anions. The N-methylimidazolium cation-modified iron oxide nanoparticles also showed the same behavior. The physico-chemical change of the surface on the iron oxide nanoparticles is useful for biomedical applications such like magnetic resonance imaging (MRI). The ionic liquid-modified iron oxide nanoparticles showed high dispersibility in water and low toxicity. MR image of the aqueous solution of the N-methylimidazolium cation-modified nanoparticles appeared stronger signal comparing to those for commercial products. Furthermore, the interaction with bio-molecules such as DNA was found.

Background

Nano-sized particles are promising materials for various applications (*1*, *2*). One of the interesting characters of the nanoparticles is wide surface area

In Ionic Liquid Applications: Pharmaceuticals, Therapeutics, and Biotechnology; Malhotra, S.;
ACS Symposium Series; American Chemical Society: Washington, DC, 0.

compared to bulk-size materials one. The surface area of 1 cm cube is 6 cm^2. The total surface area of nanoparticles (10 nm) as total volume of 1 cm^3 is approximately 600 m^2. The highly concentrated interface and the small diameter are attractive characters for nano-sized physical chemistry and their applications. For example, dispersion of gold nanoparticles shows red-purple color because of the surface Plasmon absorption on the wide surface area. The spectra depend on the diameter or intermolecular distance. Nano-sized iron oxide nanoparticles (γ-Fe_2O_3, meghemite or Fe_3O_4, magnetite) are super paramagnetic depending on the diameter. Thus, the change of status of the nanoparticles can be detected as optical or magnetic signals. The nanoparticles are expected as environmental probes. Additionally, various molecules can be attached to the surface. The nano-sized particles are unstable comparing to bulk solids because of their higher surface energy. Therefore, most of nanoparticles need coating materials as stabilizer. The coating materials can be used as functional moieties or scaffolds to attach functional molecules. The surface modification of nanoparticles is one of important technologies to develop their applications.

In these days, imaging proves based on nanoparticles are desired in biomedical field simultaneously with the development of hardware. In a case of magnetic resonance imaging (MRI), there are some kinds of contrast reagents commercially available such as iron oxide nanoparticles and gadolinium ion complex reagents. However, both types of the commercial contrast reagents have not site recognition or stimuli response ability. The contrast reagents based on the iron oxide nanoparticles are usually coated by sugar chains such as dextran to keep high dispersibility in a living body. Therefore, addition of site recognition or stimuli responsive functions is strongly needed for the development of imaging probes. Such attempts to give recognition ability have been reported using also gold nanoparticles (*3*). One of major strategies to obtain site recognition ability is attachment of recognition molecules to marker molecules of the disease. However, there should be much more variations to recognition systems because the chemical environment exchange accompanying the change of pH or oxygen content around the diseases.

On the other hand, ionic liquids have quite interesting physico-chemical properties such as the melting points, the decomposition temperature, the vapor pressure, the viscosity, and the hydrophobicity. Their properties are attracted in various research fields and applications. However, although numerous reports discussed about these properties in bulk liquids so far, nano-sized physico-chemical properties and usage of ionic liquids still have great possibility to develop the researches. Especially, the hydrophobicity would be present even on the surface of nanoparticles as the same as bulk status. And the modified ionic liquids would act as stimuli response moieties. Thus, we have prepared inorganic nanoparticles modified with ionic liquids. Our nanoparticles modified with the ionic liquid have possibility of a new type of site recognition system in a living body.

Downloaded by DUKE UNIV on June 22, 2012 | http://pubs.acs.org
Publication Date (Web): April 28, 2010 | doi: 10.1021/bk-2010-1038.ch009

Downloaded by DUKE UNIV on June 22, 2012 | http://pubs.acs.org
Publication Date (Web): April 28, 2010 | doi: 10.1021/bk-2010-1038.ch009

Objective

The objective of this study is a preparation of the ionic liquids-modified nanoparticles and their analysis of stimuli response behavior. Especially, ionic liquid-modified iron oxide nanoparticles were evaluated their stimuli responses, toxicities, and the interaction with bio-molecules concerning bio-medical applications.

Experimental

Preparation of Ionic Liquid-Modified Gold Nanoparticles

Preparation of N-methylimidazolium-modified gold nanoparticles ([MIm][Cl]-Au-NPs) was described in our previous report (*4*). Disulfide bearing N-methylimidazolium chloride (3.3'-[disulfanylbis(hexane-1,6-diyl)]bis(1-methyl-1H-imidazol-3-ium)dichloride) as shown in *Scheme* 1 was prepared as described in our paper. Into an aqueous solution of tetrachloroaurate and the disulfide, an aqueous sodium tetrahydroborate solution was added. The mixture was filtered through an ultrafiltration membrane. Modification of N-methylimidazolium chloride moiety on the gold nanoparticles surface was confirmed by FT-IR spectra.

Preparation of Ionic Liquid-Modified Iron Oxide Nanoparticles

Preparation of N-methylimidazolium chloride modified iron oxide nanoparticles ([MIm][Cl]-IO-NPs) was described in our previous report (*6*) as shown in *Scheme* 2. An aqueous ammonium hydrate solution was added at once to an aqueous solution of iron chloride (II) tetrahydrate and iron chloride (III) hexahydrate under vigorously mechanical stirring. After the produced black precipitation was washed by water, the residue was re-dispersed in ethanol.

Ionic liquids were covalently modified via silane coupling on the ion oxide nanoparticles according to procedures reported previously (*6*) as shown in *Scheme* 2. The silane coupling agent (1-methyl-3-[3-trimethoxysilyl]propaneimidazolium chloride) was synthesized according to the procedures reported previously (*6*). The synthesized silane coupling agent and distilled water were added to the ethanol dispersion. After the mixture was stirred at 70 °C for 12 hours, generated brown particles were washed by ethanol using centrifuge. The covalent bonding between N-methylimidazolium chloride and iron oxide was confirmed by FT-IR spectra.

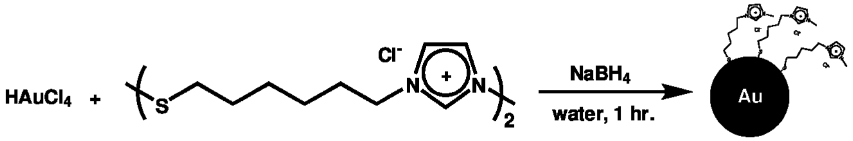

Scheme 1. Preparation of ionic liquid-modified gold nanoparticles.

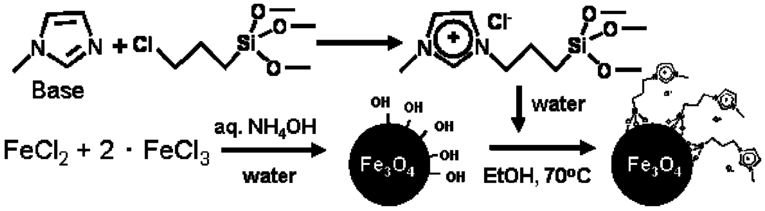

Scheme 2. Preparation of ionic liquid-modified iron oxide nanoparticles.

Analysis of the Stimuli Response

The details of the stimuli response analysis were described in each report(*4–6*). Basically, various kinds of acids or salts were added to aqueous dispersion of imidazolium-modified gold or iron oxide nanoparticles. The degree of aggregation of gold nanoparticles was observed by the appearance of the dispersion or UV-visible absorption spectra(*4*, *5*). In the case of iron oxide nanoparticles, the aggregated diameters were measured by dynamic light scattering (DLS) (*6*).

Downloaded by DUKE UNIV on June 22, 2012 | http://pubs.acs.org
Publication Date (Web): April 28, 2010 | doi: 10.1021/bk-2010-1038.ch009

The Toxicity Assay

In vitro assay of [MIm][Cl]-IO-NPs was carried out as follows. The dispersion of the nanoparticles (0.5 mg/ml saline or PBS) was added to culture wells filled with medium containing HeLa cells (1×10^4 ml^{-1} / well). The volumes of nanoparticles dispersion were as follows (μl); 1, 2.5, 5, 10, 20, 40, 80, 100, 120, 140, 160. The microscope images of the culture wells were recorded at 3 days later. The cell death and aggregations of nanoparticles were observed in these microscope images.

Details of *in vivo* assay were described in the previous paper (*6*). [MIm][Cl]-IO-NPs were dispersed in 5 wt% aqueous glucose solution, saline or PBS. The dispersion was injected from tail vessel of mice. The mice injected the glucose containing dispersion of the nanoparticles were evaluated in various parameters (*6*). The general behaviors of mice were observed after [MIm][Cl]-IO-NPs dispersed in phosphate buffered saline (PBS).

Magnetic Resonance Imaging (MRI)

MR images of water dispersion of N-methylimidazolium chloride-modified nanoparticles were acquired with a 7 T Unity Inova MR scanner (Varian, Palo Alto, CA). A surface coil 20mm in diameter was used for signal acquisition. MR imaging parameters were with 3000 ms repetition time (TR), 100ms echo time (TE), 5mm slice thickness, 60 × 60mm field-of-view (FOV) and 256 × 256 matrices.

Analysis of Interaction between Nanoparticles and Biomolecules

The details about analysis of interaction between DNA and ionic liquid-modified iron oxide nanoparticles were described in our report (*6*). The aqueous dispersions of the nanoparticles were added to the DNA solutions (Tris-HCl-EDTA buffer, pH 8). After nanoparticles were removed by magnet or centrifuge, the supernatant solutions were analyzed by electrophoresis (0.7 % agarose gel, dyeing by ethydium bromide).

Results and Discussion

Characterization of Organic Salts Modified Nanoparticles

Downloaded by DUKE UNIV on June 22, 2012 | http://pubs.acs.org
Publication Date (Web): April 28, 2010 | doi: 10.1021/bk-2010-1038.ch009

The diameter of [MIm][Cl]-Au-NPs measured in transmission electron microscopy (TEM) image was 5 nm. From thermogravimetric analysis (TGA) of [MIm][Cl]-Au-NPs, 380 of modification agent molecules were attached on the surface (*4*).

Characterizations of [MIm][Cl]-IO-NPs were described in our report (*6*). The average diameter of core iron oxide nanoparticles measured in TEM images were around 8 - 10 nm (standard deviation values were always around 1.5 nm) in every batch. The magnetite (Fe_3O_4) nanoparticles made from co-precipitation method (*7*) are tend to have higher deviation value on the diameters comparing to these for meghemite (γ-Fe_2O_3) nanoparticles made from thermal decomposition method (*8*). However, co-precipitation method does not require severe conditions such as high temperature and highly toxic reagents to produce via thermal decomposition method. From the TGA, the volume of organic compounds was around 5 wt% (*6*) even if an excess of the silane coupling agent was added to the nanoparticles. The volume means the nanoparticles have quite thin organic layer on the surface. It was confirmed that the crystal structure of Fe_3O_4 was stable before and after modification of N-methylimidazolium chloride from XRD patterns (*6*). The magnetization curve measured by SQUID also showed that the modification on the iron oxide nanoparticles with N-methylimidazolium chloride did not affect the magnetization values (*6*). As these results, these organic molecules on the surface did not change the properties of the core iron oxide nanoparticles.

Stimuli Response of [MIm][Cl]-Au-NPs

The most interesting behavior of the organic salts modified nanoparticles is the change of the hydrophobicity of the surface by anion exchange as shown in *Scheme* 3. The anion exchange between the surface and surrounding ions should be dominated by the degree of hardness of these ions. Therefore, the equilibrium tends to form ion pairs having large hydrophobic anion such like hexafluorophosphate and soft organic cations like imidazolium. Actually, after enough volume of hydrophobic anion was added to the aqueous dispersion

Downloaded by DUKE UNIV on June 22, 2012 | http://pubs.acs.org
Publication Date (Web): April 28, 2010 | doi: 10.1021/bk-2010-1038.ch009

of [MIm][Cl]-Au-NPs, the nanoparticles transferred from aqueous phase to hydrophobic ionic liquid (1-methyl-3-butylimidazolium hexafluorophosphate) phase (*4*).

Other response mechanism was also found in [MIm][Cl]-Au-NPs. When an aqueous hydrochloric acid solution was added to the dispersion of [MIm][Cl]-Au-NPs and poly(acrylic acid), precipitation was observed depending on the pH. The change was likely that the re-formation of hydrogen bonding by addition of Brønsted acid (*5*). As a result, various mechanisms except for the anion exchange are expected by modification of organic salts on the surface.

Stimuli Response of [MIm][Cl]-IO-NPs

The same ionic stimuli response as [MIm][Cl]-Au-NPs was observed in an aqueous dispersion of [MIm][Cl]-IO-NPs (*6*). The degree of aggregation after salts were added to the dispersion depended on anion species (NaCl < NaI < $NaPF_6$). Basically, the equilibrium of the anion exchange on the surface depends on the degree of hardness of the combination of ion pairs. Ion exchange between N-methylimidazolium chloride and hydrophobic anion such as sodium hexafluorophosphate proceeds to form N-methylimidazolium hexafluoro-phosphate as soft-soft ion pair. However, reversed anion exchange depending on the concentration of surrounded ions was observed in aqueous dispersion of [MIm][Cl]-IO-NPs. When N-methylimidazolium TFSI-modified nanoparticles were washed by 1M aqueous sodium chloride solution, TFSI anions were replaced to chloride anions (*6*). Such anion exchange against to HSAB principles as shown in *Scheme* 4 should be difficult in balk ionic liquids. On the other hand, the organic salts on the surface behave as interface because the salts tethered to the surface of the nanoparticles face to surrounded molecules or ions. The fact would be the reason why such unusual anion exchange was observed. The reversed anion exchange is one of the impressive behaviors based on the wide surface area of nano-sized particles. Although the change of the hydrophobicity of the iron oxide nanoparticles could be observed by addition of both salts and acids, strong acid cause decomposition of iron oxide nanoparticles.

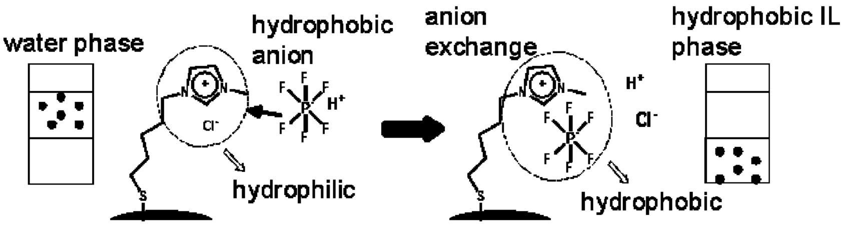

Scheme 3. Change of hydrophobicity of nanoparticles via anion exchange.

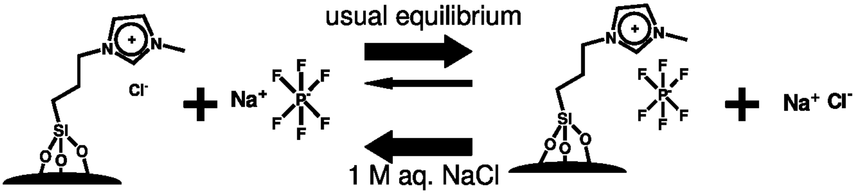

Scheme 4. The equilibrium of anion exchange on the surface.

In a living body, there are numerous kinds of ionic molecules or salts. And the acidity or an ionic environment could be changed in a specific area such like some kinds of disease. Ionic liquids are expected for sensing moiety tethered on the surface of nanoparticles. To optimize the chemical structure, specific environment in a living body would be detected.

Downloaded by DUKE UNIV on June 22, 2012 | http://pubs.acs.org
Publication Date (Web): April 28, 2010 | doi: 10.1021/bk-2010-1038.ch009

Dispersibility of [MIm][Cl]-IO-NPs

[MIm][Cl]-IO-NPs have high dispersibility in water and alcohol. The dispersibility of nanoparticles is very important concerning to use in a living body. To keep high dispersibility, sugar chains such like dextran are often used (*9*) as a coating material for commercial products as MRI contrast agents. Ethylene oxide chains such as poly(ethylene glycol) are also used to give high dispersibility in a living body (*10*). Although these hydrophilic polymers are convenient to disperse in aqueous media, the coating layer is usually thick comparing to the diameter of the core iron oxide(*11*, *12*). On the other hand, organic salt layer on the surface should be thin according to the organic molecule contents as mentioned in the previous section. Although amino group-modified iron oxide nanoparticles were also reported as aqueous dispersed nanoparticles (*13*), the dispersibility was lower than that of [MIm][Cl]-IO-NPs as shown in *Fig.* 1. In an aqueous dispersion, it takes more than 2 weeks to collect [MIm][Cl]-IO-NPs using a neodymium magnet.

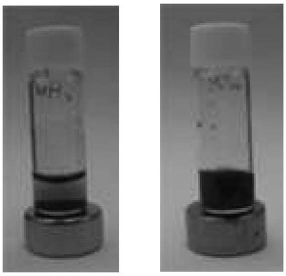

Figure 1. Photographs of the aqueous dispersion (5 mg/ml) of amino group-modified iron oxide nanoparticles (left) and [MIm][Cl]-IO-NPs(right) on neodymium magnets at 60 sec. later after dispersion by ultrasonic wave.

Toxicity of [MIm][Cl]-IO-NPs

Recently, the toxicity of ionic liquids is feared (*14*). Therefore, [MIm][Cl]-IO-NPs also make a suspicion about the toxicity in a living body. However, [MIm][Cl]-IO-NPs did not show serious toxicity in both *in vitro* and *in vivo* (*6*) assay. *Fig.* 2 and *Table* 1 show the results of *in vitro* assay of [MIm][Cl]-IO-NPs. When more than 80 Wl of the PBS dispersion of [MIm][Cl]-IO-NPs was added to the culture medium 1 ml, cell deaths were observed. Concerning of practical concentration of nanoparticles in a living body used as contrast agent for MRI, the concentrations should be lower than the wells added 40 el of dispersion. The result means that [MIm][Cl]-IO-NPs do not have serious toxicity for living cells in a practical concentration to use as a contrast agent.

In vivo assay was also carried out to evaluate sub-acute toxicity (*6*). After aqueous [MIm][Cl]-IO-NPs dispersions containing 0.5 % glucose (13.5 mg nanoparticles/kg body weight) were injected from tail vessel of mice, observation of general behavior and organs, and evaluation in various parameters were carried out. These results are almost same as commercial product (Resovist®) as control, even the concentration in a living body was 30 times higher than practical one actually using in a human body. Furthermore, in cases that the [MIm][Cl]-IO-NPs PBS dispersion (0.2 mg/ml) was injected with higher volume (19.8 and 31.4 mg/kg), also the general behavior of the mice was kept normal.

There would be some reasons that the [MIm][Cl]-IO-NPs showed low toxicity against the expectation. Generally, it is said that cationic molecules tend to act as toxic. Many of reports showed that the toxicity of imidazolium salts is increased with elongating the N-substituted alkyl group(*14–22*) because an increase of lipophilicity caused destroying lipid bilayer of cells(*14*, *22*), or interaction with the lipophilic active center of the enzyme (*16*). From this view point, short methyl substitution on the imidazolium ring on [MIm][Cl]-IO-NPs would not affect these lipophilic domains. The low volume of imidazolium salts also should be one of the reasons of the low toxicity. In the tested concentration (13.5 mg/kg), the organic component is 0.675 mg/kg according to 5 wt% as organic component measured by TGA. If 60 wt% of a mouse with 30 g as body weight was water, the total volume in the body is 2.0×10^{-2} mg, and the concentration of organic parts is 1.1×10^{-3} mg/ml. The value is lower than these for reported value that 1-butyl-3-methylimidazolium chloride showed toxicities(*15–18*). Additionally, the diffusion in living bodies was also low because the imidazolium cations were tethered via covalent bonding. These results imply that modification of cationic molecules via covalent bonding would lead to suppression of the toxicities even if the molecules were evaluated as toxic one.

Downloaded by DUKE UNIV on June 22, 2012 | http://pubs.acs.org
Publication Date (Web): April 28, 2010 | doi: 10.1021/bk-2010-1038.ch009

Downloaded by DUKE UNIV on June 22, 2012 | http://pubs.acs.org
Publication Date (Web): April 28, 2010 | doi: 10.1021/bk-2010-1038.ch009

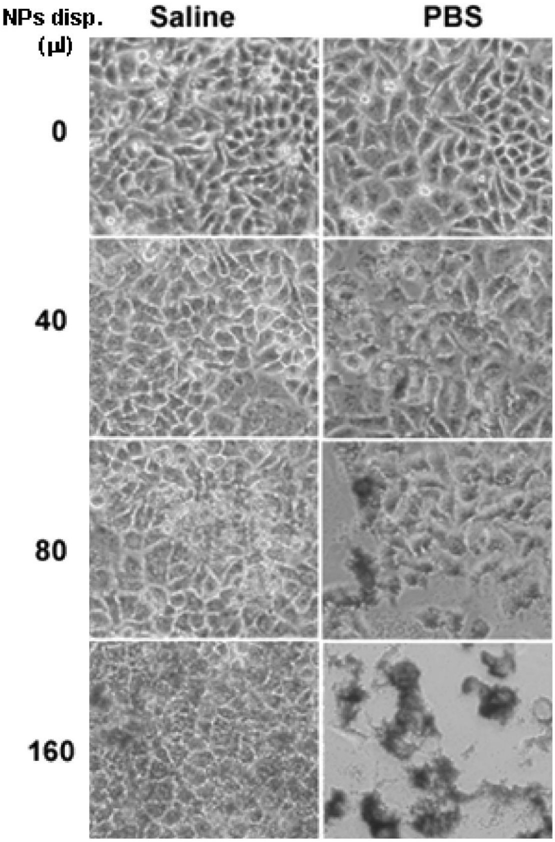

Figure 2. Microscope images of culture wells of HeLa cells at 3 days later after addition of [MIm][Cl]-IO-NPs dispersion.

MR Images of [MIm][Cl]-IO-NPs

MR images of aqueous [MIm][Cl]-IO-NPs dispersion are shown in *Fig.* 3. The results were the same as our previous report (*6*) comparing to a commercial product (Resovist®) in the same concentration. The MR images of aqueous [MIm][Cl]-IO-NPs dispersion were darker (stronger) than these of commercial product (Feridex®). This is likely that the aqueous [MIm][Cl]-IO-NPs dispersion includes higher iron content, or the thin organic layer of the surface of [MIm][Cl]-IO-NPs did not much inhibit the access of water molecules.

Table 1. Observation of cell death and aggregation of [MIm][Cl]-IO-NPs

NPs disp.	*disp. in saline*[a]		*disp. in PBS*[a]	
(μl/ml medium)	*cell death*	*aggregates*	*cell death*	*aggregates*
0	-	-	-	-
1	-	-	-	-
2.5	-	-	-	-
5	-	-	-	-
10	-	-	-	partly +
20	-	-	-	+
40	-	-	-	+
80	-	partly +	partly +	+
100	-	+	partly +	+
120	-	+	partly +	+
140	-	+	partly +	+
160	-	+	+	+

[a] Cell death and aggregates were judged in photographs.

Downloaded by DUKE UNIV on June 22, 2012 | http://pubs.acs.org
Publication Date (Web): April 28, 2010 | doi: 10.1021/bk-2010-1038.ch009

Interaction with Biomolecules

Interaction between [MIm][Cl]-IO-NPs and DNA was analyzed. DNA sticking to [MIm][Cl]-IO-NPs was also found (*6*). It was reported that iron oxide nanoparticles coated with cationic polymer stuck to DNA (*23*). The volume of DNA sticking was depending on the chemical structure of the molecules on the surface. In comparison of [MIm][Cl]-IO-NPs and [MIm][TFSI]-IO-NPs, [MIm][Cl]-IO-NPs showed higher sticking ability. Amino group-modified iron oxide nanoparticles stuck less than [MIm][TFSI]-IO-NPs. The results mean that the degree of the interaction with bio-molecules such as DNA could be controlled by change of modified molecules on the surface. In the case of organic salts, change of the anion would affect the interaction. Actually, it was reported that the ion pair of imidazolium cation and phosphate anion in DNA was formed via anion exchange (*24*). If the anion exchange is included in the sticking forces, optimization of cation structure might be also effective. One of advantages of organic salts from the view points of control of the interaction and recognition is their numerous combinations of cations and anions. The control of the interaction would be useful not only as materials for imaging probes but for bioseparation systems.

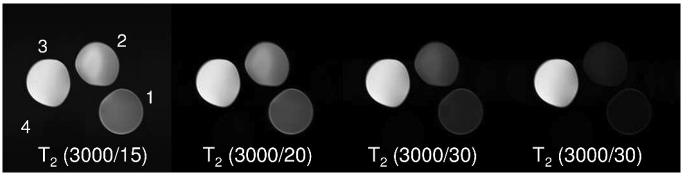

Figure 3. T2 enhanced MR images of aqueous iron oxide nanoparticles dispersions.1: [MIm][Cl]-IO-NPs (10 mg/ml aq. disp.5 µl was added to water 3 ml), 2: Feridex® (5 µl was added to water 3 ml), 3: water (H_2O), 4: water (D_2O). The numbers mean (TE/TR) values.

Conclusions

In summary, we have reported the preparation of ionic liquid-modified inorganic nanoparticles and discussed about their potential of biological applications such as contrast agents for magnetic resonance imaging (MRI) or supporting materials for bioseparation. The N-methylimidazolium chloride-modified gold nanoparticles were well-dispersed in water. The gold nanoparticles had ionic response ability due to the anion exchange between the anions on the surface and surrounded anions. The N-methylimidazolium chloride-modified iron oxide nanoparticles also showed the same ionic stimuli response. The iron oxide nanoparticles showed quite low toxicity as the same as commercial products both *in vitro* and *in vivo* assay. The aqueous solutions of the ionic liquid-modified iron oxide nanoparticles appeared stronger MR signals compared to the same concentration of commercial products due to their thin organic layer. The cationic surface was also useful to collect bio-molecules such as DNA.

Acknowledgments

The authors gratefully appreciate to Prof. Masahiro Hiraoka, Prof. Shinae Kizaka-Kondoh and Mr. Hiroyuki Tanaka (Kyoto University) for cooperation of toxicity assay, to Prof. Toshiro Inubushi and Dr. Masahito Morita (Shiga University of Medical Science) for cooperation of MR imaging, and to Prof. Susumu Kitagawa and Dr. Wakako Kaneko (Kyoto University) for cooperation of SQUID measurements.

This study is a part of joint researches, which are focusing on development of basis of technology for establishing COE of nano-medicine, carried out through Kyoto City Collaboration of Regional Entities for Advancing Technology Excellence (CREATE) assigned by Japan Science and Technology Agency (JST).

Downloaded by DUKE UNIV on June 22, 2012 | http://pubs.acs.org
Publication Date (Web): April 28, 2010 | doi: 10.1021/bk-2010-1038.ch009

Downloaded by DUKE UNIV on June 22, 2012 | http://pubs.acs.org
Publication Date (Web): April 28, 2010 | doi: 10.1021/bk-2010-1038.ch009

References

1. Laurent, S.; Forge, D.; Port, M.; Roch, A.; Robic, C.; Elst, L. V.; Muller, R. N. *Chem. Rev.* **2008**, *108*, 2064.
2. Daniel, M.-C.; Astruc, D. *Chem. Review.* **2004**, *104*, 293.
3. Dixit, V.; Van den Bossche, J.; Sherman, D. M.; Thompson, D. H.; Ronald, P.; Andres, R. P. *Bioconj. Chem.* **2006**, *17*, 603.
4. Itoh, H.; Naka, K.; Chujo, Y. *J. Am. Chem. Soc.* **2004**, *126*, 3026.
5. Naka, K.; Tanaka, H.; Chujo, Y. *Polym. J.* **2007**, *11*, 1127.
6. Naka, K.; Narita, A.; Tanaka, H.; Chujo, Y.; Morita, M.; Inubushi, T.; Nishimura, I.; Hiruta, J.; Shibayama, H.; Koga, H.; Ishibashi, S.; Seki, J.; Kizaka-Kondoh, S.; Hiraoka, M.; *Polym. Adv. Mater.*, 2008, in press.
7. Elmore, W. C. *Phys. Rev.* **1938**, *54*, 308.
8. Rockenberger, J.; Scher, E. C.; Alivisatos, A. P. *J. Am. Chem. Soc.* **1999**, *121*, 11595.
9. Shen, T.; Weissleder, R.; Papisov, M.; Bogdanov, Jr., A.; Brady, T. *Magn. Reson. Med.* **1993**, *29*, 599.
10. Bazile, D.; Prud'homme, C.; Bassoullet, M.-T.; Marlard, M.; Spenlehauer, G.; Veillard, M. *J. Pharm. Sci.* **1995**, *84*, 493.
11. For example, in a commercial product written in a description; Resovist® (Schering) in 1 ample includes 864 mg of fercarbotran as a main component containing 44.6 mg of iron.
12. Weissleder, R.; Kelly, K.; Sun, E. Y; Shtatland, T.; Josephson, L. *Nat. Biotechnol.* **2005**, *23*, 1418.
13. Yamaura, M.; Camiloa, R. L.; Sampaiob, L. C.; Macêdoc, M. A.; Nakamura, M.; Tomad, H. E. *Magn. Reson. Med.* **2004**, *279*, 210.
14. Jastorff, B.; Störmann, R.; Ranke, J.; Mölter, K.; Stock, F.; Oberheitmann, B.; Hoffmann, W.; Hoffmann, J.; Nüchter, M.; Ondruschka, B.; Filser, J. *Green Chem.* **2003**, *5*, 136.
15. Swatloski, R.P.; Holbrey, J. D.; Memon, S. B.; Caldwell, G. A.; Caldwell, K. A.; Rogers, R. D. *Chem. Commun.* **2004**, 668.
16. Stock, F.; Hoffmann, J.; Ranke, J.; Störmann, R.; Ondruschka, B.; Jastorff, B. *Green Chem.* **2004**, *6*, 286.
17. Docherty, K. M.; Kulpa, C. F., Jr. *Green Chem.* **2005**, *7*, 185.
18. Landry, T. D.; Brooks, K.; Poche, D.; Woolhiser, M. *Bull. Environ. Contam. Toxicol.* **2005**, *74*, 559.
19. Stolte, S.; Arning, J.; Bottin-Weber, U.; Matzke, M.; Stock, F.; Thiele, K.; Uerdingen, M.; Welz-Biermann, U.; Jastorffa, B.; Ranke, J. *Green Chem.* **2006**, *8*, 621.
20. Wang, X.; Ohlin, C. A.; Lu, Q.; Fei, Z.; Hub, J.; Dyson, P. J. *Green Chem.* **2007**, *9*, 1191.
21. Matzke, M.; Stolte, S.; Thiele, K.; Juffernholz, T.; Arning, J.; Ranke, J.; Welz-Biermannd, U.; Jastorff, B. *Green Chem.* **2007**, *9*, 1198.
22. Kulacki, K. J.; Lamberti, G. A. *Green Chem.* **2008**, *10*, 104.
23. McBain, S. C.; Yiu, H. H. P.; El Haj, A.; Dobson, J. *J. Mater. Chem.* **2007**, *17*, 2561.
24. Nishimura, N.; Nomura, N.; Nakamura, N.; Ohno, H. *Biomaterials* **2005**, *26*, 5558.

In Ionic Liquid Applications: Pharmaceuticals, Therapeutics, and Biotechnology; Malhotra, S.;
ACS Symposium Series; American Chemical Society: Washington, DC, 0.

Chapter 10

Preparation of Biopolymer-Based Materials Using Ionic Liquids for the Biomedical Application

Sang Hyun Lee,[1] Minoru Miyauchi,[2] Jonathan S. Dordick,[1,4,5] and Robert J. Linhardt*,[1,3,4,5]

[1]Department of Chemical & Biological Engineering, [2]Rensselaer Nanotechnology Center, [3]Department of Chemistry & Chemical Biology, [4]Department of Biology, [5]Center for Biotechnology and Interdisciplinary Studies, Rensselaer Polytechnic Institute, 110 8th Street,
Troy, New York 12180
***linhar@rpi.edu**

Downloaded by UNIV OF GUELPH LIBRARY on June 22, 2012 | http://pubs.acs.org
Publication Date (Web): April 28, 2010 | doi: 10.1021/bk-2010-1038.ch010

The insolubility of unmodified biopolymers in most organic solvents has limited the applications of biopolymer-based materials and composites. Because of their inherent biocompatibility and biodegradability, such materials have many potential applications in biomedicine, including for tissue engineering, drug delivery systems, wound treatment, dialysis membranes, and biosensors. Ionic liquids (ILs) are good solvents for polar organic, nonpolar organic, inorganic and polymeric compounds. Biopolymers such as cellulose, chitin/chitosan, silk, and DNA can be fabricated from ILs into films, membranes, fibers, spheres, and molded shapes. Various biopolymer/biopolymer and biopolymer/synthetic polymer composites also can be prepared by co-dissolution of polymers into IL mixtures. Heparin/biopolymer composites are especially of interest in preparing materials with enhanced blood compatibility.

In Ionic Liquid Applications: Pharmaceuticals, Therapeutics, and Biotechnology; Malhotra, S.;
ACS Symposium Series; American Chemical Society: Washington, DC, 0.

Downloaded by UNIV OF GUELPH LIBRARY on June 22, 2012 | http://pubs.acs.org
Publication Date (Web): April 28, 2010 | doi: 10.1021/bk-2010-1038.ch010

Introduction

Biopolymers

Bio-based materials have garnered considerable interest recently as they can decrease dependency on fossil fuel. Biopolymers are naturally obtainable macromolecules including polysaccharides, polyphenols, polyesters, polyamides, and proteins, which play an important role in biomedicine with applications in tissue engineering, regenerative medicine, drug-delivery systems, and biosensors. The inherent biocompatibility and biodegradability of these materials make them particularly useful in biomedical applications. For example, tissue engineering requires the seeding of cells into porous polymer matrices that offer channels for host cell migration and that biodegrade into non-toxic products *in vivo* (*1*). Biopolymer nanofibrous mats could be used as particle filters, wound dressings, medical textiles, and for drug delivery (*2*). However, the homogenous modification of biopolymers and preparation of unmodified biopolymer-based materials still remains a challenge. The reason for this challenge is the low solubility of unmodified biopolymers in conventional solvents making the chemical modification and the formation of biopolymer-containing composites difficult. Therefore, new solvents for the dissolution of unmodified biopolymers are of interest in developing various biopolymer-based materials.

Cellulose

Cellulose, a linear polysaccharide of D-glucose residues linked by *β*-(1→4)-glycosidic bonds, is the most abundant renewable biopolymer on earth. It has excellent thermal and mechanical properties (*3*). Unmodified cellulose offers excellent biocompatibility and is considered a promising material for biomedical applications. For example, woven cellulose pads are used as wound dressings. They are sterilizable, biocompatible, porous, elastic, easy to handle and store, and provide optimal control of wound (*4*). Hollow fibers of cellulose can be used as artificial blood vessels. The blood compatibility of vessels prepared from artificial cellulose fibers has been tested as devices in dog models (*5*). Cellulose has also been applied as a membrane to protect immobilized glucose oxidase in biosensors used to assay glucose in blood (*6*). The development of unmodified cellulose materials with various additives and cellulose composites has been hampered by the difficulty of dissolving cellulose. Cellulose is highly crystalline as a result of an extensive hydrogen bonding network, making it insoluble in most conventional organic and aqueous solvents. Although some unconventional solvents such as *N*-methylmorpholine-*N*-oxide (NMMO), CdO/ethylenediamine (*7*), LiCl/*N*,*N*-dimethylacetamide (DMAc) and near supercritical water (*8*) have been used for dissolving cellulose. Thus, greener and nontoxic solvents need to be developed for the widespread application of unmodified cellulosics (*9*). Chemically modified celluloses such as cellulose acetate, cellulose propionate and cellulose acetate-butyrate are found in a wide range of biomaterials (*10*). They are used for film coatings, dialysis membranes, solid supports, sponges and fibers in various biomedical applications. However, the chemical modification of cellulose is complicated by its high degree of crystallinity and the degree of modification for cellulose is often difficult to control due to the heterogeneous reactions.

Chitin

Chitin, a co-polymer of over 50% *N*-acetyl-glucosamine and *N*-glucosamine units, is one of the most abundant polysaccharides with an annual production just second behind cellulose. Chitin has been also successfully used for biomedical applications owing to its biodegradability and biocompatibility. For example, porous chitin matrices were used for cell transplantation applications to regenerate tissue (*11*). Chitin's monomer unit, *N*-acetyl-glucosamine, occurs in hyaluronic acid, an extracellular macromolecule that is important in wound repair (*1*). A chitin membrane, named Vinachitin, has been used to treat deep burns, orthopedic, trauma and ulcer conditions in over 300 patients (*12*). The use of chitin in many applications has also been limited due to its insolubility in most organic solvents. Chitin forms strong intermolecular and intramolecular hydrogen bonds that are difficult to break using common molecular solvents. Although few solvents, including DMAc containing 5% LiCl, methanesulfonic acid, and hexafluoro-2-propanol (HFIP), dissolve chitin, these solvents are often toxic and corrosive, and the resulting chitin solution is unstable (*2*, *13*).

Heparin

Heparin is a mixture of linear anionic polysaccharides having 2-*O*-sulfo-*α*-iduronic acid and 2-deoxy-2-sulfamino-6-*O*-sulfo-*α*-D-glucose as its major repeating disaccharide and minor amounts of *β*-D-glucuronic acid and 2-acetamido-2-deoxy-*α*-D-glucose. Heparin is widely used as an injectable anticoagulant for acute coronary syndromes (e.g., myocardial infarction, arterial fibrillation, deep-vein thrombosis and pulmonary embolism) (*14–16*). Heparin is administered, either by *intravenous* or *subcutaneous* routes, to maintain blood flow of inpatients on extracorporeal therapy (*17*). Therefore, heparin immobilized to a surface, enhances the blood compatibility of that surface, reducing platelet adhesion, the loss of blood cells, and increasing plasma recalcification time and activated partial thromboplastin time (APTT). Immobilized heparin also inhibits initial contact activation enzymes through an antithrombin-mediated pathway, and thus has enhanced anticoagulant properties (*18*, *19*). Heparinized devices, include currently used macrodevices such as kidney dialyzers in extracorporeal circuits, indwelling catheters and stents as well as implantable nanodevices and nanomachines under development for applications such as drug delivery systems (*20*). Recently, there have been many reports of using heparinization to enhance the surface properties of various polymeric materials for medical applications (*19*, *21–23*). These composites, based on their biological properties and morphology, were proposed in a variety of applications including as blood compatible, hollow fiber, and nanoporous membranes for kidney dialyzers.

Downloaded by UNIV OF GUELPH LIBRARY on June 22, 2012 | http://pubs.acs.org
Publication Date (Web): April 28, 2010 | doi: 10.1021/bk-2010-1038.ch010

Silk

Silks are spun into fibers by silkworm, spiders, scorpions, mites, and flies. *Bombyx mori* silk worms are the most thoroughly studied silk producers whose silk has been used in biomedical applications as a suture material for repairing wound injuries for centuries because of its biocompatibility, biodegradability, excellent mechanical properties, low inflammatory responses, and good oxygen and water vapor permeability (*2*, *24*, *25*). Recently, the ability to fabricate silk-based materials including films, sponges, mats, and fibers has been of great interest in the manufacturing of biomedical materials, including tissue engineering scaffolds (*26*). However, silks are insoluble in common solvents such as water, dilute acids, and alkali. A single strand of natural cocoon silk fiber from *Bombyx mori* silkworm contains two silk fibroin cores surrounded by a protective, glue-like sericin coating. The actual fibroin cores consist of 391 kDa heavy and 26 kDa light chain. The hydrogen bonded crystalline region of heavy chain is responsible for excellent mechanical properties and difficulty in its dissolution (*24*, *25*). Traditionally, the procedure to make stable silk fibroin solution includes sericin stripping by Na_2CO_3, dissolving in a high concentration of aqueous lithium salt solution, dialysis, lyopholization, and redissolving in HFIP (*24*). HFIP is extremely corrosive and toxic and the procedures to make silk solutions are very laborious. The development of environmental-friendly and efficiently silk dissolving solvent is a major interest in manufacture of silk-based materials for biomedical applications.

Downloaded by UNIV OF GUELPH LIBRARY on June 22, 2012 | http://pubs.acs.org
Publication Date (Web): April 28, 2010 | doi: 10.1021/bk-2010-1038.ch010

Ionic Liquids

Ionic liquids (ILs) are organic salts that usually melt below 100°C. Interest in ILs stems from their potential application as ‘green solvents’ (*27*). Specifically, their non-volatile character and thermal stability make them attractive alternatives to volatile organic solvents. In chemical processes, ILs exhibit excellent physical characteristics including the ability to dissolve polar and nonpolar organic, inorganic, and polymeric compounds. Moreover, the combinations of anions and cations encompassed by ILs are vast. In addition, owing to their associated synthetic flexibility, ILs are referred as ‘designer solvents’ (*28*). Recently, ILs were demonstrated to be good solvents for dissolution and reconstitution of unmodified biopolymers (*29–31*). Major merits of the procedure to make biopolymer-based materials by using ILs are high solubility of biopolymers that cannot be dissolved in general organic solvents, greener procedures using non-volatile solvents, and easy production of composites comprising of various biopolymers and synthetic polymers. In this work, the dissolution of biopolymers in ILs and the preparation of various biopolymer-based materials using ILs will be investigated.

Dissolution of Biopolymers Using ILs

Polysaccharides are highly complex, chiral organic compounds that are challenging to modify and are insoluble in most common organic solvents. Only certain polysaccharides can be dissolved and/or modified in selected polar solvents (e.g., water, pyridine, formamide, dimethylformamide and dimethylsulfoxide) (*23*, *30*, *32*, *33*). Thus, it is important to investigate new solvent systems capable of dissolving polysaccharides.

The first organic molten salts, *N*-alkylpyridinium salts, as cellulose solvents, were published in 1934. However, this was not considered as commercial solvent for cellulose because of its high melting point (118° C) (*20*, *34*). In 2002, the use of 1-alkyl-3-methylimidazolium salts as solvents for cellulose was reported by Rogers group (*9*). They tested the ability of ILs containing 1-butyl-3-methylimidazolium ([Bmim]) cation with various anions to dissolve cellulose and the most effective anion was found to be the chloride. Cellulose could be dissolved at 25 wt% in [Bmim][Cl] by microwave irradiation and dissolved cellulose can be reconstituted by the addition of an anti-solvent such as water, ethanol, and acetone. These results have opened up new paths for commercially relevant routes of homogeneous cellulose chemistry and for the preparation of various unmodified cellulose composites. NMR studies on the dissolution mechanism of cellulose in [Bmim][Cl] indicates that the $[Cl]^-$ of ILs acts as a hydrogen bond acceptor which interacts with the hydroxyl group of cellulose (*34–36*). Although [Bmim][Cl] has been reported to be chemically stable, side reactions resulting from the abstraction of the proton at position 2, high viscosity, toxicity associated with high reactivity of Cl^-, and biodegradability also need to be considered. Ren et al. synthesized 1-allyl-3-methylimidazolium chloride ([Amim][Cl]) and showed that the solubility of cellulose in [Amim][Cl] was better than [Bmim][Cl] (*37*). Heinze and coworkers reported that 1-butyl-3-methylpyridinium chloride ([Bmpy][Cl]) could dissolve up to 39 wt% Avicel, while [Bmim][Cl] dissolved at 18 wt% Avicel (*34*, *36*). Mikkola et al. used ultrasound irradiation to dissolve cellulose in [Bmim][Cl] and [Amim][Cl] (*38*). The use of high-power ultrasound dramatically intensified the dissolution process and resulted in complete dissolution within a few minutes. Recently, acetate, formate, methyl phosphate, and dicyanamide counter anions of 1-alkyl-3-methylimidazolium salts were reported as good ILs for cellulose dissolution (*39–42*). Among the room temperature ILs with low viscosity suitable for cellulose dissolution are 1-ethyl-3-methylimidazolium acetate ([Emim][Ac]) and formates of allylimidazolium based ILs. The solubility of celluloses in ILs is shown in Table 1.

There are very few results reported on the dissolution of chitin in ILs. Xie et al. showed the dissolution of 10% chitin in [Bmim][Cl], a good solvent for cellulose (*44*). However, the chitin was not fully soluble and still showed some crystallinity in these solutions. The ability to dissolve chitin in [Bmim][Cl] is highly dependent on chitin molecular weight, degree of acetylation, and its origin. Recently, Wu et al. showed the successful dissolution and regeneration of various native chitins in [Bmim][Ac] (*13*). The acetate anion in [Bmim][Ac] is a stronger hydrogen bonding acceptor than the chloride anion in [Bmim][Cl] and thus, can dissolve

Downloaded by UNIV OF GUELPH LIBRARY on June 22, 2012 | http://pubs.acs.org
Publication Date (Web): April 28, 2010 | doi: 10.1021/bk-2010-1038.ch010

higher concentrations of chitin. The acetate anion of [Bmim][Ac] is believed to strongly interact with the hydrogen bond networks in chitin by depriving the proton of the amino or hydroxyl groups from the carbonyl groups. In contrast, chitosan is more easily dissolved in [Amim][Cl], [Bmim][Cl], [Bmim][Ac], and aqueous [Bmim][BF_4] solution (*45–47*).

Heparin, like cellulose, is soluble in only a very few conventional solvents such as water, dimethylsulfoxide, dimethylformamide and formamide. Therefore, many studies have been conducted to test the solubility of various heparin-like glycosaminoglycans (GAGs) in novel solvents (*19*, *30*, *33*). Linhardt and coworkers first suggested the use of ILs for the dissolution of GAGs. They studied the synthesis and properties of ILs having benzoate as the anion and a cation comprised of alkyl substituted imidazolium, pyridinium or phosphonium moieties (*48*). The aim of this work was to find ILs that could dissolve the sodium or imidazolium salts of heparin. Four different ILs ([Emim][Ba], [Bmim][Ba], [Bmim][PF_6], and [Bmim][BF_4]) were used to study GAG solubility (*48*). A total of eight GAGs, four with sodium and four with imidazolium counterions, were tested in these dissolution studies. [Emim][Ba] showed the best dissolution of GAGs, and the imidazolium salts of GAGs dissolved better than their corresponding sodium salts. Following their initial success of heparin dissolution, [Emim][Ba] was used in the glycosylation of unprotected donors with protected acceptors (*49*) and the fabrication of blood compatible composite membranes (*19*), and the preparation of biopolymer composite fibers by electrospinning (*50*).

Downloaded by UNIV OF GUELPH LIBRARY on June 22, 2012 | http://pubs.acs.org
Publication Date (Web): April 28, 2010 | doi: 10.1021/bk-2010-1038.ch010

Table 1. Solubility of cellulose in ILs[a]

Ionic liquids	*Type of cellulose*	*Solubility*
[Emim][Cl]	Avicel (DP 286)	12% (10°C above mp.) (*43*)
	Spruce sulfite pulp (DP 593)	6% (10°C above mp.) (*43*)
	Cotton linters (DP 1198)	4% (10°C above mp.) (*43*)
	Eucalyptus pulp (DP 569)	>16% (vertical kneader) (*42*)
[Bmim][Cl]	Avicel (DP 286)	18% (80°C) (*36*)
	Spruce sulfite pulp (DP 593)	13% (80°C) (*36*)
	Cotton linters	10% (80°C) (*36*), 10 wt% (ultrasound) (*38*)
	Microcrystalline cellulose (Aldrich, 20 μm)	8 wt% (ultrasound) (*38*)
	Kraft pulp (0.35 mm)	9 wt% (ultrasound) (*38*)
	Eucalyptus pulp (DP 569)	>14% (vertical kneader) (*42*)
	Pulp (DP 1000)	3% (70°C) (*9*), 10% (100°C) (*9*), 25% (microwave) (*9*)
[Hmim][Cl]	Pulp (DP 1000)	5% (100°C) (*9*)

Continued on next page.

Downloaded by UNIV OF GUELPH LIBRARY on June 22, 2012 | http://pubs.acs.org
Publication Date (Web): April 28, 2010 | doi: 10.1021/bk-2010-1038.ch010

Table 1. (Continued). Solubility of cellulose in ILs[a]

Ionic liquids	*Type of cellulose*	*Solubility*
[Omim][Cl]	Pulp (DP 1000)	slightly soluble (100°C) (*9*)
[Bdmim][Cl]	Avicel (DP 286)	9% (10°C above mp.) (*43*)
	Spruce sulfite pulp (DP 593)	6% (10°C above mp.) (*43*)
	Cotton linters (DP 1198)	4% (10°C above mp.) (*43*)
	Eucalyptus pulp (DP 569)	>13% (vertical kneader) (*42*)
[Bmpy][Cl]	Avicel (DP 286)	39% (105°C) (*36*)
	Spruce sulfite pulp (DP 593)	37% (105°C) (*36*)
	Cotton linters (DP 1198)	12% (105°C) (*36*)
[BDTA][Cl]	Avicel (DP 286)	5% (60°C) (*36*)
	Spruce sulfite pulp (DP 593)	2% (60°C) (*36*)
	Cotton linters (DP 1198)	1% (60°C) (*36*)
[Amim][Cl]	Microcrystalline cellulose (Aldrich, 20 µm)	2-11 wt% (80-100°C) (*39*), 27 wt% (ultrasound) (*38*)
	Cotton linters	13 wt% (ultrasound) (*38*)
	Kraft pulp (0.35 mm)	8 wt% (ultrasound) (*38*)
	Cellulose	8-15 wt% (80°C) (*41*)
[Bmim][Br]	Pulp (DP 1000)	5-7% (microwave) (*9*)
[Admim][Br]	Avicel (DP 286)	12% (10°C above mp.) (*43*)
	Spruce sulfite pulp (DP 593)	4% (10°C above mp.) (*43*)
	Cotton linters (DP 1198)	4% (10°C above mp.) (*43*)
[Bmim][SCN]	Pulp (DP 1000)	5-7% (microwave) (*9*)
[Emim][Ac]	Eucalyptus pulp (DP 569)	>14% (vertical kneader) (*42*)
[Bmim][Ac]	Eucalyptus pulp (DP 569)	>13% (vertical kneader) (*42*)
[Amim][HCOO]	Microcrystalline cellulose (Aldrich , DP 250)	11-21 wt% (60-85°C) (*39*)
[Emim][(MeO)HPO$_2$]	Microcrystalline cellulose (Aldrich , DP 250)	4-10 wt% (30-45°C, 30 min) (*40*)
[Emim][(MeO)MePO$_2$]	Microcrystalline cellulose (Aldrich , DP 250)	4-10 wt% (40-55°C, 30 min) (*40*)
[Emim][(MeO)$_2$PO$_2$]	Microcrystalline cellulose (Aldrich , DP 250)	4-10 wt% (55-65°C, 30 min) (*40*)

[a] Hmim = 1-hexyl-3-methylimidazolium, Omim = 1-octyl-3-methylimidazolium, Bdmim = 1-butly-2,3-dimethylimidazolium, BDTA = benzyldimethyl(tetradecyl)ammonium, Admim = 1-allyl-2,3-dimethylimidazolium.

Downloaded by UNIV OF GUELPH LIBRARY on June 22, 2012 | http://pubs.acs.org
Publication Date (Web): April 28, 2010 | doi: 10.1021/bk-2010-1038.ch010

Table 2. Solubility of biopolymers in ILs

Biopolymer	*Ionic liquids*	*Solubility*
Heparin (imidazolium salt)	[Emim][Ba]	7.0% (35° C) (*48*)
	[Bmim][Ba]	7.0% (35° C) (*48*)
Heparan sulfate (imidazolium salt)	[Emim][Ba]	3.0% (35° C) (*48*)
	[Bmim][Ba]	2.8% (35° C) (*48*)
Chondroitin sulfate (imidazolium salt)	[Emim][Ba]	9.9% (35° C) (*48*)
	[Bmim][Ba]	5.7% (35° C) (*48*)
Hyaluronic acid (imidazolium salt)	[Emim][Ba]	10.0% (35° C) (*48*)
	[Bmim][Ba]	10.0% (35° C) (*48*)
Chitin	[Bmim][Ac]	6% (α-chitin, 110° C) (*13*), 6-7% (low MW β-chitin, 110° C) (*13*),
		3% (high MW β-chitin, 110° C) (*13*)
	[Bmim][Cl]	partially soluble (α-chitin & low MW β-chitin, 110° C) (*13*),
		>10% (110° C) (*44*)
Chitosan	[Bmim][Ac]	12% (110° C) (*13*)
	[Bmim][Cl]	10% (110° C, DAC=5%) (*13*), <10% (110° C, DAC=12%) (*44*)
	[Amim][Cl]	8% (110° C) (*13*)
Cocoon silk	[Emim][Cl]	23.3% (100° C) (*24*)
	[Bmim][Cl]	13.2% (100° C) (*24*)
	[Bdmim][Cl]	8.3% (100° C) (*24*)
	[Bmim][Br]	0.7% (100° C) (*24*)

The dissolution of various proteins such as silks (*bombyx mori* silk, spider silk, and silk-elastin fusion protein), collagen, elastin, and gelatin in ILs was also reported, although accurate solubility data for these proteins are rarely reported (*24*, *25*, *29*, *51*). Interestingly, the cocoon silk was dissolved in [Emim][Cl], [Bdmim][Cl], and [Bmim][Cl]. The silk dissolved solution indicated amorphous structure and no β-sheet which shows crystalline region. The silk ILs solutions could be diluted with water and the silk was regenerated by methanol, acetonitrile, and acetone (*24*). Table 2 shows the solubilities of biopolymers in various ILs.

Downloaded by UNIV OF GUELPH LIBRARY on June 22, 2012 | http://pubs.acs.org
Publication Date (Web): April 28, 2010 | doi: 10.1021/bk-2010-1038.ch010

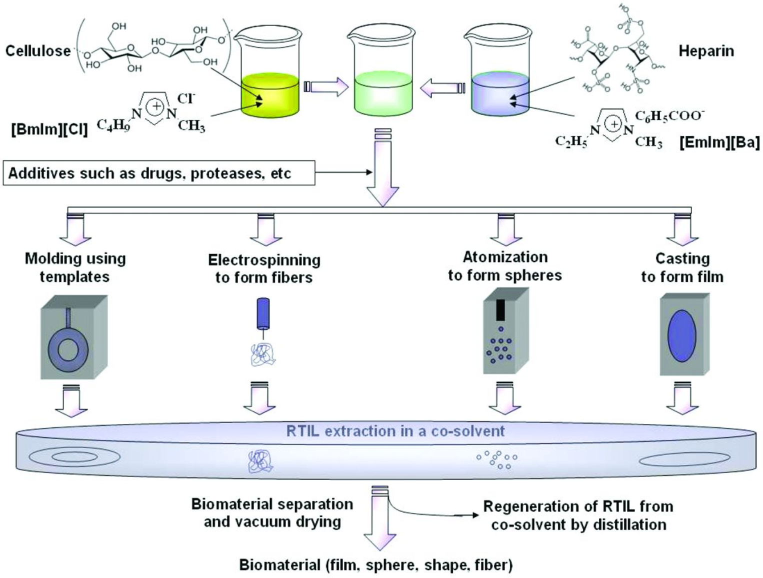
Cellulose
Heparin
[BmIm][Cl]
[EmIm][Ba]
Additives such as drugs, proteases, etc
Molding using templates
Electrospinning to form fibers
Atomization to form spheres
Casting to form film
RTIL extraction in a co-solvent
Biomaterial separation and vacuum drying
Regeneration of RTIL from co-solvent by distillation
Biomaterial (film, sphere, shape, fiber)

Figure 1. Schematic representation for the preparation of heparin/cellulose composite materials.

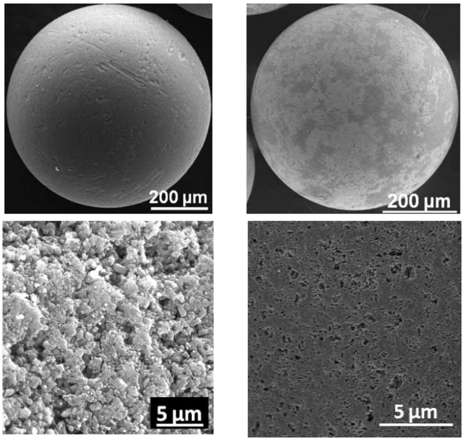
200 µm
200 µm
5 µm
5 µm

Figure 2. FESEM images: (A, B) uncoated charcoal (C, D) heparin/cellulose/charcoal composite.

Downloaded by UNIV OF GUELPH LIBRARY on June 22, 2012 | http://pubs.acs.org
Publication Date (Web): April 28, 2010 | doi: 10.1021/bk-2010-1038.ch010

Biopolymer-Based Materials Prepared by Using ILs

Film, Coating, and Membrane

The cellulose dissolution and reconstitution in ILs has great potential importance for the preparation of various biopolymer-based materials. Biopolymer-based film, coating, and biocompatible membrane can be used for biomedical application such as tissue engineering scaffolds, kidney dialysis, biosensor, drug delivery, and implantable devices.

Biopolymer-Based Materials

Rogers and coworkers have extensively explored the use of ILs to dissolve cellulose and reconstitute cellulose composites. Turner et al. used [Bmim][Cl] to encapsulate laccase into cellulose membrane (*52*). The enzyme was entrapped and the material being formed was used in producing a low-leaching bioactive films. A hydrophobic [Bmim][Tf2N] coating resulted in higher enzyme activity, by protecting the enzyme from the high and inactivating concentrations of Cl^- present in [Bmim][Cl]. Turner et al. also reported cellulose/polyamine composite films and beads from [Bmim][Cl] as solid support matrices for biocatalyst immobilization (*53*). They prepared the surface functionalized cellulose composites with primary amine functional groups necessary for chemical bonding between the enzyme and the support resulting in enhanced stability. Poplin et al. developed sensor platforms based on encapsulating a probe molecule within a cellulose matrix (*54*). The [Bmim][Cl] was used to codissolve cellulose and the hydrophobic dye/metal complexant 1-(2-pyridylazo)-2-naphthol, a good extractant and indicator for metal ions. Bagheri et al. developed a surface active cellulose films for covalent attachment of laccase by codissolution of cellulose with polyamidoamine dendrimers in [Bmim][Cl] followed by regeneration with water (*55*). These results indicate that cellulose composites can be used as supports for biosensors, biocatalysis, and novel drug delivery system. Tsioptsias and Panayiotou recently prepared cellulose and cellulose/nanohydroxyapatite composite for tissue engineering scaffolds by a particulate leaching technique, with poly(methyl methacrylate) particles as the porogen (*56*). The materials regenerated from [Bmim][Cl] solution showed different properties from the materials regenerated from *N*,*N*-dimethylacetamide and LiCl solutions. The properties of these new materials make them promising for bone regeneration applications. Additionally, the scaffold fabrication process by using [Bmim][Cl] was fast, inexpensive, and environmentally friendly.

Chitin solution in [Bmim][Ac] gels after being cooled down to room temperature. The [Bmim][Ac] could be extracted away using water or methanol (*13*). Thus, making very easy to prepare transparent soft materials. Additional removal of ILs from hydrogel and drying can also make films, membranes, coatings, and sponges. The regenerated β-chitin showed a transition to crystal structure close to α-chitin, the more stable crystal form. The regenerated chitins are also thermally more stable than the native chitin. The dissolution/regeneration process of chitin has a great potential for the preparation of chitin-based materials such as dialysis membranes, porous matrices, wound dressings, and other composites for biomedical applications, similar to previously described cellulose-based materials. Chitin-based materials prepared by casting without chemical modification show antibacterial effects, biocompatibility, and biodegradability.

Silk solutions in [Bmim][Cl] were used to cast films and the structures of regenerated films were highly dependent on the anti-solvent. Acetonitrile yields a convoluted surface structure with little crystallinity, while methanol yields a transparent film with a high degree of crystallinity, and water could not be used because of dissolution of silk film (*24*, *25*). Recently, Gupta et al. demonstrated the casting of patterned silk films and these films were found to support normal cell proliferation and differentiation(*26*) . They showed that silk films cast from silk solutions in [Bmim][Cl] did not have any detrimental effect on cell viability and gene expression, indicating that ILs can be used for the fabrication of silk scaffolds for tissue engineering applications.

Downloaded by UNIV OF GUELPH LIBRARY on June 22, 2012 | http://pubs.acs.org
Publication Date (Web): April 28, 2010 | doi: 10.1021/bk-2010-1038.ch010

Blood Compatible Biopolymer Composites

The surfaces of extracorporeal and prosthetic medical devices that come directly into contact with blood or body fluids and tissues must be biocompatible. Such devices should not trigger blood clotting, nor should they induce inflammatory responses when brought into contact with tissues. Blood compatibility is a major factor in biocompatibility because thrombogenesis is induced by surfaces of medical devices that are not blood compatible. Thrombus formation on the surface of an extracorporeal medical device or an implanted biomedical device can result in heart attack, stroke or pulmonary embolism (*19*, *20*). For example, kidney dialysis membranes should have excellent biocompatibility and blood compatibility, without activating the complement and coagulation cascade, triggering the blood clotting (*19*, *57*).

Heparin can improve the blood compatibility of synthetic polymers and biopolymers. Linhardt and coworkers reported novel biopolymer/heparin composites to enhance the blood compatibility of biopolymers, making it unnecessary to chemically couple heparin to these biopolymers. To fabricate these blood compatible composites, they exploited the ability of [Emim][Ba] to dissolve heparin. The mixtures of heparin containing [Emim][Ba] and cellulose containing [Bmim][Cl] were prepared. The resulting solution of cellulose and heparin could be fabricated into cellulose/heparin composite materials in various shapes and forms, including films and membranes, micro- or nanospheres, micro- or nanofibers, or any other shapes molded by using templates (Figure 1) (*19*, *50*, *58*). This simple approach uses IL mixtures to prepare various biopolymer/biopolymer or biopolymer/synthetic polymer composites. Heparin/cellulose composite membranes, prepared by this method, showed uniformly distributed heparin throughout the cellulose matrix. APTT and thromboelastography demonstrated that this composite had excellent blood compatibility when compared to other existing biomaterials prepared through the covalent bonding of heparin. The composite membrane was also used to test the potential for kidney dialyzers through an equilibrium experiments on urine and bovine serum albumin (BSA). Urea reached equilibrium within 60 h in while BSA did not reach equilibrium even after 45 h. Thus, these membranes show appropriate selectivity for urea (*19*). Recently, Park et al. reported novel cellulose/heparin/charcoal composites by using [Bmim][Cl] and [Emim][Ba] mixture (*58*). Activated charcoal is useful for treating individuals in danger from oral drug overdose of depressants such as alcohol, barbiturates, and benzodiazepines, or stimulants. However, uncoated activated charcoal generally results in thromboresistance when used in direct hemoperfusion. Although various polymers such as modified cellulose, agarose, chitosan, and synthetic copolymers were used to coat or entrap charcoal to increase blood compatibility of charcoal composite (*59*, *60*), the use of charcoal composites in hemoperfusion still requires the transfusion of whole blood or the addition of human serum albumin. To solve this problem, Park et al. prepared blood compatible heparin/cellulose/activated charcoal bead composites to enhance the biocompatibility and blood compatibility of activated charcoal beads while decreasing the size of their active pores (*58*). The FESEM image of heparin/cellulose/charcoal composites showed the smooth, uniformly coated surface with a large number of small, nano-sized pores (Figure 2). The surface morphology indicates that the composite is potentially capable of inhibiting the adsorption of proteins while permitting small drug molecules to adsorb to the underlying charcoal bead. APTT results and adsorption efficiency of phenytoin compared to BSA showed that the coating of activated charcoal with cellulose/heparin are useful for direct hemoperfusion to remove free-diluted and protein-bound toxins of small size or useful as potential oral agents in the cases when strict preservation of large molecules is necessary.

Downloaded by UNIV OF GUELPH LIBRARY on June 22, 2012 | http://pubs.acs.org
Publication Date (Web): April 28, 2010 | doi: 10.1021/bk-2010-1038.ch010

Fibers

Natural biopolymer fibers have been used in a variety of biomedical applications. For example, silk fibers are used as suture thread and absorbent cotton in medical dressings. Fibers and fibrous membranes have a number of potential biomedical applications due to their flexibility, permeability, high liquid retention and high surface area. Biopolymer-based fibers such as cellulose, chitosan, alginate, gelatin and silk fiber have been fabricated and evaluated for biomedical applications.

Dry-Jet Wet Spinning Using ILs

Cellulose fibers are the most widely used biopolymer-based fibers and are renewable, biocompatible and biodegradable. Although NMMO has been used industrially in dry-jet wet spinning processes (*61*), the development of a greener and easily recyclable system using non-toxic and non-volatile solvents would be advantageous. Recently, several groups obtained unmodified cellulose fibers with dry-jet wet spinning process using ILs such as [Emim][Cl], [Bmim][Cl],

[Amim][Cl], [Emim][Ac] and [Bmim][Ac] (*42*, *62*, *63*). Synthetic polymers, such as poly(m-phenylene-isophthalamide) (*64*) and polyacrylonitrile (*65*), were also similarly fabricated into fiber. In a typical dry-jet wet spinning process using ILs as solvents, the spin dope is prepared from cellulose solution in ILs. The spinning is performed by extruding the spin dope across an air gap into coagulation bath. The solvent of coagulation bath is miscible with ILs and immiscible with cellulose. Water and alcohols can be used for such solvent. Hence, as the fiber is formed, the solvent of coagulation bath removes ILs from fiber. In the extracting process, it is possible to draw the fiber to enhance the fiber properties. After that, ILs can be recycled easily from co-solvent of coagulation bath due to its non-volatility. Various biopolymer fibers were also obtained by dry-jet wet spinning using ILs. Silk fiber from [Emim][Cl] solution (*25*) and DNA fiber from [Bmim][BF_4] solution (*66*) were reported. Biopolymer composite fibers such as wool keratin/cellulose with improved mechanical property and cellulose/m-aramid with enhanced antimicrobial activity were also fabricated by using [Bmim][Cl] (*67*, *68*).

Electrospinning Using ILs

The electrospinning has been recognized as a simple and versatile method for producing ultrathin fiber with an extremely high surface area on a sub-cellular scale. In medical field, fabric materials made of electrospun fiber are anticipated to be candidates for tissue engineering scaffolds, in wound dressing and as protective clothing (*2*, *69*). In a typical electrospinning process, a strong electric field is applied to a droplet formed by a solution of polymer and volatile solvent at the tip of a die which acts as one of the electrode. The droplet is deformed as it is charged and forms a jet that is accelerated in the direction of the collector electrode with an evaporation of the solvent. This conventional electrospinning method using volatile solvents can be defined as a dry spinning process (*70*). Because the evaporation of volatile solvents is involved, this process is sensitive to state of the atmosphere such as temperature and humidity (*71*). The recovery of evaporated organic solvent is usually difficult. Especially, in case of the inflammable solvent where ignition by a spark can take place.

Recently, electrospinning methods have used non-volatile ILs as solvents to fabricate ultrathin fibers of unmodified cellulose (*50*). This method can be defined as a dry-jet wet electrospinning process, which forms biopolymer-based ultrathin fibers fabricated by collecting the jet in a grounded coagulation bath. The dry-jet wet electrospinning process with ILs is stable system at atmosphere, no need of gas recovery, and a fire-safety system. Although the high viscosity of the ILs is a presumed disadvantage for electrospinning, nanoscale (about 500 nm) fibers could be observed. The success of this method might result from the jet of highly conductive ILs solution might be subjected to a greater tensile force in the presence of an electric field. Zhang et al. reported that diameter of electrospun fiber decreased with increasing the solution conductivity (*72*). The control of solution properties such as the viscosity, the surface tension and conductivity were also reported using a mixed solvent approach (*73*, *74*). By addition of

Downloaded by UNIV OF GUELPH LIBRARY on June 22, 2012 | http://pubs.acs.org
Publication Date (Web): April 28, 2010 | doi: 10.1021/bk-2010-1038.ch010

Downloaded by UNIV OF GUELPH LIBRARY on June 22, 2012 | http://pubs.acs.org
Publication Date (Web): April 28, 2010 | doi: 10.1021/bk-2010-1038.ch010

dimethylsulfoxide or dimethylformamide as co-solvents to cellulose solution in [Amim][Cl], the viscosity and surface tension could be decreased and the conductivity could be increased. Electrospinnability was improved and thinner fiber was obtained. They also demonstrated that cellulose coagulation could be accomplished using water vapor. The water vapor such as 80% relative humidity of the environment caused the cellulose solidification from the surface of the jet and then fiber form could be obtained without the use of a coagulation bath. The combination of ILs and the dry-jet wet electrospinning can be also applied to synthetic polymers (*75*) and has more potential because ILs are 'designer solvents' that can be modified specifically for this electrospinning process.

Linhardt and coworkers prepared a cellulose/heparin composite fiber by electrospinning using [Bmim][Cl] and [Emim][Ba] mixture (*50*). FESEM images showed the formation of both micron- and nanosized fibers. The cellulose fiber showed a smooth surface, while cellulose/heparin composite fibers had a rough surface morphology (Figure 3). Cellulose/heparin composite fibers showed anticoagulant activity, demonstrating the activity of heparin remained unaffected even on exposure to a high voltage involved in electrospinning. Cellulose/heparin fibers have a great potential for use in the construction of artificial vessels with excellent blood compatibility. Table 3 shows various fiber prepared by spinning from ILs.

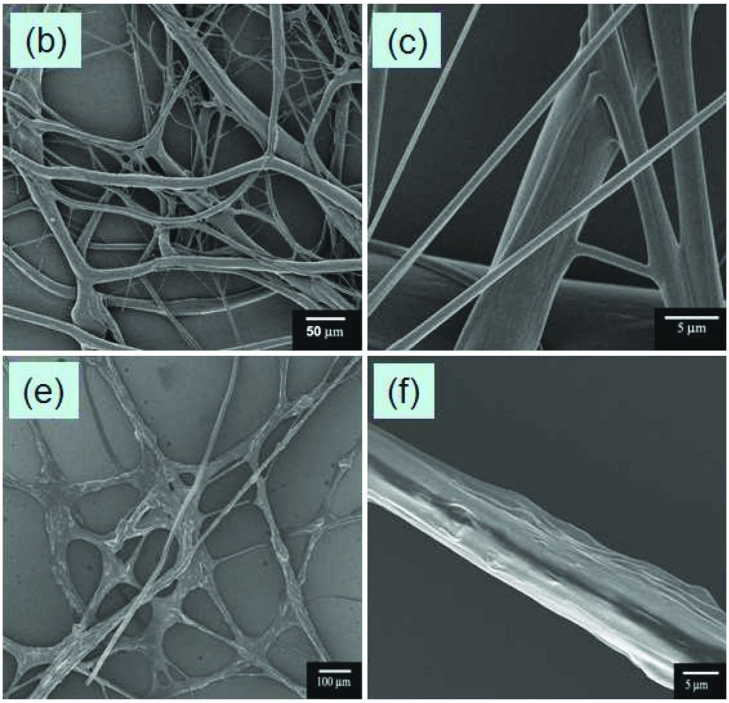

Figure 3. FESEM images: (A, B) cellulose fiber, (C, D) heparin/cellulose composite fiber.

Downloaded by UNIV OF GUELPH LIBRARY on June 22, 2012 | http://pubs.acs.org
Publication Date (Web): April 28, 2010 | doi: 10.1021/bk-2010-1038.ch010

Electrochemical Device Platforms

The direct electrochemistry of redox proteins recently has gained considerable interests, because it is helpful for understanding the electron-transfer mechanism in biological systems and for constructing biofuel cells and biosensors (*51*, *76*). Various systems have been developed to enhance the direct electron transfer and protein stability, because electroactive centers of redox proteins are embedded in the molecules and proteins are usually unstable. For these purpose, host materials should be able to immobilize proteins well and promote the direct electrochemistry. These materials also should be nontoxic, stable, and biocompatible (*77*, *78*). Biopolymers can provide a favorable microenvironment for redox proteins and enzymes to fabricate excellent biosensors. ILs have also been used in electrochemistry and electroanalysis, because of their high ionic conductivity and wide electrochemical windows (*79*). ILs also allow efficient direct electron transfer of various proteins such as microperoxidase (*80*), hemoglobin, horseradish peroxdiase (*45*), and glucose oxidase (*47*, *81*). Therefore, biopolymer/ILs composite systems might represent unique materials that could open up new opportunities for direct electrochemistry.

Lu et al. proposed a chitosan/[Bmim][BF_4] composite material and the composites were used as immobilization matrices to entrap hemoglobin (Hb) and horseradish peroxidase (HRP) (*45*, *46*). A reagentless HRP biosensor based on chitosan/[Bmim][BF_4] composite showed direct bioelectroanalysis toward H_2O_2. Both biocompatibility of chitosan and inherent conductivity of [Bmim][BF_4] enable the composite material to become an biosensing platform for direct electrochemistry and electrocatalysis of HRP. Wang et al. developed a chitosan/[Bmim][BF_4]/HRP/muti-walled carbon nanotubes (MWNTs) composite (*47*). This composite could form a relative uniform film with unique structure on electrode surface. The composite electrode showed good analytical performance such as low detection limit, good regeneration, and anti-fouling properties for determination of NADH. Sun et al. used [Bmim][PF_6] as binder to fabricate a carbon IL electrode (CILE) (*82*). Hemoglobin was immobilized on the surface of CILE with the sodium alginate (SA), a linear hydrophilic polysaccharide composed of β-mannuronic acids and α-L-guluronic acids, hydrogel film to form a SA/Hb/CILE. The SA/Hb/CILE composite showed good electrocatalytic activity to H_2O_2 and nitrate. They also made SA/SiO_2 nanoparticle/[Bmim][PF_6]/Hb/carbon paste electrode composite. This composite showed dramatically enhanced electrocatalytic activity to the reduction oftrichloroacetic acid, H_2O_2, and oxygen (*83*). Ding et al. developed a composite material based on *N*-butylpyridinium hexafluorophosphate, SA, and graphite to construct a HRP biosensor for the determination of H_2O_2 (*84*). The resulting biosensor not only had economic and disposable property but also showed good detection precision, bioactivity, storage stability, and reproducibility. Yan et al. developed a gelatin/dimethylformamide/[Omim][PF_6] hydrogel film to provide a favorable microenvironment for the direct electrochemistry of HRP at glassy carbon electrode (*51*). The enzyme electrode has good catalytic activity to the reduction of hydrogen peroxide, thermal stability, and reproducibility.

In Ionic Liquid Applications: Pharmaceuticals, Therapeutics, and Biotechnology; Malhotra, S.;
ACS Symposium Series; American Chemical Society: Washington, DC, 0.

Table 3. Polymer fibers prepared by spinning using ILs[a]

Spinning method	*Polymer*	*Spinning solvent*	*Polymer conc. (wt%)*	*Coagulation solvent*	*Fiber thickness*	*Ref.*
Wet spinning	Cellulose	[Amim][Cl]	4	water	ND[b]	(*62*)
		[Bmim][Cl]	3.5, 13.6	water, ND	1.46, 24.3 dtex[c]	(*42*, *68*)
		[Emim][Cl]	3.8-11.5,15.8	water, ND	1.84 dtex	(*42*, *63*)
		[Bd-mim][Cl]	13.2	ND	1.67 dtex	(*42*)
		[Bmim][Ac]	18.9	ND	1.64 dtex	(*42*)
		[Emim][Ac]	19.6	ND	1.76 dtex	(*42*)
	Cellulose/keratin	[Bmim][Cl]	10	methanol	ND	(*67*)
	Cellulose/m-aramid	[Bmim][Cl]	3.5	water	24.3-30.1 dtex	(*68*)
	Cellulose/MWNT	[Amim][Cl]	4	water	ND	(*62*)
	Cellulose/Fe_3O_4	[Emim][Cl]	3.8-11.4	water	ND	(*63*)
	Silk	[Emim][Cl]	10	methanol	150 μm	(*25*)
	DNA	[Bmim][BF_4]	5	water/[Bmim][BF_4]	200 μm	(*66*)
	PMIA	[Bmim][Cl]	14-18	water,water/[Bmim][Cl]	9.2-13.2 dtex	(*64*)
	PAN	[Bmim][Cl]	14-20	water/[Bmim][Cl]	ND	(*65*)
Electrospinning	Cellulose	[Bmim][Cl]	10	ethanol	500 nm	(*50*)
		[Amim][Cl]/DMSO	1-5	water vapor	100-800 nm	(*73*)
		[Amim][Cl]/DMF	2-3.5	water	100-500 nm	(*74*)

Continued on next page.

Downloaded by UNIV OF GUELPH LIBRARY on June 22, 2012 | http://pubs.acs.org
Publication Date (Web): April 28, 2010 | doi: 10.1021/bk-2010-1038.ch010

Downloaded by UNIV OF GUELPH LIBRARY on June 22, 2012 | http://pubs.acs.org
Publication Date (Web): April 28, 2010 | doi: 10.1021/bk-2010-1038.ch010

Table 3. (Continued). Polymer fibers prepared by spinning using ILs[a]

Spinning method	*Polymer*	*Spinning solvent*	*Polymer conc. (wt%)*	*Coagulation solvent*	*Fiber thickness*	*Ref.*
	Cellulose/heparin	[Bmim][Cl]/ [Emim][Ba]	7	ethanol	ND	(*50*)
	PMIA	[Bmim][BF_4]	6-8	water	Less than 1 µm	(*75*)

[a] PMIA = poly(m-phenyleneisophthalamide), MWNT = multi walled carbon nanotube, PAN = polyacrylonitrile. [b] no data. [c] dtex = g/(10000 m of fiber).

Prospects

Fabrication of unmodified biopolymer-based materials and composites has been traditionally hampered by the difficulty of dissolving biopolymers due to their highly crystalline nature. ILs have a great potential to dissolve biopolymers and develop biopolymer-based materials, because of their synthetic flexibility by changing the combinations of cation and anion, and green solvent properties such as non-volatility, non-flammability and recyclability. Biopolymers such as cellulose, chitin/chitosan, silk, and gelatin can be easily fabricated into films, membranes, fibers, spheres, and molded shapes by dissolution in ILs and reconstitution in anti-solvent. Biopolymer-based materials with ILs should be useful for the biomedical applications such as tissue engineering scaffolds, wound dressing, drug delivery, implantable devices, and biosensors owing to their inherent biocompatibility and biodegradability. Additionally, heparin/biopolymer composites which can be prepared by using ILs mixtures will be beneficial to enhance the blood compatibility of biopolymer.

References

1. Khor, E.; Lim, L. *Biomaterials* **2003**, *24*, 2339.
2. Schiffman, J. D.; Schauer, C. L. *Polym. Rev.* **2008**, *48*, 317.
3. Brown, R. M. *J. Polym. Sci., Part A: Polym. Chem.* **2004**, *42*, 487.
4. *Biopolymers for Medical and Pharmaceutical Applications*; Steinbüchel, A., Marchessault, R. H., Eds.; Wiley-VCH, GmbH & Co. KGaA: Weinheim, Germany, 2005; pp 329−382.
5. Yamanaka S.; Yatanabe K.; Suzuki Y. European Patent 0396344A2, 1990
6. Eisele, S.; Ammon, H. P. T.; Kindervater, R.; Grobe, A.; Gopel, W. *Biosens. Bioelectro.* **1994**, *9*, 119.
7. Rosenau, T.; Potthast, A.; Adorjan, I.; Hofinger, A.; Sixta, H.; Firgo, H.; Kosma, P. *Cellulose* **2002**, *9*, 283.
8. Strlič, M.; Kolar, J. *J. Biochem. Biophys. Methods* **2003**, *56*, 265.

9. Swatloski, R. P.; Spear, S. K.; Holbrey, J. D.; Rogers, R. D. *J. Am. Chem. Soc.* **2002**, *124*, 4974.
10. Yan, L.; Ishihara, K. *J. Polym. Sci., Part A: Polym. Chem.* **2008**, *46*, 3306.
11. Chow, K. S.; Khor, E.; Wan, A. C. A. *J. Polym. Res.* **2001**, *8*, 27.
12. *Chitin and Chitosan in Life Science*; Uragami, T., Kurita, K., Fukamizo, T., Eds.; Kodansha Scientifiv, Ltd.: Tokyo, Japan, 2001; pp 27−230.
13. Wu, Y.; Sasaki, T.; Irie, S.; Sakurai, K. *Polymer* **2008**, *49*, 2321.
14. Linhardt, R. J. *Chem. Indus.* **1991**, *2*, 45.
15. Linhardt, R. J.; Gunay, N. S. *Semin. Thromb. Hemostasis* **1999**, *25*, 5.
16. Murugesan, S.; Xie, J.; Linhardt, R. J. *Curr. Top. Med. Chem.* **2008**, *8*, 80.
17. Brieterman-Whits, R. *ANNA J.* **1995**, *22*, 491.
18. Sanchez, J.; Elgue, G.; Riesenfeld, J.; Olsson, P. *Thromb. Res.* **1998**, *89*, 41.
19. Murugesan, S.; Mousa, S.; Vijayaraghavan, A.; Ajayan, P. M.; Linhardt, R. J. *J. Biomed. Mater. Res., Part B* **2006**, *79*, 298.
20. Park T. J.; Murugesan S.; Linhardt R. J. Polysaccharide Materials, *ACS Symposium Series*, 2008a, in press.
21. Murugesan, S.; Park, T. J.; Yang, H. C.; Mousa, S.; Linhardt, R. J. *Langmuir* **2006**, *22*, 3461.
22. Li, Y.; Neoh, K. G.; Cen, L.; Kang, E. T. *Biotech. Bioeng.* **2003**, *84*, 305.
23. Oliveira, G. B.; Carvalho, L. B.; Silva, M. P. C. *Biomaterials* **2003**, *24*, 4777.
24. Phillips, D. M.; Drummy, L. F.; Conrady, D. G.; Fox, D. M.; Naik, R. R.; Stone, M. O.; Trulove, P. C.; De Long, H. C.; Mantz, R. A. *J. Am. Chem. Soc.* **2004**, *126*, 14350.
25. Phillips, D. M.; Drummy, L. F.; Naik, R. R.; De Long, H. C.; Fox, D. M.; Trulove, P. C.; Mantz, R. A. *J. Mater. Chem.* **2005**, *15*, 4206.
26. Gupta, M. K.; Khokhar, S. K.; Phillips, D. M.; Sowards, L. A.; Drummy, L. F.; Kadakia, M. P.; Naik, R. R. *Langmuir* **2007**, *23*, 1315.
27. Sheldon, R. A.; Lau, R. M.; Sorgedrager, M. J.; van Rantwijk, F. *Green Chem.* **2002**, *4*, 147.
28. Freemantle, M. *Chem. Eng. News* **1998**, *76*, 32.
29. Novoselov, N. P.; Sashina, E. S.; Kuźmina, O. G.; Troshenkova, S. V. *Russ. J. Gen. Chem.* **2007**, *77*, 1395.
30. El Seoud, O. A.; Koschella, A.; Fidale, L. C.; Dorn, S.; Heinze, T. *Biomacromol.* **2007**, *8*, 2629.
31. Mantz, R. A.; Fox, D. M.; Green, J. M.; Fylstra, P. A.; De Long, H. C.; Trulove, P. C. *Z. Naturforsch., A: Phys. Sci.* **2007**, *62*, 275.
32. Chheda, J. N.; Dumesic, J. A. *Catal. Today.* **2007**, *123*, 59.
33. Murugesan, S.; Linhardt, R. J. *Curr. Org. Synth.* **2005**, *2*, 437.
34. Liebert, T.; Heinze, T. *BioResources* **2008**, *3*, 576.
35. Moulthrop, J. S.; Swatloski, R. P.; Moyna, G; Rogers, R. D. *Chem. Commun.* **2005**, 1557.
36. Heinze, T.; Schwikal, K.; Barthel, S. *Macromol. Biosci.* **2005**, *5*, 520.
37. Ren, Q.; Wu, J.; Zhang, J.; He, J. S. *Acta Polym. Sin.* **2003**, 448.
38. Mikkola, J. P.; Kirilin, A.; Tuuf, J. C.; Pranovich, A.; Holmbom, B.; Kustov, L. M.; Murzin, D. Y.; Salmi, T. *Green Chem.* **2007**, *9*, 1229.
39. Fukaya, Y.; Sugimoto, A.; Ohno, H. *Biomacromol.* **2006**, *7*, 3295.
40. Fukaya, Y.; Hayashi, K.; Wada, M.; Ohno, H. *Green Chem.* **2008**, *10*, 44.

Downloaded by UNIV OF GUELPH LIBRARY on June 22, 2012 | http://pubs.acs.org
Publication Date (Web): April 28, 2010 | doi: 10.1021/bk-2010-1038.ch010

41. Zhao, H.; Baker, G. A.; Song, Z. Y.; Olubajo, O.; Crittle, T.; Peters, D. *Green Chem.* **2008**, *10*, 696.
42. Kosan, B.; Michels, C.; Meister, F. *Cellulose* **2008**, *15*, 59.
43. Barthel, S.; Heinze, T. *Green Chem.* **2006**, *8*, 301.
44. Xie, H. B.; Zhang, S. B.; Li, S. H. *Green Chem.* **2006**, *8*, 630.
45. Lu, X. B.; Hu, J. Q.; Yao, X.; Wang, Z. P.; Li, J. H. *Biomacromol.* **2006**, *7*, 975.
46. Lu, X. B.; Zhang, Q.; Zhang, L.; Li, J. H. *Electrochem. Commun.* **2006**, *8*, 874.
47. Wang, Q.; Tang, H.; Me, Q. J.; Tan, L.; Zhang, Y. Y.; Li, B.; Yao, S. Z. *Electrochim. Acta* **2007**, *52*, 6630.
48. Murugesan, S.; Wiencek, J. M.; Ren, R. X.; Linhardt, R. J. *Carbohyd. Polym.* **2006**, *63*, 268.
49. Park, T. J.; Weiwer, M.; Yuan, X. J.; Baytas, S. N.; Munoz, E. M.; Murugesan, S.; Linhardt, R. J. *Carbohyd. Res.* **2007**, *342*, 614.
50. Viswanathan, G.; Murugesan, S.; Pushparaj, V.; Nalamasu, O.; Ajayan, P. M.; Linhardt, R. J. *Biomacromol.* **2006**, *7*, 415.
51. Yan, R.; Zhao, F.; Li, J.; Xiao, F.; Fan, S.; Zeng, B. *Electrochim. Acta* **2007**, *52*, 7425.
52. Turner, M. B.; Spear, S. K.; Holbrey, J. D.; Rogers, R. D. *Biomacromol.* **2004**, *5*, 1379.
53. Turner, M. B.; Spear, S. K.; Holbrey, J. D.; Daly, D. T.; Rogers, R. D. *Biomacromol.* **2005**, *6*, 2497.
54. Poplin, J. H.; Swatloski, R. P.; Holbrey, J. D.; Spear, S. K.; Metlen, A.; Gratzel, M.; Nazeeruddin, M. K.; Rogers, R. D. *Chem. Commun.* **2007**, 2025.
55. Bagheri, M.; Rodriguez, H.; Swatloski, R. P.; Spear, S. K.; Daly, D. T.; Rogers, R. D. *Biomacromol.* **2008**, *9*, 381.
56. Tsioptsias, C.; Panayiotou, C. *Carbohydr. Polym.* **2008**, *74*, 99.
57. Modi, G. K.; Pereira, B. J. G.; Jaber, B. L. *Semin. Dial.* **2001**, *14*, 318.
58. Park, T. J.; Lee, S. H.; Trevor, J. S.; Martin, J. G.; Mousa, S. A.; Snezhkova, E. A.; Sarnatskaya, V. V.; Nikolaev, S. G.; Linhardt, R. J. *Chem. Commun.* **2008**, in press.
59. Hasirci, N; Akovali, G. *J. Biomed. Mater. Res.* **1986**, *20*, 963.
60. Chandy, T.; Sharma, C. P. J. *Biomater. Appl.* **1998**, *13*, 128.
61. Perepelkin, K. E. *Fibre Chem.* **2007**, *39*, 163.
62. Zhang, H.; Wang, Z. G.; Zhang, Z. N. *Adv. Mater.* **2007**, *19*, 698.
63. Sun, N.; Swatloski, R. P.; Maxim, M. L. *J. Mater. Chem.* **2008**, *18*, 283.
64. Zhao, T.; Wang, H.; Zhang, Y. *Int. J. Mol. Sci.* **2008**, *8*, 680.
65. Zhang, Y. M.; Tu, X. P.; Liu, W. W. *Polym. Eng. Sci.* **2008**, *48*, 184.
66. Lee, C. K.; Shin, S. R.; Lee, S. H.; Jeon, J. H.; So, I.; Kang, T. M.; Kim, S. I.; Mun, J. Y.; Han, S. S.; Spinks, G. M.; Wallace, G. G.; Kim, S. J. *Angew. Chem., Int. Ed.* **2008**, *47*, 2470.
67. Xie, H. B.; Li, S. H.; Zhang, S. B. *Green Chem.* **2005**, *7*, 606.
68. Lee, J.; Broughton, R. M.; Worley, S. D. *AATCC Rev.* **2008**, *8*, 43.
69. Sill, T. J.; von Recum, H. A. *Biomaterials* **2008**, *29*, 1989.
70. Rutledge, G. C.; Fridrikh, S. V. *Adv. Drug Delivery Rev.* **2007**, *59*, 1384.

Downloaded by UNIV OF GUELPH LIBRARY on June 22, 2012 | http://pubs.acs.org
Publication Date (Web): April 28, 2010 | doi: 10.1021/bk-2010-1038.ch010

71. Costolo, M. A.; Lennhoff, J. D.; Pawle, R. *Nanotechnology* **2008**, *19*, 35707.
72. Zhang, C. X.; Yuan, X. Y.; Wu, L. L. *Eur. Polym. J.* **2005**, *41*, 423.
73. Xu, S. S.; Zhang, J.; He, A. H. *Polymer* **2008**, *49*, 2911.
74. Sui, S.; Yuan, J.; Yuan, W.; Zhou, M. *Chem. Lett.* **2008**, *37*, 114.
75. Yang, W.; Yu, H.; Zhu, M. F. *J. Macromol. Sci., Part B: Phys.* **2006**, *45*, 573.
76. Jia, J. B.; Wang, B. Q.; Wu, A. G.; Cheng, G. J.; Li, Z.; Dong, S. J. *Anal. Chem.* **2002**, *74*, 2217.
77. Simionsecu, C.; Popa, M.; Dumitru, S. *Biotechnol. Bioeng.* **1987**, *29*, 361.
78. Iwasaki, Y.; Nakagawa, C; Ohtomi, M; Akiyosi, K. *Biomacromol.* **2004**, *5*, 1110.
79. Buzzeo, M. C.; Evans, R. G.; Compton, R. G. *ChemPhysChem* **2004**, *5*, 1106.
80. Zhao, F.; Wu, X. E.; Wang, M. K.; Liu, Y.; Gao, L. X.; Dong, S. J. *Anal. Chem.* **2004**, *76*, 4960.
81. Li, J. W.; Yu, J. J.; Zhao, F. Q.; Zeng, B. Z. *Anal. Chem.* **2007**, *587*, 33.
82. Sun, W.; Wang, D.; Gao, R.; Jiao, K. *Electrochem. Commun.* **2007**, *9*, 1159.
83. Sun, W.; Wang, D.; Zhong, J.; Jiao, K. *J. Sold State Electrochem.* **2008**, *12*, 655.
84. Ding, C.; Zhang, M.; Zhao, F.; Zhang, S. *Anal. Biochem.* **2008**, *378*, 32.

Downloaded by UNIV OF GUELPH LIBRARY on June 22, 2012 | http://pubs.acs.org
Publication Date (Web): April 28, 2010 | doi: 10.1021/bk-2010-1038.ch010

In Ionic Liquid Applications: Pharmaceuticals, Therapeutics, and Biotechnology; Malhotra, S.;
ACS Symposium Series; American Chemical Society: Washington, DC, 0.

Downloaded by STANFORD UNIV GREEN LIBR on June 22, 2012 | http://pubs.acs.org
Publication Date (Web): April 28, 2010 | doi: 10.1021/bk-2010-1038.ch011

Chapter 11

Toxicological Evaluation of Ionic Liquids

Effect of Ionic Liquids on Human Colon Carcinoma HT-29 and CaCo-2 Cell Lines

**Raquel F. M. Frade,[*,1] Ana Matias,[1] Luis C. Branco,[2,3]
Nuno M. T. Lourenço,[3] João N. Rosa,[3] Carlos A. M. Afonso,[3]
and Catarina M. M. Duarte[1,4]**

**[1]Instituto de Biologia Experimental e Tecnológica, Av. Da
República, Quinta-do-Marquês, Estação Agronómica, Apartado12,
2781-901 Oeiras, Portugal
[2]REQUIMTE, Departamento de Química, Faculdade de Ciências e
Tecnologia, Universidade Nova de Lisboa, 2829-516 Caparica, Portugal
[3]IBB- Instituto de Biotecnologia e Bioengenharia, Centro de Engenharia
Biológica e Química (CEBQ), Instituto Superior Técnico, Av. Rovisco Pais,
P-1049-001 Lisboa, Portugal
[4]Instituto de Tecnologia Química e Biológica, Universidade Nova
de Lisboa, Avenida da República, Estação Agronómica Nacional,
2780-157 Oeiras, Portugal
[*]raquel.frade@ist.utl.pt**

Introduction

Toxicological evaluation of ionic liquids was performed on colon carcinoma cells. Methylimidazolium (MIM) toxicity increases with the chain length, however toxicity is greatly decreased when a carboxylic group is added at the end of a C_{10} chain. MIM toxicity does not depend on the anion, in contrast to aliquat and dimethylguanidinium based cations, whose toxicity was strongly reduced with bistrifluoromethane-sulfonimidate.

In Ionic Liquid Applications: Pharmaceuticals, Therapeutics, and Biotechnology; Malhotra, S.;
ACS Symposium Series; American Chemical Society: Washington, DC, 0.

Downloaded by STANFORD UNIV GREEN LIBR on June 22, 2012 | http://pubs.acs.org
Publication Date (Web): April 28, 2010 | doi: 10.1021/bk-2010-1038.ch011

Models Used for Toxicological Evaluation

Ionic liquids (ILs) have been classified as “green solvents” due to their low volatility, which contrasts to conventional organic solvents. However, many are water-miscible and therefore, if they escape to the environment, they will possible have a negative impact in the ecossistems and human lives. As an attempt to predict this impact, toxicological evaluations have been undertaken in several models of the aquatic (algae, fish, plants) and terrestrial (plants, soil microorganisms) environment (*1–10*). More recently, some publications have come out with interesting experimental work carried out in rat and human cell lines. These cell lines have their origin on carcinomas from the brain (rat C6 cell line) (*1*), blood and bone marrow (rat IPC-81) (*7*, *8*, *11*), cervical region (human HeLa) (*12*) and the colon (human HT-29 and CaCo-2) (*13*, *14*). By studying the effect of the ILs on these cell models, it is possible to predict likely consequences for animals and human beings.

Toxicological Assays Performed on HT-29 and CaCo-2 Cell Lines

In our experimental study, two colon carcinoma cell lines were used: HT-29 and CaCo-2. This last has the remarkable advantage of mimicking intestinal epithelium once cells have reached confluence (*15*, *16*). These cells are grown on to a surface and consequently, spaces between them get shorter and shorter during cellular division. When they reach confluency, they stop dividing and differentiate, acquiring typical characteristics of human intestinal epithelial cells. Consequently, compounds that are toxic to confluent CaCo-2 will likely be harmful to human intestine.

Contrary to confluent CaCo-2 cell line, HT-29 cells still divide when they reach confluency. Compounds that are not toxic to confluent CaCo-2 cells, but are toxic to HT-29, are possible acting as anti-cancer agents. Accordingly, it is extremely useful to compare the data obtained for HT-29 and CaCo-2 cells.

Based on the above explanation, CaCo-2 cells were assayed in a confluent state and were left incubating with the ILs for 4 hours. In case of cell viability decreasing, this is due to induced cell death. HT-29 cells were used at a low confluence in order to investigate if the ILs would also have an effect on the proliferation cell rate. To allow cells to divide and proliferate during the experiment, cells were left for an additional period of 24 hours, after the 4 hours treatment with the ILs, and before viability assessment. In this situation, decreasing of cell viability can be a result of a lower proliferation cell rate (in comparison to the control samples) and / or to induced cell death. To confirm that tested compounds are inducing cell death, microscopic observations are indispensable; cell detachment and presence of cell fragments are indicators of cellular toxicity.

Determination of Cell Viability – MTT Assay

In this study, we have used the reagent 3-(4,5-dimethylthiazolyl-2)-2,5-diphenyltetrazolium bromide (MTT) to detect metabolic active cells (viable cells). MTT assay was developed in 1983 and it has been extensively documented (*17*, *18*). MTT is reduced by mitochondrial succinic dehydrogenases in viable cells and the resultant formazan crystals can be solubilized and detected spectrometrically. Consequently, determination of cellular viability can be assessed by quantification of the amount of reduced MTT in ILs-treated cells and non-treated cells (control). Relative viability is the quocient between both absorbances.

Downloaded by STANFORD UNIV GREEN LIBR on June 22, 2012 | http://pubs.acs.org
Publication Date (Web): April 28, 2010 | doi: 10.1021/bk-2010-1038.ch011

Results and Discussion

All the assays were performed in triplicate and the averages were used to plot the relative viability as a function of the IL concentration (μM). Concentrations up to 6000 μM were used and several concentrations were experimented for each IL.

We have investigated several classes of cations, being methylimidazolium (MIM) the most extensively studied. Dimethylguanidinium (DMG), tri-*n*-hexyl-tetra-*n*-decylphosphonium (P66614), tri-*n*-octyl-methylammonium (Aliquat) and choline were the other studied cations. The studied anions were tetrafluoroborate (BF_4), hexafluorophosphate (PF_6), acesulfame (ACS), saccharin (SAC), dicyanoamide (DCA), bis(trifluoromethanesulfonyl)imide (NTf_2), *N*-cyanobenzenesulfonamide (CBS) and *N*-cyanomethanesulfonamide (CMS) (see Table I).

Compounds that decreased cell viability in about 50% or more were considered toxic (T). And, in the situations where viability was considerably decreased (> 30%), but never reached 50%, compounds were classified as slightly toxic (ST). Compounds that are toxic for confluent CaCo-2 cells are not interesting and therefore, they were not considered for toxicity evaluation on HT-29 cells.

Methylimidazolium Cation

Several variations on the cation structure were taken into account: different lengths of the alkyl chains and absence or presence of functionalized alkyl chains (OH, R-O-R, R-COOH and $RCOO-CH_2CH_3$; R-variable group). Moreover, MIM cation was studied in combination with several anions: BF_4, PF_6, ACS, SAC, DCA, NTf_2, CMS and CBS.

Independently of the anion, MIM with a 4 carbons-alkyl-chain (C_4: CH_2-CH_2-CH_2-CH_3) is not toxic to CaCo-2 and HT-29, within the studied concentration range. However, viability decreases substantially when C_8 and C_{10} chains are used instead; and the increase in toxicity correlates with the length of the chain.

Downloaded by STANFORD UNIV GREEN LIBR on June 22, 2012 | http://pubs.acs.org
Publication Date (Web): April 28, 2010 | doi: 10.1021/bk-2010-1038.ch011

Table I. Types of anions and cations used in this experimental study

Types of anions		*Types of cations*	
BF$_4$	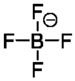	C_4MIM	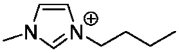
PF$_6$	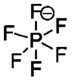	C_8MIM	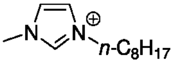
ACS	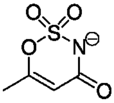	C_{10}MIM	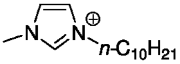
SAC	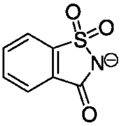	BDMIM	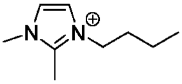
DCA	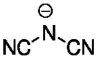	C_2OHMIM	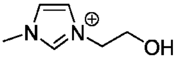
NTf$_2$	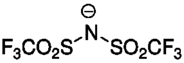	C_5O_2MIM	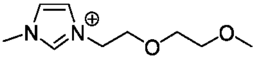
CMS	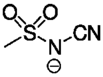	$C_{10}O_2$EtMIM	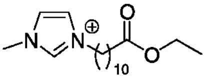
CBS	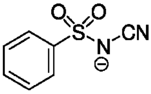	$C_{10}O_2$HMIM	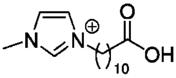
		Aliquat	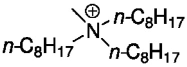
		P66614	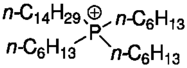
		DMG	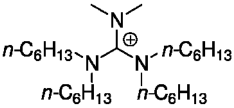
		Choline	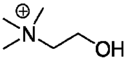

Downloaded by STANFORD UNIV GREEN LIBR on June 22, 2012 | http://pubs.acs.org
Publication Date (Web): April 28, 2010 | doi: 10.1021/bk-2010-1038.ch011

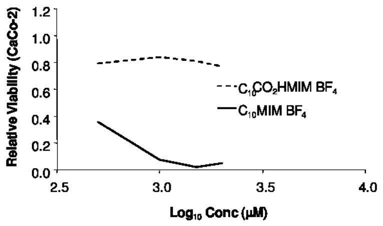

Figure 1. Relative viability of CaCo-2 cells after 4 hours treatment with $[C_{10}MIM]$ $[BF_4]$ and $[C_{10}CO_2HMIM]$ $[BF_4]$.

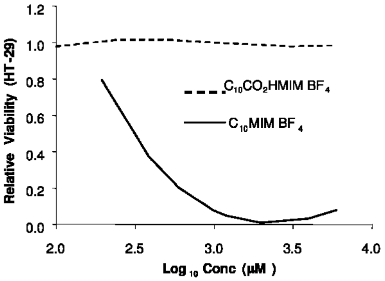

Figure 2. Relative viability of HT-29 cells following 4 hours treatment with $[C_{10}MIM]$ $[BF_4]$ and $[C_{10}CO_2HMIM]$ $[BF_4]$ and a 24 hours proliferation period.

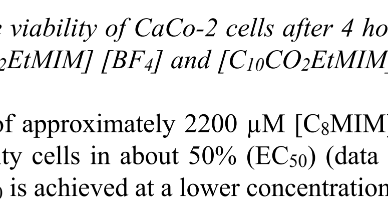

Figure 3. Relative viability of CaCo-2 cells after 4 hours treatment with $[C_{10}CO_2EtMIM]$ $[BF_4]$ and $[C_{10}CO_2EtMIM]$ $[PF_6]$.

A concentration of approximately 2200 µM $[C_8MIM]$ $[BF_4]$ is sufficient to reduce CaCo-2 viability cells in about 50% (EC_{50}) (data not shown). And, for $[C_{10}MIM]$ $[BF_4]$, EC_{50} is achieved at a lower concentration of approximately 600 µM (Figure 1).

Surprisingly, the presence of a carboxylic group at the end of the C_{10} chain ($(CH_2)_{10}$-COOH) decreases greatly toxicity. As seen in Figure 1, $[C_{10}CO_2HMIM]$ $[BF_4]$ is not toxic to CaCo-2 cells. Results are similar to $[C_{10}CO_2HMIM]$ $[PF_6]$ and $[C_{10}CO_2HMIM]$ [DCA] ILs (data not shown). Moreover, these ILs are not toxic for HT-29 cell line (Figure 2).

Downloaded by STANFORD UNIV GREEN LIBR on June 22, 2012 | http://pubs.acs.org
Publication Date (Web): April 28, 2010 | doi: 10.1021/bk-2010-1038.ch011

In contrast to, the change of the carboxylic group to an ester ($(CH_2)_{10}$-COO-CH_2-CH_3) induces a high toxicity. CaCo-2 cells were all death at higher doses as shown in the cytotoxicity curves presented in Figure 3.

When an additional CH_3 group is added to C_4MIM cation at position 2 of the imidazolium ring (BDMIM), the cation does not induce cytotoxicity for CaCo-2 cells, whereas for HT-29 cells it can be a little toxic. Furthermore, there is no cytotoxicity when C_4 chain is replaced for C_2OH (CH_2-CH_2-OH) or C_5O_2 (CH_2-CH_2-O-CH_2-CH_2-O-CH_3) chains, independently on the anion (data not shown). Results for MIM ILs can be found summarized in Table II.

Table II. Toxicity of methylimidazolium class of ionic liquids

Cations	*R*	*Anions*	*HT-29*	*CaCo-2*
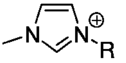	*n*-C_4H_9 (*n*-C_8H_{17}/*n*-$C_{10}H_{21}$)	BF_4	ST (-/-)	NT (T/T)
		PF_6	NT (-/-)	NT (T/T)
		NTf_2	NT	NT
		ACS	NT	NT
		SAC	NT	NT
		DCA	NT	NT
		CBS	ST	NT
		CMS	NT	NT
	$C_{10}H_{20}CO_2Et$	Br	-	T
		BF_4 / PF_6 / DCA	-	T
	$C_{10}H_{20}CO_2H$	BF_4 / PF_6 / DCA	NT	NT
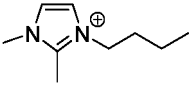		BF_4 /CMS	ST	NT
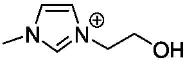		BF_4 / PF_6 / ACS / SAC / CMS / CBS	NT	NT
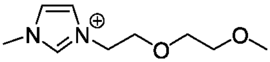		BF_4 / PF_6	NT	NT

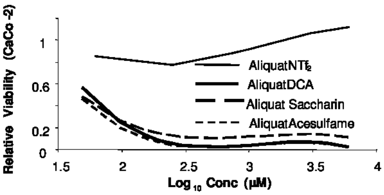

Figure 4. Viability of CaCo-2 cells following 4 hours treatment with [Aliquat] [NTf$_2$], [Aliquat] [DCA], [Aliquat] [Saccharin] and [Aliquat] [Acesulfame].

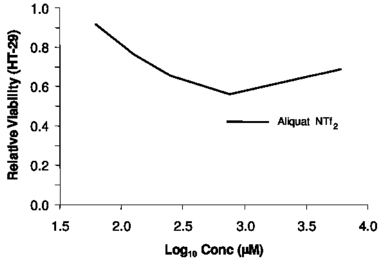

Figure 5. Viability of HT-29 cells following 4 hours treatment with [Aliquat] [NTf$_2$] and a 24 hours proliferation period.

Downloaded by STANFORD UNIV GREEN LIBR on June 22, 2012 | http://pubs.acs.org
Publication Date (Web): April 28, 2010 | doi: 10.1021/bk-2010-1038.ch011

Tri-*n*-octyl-methylammonium Cation

Many of the ILs containing this cation are highly toxic for CaCo-2 cells. [Aliquat] [NTf$_2$] is the only exception. It is not cytotoxic for these cells (Figure 4) and dimishes HT-29 cells viability to a certain extend, but it never goes below 50% (Figure 5).

The trends obtained for [Aliquat] [NTf$_2$] are quite different in both of the cell lines. In Figure 4, this IL is likely generating interference signals that keep rising with the concentration, because there is not toxic effect associated to this IL on this cell line. Otherwise, interference would be masked by viability decrease at cytotoxic concentrations. In Figure 5, viability increasing at higher concentrations may be due to a mitogenic effect.

Tetra-*n*-hexyl-dimethylguanidinium Cation

Tetra-*n*-hexyl-dimethylguanidinium (DMG) toxicity also depends strongly on the anion. CaCo-2 viability in the presence of [DMG] [PF$_6$] stays within the range 30-40% for all the studied concentrations, as seen in Figure 6. However, [DMG] [DCA] and [DMG] [NTf$_2$] ILs are not toxic for this cell line (Figure 6). [DMG] [DCA] decreases a little more HT-29 cells viability than CaCo-2 cells viability, whereas [DMG] [NTf2] induces a similar response at the highest concentration. However, its cytotoxicity profiles are quite different (Figure 6,7). Increasing on HT-29 cells viability in the presence of lower concentrations of [DMG] [NTf2] can also be attributed to a mitogenic effect. Toxicity of DMG and other classes of ionic liquids is summarized in Table III.

Tri-*n*-hexyl-tetra-*n*-decylphosphonium Cation

Tri-*n*-hexyl-tetra-*n*-decylphosphonium cation (P66614) was studied in combination with NTf_2. It is not toxic for CaCo-2 cells (Figure 6), however it decreases HT-29 viability in about 50% at the highest concentration (Figure 7).

Downloaded by STANFORD UNIV GREEN LIBR on June 22, 2012 | http://pubs.acs.org
Publication Date (Web): April 28, 2010 | doi: 10.1021/bk-2010-1038.ch011

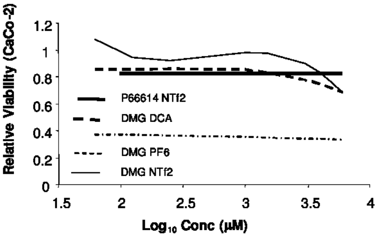

Figure 6. Viability of CaCo-2 cells after 4 hours treatment with [DMG] [NTf_2], [DMG] [DCA], [DMG] [PF_6] and [P66614] [NTf_2].

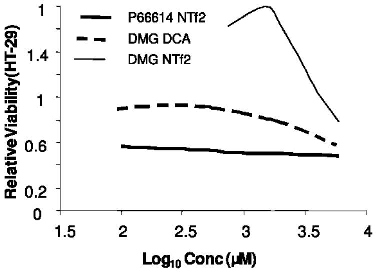

Figure 7. Viability of HT-29 cells following 4 hours treatment with [DMG] [NTf_2], [DMG] [DCA] and [P66614] [NTf_2] and a 24 hours proliferation period.

Downloaded by STANFORD UNIV GREEN LIBR on June 22, 2012 | http://pubs.acs.org
Publication Date (Web): April 28, 2010 | doi: 10.1021/bk-2010-1038.ch011

Table III. Toxicity of different classes of ionic liquids[a]

Cations	*Anions*	*HT-29*	*CaCo-2*
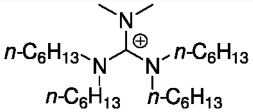	PF_6	-	T
	NTf_2	NT	NT
	DCA	ST	NT
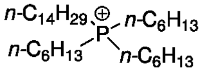	NTf_2	T	NT
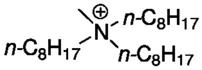	ACS / SAC	-	T
	NTf_2	ST	NT
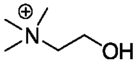	ACS / SAC	NT	NT

[a] ST-slightly toxic (>30% and < 50%); T-toxic (>50%); NT-not toxic.

Choline Cation

Choline was studied in combination with the anions ACS and SAC and both combinations were not toxic for any of the tested colonic cell lines (data not shown).

Conclusions

Two colon carcinoma HT-29 and CaCo-2 cell lines were used as tools to investigate toxicity of several ILs on human intestinal epithelium. Negative results were obtained for some of the tested ILs which excludes their utilization when searching for human inoffensive ILs. If this is a priority, MIM cations with long alkyl chains will be putted aside, together with most of the Aliquat cations (Figures 1,2,3,4). Within the tested combinations, only [Aliquat] [NTf_2] is not toxic for CaCo-2 cells (Figure 4). Furthermore, DMG cation can also be harmful for human intestine when combined with some anions, such as PF_6 (Figure 6). Toxicity of these two last classes of cations were seen to depend greatly on the anion (Figure 4, 6). Amanzingly, NTf_2 anion changes completely cytotoxicity of Aliquat and DMG ILs: they are no longer cytotoxic to CaCo-2 cells dispite decreasing to a certain extent HT-29 cells viability (Figures 4,5,6,7). Similar result was also obtained for [P66614] [NTf2] which reduced the number of metabolic active HT-29 cells, without significant effect on CaCo-2 cells viability (Figure 6,7). Therefore, the presence of NTf_2 reduces significantly CaCo-2 cytotoxicity and it seems to be acting as an anticarcinogenic agent in HT-29 cells.

Within the extensively studied MIM cation class, it is very interesting to note that toxicity of C_{10}MIM can be overcomed in the presence of a carboxylic group at the end of the alkyl chain (Figure 1,2). But, this still needs more studies.

It would be extremely important to explore these results and to understand how cell toxicity of ILs is ruled out. In a near future, we would like to be able to explain these mechanisms. But, it is necessary to highlight that non toxic ILs for CaCo-2 do not mean they are safe for humans. These results can work as a primary screening, but to be completely sure that ILs are human-safe, toxicity has to be evaluated in a broad number of cell types from different origins, since toxicity of a compound can be organ-specific.

References

1. Ranke, J.; Molter, K.; Stock, F.; Bottin-Weber, U.; Poczobutt, J.; Hoffman, J.; Ondruschka, B.; Filser, J.; Jastorff, B. *Ecotoxicol. Environ. Saf.* **2003**, *58* (3), 396–404.
2. Swatloski, R. P.; Holbrey, J. D.; Memon, S. B.; Caldwell, G. A.; Caldwell, K. A.; Rogers, R. *Chem. Commun.* **2004**, *6*, 668–669.
3. Lee, S.; Chang, W.; Choi, A.; Koo, Y. *Korean J. Chem. Eng.* **2005**, *22* (5), 687–690.
4. Latala, A.; Stepnowski, P.; Nedzi, M.; Mrozik, W. *Aquat. Toxicol.* **2005**, *73*, 91–98.
5. Ganske, F.; Bornscheuer, U. T. *Biotechnol. Lett.* **2006**, *28*, 465–469.
6. Pretti, C.; Chiappe, C.; Pieraccini, D.; Gregori, M.; Abramo, F.; Monni, G.; Intorre, L. *Green Chem.* **2006**, *8*, 238–240.
7. Matzke, M.; Stolte, S.; Thiele, K. ; Juffernholz, T.; Arning, J.; Ranke, J.; Welz-Biermann, U.; Jastorff, B. *Green Chem.* **2007**, *9*, 1198–1207.
8. Stolte, S.; Matzke, M.; Arning, J.; Boschen, A.; Pitner, W.; Welz-Biermann, U.; Jastorff, B.; Ranke, J. *Green Chem.* **2007**, *9*, 1170–1179.
9. Kulacki, K. J.; Lamberti, G. A. *Green Chem.* **2008**, *10*, 104–110.
10. Cho, C.; Pham, T. P. T.; Jeon, Y.; Yun, Y. *Green Chem.* **2008**, *10*, 67–72.
11. Stolte, S.; Arning, J.; Bottin-Weber, U.; Matzke, M.; Stock, F.; Thiele, K.; Uerdingen, M.; Welz-Bierman, U.; Jastorff, B.; Ranke, J. *Geen Chem.* **2006**, *8*, 621–629.
12. Stepnowski, P.; Skladanowski, A. C.; Ludwiczak, A.; Laczynska, E. *Hum. Exp. Toxicol.* **2004**, *23*, 513–517.
13. Frade, R. F. M.; Matias, A.; Branco, L. C.; Afonso, C. A. M.; Duarte, C. M. M. *Green Chem.* **2007**, *9*, 873–877.
14. Garcia-Lorenzo, A.; Tojo, E.; Tojo, J.; Teijeira, M.; Rodríguez-Berrocal, F. J.; González, M. P.; Martínez-Zorzano, V. S. *Green Chem.* **2008**, *10*, 508–510.
15. Jumarie, C.; Malo, C. *J. Cell Physiol.* **1991**, *149*, 24–33.
16. Giuliano, A. R.; Word, R. J. *Am. J. Physiol.* **1991**, *276*, G958–G964.
17. Mosmann, T. *J. Immunol. Methods* **1983**, *65*, 55–63.
18. Hamid, R.; Rotshteyn, Y.; Rabadi, L.; Parikh, R.; Bullock, P. *Toxicol. in Vitro* **2004**, *18*, 703–710.

Downloaded by STANFORD UNIV GREEN LIBR on June 22, 2012 | http://pubs.acs.org
Publication Date (Web): April 28, 2010 | doi: 10.1021/bk-2010-1038.ch011

Downloaded by DUKE UNIV on June 22, 2012 | http://pubs.acs.org
Publication Date (Web): April 28, 2010 | doi: 10.1021/bk-2010-1038.ch012

Chapter 12

Formation of Anhydrosugars from Polysaccharides in Ionic Liquids by Microwave Irradiation

**Hiroe Satoh,[1,4] Momoko Hayashi,[1] Toshifumi Satoh,[2]
Toyoji Kakuchi,[2] Harumi Kaga,[3] and Kenji Takahashi*,[1]**

[1] Division of Material Science, Graduate School of Natural Science and Technology, Kanazawa University, Kanazawa 920-1192, Japan
[2] Division of Biotechnology and Macromolecular Chemistry, Graduate School of Engineering, Hokkaido University, Sapporo 060-8628, Japan
[3] National Institute of Advanced Industrial Science and Technology (AIST), Sapporo 062-8517, Japan
[4] Technical Center, Seiren Co., Ltd., Fukui 913-0036, Japan
***ktkenji@t.kanazawa-u.ac.jp**

It is known that some ionic liquids can dissolve cellulose, and that ionic liquids can be heated very rapidly using microwave irradiation. These characteristics make it possible to use ionic liquids as a reaction medium to form anhydrosugars from polysaccharides by microwave irradiation. In the present study, we examined formation of anhydroglucose from glucose, cellobiose, and cellulose using microwave irradiation in several ionic liquids. A single-mode microwave was used to carry out the reactions. The yield of anhydroglucose from cellobiose was quite high: a 60 mol% yield at 270 °C after 4 min of heating time. It has also been found that in the ionic liquids, diethyl-methyl-(2-methoxyethyl)ammonium bis(trifluoromethanesulfonyl)imide and butyl-methylimidazolium bis(trifluoromethanesulfonyl)imide, a few products were obtained from depolymerization of cellulose and cellobiose. The main products were identified as 1,6-anhydro-β-D-glucopyranose and 1,6-anhydro-β-D-glucofuranose. In contrast, in the ionic liquid butyl-methylimidazolium chloride after a few minutes

In Ionic Liquid Applications: Pharmaceuticals, Therapeutics, and Biotechnology; Malhotra, S.;
ACS Symposium Series; American Chemical Society: Washington, DC, 0.

of microwave heating, the samples turned dark brown; no anhydrosugars were produced. These results suggest the importance of proper selection of the anion in the ionic liquids to produce anhydrosugars.

Introduction

1,6-Anhydro-β-D-glucopyranose (AGP) is a typical anhydrosugar. AGP can be prepared by depolymerization of a sugar source such as cellulose and cellobiose. In line with the increasing interest in sustainable development, the synthesis of AGP is an important possibility for development of applications, using it as a chemical and fuel feedstock. For example, AGP can be used as a monomer in the production of biodegradable surfactants, stereoregular polysaccharides, and hyperbranched polysaccharides (*1*, *2*). Figure 1 depicts a reaction scheme for producing anhydroglucose from glucose or cellobiose and for synthesis of hyperbranched polysaccharides.

It is known that ionic liquids can be heated very efficiently by microwave irradiation (*3*), are very stable even at high temperatures, are non-flammable, and have negligible vapor pressure. These desirable qualities have led to an interest in ionic liquids as reaction media to use with microwave irradation, which leads to large reductions in reaction times, and enhancements in conversions and selectivity. These improvements offer several advantages for an eco-friendly process. The improvements produced by microwave irradiation are thought to be caused by both thermal and non-thermal effects. The thermal effect is that solvent is heated rapidly and uniformly, so that reaction rates are faster than with conventional heating, even at the same temperature. The non-thermal effect is that the electric and magnetic fields induced by microwave irradiation are thought to enhance reaction rates. However, it is not yet clear why microwave irradiation leads to reaction enhancement. Although the microwave non-thermal effect on chemical reactions is a very interesting topic, we will not argue this effect in the present study.

There have been several studies regarding the formation of anhydrosugars, but in those previous methods, the yields and selectivity were limited (*4*–*7*). We therefore explored the combination of ionic liquids and microwave heating for the potential of that combination to obtain anhydrosugars with very high selectivity.

In this study, we present a method to produce anhydroglucose from carbohydrates such as glucose, cellulose, and cellobiose, using microwave radiation in a hydrophobic ionic liquid; the hydrophobic nature of the reaction medium makes aqueous extraction of reaction products possible.

Downloaded by DUKE UNIV on June 22, 2012 | http://pubs.acs.org
Publication Date (Web): April 28, 2010 | doi: 10.1021/bk-2010-1038.ch012

Downloaded by DUKE UNIV on June 22, 2012 | http://pubs.acs.org
Publication Date (Web): April 28, 2010 | doi: 10.1021/bk-2010-1038.ch012

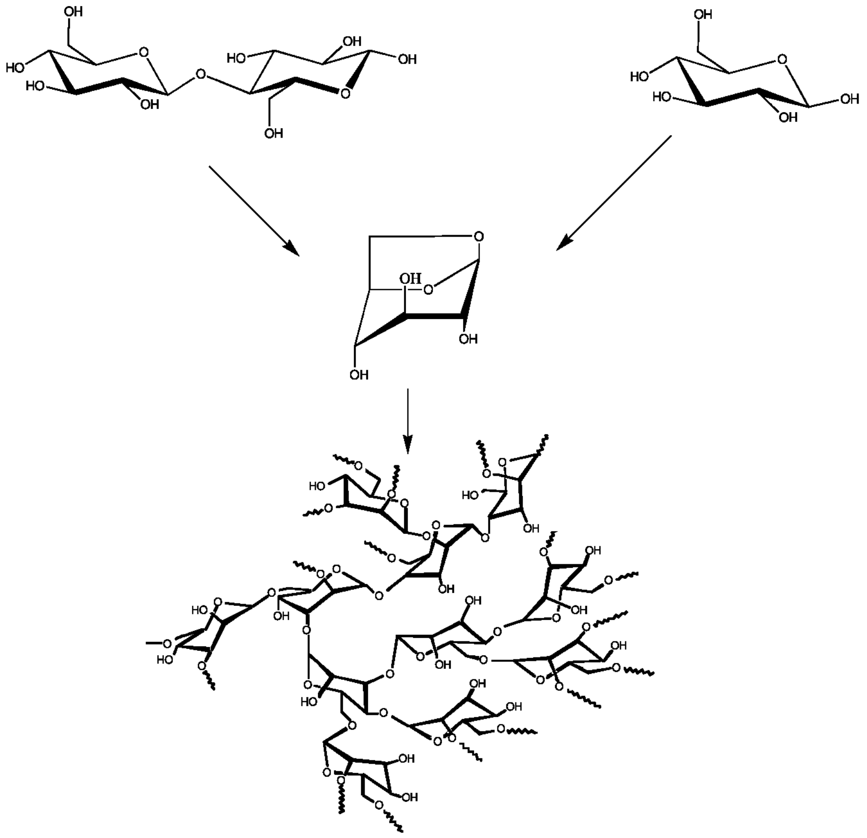

Figure 1. Reaction scheme for formation of an anhydrosugar from cellobiose and glucose, and synthesis of a hyperbranched polysaccharide.

Experimental

Cellulose (50 mg, microcrystalline, MERCK), cellobiose (50 mg, Kanto Kagaku), or glucose (50 mg, Kanto Kagaku) was dispersed in 5 g of ionic liquid. *N*,*N*-Diethyl-*N*-methyl-*N*-(2-methoxyethyl)ammonium bis(trifluoromethanesulfonyl)imide (DEME-TFSI) was kindly donated by Nisshinbo Industries Inc. Physical properties reported for DEME-TFSI are conductivity 2.62 mS·cm^{-1}, density 1.42 g·cm^{-3}, and viscosity 120 mPa·s. Ionic liquid butyl-methylimidazolium bis(trifluoromethanesulfonyl)imide was purchased from Solvent Innovation GmbH (abbreviated as Bmim-TFSI(S)) and Toyo Gosei Co., Ltd. (abbreviated as Bmim-TFSI(T)), respectively. *N*,*N*,*N*-trimethyl-*N*-propylammonium bis(trifluoromethylsulfonyl)imide (TMPA-TFSI) was purchased from Kanto Chemical Co., Ltd., ethyl-methylimidazolium bis(trifluoromethanesulfonyl)imide (Emim-TFSI) and methyltrioctylammonium bis(trifluoromethanesulfonyl)imide (TOM-TFSI), both from Solvent Innovation

GmbH. The ionic liquids were dried at 60 °C for 3 h before use. Reactions were performed using a single-mode microwave oven (IDX, green motif Ib). The microwave frequency was 2.45 GHz, and the maximum output power was 300 W. The reaction was carried out at 200 to 270 °C. The sample was purged with argon. The reaction temperature was monitored by a K-type thermocouple; the sample required only 50 s to reach 270 °C. After the desired reaction time had elapsed, the sample was immediately cooled by air flow to terminate the reactions. Anhydroglucose produced in the ionic liquid was extracted by water, and analyzed by HPLC (Shimadzu HIC-6A, Column: Shodex SUGER KS-801). We used 4 ml water for the extraction process, and repeated it four times.

Downloaded by DUKE UNIV on June 22, 2012 | http://pubs.acs.org
Publication Date (Web): April 28, 2010 | doi: 10.1021/bk-2010-1038.ch012

Results and Discussion

Anhydrosugars from Glucose

Temperature Effect in TMPA-TFSI

By analyzing the samples after the reaction of glucose in ionic liquids, two anhydrosugars were detected: 1,6-anhydro-β-D-glucopyranose (AGP), also known as levoglucosan, and 1,6-anhydro-β-D-glucofuranose (AGF) (Fig. 2). We have previously reported that in reactions of glucose in subcritical water (a very dry and high-temperature steam), AGP was the main product (*8*). However, it has been found that the reaction kinetics in ionic liquids are quite different from those in subcritical water. The reaction rates of glucose transformation in ionic liquids are very much slower than that in subcritical water, even at the same reaction temperature. Figure 3 shows an Arrhenius plot of the glucose transformation rate constants. At 200 °C, the first-order rate constant is 0.16 min^{-1} in the ionic liquid TMPA-TFSI. However, in subcritical water, the first-order rate constant is 3.0 min^{-1} (*8*). Therefore, the reaction rate of glucose transformation in the ionic liquid TMPA-TFSI is twenty times slower than that in subcritical water. We have also found that the activation energy for glucose transformation in TMPA-TFSI is 176 $\mathrm{kJ \cdot mol^{-1}}$, three times higher than that in subcritical water.

Because the glucose transformation reaction is slow in the ionic liquid TMPA-TFSI, we examined conversion of glucose at several different reaction times and temperatures. We also noted the maximum reaction temperature at which ionic liquids can be reused without any degradation. It was found that when the reaction is performed at 200 °C for 17 min, there is no significant change in the UV-Vis absorption spectra of the ionic liquid TMPA-TFSI after the reaction, and the conversion of glucose was acceptable. Therefore, in the following experiments for the glucose transformation, we examined the formation of anhydroglucose mainly at 200 °C.

Downloaded by DUKE UNIV on June 22, 2012 | http://pubs.acs.org
Publication Date (Web): April 28, 2010 | doi: 10.1021/bk-2010-1038.ch012

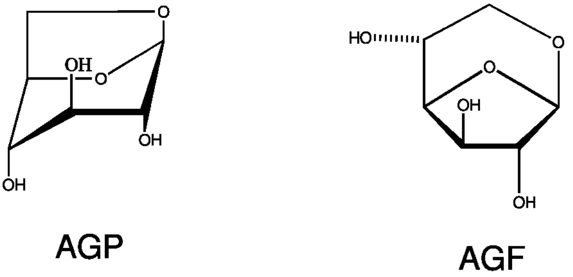

Figure 2. Structure of 1,6-anhydro-β-D-glucopyranose (AGP) and 1,6-anhydro-β-D-glucofuranose (AGF).

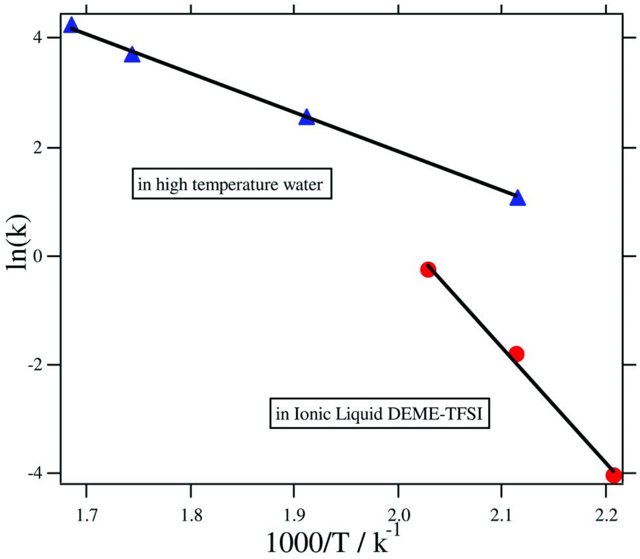

Figure 3. Arrhenius plot of glucose transformation reaction rate in ionic liquid TMPA-TFSI. For comparison, the reaction rates in high temperature water were also plotted.

Effect of the Ionic Liquid Cation

The yields of AGP and AGF in several ionic liquids after the 17-min reaction time at 200 °C are summarized in Table 1. The highest yields were obtained when the ionic liquids DEME-TFSI, TMPA-TFSI, and Bmim-TFSI(T) were used. However, in the ionic liquid Emim-TFSI, the yield was quite low, even though there is no significant difference between Bmim-TFSI and Emim-TFSI. We suspected that the difference in yield might have been caused by impurities in the ionic liquid Emim-TFSI, because after washing it with water, the yield of

AGP increased significantly (Table 1, numbers in parentheses). We suspected that the main impurity that affects the conversion and yields might be chloride ion; this issue will be discussed later in the article.

Table 1. Yield and selectivity of anhydrosugars in several ionic liquids[a]

Ionic liquid	X_A/mol/%	S_{AGP}/mol/%	S_{AGF}/mol%
TMPA-TFSI	93.8	40.7	24.4
DEME-TFSI	93.0	39.0	23.2
Emim-TFSI	42.7(97.0)	19.3(49.4)	21.2(28.1)
Bmim-TFSI(S)	80.6	37.6	25.3
Bmim-TFSI(T)	96.9	54.5	25.5
TOM-TFSI	26.5	5.9	5.4

[a] X_A, glucose conversion; S_{AGP}, selectivity of AGP; and S_{AGF}, selectivity of AGF. All experiments were performed at 200 °C and microwave irradiation for 17 min. Numbers in parentheses are the yields after washing the ionic liquid with water.

Downloaded by DUKE UNIV on June 22, 2012 | http://pubs.acs.org
Publication Date (Web): April 28, 2010 | doi: 10.1021/bk-2010-1038.ch012

Anhydrosugars from Cellobiose and Cellulose

Figure 4(a) shows the conversions of cellulose and cellobiose as a function of microwave irradiation time in the ionic liquid DEME-TFSI at a reaction temperature of 270 °C.

The conversion of cellobiose reached almost 100 wt% after 4 min of reaction time. This suggests that, in the ionic liquid DEME-TFSI, cellobiose is quite easily transformed into other molecules by microwave irradiation. In contrast, it was found that the reaction of cellulose is quite slow in the ionic liquid DEME-TFSI. The required reaction time was about 120 min to achieve 90 wt% conversion. Because one structural difference between cellobiose and cellulose is a hydrogen bond, this result suggests that the strong inter- and intra-molecular hydrogen bonds between the hydroxyl group of the glucose residues are difficult to weaken in microwave-heated ionic liquid, even at 270 °C.

Figure 4(b) shows the yields of AGP from cellulose and cellobiose in DEME-TFASI. For cellobiose, the maximum yield of 60 wt% was obtained after a reaction time of 4 min. As the reaction time was increased, the yield of AGP decreased gradually. Since the conversion of cellobiose at 4 min is almost 100% and the yield at 4 min is at the maximum, the reaction that occurred after 4 min can be assumed to be mainly decomposition of AGP.

For the reactions of cellulose, the change of yield as a function of time is quite different from the results for cellobiose—the yield increased very slowly with increasing reaction time, and the highest yield was obtained at 60 min (Fig. 4(b)). This yield change suggests that formation of AGP from cellulose can be represented by a typical successive reaction, in which AGP is an intermediate.

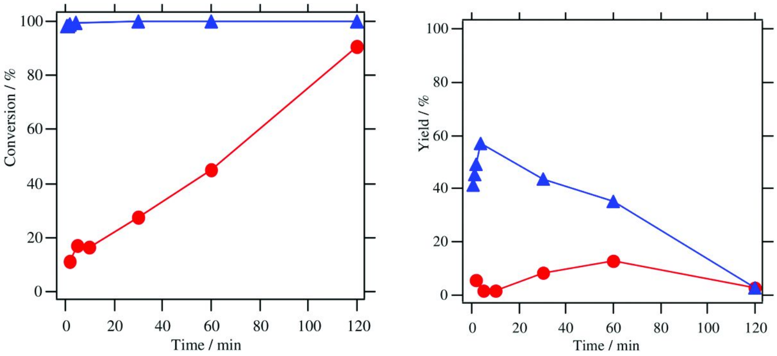

Figure 4. (a) Conversions of cellulose (circles) and cellobiose (triangles) in ionic liquid DEME-TFSI at 270 °C. (b) Yields of AGP from cellulose (circles) and cellobiose (triangles) in ionic liquid DEME-TFSI at 270 °C. (see color insert)

Downloaded by DUKE UNIV on June 22, 2012 | http://pubs.acs.org
Publication Date (Web): April 28, 2010 | doi: 10.1021/bk-2010-1038.ch012

Effect of Chloride Ion on Formation of Anhydrosugars

As has been shown in the previous section, chloride ion contained in ionic liquids was suspected to be the impurity that affects the yield of anhydrosugars. To examine the effect of chloride ion on the yield of AGP, the reaction was performed in Bmim-TFSI and a mixed ionic liquid (Bmim-TFSI + Bmim-Cl) at 200 °C for 10 min. The results are summarized in Table 2. In pure Bmim-TFSI, the yield of AGP was 30.3 mol%, while in the mixed ionic liquid, the yield decreased dramatically to 7.7 mol%. Therefore, it is clear that the chloride ion has a significant effect on the formation of AGP, even at a very low concentration. It is known that among the anions that interact with the hydroxyl group in glucose, chloride interacts most strongly (*9*). We speculate that in our reaction, chloride ion is interacting strongly with the hydroxyl groups in glucose, resulting in production of hydrogen ions. These hydrogen ions may react with the oxygen ring in AGP, opening it easily, and thus lowering the yield of AGP significantly. The TFSI anion is also known to be derived from a strong acid; however, it can be postulated that the TFSI anion interacts weakly with OH in glucose.

Table 2. Effect of chloride ion on formation of anhydrosugar

Ionic liquid	*[Bmim-Cl]/mol/%*	*X_A/mol/%*	*Y_{AGP}/mol/%*
Bmim-TFSI(S)	0	80.6	30.3
Bmim-TFSI	5	99.1	7.7

Downloaded by DUKE UNIV on June 22, 2012 | http://pubs.acs.org
Publication Date (Web): April 28, 2010 | doi: 10.1021/bk-2010-1038.ch012

Because of the possible presence of chloride ion in the ionic liquids, we also examined the possibility of reusing the ionic liquids to produce anhydrosugars. However, in all the ionic liquids we examined, either there was no significant change in the yields, or the yields of AGP and AGF increased, after reusing the ionic liquids several times. We speculate that the concentration of impurities, especially chloride ion, decreases after reuse. Also, because the ionic liquids used are very stable at high temperatures, decomposition is not a problem.

Applications of Anhydrosugars as Hyperbranched Polysaccharides

As already mentioned in the Introduction, one of the applications of anhydrosugars is to make hyperbranched polysaccharides. These products are preferred building blocks for the core of amphiphiles, because they possess spherical three-dimensional architecture and numerous functional groups on the exterior of the molecules. The amphiphilic macromolecule is a very useful nanoscale material. An amphiphilic structure consisting of a covalently linked dendritic core and shell parts has the potential to exist as a unimolecular micelle in solution, which could remain stable under conditions of varying concentration, temperature, and pH. The high stability as a unimolecular micelle can be produced in the hyperbranched polysaccharides, and this space could encapsulate suitable guest molecules. An example of a hyperbranched unimolecular reversed micelle is shown in Figure 5. When dispersed in chloroform, this hyperbranched polysaccharide has encapsulation ability for water-soluble molecules, such as rose bengal, thymol blue, and alizarin yellow. The encapsulation ability depends on the hydrophilicity of the hyperbranched polysaccharides and the molecular size of the dye. The rose bengal-encapsulated polymer showed a slow release from this system into water at neutral pH, while the release rate was significantly accelerated by hydrolysis of the hydrophobic polymer shell under basic conditions (*10*).

Conclusion

We found that the anhydrosugars AGP and AGF can be produced with very high selectivities in ionic liquids, compared with that in high-temperature water. The reaction rates of glucose transformation in ionic liquids are slower than that in high-temperature water. The activation energy of glucose transformation in TMPA-TFSI is 176 $kJ \cdot mol^{-1}$. There were no significant effects of ionic liquid cations, while the ionic liquid anion—especially if a chloride ion is present—has a large effect. By adding chloride anions, the yields of anhydrosugars decreased significantly.

Downloaded by DUKE UNIV on June 22, 2012 | http://pubs.acs.org
Publication Date (Web): April 28, 2010 | doi: 10.1021/bk-2010-1038.ch012

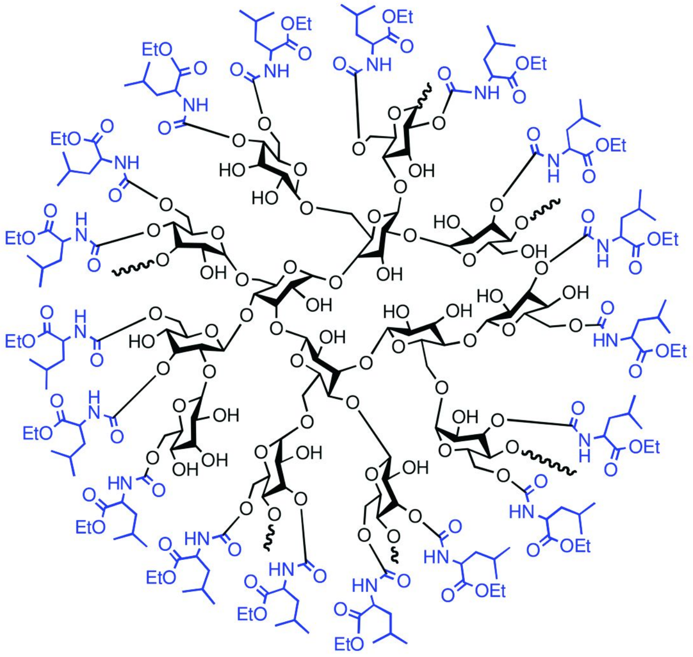

Figure 5. Hyperbranched D-glucan with L-leucine moieties as the unimolecular reverse micelle. (see color insert)

Acknowledgments

The DEME TFSI was kindly provided by Nisshinbo Industries Inc. This study was supported by Industrial Technology Research Grant Program in 2007 from New Energy and Industrial Technology Development Organization (NEDO) of Japan, and the Grant-in-Aid for Scientific Research in Priority Area "Science of Ionic Liquids" from Ministry of Education, Culture, Sports, Science and Technology.

References

1. Satoh, T.; Imai, T.; Ishihara, H.; Maeda, T.; Kitajyo, Y.; Sakai, Y.; Kaga, H.; Kaneko, N.; Ishii, F.; Kakuchi, T. *Macromolecules* **2005**, *38*, 4202–4210.
2. Kitajyo, Y.; Nawa, Y.; Tamaki, M.; Tani, H.; Takahashi, K.; Kaga, H.; Satoh, T.; Kakuchi, T. *Polymer* **2007**, *48*, 4683–4690.
3. Leadbeater, N. E.; Torenius, H. M. *J. Org. Chem.* **2002**, *67*, 3145–3148.
4. Shafizadeh, F.; Fu, Y. L. *Carbohydr. Res.* **1973**, *29*, 113–122.
5. Kwon, G.-J.; Kuga, S.; Hori, K.; Yatagai, M.; Ando, K.; Hattori, N. *J. Wood Sci.* **2006**, *52*, 461–465.

6. Miura, M.; Kaga, H.; Tanaka, S.; Takahashi, K.; Ando, K. *J. Chem. Eng. Jpn.* **2000**, *33*, 299–302.
7. Kawamoto, H.; Saito, S.; Hatanaka, W.; Saka, S. *J. Wood Sci.* **2007**, *53*, 127–133.
8. Satoh, H.; Takahashi, K.; Kaga, H. *Abstracts of Papers*, 10th Asian Pacific Confederation of Chemical Engineering (APCChE) Congress, Kokura, Japan, October 2004; 3P-03-018, [CD-ROM].
9. Jiang, Y.; Cole, R. B. *J. Am. Soc. Mass Spectrom.* **2005**, *16*, 60–70.
10. Kitajyo, Y.; Imai, I.; Sakai, Y.; Tamaki, M.; Tani, H.; Takahashi, K.; Narumi, A.; Kaga, H.; Kaneko, N.; Satoh, T.; Kakuchi, T. *Polymer* **2007**, *48*, 1237–1244.

Downloaded by DUKE UNIV on June 22, 2012 | http://pubs.acs.org
Publication Date (Web): April 28, 2010 | doi: 10.1021/bk-2010-1038.ch012

Chapter 13

Chiral Pyrrolidine-Substituted Ionic Liquid-Mediated Activation of Enzyme

**Toshiyuki Itoh,*,[1] Yoshikazu Abe,[1] Takuya Hirakawa,[1]
Nagisa Okano,[1] Shino Nakajima,[1] Shuichi Hayase,[1]
Motoi Kawatsura,[1] Tomoko Matsuda,[2] and Kaoru Nakamura[3]**

**[1]Department of Chemistry and Biotechnology, Graduate School
of Engineering, Tottori University, Koyama Minami 4-101,
Tottori 680-8552, Japan
[2]Department of Bioengineering, Graduate School of Bioscience and
Biotechnology, Tokyo Institute of Technology, 4259 Nagatsuta, Midori-ku,
Yokohama 226-8501, Japan
[3]Insititute for Chemical Research, Kyoto Univeristy,
Uji Gokasho 611-0011, Japan
*Fax: +81-857-31-5259. E-mail: titoh@chem.tottori-u.ac.jp.**

Downloaded by STANFORD UNIV GREEN LIBR on June 22, 2012 | http://pubs.acs.org
Publication Date (Web): April 28, 2010 | doi: 10.1021/bk-2010-1038.ch013

(*R*)-Pyrrolidine-substituted imidazolium cetyl-PEG10-sulfate (D-ProMe) derived from D-proline worked as an excellent activating agent of *Burkholderia cepacia* lipase; it is particularly interesting that (*R*)-isomer of the imidazolium salt worked better than (*S*)-isomer. This suggests that the imidazolium cation group directly interacts with the enzyme protein and causes preferable modification of the reactivity.

1. Introduction

Enzymatic reactions are now widely recognized as useful tools for organic syntheses. Lipases are the most widely used enzymes applicable for various substrates, however, the enantioselectivity is significantly dependent on both substrates and reaction media (*1*). Therefore, development of a strategy to improve lipase reaction performance is desirable (*1*, *2*). Several methods have been reported for activation of lipases in a non aqueous medium: lipid coating mediated activation (*3*), entrapment of lipases in hydrophobic sol-gel

In Ionic Liquid Applications: Pharmaceuticals, Therapeutics, and Biotechnology; Malhotra, S.;
ACS Symposium Series; American Chemical Society: Washington, DC, 0.

Downloaded by STANFORD UNIV GREEN LIBR on June 22, 2012 | http://pubs.acs.org
Publication Date (Web): April 28, 2010 | doi: 10.1021/bk-2010-1038.ch013

materials (*4*), molecular bioimprinting (*5*), salt-mediated activation (*6–8*), and use of some surfactants such as polyoxyethylenealkyl ether (*9*). Recently, we reported an efficient activation protocol of lipases by the coating of [1-butyl-2,3-dimethylimidazolium][cetyl-PEG10-sulfate](BDMIM-PEG) (*8*). Although the activation effect was dependent on the substrate, more than 1000-fold acceleration was accomplished for some substrates with excellent enantioselectivity when *Burkholderia cepacia* lipase (lipase PS) (*10*) or *Candida rugosa* lipase was coated with BDMIM-PEG *(8b)*. MALD-TOF Mass experiments suggested that BDMIM-PEG binds with the enzyme protein, therefore it was assumed that the modified activity of lipase might be due to flexibility or conformation change of the lipase protein by the **B**DMIM-PEG-binding *(8b)*. Furthermore, it was established that imidazolium cation affected the enantioselectivity of the lipase; 1-butyl-2,3-dimethyimidazolium salt-coated lipase PS gave better enantioselectivity than a 1-butyl-3-methylimidazolium salt-coated one. Based on these results, we attempted to refine the design of activating agent for lipase by modification of the imidazolium group. Our idea is that introduction of an appropriate chiral functional group on the imidazolium group may create more efficient activation of an enzyme (Figure 1).

We hypothesized that chiral pyrrolidine moiety substituted imidazolium cetyl-PEG10-sulfate may have capability desired to control stereochemistry of the enzymatic reaction. In this chapter, we report the results of designing a novel ionic liquid type activating agent for enzymes (*11*).

2. Cooperative Activation of a Lipase Using Amino Acid with [1-Butyl-2,3-dimethylimidazolium][cetyl-PEG10-sulfate]

Amino acids have been used as stabilizers of an enzyme during the purification process; commercial lipase PS from *Burkholderia cepacia* involves ca. 20 wt% of glycine as an essential stabilizer during preparation of the lipase protein by the lyophilization process (*8*, *10*). We were intrigued by this glycine-mediated stabilization of lipase protein and investigated the roll of glycine; it was found to work only as a stabilizer of the enzyme and had no influence on the reactivity of lipase PS *(8b)*. The resulting glycine free protein was dissolved in cold deionized water, dried by lyophilization to give GF-PS powder and stored under argon in a refrigerator (*12*). Since it was anticipated that chiral amino acid may modify the enantioselectivity of an enzymatic reaction, we prepared amino acid coated PS (i.e., L-Phe and L-Pro) and investigated their properties for activation of lipase PS (Eq. 1) (*11*). Amino acid coated lipase was prepared by mixing the corresponding amino acid (100 mol eq. vs. lipase protein) with glycine free lipase PS protein and drying by lyophilization. With this data, we evaluated lipase-catalyzed reactions using the same amount of amino acid coated lipase PS as of enzyme protein.

Downloaded by STANFORD UNIV GREEN LIBR on June 22, 2012 | http://pubs.acs.org
Publication Date (Web): April 28, 2010 | doi: 10.1021/bk-2010-1038.ch013

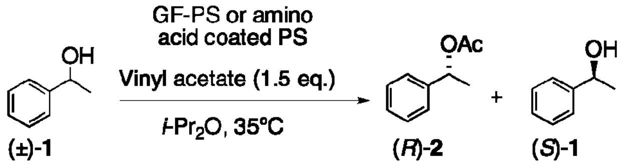
GF-PS or amino acid coated PS
Vinyl acetate (1.5 eq.)
i-Pr2O, 35°C
OH
(±)-1
OAc
(R)-2
+
OH
(S)-1

(1)

As can be seen in Figure 2, however, coating of lipase PS protein by L-Phe (column 3) neither accelerated nor enhanced enantioselectivity. On the contrary, a slight reduction of enantioselectivity was recorded when the reaction was carried out using L-Pro-PS and the E value (*13*) dropped to 91 (column 4) from >200 which was obtained for GF-PS-catalyzed reaction (column 1). Coating treatment by glycine somewhat reduced enantioselctivity of the enzymatic reaction (column 2) and a similar reaction rate to those of L-Phe coating enzyme or L-Pro coating enzyme was obtained. BDMIM-PEG coating (column 5), on the other hand, caused great acceleration of the enzymatic reaction for GF-PS (column 1).

To our delight, we discovered very interesting cooperative activation of an enzyme for BDMIM-PEG with an amino acid. Great acceleration was obtained for L-Pro-BDMIM-PEG-PS (column 7), which was prepared by treatment of glycine free PS with 100 mol eq. of L-Pro and IL1, and the reaction conversion reached 38% in only 4 h (9.5 % conv./h); on the contrary, there was only 19% conversion in 60 h for L-Pro-PS-catalyzed reaction (column 4: 0.32% conv./h). It was thus found that the combination of BDMIM-PEG and amino acid, particularly L-Pro with BDMIM-PEG, was essential for realizing effective activation of the lipase.

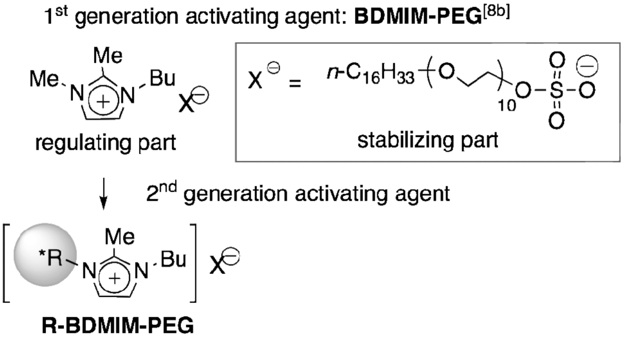
1st generation activating agent: BDMIM-PEG[8b]
Me
Me
N
N
Bu
X⊖
regulating part
X⊖ =
n-C16H33
O
10
O
S
O
O
O
⊖
stabilizing part
2nd generation activating agent
*R
Me
N
N
Bu
X⊖
R-BDMIM-PEG

Figure 1. Design of 2nd generation ionic liquid type activating agents for enzymes

Downloaded by STANFORD UNIV GREEN LIBR on June 22, 2012 | http://pubs.acs.org
Publication Date (Web): April 28, 2010 | doi: 10.1021/bk-2010-1038.ch013

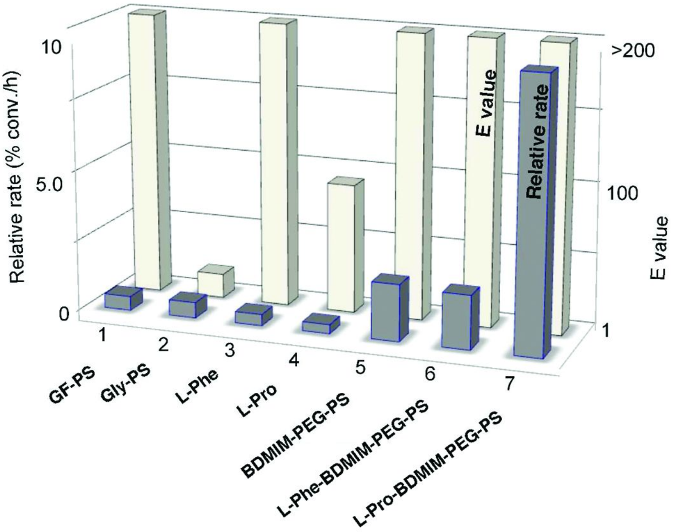

*Figure 2. Transesterification of 1-phenylethanol by glycine free lipase PS or amino acid coated lipase PS. When the reaction was carried out using amino acid coated enzyme, we used 7.5 mg of L-Phe-PS, 6.8 mg of L-Pro-PS, 6.1 mg of Gly-PS, 26.3 mg of BDMIM-PEG-PS, and 27.8 mg of L-Phe-BDMIM-PEG-PS or L-Pro-BDMIM-PEG-PS per 50 mg of (±)-**1**.*

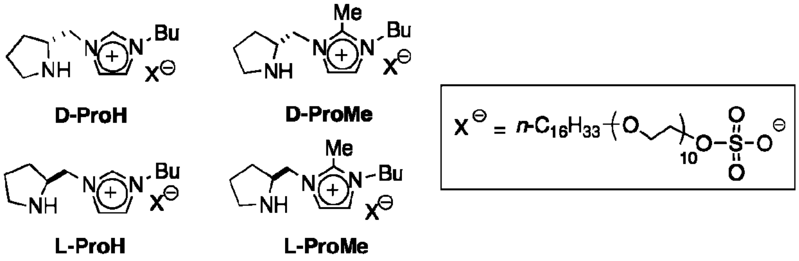

Figure 3. Design of chiral pyrrolidine-substituted-BDMIM-PEG

Downloaded by STANFORD UNIV GREEN LIBR on June 22, 2012 | http://pubs.acs.org
Publication Date (Web): April 28, 2010 | doi: 10.1021/bk-2010-1038.ch013

3. Design of a Novel Enzyme Activating Agent

3-1. Activation of a Lipase by Chiral Pyrrolidine-Substituted Imidazolium Salt

Recently Cheng and co-workers reported the synthesis of imidazolium ionic liquid derived from L-proline and used it as an efficient asymmetric organocatalyst (*14*). Following their method, we prepared pyrrolidine-substituted imidazolium bromide and converted it to cetyl-PEG10-sulfate by the metal exchange reaction. Since it was anticipated that stereochemistry of the proline moiety to which the imidazolium ring was attached may influence the enantioselectivity of the enzyme, we prepared four types of chiral pyrrolidine-substituted imidazolium cetyl-PEG10-sulfate as listed in Figure 3 (*11*). Using these four types of ionic liquid coating materials, we prepared ionic liquid coated lipase PS and evaluated their activities.

Although glycine free lipase PS was employed for the initial experiments described in Figure 2, commercial lipase PS was this time used as a source of lipase protein, which involved 20 wt% of glycine as stabilizing agent, because glycine had no modification property in enantioselectivity. Figure 4 summarizes the results of transesterification of (±)-1-phenylethanol (**1**) using commercial lipase PS and four types of 2nd generation imidazolium salt-coated lipase PS using two kinds of acyl donor (Eq. 2). We conducted the reaction using 1.5 eq. of vinyl acetate or 2,2,2-trifluoroethyl acetate as acylating reagent; the results were very satisfactory. The reaction rate of commercial PS-catalyzed reaction proceeded faster than that of GF-PS (column 1), although the enantioselectivity of commercial lipase PS was inferior to that of GF-PS (see Table 1, Entry 1). As we previously reported *(8b)*, coating of lipase PS protein by IL1 (1st generation activating agent) caused great acceleration and enhanced enantioselectivity (column 2).

As expected, it was established that chiral pyrrolidine-substituted imidazolium salt worked as an excellent activator of lipase PS. In particular, (*R*)-pyrrolidine-substituted salt (D-ProMe), which was derived from unnatural D-proline, was found to be the best agent: an extraordinary acceleration was accomplished with perfect enantioselectivity for D-ProMe-PS-catalyzed reaction and 58 times faster reaction (vs. lipase PS) was recorded (column 6). L-ProMe-PS also showed significant acceleration (column 5), but it was obviously inferior to that of D-ProMe-PS. As we previously reported (*8*), the functional group on the 2-position of the imidazolium ring had a certain impact on the modified property. Both L- and D-ProMe gave better results than those of corresponding L- and D-ProH salts.

The results seem to suggest that the cationic part of the imidazolium salt bound with the lipase protein and affected its reaction profile; this may explain why our ionic liquid coating activation of enzyme depends on the substrate. It was thus established that D-ProMe worked as an excellent activator of lipase PS. No significant difference in the reaction rate between acyl agents was obtained, while better enantioselectivity was recorded when esterification of (±)- **1** was carried out in the presence of 2,2,2-trifluoroethyl acetate as acyl donor (column 7). Remarkable acceleration was again obtained for D-ProMe-PS-catalyzed reaction

Downloaded by STANFORD UNIV GREEN LIBR on June 22, 2012 | http://pubs.acs.org
Publication Date (Web): April 28, 2010 | doi: 10.1021/bk-2010-1038.ch013

even when 2,2,2-trifluoroethyl acetate was employed as acyl donor (column 8), although a slightly reduced activation was observed compared to that of vinyl acetate mediated reaction using the same enzyme (column 6). Therefore, we assume that the origin of activation property might be unaffected by the acylation agent.

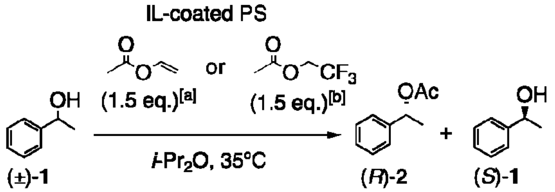

(2)

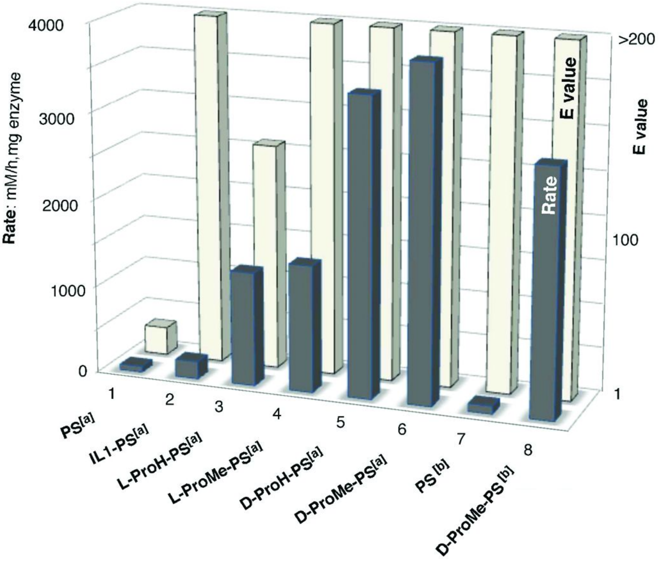

Figure 4. Activation of lipase PS by the imidazolium salt coating. [a] The reaction was carried out using vinyl acetate as acyl donor. [b] 2,2,2-trifluoroethyl acetate was used as acylating reagent.

Downloaded by STANFORD UNIV GREEN LIBR on June 22, 2012 | http://pubs.acs.org
Publication Date (Web): April 28, 2010 | doi: 10.1021/bk-2010-1038.ch013

We next tested the possibility of recyclable use of D-ProMe-PS in an ionic liquid solvent system (Figure 5). We recently reported that lipase PS-catalyzed transesterification of secondary alcohols was accomplished very rapidly when phosphonium ionic liquid $[MEBu_3P]NTf_2$ (*15*) was used as solvent, and afforded the first example of a reaction rate superior to that in diisopropyl ether (*15*). As expected, D-ProMe-PS worked very well in $[MEBu_3P]NTf_2$ and it was possible to use it repeatedly in this solvent. To a mixture of (±)-**1** (50 mg, 0.41 mmol) and vinyl acetate (52 mg, 0.60 mmol) in $[MEBu_3P]NTf_2$ (1.0 mL) was added D-ProMe-PS (6.0 mg, corresponding to 0.25 mg of enzyme) and the mixture was stirred at 35 °C for 35 min. The reaction course was monitored by capillary GC-analysis and silica gel TLC and the reaction was stopped by addition of 1.5 mL of a mixed solvent of hexane and diethyl ether (3:1). This formed biphasic layers and product acetate (*R*)-**2** and alcohol (*S*)-**3** were isolated from the ether layer. The combined extracts were evaporated and preparative silica gel TLC to give (*R*)-**2** (99.1% ee) in 46% and alcohol (*S*)-**3** (91% ee) in 44% yield. Since the lipase remained in the ionic liquid layer, its recyclable use of lipase was demonstrated (Figure 5); after extraction of the products, the ionic layer was placed under reduced pressure (2 torr) at rt for 15 min to remove the organic solvent and to the resulting ionic layer was added (±)-**1** and vinyl acetate and the mixture was stirred at 35°C. The desired second reaction proceeded smoothly and (*R*)-**2** and (*S*)-**3** were again obtained while maintaining perfect enantioselectivity and reaction rate. After repeating the same process ten times, we succeeded in obtaining (*R*)-**2** in 37% with 99% ee and (*S*)-**3** in 42% with 92% ee by 55 min of reaction. Recyclable use of D-ProMe-PS was in fact possible in an ionic liquid solvent system (Figure 5) (*11*).

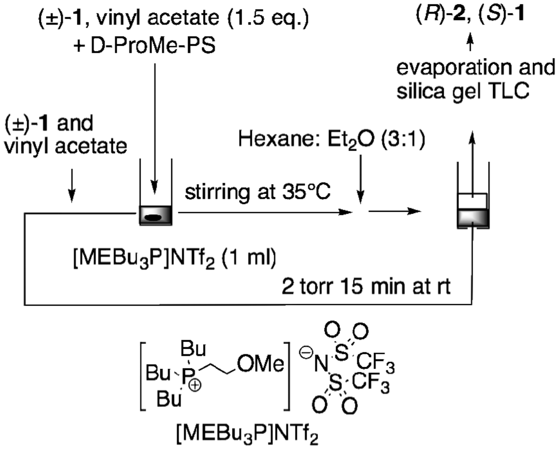

Figure 5. Recyclable use of D-ProMe-PS in an ionic liquid solvent system

3-2. Activation of *Geotrichum candidum* Dehydrogenase by the Coating of Chiral Pyrrolidine-Substituted Imidazolium Salt

The lipase-catalyzed transesterification of alcohols in ionic liquids has now been completely established, however, there are only a few reports on alcohol dehydrogenase catalyzed reaction in ionic liquids *(1c*, *2c)*, in spite of the fact that asymmetric reduction of ketones and oxidation of alcohols is one of the most important reactions for organic synthesis. Recently, Matsuda and co-workers reported a method using alcohol dehydrogenase in ionic liquids (*16*). The asymmetric reduction of ketones by *Geotrichum candidum* NBRC 5767 (*17*) in ionic liquids proceeded smoothly with excellent enantioselectivity when the cell was immobilized on water-absorbing polymer containing water inside the polymer, while the reaction without the polymer did not proceed.

It has been established that dried cells of this microbe worked as excellent dehydrogenase source without purification and accomplished asymmetric reduction of various types of ketones with excellent enantioselectivity (*17*, *18*). We hypothesized that our ionic liquid coating may make it possible for *Geotrichum candidum* to work in a pure ionic liquid solvent because the alkyl PEG sulfate group involves a significant amount of water and may act to prevent removal of the water from the enzyme surface. So we prepared ionic liquid coated Geotrichum candidum dried cells, in the presence of 50 wt% of BDMIM-PEG (*19*) with MES buffer (pH 7.0) and tested it for asymmetric reduction of acetophenone (**3**) in [bmim][NTf$_2$] solvent system. However, the ionic liquid coated enzyme showed no reactivity in a pure ionic liquid solvent and it was essential to use an ionic liquid which contained at least 5 volume % of water, as Kragl and co-workers previously reported for the reaction of dehydrogenase in an ionic liquid solvent (*20*).

Although stabilization of *Geotrichum candidum enzyme* by the BDMIM PEG-coating was unsuccessful for it to work in a pure ionic liquid solvent, we found an unexpected activation effect of the coating (Table 1): the initial rate of the enzymatic reaction was significantly increased when the BDMIM PEG-coating enzyme was used in the MES buffer solution (Eq. 3). In particular, the desired alcohol (*S*)-**1** was obtained in 88% yield for just 0.5 h reaction for D-ProH coated enzyme (Entry 7), while the product yield was insufficient (56%) at the same reaction time when the native dried cell was used as catalyst (Entry 8).

Interestingly, D-ProH gave a better result than D-ProMe, although the latter acted as a stronger activator for lipase PS as mentioned in the previous section (see Figure 3). However, this effect of the imidazolium salt coating was only limited for acceleration of the initial rate and neither increased product yield nor modified enantioselectivity was recorded after 24 h reaction for D-ProH coated enzyme (Entry 10) compared to that of native enzyme-catalyzed reaction (Entry 11).

Downloaded by STANFORD UNIV GREEN LIBR on June 22, 2012 | http://pubs.acs.org
Publication Date (Web): April 28, 2010 | doi: 10.1021/bk-2010-1038.ch013

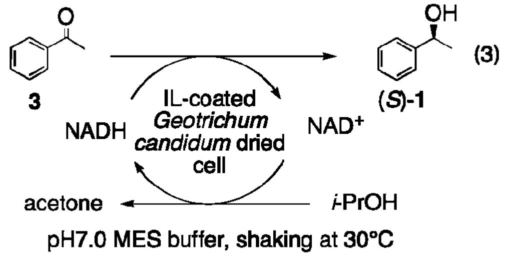
3
(S)-1
NADH
NAD+
IL-coated Geotrichum candidum dried cell
acetone
i-PrOH
pH7.0 MES buffer, shaking at 30°C
(3)

Downloaded by STANFORD UNIV GREEN LIBR on June 22, 2012 | http://pubs.acs.org
Publication Date (Web): April 28, 2010 | doi: 10.1021/bk-2010-1038.ch013

Table 1. Asymmetric reduction of acetophenone (3) using ionic liquid coated-*Geotrichum candidum* dried cells

Entry	*Coating agent*	*Time (h)*	*Yield of (S)-**1** (%)*	*ee (%)*[a]
1	BDMIM-PEG	1	78	>99
2	BMIM-PEG	1	76	>99
3	L-ProMe	1	74	>99
4	L-ProH	1	71	>99
5	D-ProMe	1	77	>99
6	D-ProH	1	91	>99
7	D-ProH	0.5	88	>99
8	none	0.5	56[b]	>99
9	none	1	80	>99
10	D-ProH	24	90	>99
11	none	24	91	>99

[a] Determined by HPLC. [b] TLC analysis showed that a large amount of substrate **3** still remained at this reaction time, though the recovered yield was less than 5 %.

The D-ProH-coated enzyme protein did not dissolve in the MES buffer and no free imidazolium salt was detected in this buffer layer at an initial stage of the reaction, while D-ProH itself dissolved easily in the MES buffer solution. But it was observed that gradual elution of free D-ProH from the coated enzyme to the buffer took place during shaking of the reaction mixture. From these results, we assume that ionic liquid may bind with the enzyme protein and form an ionic liquid layer on the protein surface; since our ionic liquid has amphiphilic property, this contributes to concentrate the hydrophobic substrate on the enzyme protein and thus initial acceleration of the rate might be realized. However, because the binding property of the imidazolium salt with the enzyme is not strong, the coating effect is gradually lost during the course of the reaction. The present ionic liquid was, therefore, not appropriate to activate *Geotrichum candidum* effectively, but we expect that we can suggest a possibility to realize activation of dehydrogenase using a very simple technology and hope that this may become more promising after refinement of the molecular design of the coating material.

4. Conclusion

In summary, we succeeded in developing a very effective 2nd generation activation agent for lipase protein: a novel chiral imidazolium cetyl-PEG10-sulfate (D-ProMe) derived from D-proline worked as an excellent activator of lipase PS and was ca. 20 fold stronger than the BDMIM-PEG. It is particularly noteworthy that (*R*)-isomer of the imidazolium salt worked better than (*S*)-isomer. This suggests that the imidazolium cation group directly interacts with the enzyme protein and causes modification of the reactivity. We anticipate that introduction of an appropriate amino acid or oligo peptide moiety on the imidazolium ring may make it possible to design more efficient activating agents for various types of enzymes. We next attempted to activate dehydrogenase by the imidazolium salt coating, however, only limited activation was obtained. At present, our activation technology of enzymes using alkylPEG imidazolium salt coating is particularly effective for a lipase, but is not significant for *Geotrichum candidum*. We believe that further investigation of the scope and limitation of this salt mediated activation of enzymes will make it even more valuable.

Downloaded by STANFORD UNIV GREEN LIBR on June 22, 2012 | http://pubs.acs.org
Publication Date (Web): April 28, 2010 | doi: 10.1021/bk-2010-1038.ch013

5. Experimental Section

5.1. Preparation of Amino Acid-Coated Lipase PS (*11*)

Typically, celite free PS (10 mg) was dissolved in 0.50 ml of deionized water at 4°C in a centrifugal filter device equipped with ultracel YM-10 (Microcon, Millipore) and centrifuged at 13,000 rpm at 4°C for 10 min., repeating the same process several times until (after ca. 10 times) no more glycine was detected from the filtrate. Since the glycine free lipase protein is unstable, it was immediately used for amino acid coated lipase PS. The resulting glycine free protein was dissolved in cold deionized water, dried by lyophilization to give GF-PS powder and stored under argon in a refrigerator. For example, since 8.0 mg of GF-PS (10 mg of the starting celite-free PS) corresponded to 2.5 X 10^{-4} mmol of lipase PS protein (32 K dalton), the amount of enzyme protein involved in each amino acid coated enzyme was estimated to be: L-Phe-PS: 66 wt%, L-Pro-PS: 73 wt%, Gly-PS: 81wt%, BDMIM-PEG-PS: 19wt%, L-Phe-BDMIM-PEG-PS: 18 wt%, L-Pro-BDMIM-PEG-PS: 18wt%.

Downloaded by STANFORD UNIV GREEN LIBR on June 22, 2012 | http://pubs.acs.org
Publication Date (Web): April 28, 2010 | doi: 10.1021/bk-2010-1038.ch013

5.2. Lipase-Catalyzed Transesterification Using Amino Acid-Coated Lipase PS (*11*)

To a solution of (±)-**1** (50 mg, 0.41 mmol) and vinyl acetate (55 mg, 0.64 mmol) in *i*-Pr_2O (2.0 mL) was added GF-PS (5.0 mg) and the mixture was stirred at 35 °C. The reaction course was monitored by capillary GC-analysis and silica gel TLC. (*R*)-**2** and (*S*)-**1** were obtained by preparative silica gel thin layer chromatography (TLC). The enantioselectivity was determined by HPLC analysis on a chiral column (Chiralcel OB, hexane: 2-propanol = 9 : 1). When the reaction was carried out using amino acid coated enzyme, we used 7.5 mg of L-Phe-PS, 6.8 mg of L-Pro-PS, 6.1 mg of Gly-PS, 26.3 mg of IL1-PS, and 27.8 mg of L-Phe-IL1-PS or L-pro-IL1-PS per 50 mg of (±)-**1**.

5.3. Preparation of (D)-ProMe-Supported Lipase PS (D-ProMe-PS) by Lyophilization (*11*)

Lipase PS (Amano) (1.0 g, since this contained 20 wt % of glycine and 1.0 wt % of lipase protein, the amount of lipase protein was estimated as $3.1x10^{-4}$ mmol) was dissolved in 8.0 ml of 0.1 M potassium phosphate buffer (pH 7.2) and the mixture was centrifuged at 3,500 rpm for 5 min (3 times). 2.0 ml of 0.1 M potassium phosphate buffer (pH 7.2) of D-ProMe[11] (30 mg; ca. 3.1×10^{-2} mmol because the estimated molecular weight of the salt was 984.37.) was mixed with the resulting supernatant and dried by lyophilization to give D-ProMe-PS (219 mg) as a hygroscopic white powder. The estimated lipase protein of this enzyme powder was therefore estimated as 4.2 wt%.

5.4. D-ProMe-PS-Catalyzed Acylation of (±)-1-Phenylethanol (1) in *i*-Pr_2O

To a solution of (±)-**1a** (50 mg, 0.41 mmol) and vinyl acetate (52.9 mg, 0.62 mmol) in *i*-Pr_2O (2.0 mL) was added D-ProMe-PS (5.9 mg, corresponding to 0.25 mg of enzyme) and the mixture was stirred at 35°C. The reaction course was monitored by capillary GC-analysis and silica gel TLC. (*R*)-**2** and (*S*)-**1** were obtained by preparative silica gel thin layer chromatography (TLC). The enantioselectivity was determined by HPLC analysis using a chiral column (Chiralcel OB, hexane: 2-propanol = 9: 1).

5.5. Preparation of D-ProH-Coated *Geotrichum candidum* Dried Cell

Geotrichum candidum acetone powder (120 mg) and NAD^+ (30 mg) was mixed in 10 mL of MES buffer (pH 7.0) solution of D-ProH (*11*) (60 mg). The resulting mixture was shaken at rt for 15 min, then dried by lyophilization to give D-ProH-coated enzyme (329 mg). It was possible to keep the enzyme for over one month in a refrigerator without any loss of activity, though the IL-coated enzyme showed a hygroscopic property.

5.6. Asymmetric Reduction of Acetophenone by Ionic Liquid Coated *Geotrichum candidum* Dried Cells

A mixture of acetophenone (**3**) (10.7 mg, 0.080 mmol), 2-propanol (0.10 mL), D-ProH-enzyme (20.9 mg) and NAD^+ (5.0 mg) in 3.0 mL of MES buffer (pH 7.0) was shaken at 135 rpm at 30°C for 1 h. The reaction mixture was filtered through a glass-sintered filter with a celite pad to remove the enzyme, the filtrate was evaporated and the residue was chromatographed on silica gel TLC to give (*S*)-**1** (9.0 mg, 0.073 mmol) in 91 % yield.

Downloaded by STANFORD UNIV GREEN LIBR on June 22, 2012 | http://pubs.acs.org
Publication Date (Web): April 28, 2010 | doi: 10.1021/bk-2010-1038.ch013

Acknowledgments

The present work was supported by a Grant-in-Aid for Scientific Research in a Priority Area, "Science of Ionic Liquids", from the Ministry of Education, Culture, Sports, Science and Technology of Japan.

References

1. For reviews see: (a) Wong, C. -H.; Whitesides, G. M. *Enzymes in Synthetic Organic Chemistry*; Pergamon: Oxford, U.K., 1994. (b) Bornscheuer, U. T.; Kazlauskas, R. J. *Hydrolases in Organic Synthesis: Regio- and Stereoselective Biotransformations*; John Wiley & Sons, Inc.: Chichester, U.K., 1999.
2. For reviews see: (a) Klivanov, M. *Trends Biotechnol.* **1997**, *15*, 97. (b) Itoh, T.; Takagi, Y.; Tsukube, H. *Trends Org. Chem.* **1997**, *6*, 1−22. (c) Theil, H. *Tetrahedron* **2000**, *56*, 2905−2919. (d) Itoh, T. *Future Directions in Biocatalysis*, T. Matsuda, Ed.; Elsevier Bioscience: The Netherlands, 2007, pp 3−20.
3. (a) Okahata, Y.; Ijiro, K. *J. Chem. Soc., Chem. Commun.* **1988**, 1392−1394. (b) Okahata, Y.; Fujimoto, Y.; Ijiro, K. *Tetrahedron Lett.* **1988**, *29*, 5133−5134. (c) Okahata, Y.; Ijiro, K. *Bull. Chem. Soc. Jpn.* **1992**, *65*, 2411−2420. (d) Tsuzuki, W.; Okahata, Y.; Katayama, O.; Suzuki, T. *J. Chem. Soc., Perkin Trans. 1* **1991**, 1245−1247. (e) Okahata, Y.; Fujimoto, K.; Ijiro, K. *J. Org. Chem.* **1995**, *60*, 2244−2250. (f) Okahata, Y.; Hatano, A.; Ijiro, K. *Tetrahedron: Asymmetry* **1995**, *6*, 1311-1322. (g) Okahata, Y.; Mori, T. *Trends Biotechnol.* **1997**, *15*, 50−54. (h) Mori, T.; Okahata, Y. Methods in Biotechnology. In *Enzymes in Non-aqueous Solvents: Methods and Protocols*, Halling, E. N., Holland, H. L., Eds.; Humana Press, Inc.: Totowa, NJ, 2001; Vol. 15, Chapter 9, pp 83−94. (i) Mori, T.; Kishimoto, S.; Ijiro, K.; Kobayashi, A.; Okahata, Y. *Biotech. Bioeng.* **2001**, *76*, 157−163. (j) Nishino, H.; Mori, T.; Okahata, Y. *Chem. Commun.* **2002**, 2684−2685.
4. (a) Reetz, M. T.; Zonta, A.; Simpelkamp, J. *Angew. Chem., Int. Ed. Engl.* **1995**, *34*, 301−303. (b) Reetz, M. T.; Zonta, A.; Simpelkamp, J.; Könen, W. *Chem. Commun.* **1996**, 1397−1398.
5. (a) Mingarro, I.; Abad, C.; Braco, L. *Proc. Natl. Acad. Sci. U.S.A.* **1995**, *92*, 3308−3312. (b) Mingarro, I.; Gonzalez-Navarro, H.; Braco, L. *Biochemistry*

1996, *35*, 9935−9944. (c) Gonzalez-Navarro, H.; Braco, L. *J. Mol. Catal. B: Enzym.* **1997**, *3*, 111−119. (d) Gonzalez-Navarro, H.; Braco, L. *Biotechnol. Bioeng.* **1998**, *59*, 122−127.

6. (a) Khmelnitsky, Y. L.; Welch, S. H.; Clark, D. S.; Dordick, J. S. *J. Am. Chem. Soc.* **1994**, *116*, 2647−2648. (b) Ru, M. T.; Hirokane, S. Y.; Lo, A. S.; Dordick, J. S.; Reimer, J. A.; Clark, S. S. *J. Am. Chem. Soc.* **2000**, *122*, 1565−1571. (c) Lindsay, J. P.; Clark, D. S.; Dordick, J. S. *Biotechnol. Bioeng.* **2004**, *85*, 553−560.
7. Lee, J. K.; Kim, M-J. *J. Org. Chem.* **2002**, *67*, 6845–6847.
8. (a) Itoh, T.; Han, S-H.; Matsushita, Y.; Hayase, S. *Green Chem.* **2004**, *6*, 437−439. (b) Itoh, T.; Matsushita, Y.; Abe, Y.; Han, S-H.; Wada, S.; Hayase, S.; Kawatsura, M.; Takai, S.; Morimoto, M.; Hirose, Y. *Chem. Eur. J.* **2006**, *12*, 9228−9237.
9. For examples see: (a) Park, S.; Kazlauskas, R. J. *J. Org. Chem.* **2001**, *66*, 8395-8401. (b) Maruyama, T.; Nagasawa, S.; Goto, M. *Biotechnol. Lett.* **2002**, *24*, 1341−1345. (c) Bora, U.; Saikia, C. J.; Chetia, A.; Mishra, A. K.; Kumar, B. S. D.; Boruah, R. C. *Tetrahedron Lett.* **2003**, *44*, 9099−9102.
10. BDMIM-PEG-PS is commercially available from Tokyo Chemical Industry Co., Ltd. Telephone: +81-3-5640-8857. Fax: +81-3-5640-8868.
11. Abe, Y.; Hirakawa, T.; Nakajima, S.; Okano, N.; Hayase, S.; Kawatsura, M.; Hirose, Y.; Itoh, T. *Adv. Synth. Catal.* **2008**, *350*, in press.
12. Commercial lipase PS (Amano) was supported by a Celite with 20 wt% of glycine. Protein content of PS is stated to have 1.0 wt% by Amano Enzyme, Ltd. The amino acid sequence of this lipase is known, so the molecular weight can be given precisely as 32 K dalton. Glycine-free PS was prepared by the Celite-free lipase PS, which was provided by Amano Enzyme *(11)*. Celite free lipase PS was provided by Amano Enzyme, Ltd. and included 20 wt% of glycine as a stabilizer.
13. Chen, C. -S.; Fujimoto, Y.; Girdauskas, G.; Sih, C. J. *J. Am. Chem. Soc.* **1982**, *102*, 7294–7298.
14. Luo, S.; Mi, X.; Zhang, L.; Liu, S.; Xu, H.; Cheng, J-P. *Angew. Chem., Int. Ed.* **2006**, *45*, 3093–3097.
15. Abe, Y.; Kude, K.; Hayase, S.; Kawatsura, M.; Itoh, Y. *J. Mol. Catal B: Enzym.* **2008**, *51*, 81–85.
16. Matsuda, T.; Yamagishi, Y.; Koguchi, S.; Iwai, N.; Kitazume, T. *Tetrahedron Lett.* **2006**, *47*, 4619–4621.
17. Nakamura, K.; Matsuda, T. *J. Org. Chem.* **1998**, *63*, 8957–8964.
18. (a) Matsuda, T.; Harada, T.; Nakamura, K. *Chem. Commun.* **2000**, 1367−1368. (b) Matsuda, T.; Watanabe, K.; Kamitanaka, T.; Harada, T.; Nakamura, K. *Chem. Commun.* **2003**, 1198−1199.
19. We prepared four types of BDMIM-PEG coated-*Geotrichum candidum* dried cells, which have ionic liquids with different contents of 5, 10, 50, and 100 wt% vs dried cells and evaluated their activity for the asymmetric reduction of acetophenone (**3**). The best activity was obtained for the enzyme that was prepared in the presence of 50 wt% of BDMIM-PEG *(8b)*.
20. Eckstein, M.; Filho, M. V.; Liese, A.; Kragl, U. *Chem. Commun.* **2005**, 1084–1085.

Downloaded by STANFORD UNIV GREEN LIBR on June 22, 2012 | http://pubs.acs.org
Publication Date (Web): April 28, 2010 | doi: 10.1021/bk-2010-1038.ch013

Downloaded by CORNELL UNIV on June 22, 2012 | http://pubs.acs.org
Publication Date (Web): April 28, 2010 | doi: 10.1021/bk-2010-1038.ch014

Chapter 14

Deep Eutectic Solvents for *Candida antarctica* Lipase B-Catalyzed Reactions

Johnathan T. Gorke,[1,2] Friedrich Srienc,[1,2] and Romas J. Kazlauskas[*,2,3]

[1]Department of Chemical Engineering and Materials Science, University of Minnesota, Minneapolis, MN 55455
[2]BioTechnology Institute, University of Minnesota, Saint Paul, MN 55108
[3]Department of Biochemistry, Molecular Biology, and Biophysics, University of Minnesota, Saint Paul, MN 55108
[*] rjk@umn.edu

Many deep eutectic solvents (DES's) are mixtures of ammonium salts and hydrogen-bond donors; e.g., a 1:2 mixture of choline chloride and urea. Like room temperature ionic liquids, DES's are polar, viscous solvents with low vapor pressure and flammability. However, synthesis of DES's is simpler – requiring only mixing of components – and the components are non-toxic and approximately ten-fold less expensive than the components for ionic liquids. Even though components of DES's can include protein denaturants like urea, we found that immobilized *Candida antarctica* lipase B retains activity in a wide range of DES's. Rates of transesterification, aminolysis of esters, perhydrolysis were similar to those in organic solvents and several-fold faster than those in ionic liquids. In a few cases, side reactions with the components of the DES occurred. DES's containing sugars were highly viscous and required temperatures ≥60 °C to permit stirring.

Introduction

Room temperature ionic liquids (RTILs) are liquids composed entirely of cations and anions, e.g. 1-butyl-3-methyl imidazolium tetrafluorborate (*1–3*).

In Ionic Liquid Applications: Pharmaceuticals, Therapeutics, and Biotechnology; Malhotra, S.;
ACS Symposium Series; American Chemical Society: Washington, DC, 0.

Most ionic liquids are non-volatile, thermally stable, and varying the cation and anion varies their polarity and other physical properties. Ionic liquids may be better than traditional organic solvents as solvents for extractions (*4*, *5*) chemical reactions (*6–8*) and biotransformations (*9–13*). Some limitations of the most common ionic liquids are toxicity similar to or higher than organic solvents (*14–16*), high cost, and the need for high purity, as even trace impurities can affect physical properties (*17*, *18*).

Deep eutectic solvents (DES's) are eutectic mixtures that are liquids at room temperature. Many DES's are 1:1 or 1:2 mixtures of an ammonium or metal salt and a hydrogen-bond donor, e.g. a 1:2 mixture of choline chloride and urea (*19*). DES's are alternatives to ionic liquids as replacements for organic solvents because DES's have low volatility and flammability, high thermal stability and varying the components varies the physical properties of solvent. DES's are not ionic liquids because they contain uncharged components – urea in the example above. Nevertheless, strong hydrogen bonding between the components makes their physical properties similar to those for ionic liquids (*20*).

The advantages of DES's over ionic liquids are lower cost and lower toxicity. The components of common DES's are inexpensive. Most DES's are mixtures of amine chloride salts and urea, glycerol, or ethylene glycol. Scheme 1 lists the components used in this work. Another reason for the low cost is the simple synthesis, which involves only warming and stirring the components for an hour or so. In contrast, synthesis of ionic liquids usually requires removal of salts, which can require multiple precipitations followed by chromatography to remove remaining traces. The components of DES's also are non-toxic; for example, glycerol and choline chloride are used as food additives. It is possible to use expensive or toxic components to make a DES, but the most common ones use inexpensive and nontoxic components. Other possibilities for DES components include: a wide range of organic acids (*21*, *22*) and fluorinated hydrogen bond donors (*23*).

Researchers have already reported numerous applications of DES's. For example, Abbott and coworkers dissolved silver salts in the DES's to dip coat copper surfaces with silver without the need for catalysts (*24*, *25*). Choline chloride-based DES's replaced phosphoric and sulfuric acids for electropolishing stainless steel (*26*, *27*). Adding choline chloride to a biodiesel preparation removed the glycerol side product by forming a choline chloride-glycerol DES as a second phase (*28*). Ma and workers sequestered CO_2 by reacting it with an epoxide to form a cyclic carbonate using immobilized choline chloride-urea as a catalyst (*29*). DES's containing $ZnCl_2$ in place of either the hydrogen bond donor or ammonium salt component are conductive (*30*, *31*) and also dissolve starch (*32*).

Some applications involve reactions of the components of the DES's. Heating a choline-chloride-urea DES caused a breakdown of the urea to an amine, which reacted to form aluminophosphonate materials (*33*). Different urea derivatives yielded different aluminophosphonate structures. To derivatize cellulose with ether links, Abbott and coworkers heated it in a DES containing alkylating agent chlorocholine chloride instead to choline chloride. (*34*).

Downloaded by CORNELL UNIV on June 22, 2012 | http://pubs.acs.org
Publication Date (Web): April 28, 2010 | doi: 10.1021/bk-2010-1038.ch014

Our preliminary report of lipase-catalyed transesterification and aminolysis in deep eutectic solvents (*35*) was surprising for two reasons. First, even though immobilized *Candida antarctica* lipase B (iCALB) denatures in solutions of urea, it did not denature in DES's containing 10 M urea. Second, even though alcohols and amines were reactants in these reactions, the alcohol or amine components of DES's showed up to 200-fold reduced chemical reactivity and usually did not interfere with these reactions. We hypothesized that strong hydrogen bonds between DES components lowered their reactivity. We also reported enzyme-catalyzed hydrolyses in mixtures of water and DES. In one case – hydrolysis of styrene oxide catalyzed by epoxide hydrolase – the reaction rate was 20-fold faster in a water/DES mixture than in water.

In this work we expand these findings to wider range of DES's and reaction types. The new DES components include very strong hydrogen bond donors such as formamide, ammonium salts with more hydrophobic substituents, and sugars. The new reaction types are lipase-catalyzed perhydrolysis and ring-opening polymerization (Scheme 2).

Downloaded by CORNELL UNIV on June 22, 2012 | http://pubs.acs.org
Publication Date (Web): April 28, 2010 | doi: 10.1021/bk-2010-1038.ch014

Experimental Section

General

Reagents and enzymes were purchased from Sigma-Aldrich, except where noted otherwise. Ionic liquids were purchased from Solvent Innovation (Cologne, Germany). Blank reactions (no enzyme) gave negligible conversion as compared to the enzyme-containing reactions. Gas chromatography used a flame ionization detector with the detector temperature at 275 °C and injector temperature at 250 °C.

Synthesis of Deep Eutectic Solvents

Ammonium-based DES's were prepared according to Abbott and coworkers method (*19*). For amide and glycerol-based DES's, ammonium salt (0.050 mol) and hydrogen bond donor (0.100 mol) were combined in a 20-mL vial and stirred at 60 to 80 °C until a homogeneous liquid formed, typically one hour. For sugar-based DES's, ammonium salt (0.050 mol) and sugar (0.050 mol) were combined as above, and stirred at 100 °C until a homogeneous liquid formed, typically several hours. The sugar-based DES's are very viscous, so they were warmed to 60 °C before use. The zinc-chloride-based DES was prepared by combining zinc chloride (0.050 mol) and urea (0.175 mol) and stirring at 80 °C.

Downloaded by CORNELL UNIV on June 22, 2012 | http://pubs.acs.org
Publication Date (Web): April 28, 2010 | doi: 10.1021/bk-2010-1038.ch014

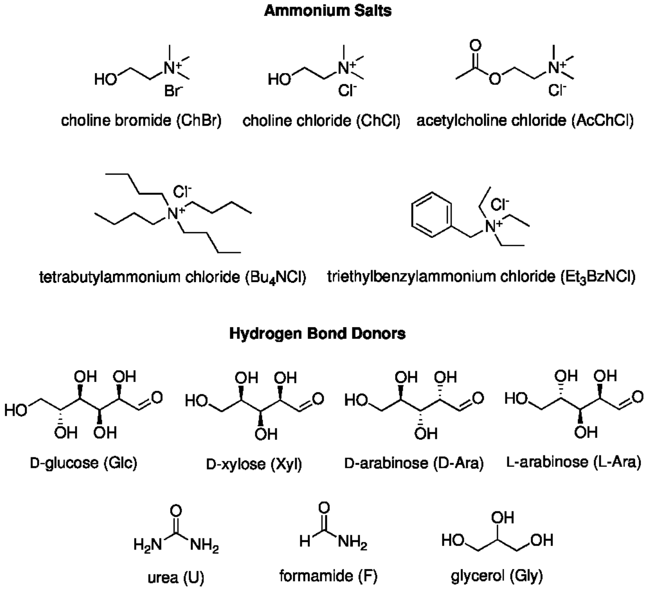
Ammonium Salts
choline bromide (ChBr)
choline chloride (ChCl)
acetylcholine chloride (AcChCl)
tetrabutylammonium chloride (Bu4NCl)
triethylbenzylammonium chloride (Et3BzNCl)
Hydrogen Bond Donors
D-glucose (Glc)
D-xylose (Xyl)
D-arabinose (D-Ara)
L-arabinose (L-Ara)
urea (U)
formamide (F)
glycerol (Gly)

Scheme 1. Many deep eutectic solvents are 1:1 or 1:2 mixtures of an ammonium salts and a hydrogen bond donor. These components were used in this work.

Transesterification

Immobilized CALB (iCALB, 1.0 mg of immobilized enzyme preparation) was suspended in solvent (0.20 mL) in a glass vial. Ethyl valerate (3.0 µL, 100 mM) and 2-butanol (3.7 µL, 200 mM) were added to the suspension and the resulting mixture was stirred at 40 °C for 15 min (60 °C for 30 min for the sugar-based DES's). The reaction products were extracted with toluene (1.0 mL) and analyzed by gas chromatography (Varian CP 7502 column, 25 m x 0.25 mm inner diameter and 0.25 µm film thickness). The initial column temperature of 50 °C was held for 8 min, then increased to 200 °C at 10 °C min^{-1} held at 200 °C for 5 min.

Perhydrolysis

Immobilized CALB (iCALB, 5.0 mg of immobilized enzyme preparation) was suspended in solvent (1.0 mL) in a glass vial. Cyclohexene (0.30 mL, 3.0 M final concentration) and octanoic acid (60 µL, 400 mM) were added to the suspension and the resulting mixture was stirred at room temperature. Hydrogen peroxide (0.18 mL of a 50 wt% solution in water, 440 mM final concentration) was added in six portions over the first five hours of reaction. After 24 h, the reaction products were extracted with toluene (1.0 mL) and analyzed by gas chromatography on an HP-5 column (J&W Scientific, Folsom, CA, 30 m x 0.32 mm inner dia and 0.25 µm film thickness). The initial column temperature of

60 °C was held for 6 min, then increased to 165 °C at 15 °C min^{-1}, then further increased to 200 °C at 25 °C min^{-1} and held at 200 °C for 5 min.

Polymerization

ε-Caprolactone (0.10 mL) was added to a magnetically-stirred suspension of immobilized CALB (iCALB, 3.3 mg of immobilized enzyme preparation) in solvent (0.20 mL) in a glass vial. After 24 h at 70 °C, the reaction was stopped by the addition of methanol (1.0 mL) and the vials were stored at 4 °C for 1 h to precipitate any polymer formed. Control reactions without enzyme or without lactone gave no precipitate.

Downloaded by CORNELL UNIV on June 22, 2012 | http://pubs.acs.org
Publication Date (Web): April 28, 2010 | doi: 10.1021/bk-2010-1038.ch014

Results

Wider Range of DES's

We previously reported that iCALB was active in DES's composed of choline chloride or ethylammonium chloride combined with an amide- hydroxyl- or acid-containing hydrogen bond donor (*35*). In this study, we examined a wider range of DES's and found that iCALB was active in all of them (Scheme 1 and Table I). These include several quarternary ammonium salts combined with glycerol or urea; choline chloride combined with sugars or with formamide, and even zinc chloride coupled to urea. Thus, a wide range of DES's are potential solvents for iCALB-catalyzed reactions.

Stability

Previously, we found that iCALB is at least 20 times more stable in ChCl:U than in either a 5 M choline chloride or 10 M urea solution. The enzyme lost < 1% activity in 90 min at 60 °C as compared with 25% loss in the choline chloride solution and 70% loss in the urea solution. Here we tested the long-term stability of iCALB in a glycerol-based DES. We incubated free iCALB in either toluene or ChCl:Gly for 18 h at 60 °C and tested the initial rate of transesterification of ethyl valerate to butyl valerate. In toluene, the activity dropped 12% compared to the rate before incubation, but in ChCl:Gly, it dropped only 5%. Thus, for this glycerol-based DES, iCALB is more stable than in toluene.

Activity in Transesterification

The initial activity of iCALB in the transesterification of ethyl valerate (100 mM) with 2-butanol (200 mM) in DES's was comparable to that in toluene (Table I). Initial rates were calculated from the conversion of ethyl valerate to

Downloaded by CORNELL UNIV on June 22, 2012 | http://pubs.acs.org
Publication Date (Web): April 28, 2010 | doi: 10.1021/bk-2010-1038.ch014

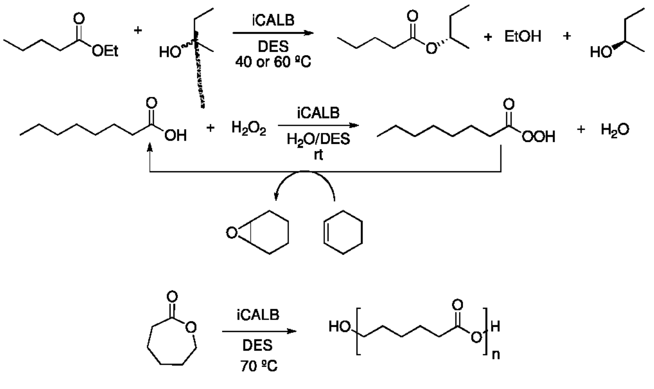

Scheme 2. iCALB-catalyzed reactions in DES's. Transesterification of ethyl valerate with 2-butanol (top), perhydrolysis of octanoic acid with the simultaneous epoxidation of cyclohexene (center), and ring-opening polymerization of ε-caprolactone (bottom).

2-butyl valerate after 15 minutes of reaction at 40 °C. Typical conversions were 10-45%, but the best solvent - ChCl:U – gave a conversion of 74%. Immobilized CALB was most active in ChCl:U, ChCl:Gly, ChBr:Gly, and Et_3BzNCl:Gly, with initial activities of 990, 640, 580, and 450 mU mg^{-1}, respectively. Immobilized CALB was less active in AcChCl:Gly (410 mU mg^{-1}), $ZnCl_2$:U (260 mU mg^{-1}), Bu_4NCl:Gly (200 mU mg^{-1}), and ChCl:F (150 mU mg^{-1}) than in toluene (430 mU mg^{-1}). These lower activities are all higher than those in the ionic liquid 1-butyl-3-methylimidazolium bis(trifluoromethanesulfonyl)-imide (BMIM[TF_2N], 140 mU mg^{-1}).

The activity of iCALB was slightly higher in the more viscous sugar-based DES's, likely due to the higher temperature used for these reactions (60 °C instead of 40 °C). The high viscosity of these sugar-based DES's required the higher temperature. Immobilized CALB had a higher initial activity in each sugar-based DES than toluene (660 mU mg^{-1}). The activity of iCALB in sugar-based DES's decreased as the viscosity increased: ChCl:Glc (750 mU mg^{-1}) was qualitatively the most viscous, ChCl:D-Ara (800 mU mg^{-1}) and ChCl:L-Ara (830 mU mg^{-1}) were less viscous, and ChCl:Xyl (880 mU mg^{-1}) was least viscous. This heterogenous reaction may be limited by slow diffusion in these viscous solvents.

Enantioselectivity

The enantioselectivity of iCALB toward 2-butanol is low ($E = 9.9$ in toluene at 40 °C) likely due to the difficulty in distinguishing the methyl and ethyl substituents at the stereocenter. This enantioselectivity decreased by a factor to two or more in both BMIM[Tf_2N] and in DES's. The enantioselectivity in DES's were generally higher than in BMIM[Tf_2N] (3.1), with Bu_4NCl:Gly (2.8) as the exception. Et_3BzNCl:Gly gave the highest enantioselectivity of any DES (5.2),

Downloaded by CORNELL UNIV on June 22, 2012 | http://pubs.acs.org
Publication Date (Web): April 28, 2010 | doi: 10.1021/bk-2010-1038.ch014

Table I. Initial Activity and Enantioselectivity of CALB-Catalyzed Transesterification of Ethyl Valerate and Butanol in DES's[a]

Solvent	*Type of Solvent*	*Alcohol*	*Initial Activity ($mU\ mg^{-1}$)*	*Enantio-selectivity*
Toluene	Organic	1-butanol	620 (*35*)	N/A
Toluene	Organic	2-butanol	430	9.9
Toluene	Organic	2-butanol	660 [b]	6.2
BMIM[Tf_2N]	RTIL	1-butanol	400 (*35*)	N/A
BMIM[Tf_2N]	RTIL	2-butanol	140	3.1
AcChCl:Gly	DES	2-butanol	410	5.0
Bu_4NCl:Gly	DES	2-butanol	200	2.8
ChBr:Gly	DES	2-butanol	580	4.5
ChCl:F	DES	2-butanol	150	4.4
ChCl:Gly	DES	1-butanol	560 (*35*)	N/A
ChCl:Gly	DES	2-butanol	640	4.9
ChCl:U	DES	1-butanol	340 (*35*)	N/A
ChCl:U	DES	2-butanol	990	3.6
$ZnCl_2$:U	DES	2-butanol	260	7.2
Et_3BzNCl:Gly	DES	2-butanol	450	5.2
ChCl:D-Ara	DES	2-butanol	800 [b]	3.7
ChCl:L-Ara	DES	2-butanol	830 [b]	3.2
ChCl:Glc	DES	2-butanol	750 [b]	4.0
ChCl:Xyl	DES	2-butanol	880 [b]	2.8

[a] Conditions: 2-butanol – 15 min, 40 °C, 5 mg mL^{-1} iCALB, 100 mM ethyl valerate, 200 mM 2-butanol. [b] 30-min reaction, 60 °C. 1-butanol – 15 min, 60 °C, 2.5 mg mL^{-1} iCALB, 40 mM ethyl valerate, 400 mM 1-butanol. 1 U = 1 μmol product formed min^{-1}. N/A = not applicable.

followed by AcChCl:Gly (5.0), ChCl:Gly (4.9), ChBr:Gly (4.5), ChCl:F (4.4), and ChCl:U (3.6).

The enantioselectivity of iCALB was also reduced in the sugar-based DES's compared to toluene ($E = 6.2$ at 60 °C). ChCl:Glc had the highest enantioselectivity of the DES's (4.0), while ChCl:D-Ara (3.7), ChCl:L-Ara (3.2), and ChCl:Xyl (2.8) were marginally lower. The two DES's containing enantiomeric arabinoses as components had similar enantioselectivities, suggesting that the arabinoses do not interact strongly with either the substrate or enzyme.

Perhydrolysis in DES-Water Mixtures

DES's were comparable to an ionic liquid for an iCALB-catalyzed perhydrolysis, but not as good as acetonitrile (Table II). Perhydrolysis of octanoic acid by hydrogen peroxide yielded the peracid, which reacted with cyclohexene to form cyclohexene oxide. The reaction mixture included ~10 vol% water from the added hydrogen peroxide solution. The conversion of cyclohexene to cyclohexene oxide was similar in ChCl:U (8%), ChCl:Gly (22%) and BMIM[BF_4] (15%), but substantially higher in acetonitrile (79%). Sheldon and coworkers also found that acetonitrile was the best solvent for this reaction (*9*).

Polymerization

Immobilized CALB also catalyzed ring-opening polymerization of ε-caprolactone in four DES's. We avoided DES's containing hydroxyl groups to prevent side reactions with the DES components. Trace water bound to the immobilized enzyme preparation initiated the polymerization. Similar amounts of polymer precipitate formed in AcChCl:U and Bu_4NCl:U as in toluene. A smaller amount of polymer precipitate formed in ChCl:U, and ChCl:F, but none in $ZnCl_2$:U. Further characterization of the polymer is in progress.

Discussion

CALB is active in a wide variety of DES's. We have expanded the range of DES's that may be suitable for enzymatic transformations into the realm of very strong hydrogen bond donors such as formamide, ammonium salts with more hydrophobic substituents, and sugars as hydrogen bond donors. Immobilized CALB was active in all combinations of ammonium salt and amide- or polyol-based hydrogen bond donor that we tested. The requirements for a suitable solvent appear to be: i) the components can form a homogeneous mixture, ii) the hydrogen bonds between DES components are strong enough to reduce the reactivity and hydrogen bond basicity of the two components, iii) the ammonium salt has no potential for proton exchange with desired substrates.

Requirements ii and iii depend on the specific reaction (Scheme 3). For instance, EAC:Gly is a suitable solvent for transesterification between ethyl valerate and butanol, but not for aminolysis of ethyl valerate. Little or no side products form in the transesterification, but the amine reacted with the ethyl ammonium component to make ethyl amine, resulting in significant amounts of aminolysis to ethyl amides instead of the desired amide (*35*). In another example, ChCl:EG was not a suitable solvent for transesterifications. Although the reactivity of the ethylene glycol component was reduced in the DES, it remained significant and the side reaction with ethylene glycol accounted for more than half of total conversion of ester.

Downloaded by CORNELL UNIV on June 22, 2012 | http://pubs.acs.org
Publication Date (Web): April 28, 2010 | doi: 10.1021/bk-2010-1038.ch014

Table II. Oxidation of cyclohexene to cyclohexene oxide by peroctanoic acid formed by iCALB-catalyed perhydrolysis of octanoic acid[a]

Solvent	*Type of solvent*	*Conversion (%)*
MeCN	Organic	79
BMIM[BF_4]	RTIL	15
ChCl:Gly	DES	22
ChCl:U	DES	8

[a] Conditions: 0.18 mL 50 wt% hydrogen peroxide added in six portions over 5 h to a mixture of 1.0 mL solvent, 0.3 mL cyclohexene, 60 µL octanoic acid, and 5 mg iCALB; stirred for 24 h total.

Downloaded by CORNELL UNIV on June 22, 2012 | http://pubs.acs.org
Publication Date (Web): April 28, 2010 | doi: 10.1021/bk-2010-1038.ch014

Another consideration for using DES's is viscosity. High viscosity makes handling and filtration difficult and may limit the reaction rates of heterogenous reactions where diffusion is important. The sugar-based DES's had viscosities likely too high for practical use without additives to decrease viscosity.

While iCALB typically had comparable and often higher activity in DES's compared to toluene, its enantioselectivity was lower. We can suggest three possible reasons. First, the molecular volume of a DES may be substantially larger than toluene, so that the substrate will displace different numbers of solvent molecules from active site. The different numbers will yield different entropy contributions to the reaction rate. Further, if the substrate enantiomers displace different numbers of solvent molecules in the two cases, then the different entropy contributions can change the enantioselectivity (*36*).

A second explanation is that some catalysis in DES's occurred outside the active site. Ma and coworkers reported that ChCl:U catalyzed the reaction of CO_2 with epoxides (*29*), so it is conceivable that DES's might catalyze transesterification. Control reactions showed that no product formed without enzyme, so this explanation would require the catalyst to be some type of adduct of DES and enzyme.

A third explanation is that the enzyme conformation in the polar DES's differs from that in toluene. Support for this notion comes from recent computer simulations that suggest that CALB changes its conformation in different organic solvents (*37*). Such changes could alter enantioselectivity, especially if the changes involve residues in the alcohol-binding site.

Both BMIM[BF_4] and DES's were poorer solvents than acetonitrile for perhydrolysis. This difference may be due to the reaction conditions, especially the ~10 vol% water. Seddon's group reported that the CALB perhydrolysis activity was comparable in both BMIM[BF_4] and acetonitrile, but they used less water (a more concentrated hydrogen peroxide solution) (*9*). Another possibility in the case of urea-containing DES's is that the urea acted as a base-catalyst for the hydrolysis of peracid.

Downloaded by CORNELL UNIV on June 22, 2012 | http://pubs.acs.org
Publication Date (Web): April 28, 2010 | doi: 10.1021/bk-2010-1038.ch014

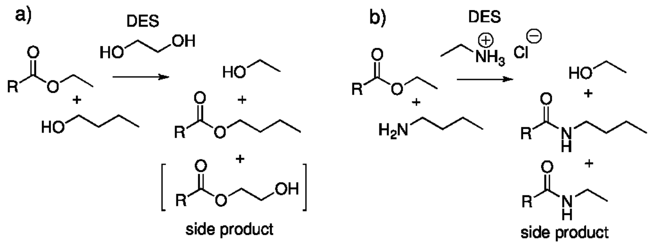

Scheme 3. Two side reactions of DES's in lipase-catalyzed reactions. a) The ethylene glycol component in DES competed with 1-butanol in an iCALB-catalyzed transesterification. The brackets indicate that gas chromato-graphy did not detect this presumed side product. DES's containing glycerol did not show this side reaction. b) The ethylamine component in DES competed with butylamine in an iCALB-catalyzed aminolysis. This side reaction does not occur in transesterifications, presumably because the ethylamine remains protonated and unreactive.

Conclusion

CALB is active in a variety of ammonium-ion-based DES's, despite the presence of chlorides and strong hydrogen bond donors such as formamide and urea. CALB is also active in DES's containing sugars such as hydrogen bond donors. Generally, the activity of CALB for tranesterifications in most DES's was comparable to toluene, but the enantioselectivity was lower. DES's were comparable to BMIM[BF_4] as solvents for perhydrolysis, but were not as good as acetonitrile.

Acknowledgments

We thank the University of Minnesota's Initiative for Renewable Energy and the Environment and the National Institutes of Health Biotechnology Training Grant for financial support.

References

1. Welton, T. *Chem. Rev.* **1999**, *99*, 207.
2. Wasserscheid, P.; Keim, W. *Angew. Chem., Int. Ed.* **2000**, *39*, 3772.
3. Wasserscheid, P.; Welton, T. *Ionic Liquids in Synthesis*; Wiley-VCH: Weinheim, Germany, 2003.
4. Huddleston, J. G.; Visser, A. E.; Swatlowski, R. P.; Reichert, W. M.; Griffin, S. T.; Rogers, R. D. *Ind. Eng. Chem. Res.* **2000**, *29*, 3596.
5. Zhao, H.; Xia, S.; Ma, P. *J. Chem. Technol. Biotechnol.* **2005**, *80*, 1089.
6. Zhao, H.; Moltrova, S. V. *Aldrichimica Acta* **2002**, *35*, 75.
7. Gordon, C. M. *Appl. Catal., A* **2001**, *222*, 101.

8. Jain, N.; Kumar, A.; Chauhan, S.; Chauhan, S. M. S. *Tetrahedron* **2005**, *61*, 1015.
9. Lau, R. M.; van Rantwijk, F.; Seddon, K. R.; Sheldon, R. A. *Org. Lett.* **2000**, *2*, 4189.
10. Lozano, P.; De Diego, T.; Carrié, D.; Vaultier, M.; Iborra, J. L. *Biotechnol. Lett.* **2001**, *23*, 1529.
11. Kragl, U.; Eckstein, M.; Kaftzik, N. *Curr. Opin. Biotechnol.* **2002**, *13*, 565.
12. Sheldon, R. A.; Lau, R. M.; Sorgedrager, M. J.; van Rantwijk, F.; Seddon, K. R. *Green Chem.* **2002**, *4*, 147.
13. Park, S.; Kazlauskas, R. J. *Curr. Opin. Biotechnol.* **2003**, *14*, 432.
14. Jastorff, B.; Störmann, R.; Ranke, J.; Mölter, K.; Stock, F.; Oberheitmann, B.; Hoffmann, W.; Hoffmann, J.; Nüchter, M.; Ondruschka, B.; Filser, J. *Green Chem.* **2003**, *5*, 136.
15. Ranke, J.; Mölter, K.; Stock, F.; Bottin-Weber, U.; Poczobutt, J.; Hoffmann, J; Ondruschka, B.; Filser, J.; Jastorff, B. *Ecotoxicol. Environ. Saf.* **2004**, *58*, 396.
16. Stolte, S.; Arning, J.; Bottin-Weber, U.; Matzke, M.; Stock, F.; Thiele, K.; Uerdingen, M.; Welz-Biermann, U.; Jastorff, B.; Ranke, J. *Green Chem.* **2006**, *8*, 621.
17. Seddon, K. R.; Stark, A.; Torres, M. *Pure Appl. Chem.* **2000**, *72*, 2275.
18. Burrell, A. K.; Del Sesto, R. E.; Baker, S. N.; McCleskey, T. M.; Baker, G. A. *Green Chem.* **2007**, *9*, 449.
19. Abbott, A. P.; Capper, G.; Davies, D. L.; Rasheed, R. K.; Tambyrajah, V. *Chem. Commun.* **2003**, 70–71.
20. Abbott, A. P.; Harris, R. C.; Ryder, K. S. *J. Phys. Chem. B* **2007**, *111*, 4910.
21. Abbott, A. P.; Boothby, D.; Capper, G.; Davies, D. L.; Rasheed, R. K. *J. Am. Chem. Soc.* **2004**, *126*, 9142.
22. Abbott, A. P.; Capper, G.; Davies, D. L.; McKenzie, K. J.; Obi, S. U. *J. Chem. Eng. Data* **2006**, *51*, 1280.
23. Abbott, A. P.; Capper, G.; Gray, S. *Chem. Phys. Chem.* **2006**, *7*, 803.
24. Abbott, A. P.; Griffith, J.; Nandhra, S.; O'Connor, C.; Postlethwaite, S.; Ryder, K. S.; Smith, E. L. *Surf. Coat. Technol.* **2008**, *202*, 2033.
25. Abbott, A. P.; Nandhra, S.; Postlethwaite, S.; Smith, E. L.; Ryder, K. S. *Phys. Chem. Chem. Phys.* **2007**, *9*, 3735.
26. Abbott, A. P.; Capper, G.; Swain, B. G.; Wheeler, D. A. *Transact. Inst. Met. Finish.* **2005**, *83*, 51.
27. Abbott, A. P.; Capper, G.; McKenzie, K. J.; Glidle, A.; Ryder, K. S. *Phys. Chem. Chem. Phys.* **2006**, *8*, 4214.
28. Abbott, A. P.; Cullis, P. M.; Gibson, M. J.; Harris, R. C.; Raven, E. *Green Chem.* **2007**, *9*, 868.
29. Zhu, A.; Jiang, T.; Han, B.; Zhang, J.; Xie, Y.; Ma, X. *Green Chem.* **2007**, *9*, 169.
30. Abbott, A. P.; Capper, G.; Davies, D. L.; Munro, H. L.; Rasheed, R. K.; Tambyrajah, V. *Chem. Commun.* **2001**, 2010.
31. Abbott, A.P.; Barron, J. C.; Ryder, K. S.; Wilson, D. *Chem. Eur. J.* **2007**, *13*, 6495.

Downloaded by CORNELL UNIV on June 22, 2012 | http://pubs.acs.org
Publication Date (Web): April 28, 2010 | doi: 10.1021/bk-2010-1038.ch014

32. Biswas, A.; Shogren, R. L.; Stevenson, D. G.; Willett, J. L.; Bhowmik, P. K. *Carbohydr. Polym.* **2006**, *66*, 546.
33. Parnham, E. R.; Drylie, E. A.; Wheatley, P. S.; Slawin, A. M. Z.; Morris, R. E. *Angew. Chem., Int. Ed.* **2006**, *45*, 4962.
34. Abbott, A. P.; Bell, T. J.; Handa, S.; Stoddart, B. *Green Chem.* **2006**, *8*, 784.
35. Gorke, J. T.; Srienc, F.; Kazlauskas, R. J. *Chem. Commun.* **2008**, *10*, 1235.
36. Ottosson, J.; Fransson, L.; King, J. W.; Hult, K. *Biochim. Biophys. Acta, Prot. Struct. Mol. Enzymol.* **2002**, *1594*, 325–334.
37. Trodler, P.; Pleiss, J. *BMC Struct. Biol.* **2008**, *8*, 9.

Downloaded by CORNELL UNIV on June 22, 2012 | http://pubs.acs.org
Publication Date (Web): April 28, 2010 | doi: 10.1021/bk-2010-1038.ch014

Chapter 15

Enzyme Catalysis in Ionic Liquids and Supercritical Carbon Dioxide

Pedro Lozano,*,[1] Teresa De Diego,[1] Michel Vaultier,[2]
and José L. Iborra[1]

[1] Departamento de Bioquímica y Biología Molecular B e Inmunología,
Facultad de Química, Universidad de Murcia, P.O. Box 4021,
E-30100 Murcia, Spain
[2] UMR-CNRS 6510, Université de Rennes, Campus de Beaulieu. Av.
Général Leclerc, 35042 Rennes, France
*** plozanor@um.es**

Downloaded by CORNELL UNIV on June 22, 2012 | http://pubs.acs.org
Publication Date (Web): April 28, 2010 | doi: 10.1021/bk-2010-1038.ch015

Enzymatic reactions based on ionic liquids (ILs) and supercritical carbon dioxide ($scCO_2$), are interesting alternatives to organic solvents for designing clean synthetic chemical processes that provide pure products directly. The classical advantages of $scCO_2$ to extract, dissolve and transport chemicals are tarnished in the case of enzymatic processes because of its denaturative effect on enzymes. ILs have shown themselves to be excellent non-aqueous environments for enzyme catalysis. Biphasic systems based on ILs and supercritical carbon dioxide have been proposed as the first approach to achieving integral green bioprocesses in non-aqueous media.

Enzyme Catalysis in Non-Aqueous Environments

Green Chemistry is based on the use of safer solvents and reaction conditions, and encourages the use of environmentally benign non-aqueous solvents and efficient catalysts for chemical reactions and/or processes (*1*). Enzymes, as catalysts of living systems, clearly constitute powerful green tools for chemical processes, since their activity and selectivity (stereo-, chemo- and regioselectivity) for catalyzed reactions are far-ranging. However, the catalytic activity of an enzyme strongly depends on this 3-D structure or native conformation, which is

In Ionic Liquid Applications: Pharmaceuticals, Therapeutics, and Biotechnology; Malhotra, S.;
ACS Symposium Series; American Chemical Society: Washington, DC, 0.

maintained by a high number of weak internal interactions (*e.g.* hydrogen bonds, van der Walls, etc.), as well as interactions with other molecules, mainly water, as natural solvent of living systems. Enzymes are designed to function in aqueous solutions within a narrow range of environmental conditions (pH, temperature, etc), which in fact represent the limits of life. Outside these conditions, enzymes are usually deactivated as a consequence of a loss of native conformation through unfolding (*2*).

In this context, the market for enantiopure fine chemicals is continuously growing, making enzymes the most suitable catalysts for green synthetic processes. However, the use of biocatalysts in aqueous media is limited because most chemicals of interest are insoluble in water. Furthermore, water is not an inert compound and usually gives rise to undesired side reactions, as well bringing about the degradation of substrates (*3*).

Downloaded by CORNELL UNIV on June 22, 2012 | http://pubs.acs.org
Publication Date (Web): April 28, 2010 | doi: 10.1021/bk-2010-1038.ch015

There are numerous potential advantages in employing enzymes in non-aqueous environments or media with a reduced water content (*e.g.* in the presence of organic solvents and/or additives) (*4*). These advantages include the higher solubility they permit in the case of hydrophobic substrates, the insolubility of enzymes, which makes them easy to reuse, and the elimination of microbial contamination in reactors. Probably the most interesting advantage of using non-aqueous environments for enzyme catalysis arises when hydrolytic enzymes (*e.g.* lipases, esterases, proteases, glycosidases, etc.) are applied, because of the ability of these enzymes to catalyze synthetic reactions. Additionally, enzymes are able to stereoespecifically recognize only one isomer from a racemic mixture of substrates, resulting in asymmetric synthetic reactions. However, switching from water to non-aqueous solvents, as reaction medium for enzyme-catalyzed reactions is not always a simple answer because the native structure of the enzyme can easily be destroyed, resulting in deactivation. Water is the key component of all non-conventional media, because of the importance that enzyme-water interactions have in maintaining the active conformation of the enzyme. Few clusters of water molecules are required for the catalytic function, in which hydrophobic solvents typically afford higher enzymatic activity than hydrophilic ones due to the latter have a tendency to strip some of these essential water molecules (see Figure 1) (*2*).

In this context, ionic liquids (ILs) and supercritical fluids (SCFs) are the non-aqueous green solvents which have received most attention worldwide for use in enzyme catalysis. The use of both ILs and $scCO_2$ neoteric solvents has enhanced the potential of enzymes because of improvements to their catalytic properties and operational stability. The combination of these neoteric solvents with enzymes may represent the most important "arsenal" of green tools to develop integral clean chemical processes of industrial interest in the near future (*5*).

Green Non-Aqueous Reaction Media

Solvents are key elements in chemical processes, where they acts as media for mass-transport, reaction and product separation. They are responsible for a major part of the environmental performance of processes in the chemical industry and have a great impact on cost, safety and health (*6*). The search for new environmentally benign non-aqueous solvents or green solvents, which can easily be recovered/recycled and which permit enzymes to operate efficiently in them, is a priority in the development of integral green chemical processes. Both ILs and SCFs are the main centres of interest for use as non-aqueous green solvents on the current academic and industrial agenda.

An SCF is defined as a state of matter at a pressure and temperature higher than its critical point, but below the pressure required to condense it into a solid. The exceptional properties of SCFs as solvents for extraction, reaction, fractionation and analysis have been reported (*7*). With respect to enzymatic catalysis, the number of fluids assayed in supercritical conditions is relatively low because of the inherent nature of proteins, which unfold and deactivate at high temperatures. Furthermore, supercritical fluids are low polar solvents, which preferentially dissolve hydrophobic compounds and have been applied in the biotransformation of this kind of compound. The most popular SCF in enzyme catalysis is $scCO_2$, which is considered as a green solvent, because it is chemically inert, non-toxic, non-flammable, cheap and readily available, exhibiting relatively low critical parameters that are compatible with biocatalysis, being used in reaction, extraction and fractionation processes. Other SCFs are less attractive because of their flammability (e.g. ethane, propane, etc), high cost (*e.g.* CHF_3) or poor solvent power (*e.g.* SF_6), and are therefore used in few research works (*8*).

ILs have recently emerged as exceptionally interesting non-aqueous reaction media for enzymatic transformations, and research interest in this area has increased widely in recent years. They are simply salts, and therefore entirely composed of ions, that are liquid below 100°C or even close to room temperature. Typical room temperature ionic liquids (RTILs) are based on organic cations, *e.g.* 1,3-dialkylimidazolium, N-alkylpyridinium, tetraalkylammonium and tetraalkylphosphonium, paired with a variety of anions that have a strongly delocalized negative charge (*e.g.* BF_4, PF_6, NTf_2, etc), resulting in colourless easily handled materials of low viscosity (see Figure 2). The interest of ILs as green solvents resides in their negligible vapour pressure, excellent thermal stability (up to 300 °C in many cases), ability to dissolve a wide range of organic and inorganic compounds, including gases (*e.g.* H_2, CO_2, etc), and their non-flammable nature (*9*). Moreover, the hydrophilicity/hydrophobicity and solvent miscibility of ILs can be tuned by selecting the appropriate cation and anion.

Downloaded by CORNELL UNIV on June 22, 2012 | http://pubs.acs.org
Publication Date (Web): April 28, 2010 | doi: 10.1021/bk-2010-1038.ch015

Downloaded by CORNELL UNIV on June 22, 2012 | http://pubs.acs.org
Publication Date (Web): April 28, 2010 | doi: 10.1021/bk-2010-1038.ch015

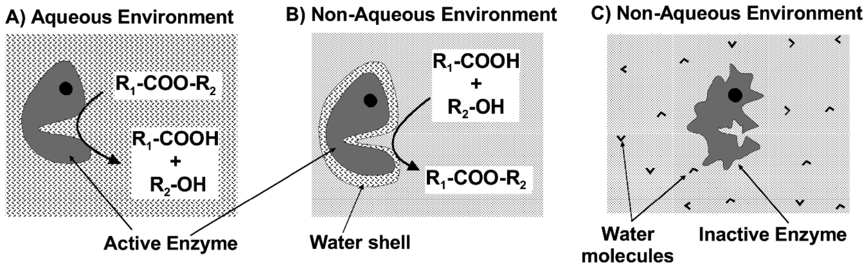
A) Aqueous Environment
B) Non-Aqueous Environment
C) Non-Aqueous Environment
R1-COO-R2
R1-COOH
+
R2-OH
R1-COOH
+
R2-OH
R1-COO-R2
Active Enzyme
Water shell
Water molecules
Inactive Enzyme

Figure 1. Schema of the role of water in different enzyme environments

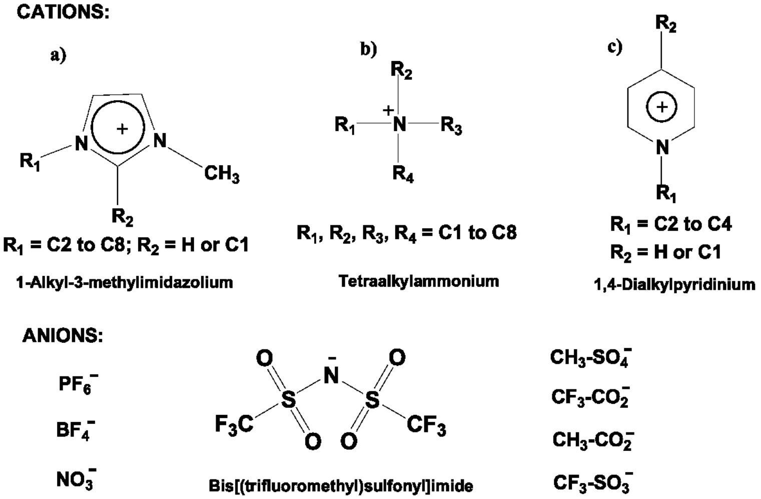
CATIONS:
a)
b)
c)
R1
R2
R3
R4
CH3
N
+
R1 = C2 to C8; R2 = H or C1
1-Alkyl-3-methylimidazolium
R1, R2, R3, R4 = C1 to C8
Tetraalkylammonium
R1 = C2 to C4
R2 = H or C1
1,4-Dialkylpyridinium
ANIONS:
PF6-
BF4-
NO3-
F3C
CF3
O
S
Bis[(trifluoromethyl)sulfonyl]imide
CH3-SO4-
CF3-CO2-
CH3-CO2-
CF3-SO3-

Figure 2. Typical structures of cations and anions involved in ILs that have been applied in enzyme catalysis

The polar character of ILs contrasts with the non-miscibility with water of some of them, which is an interesting property for enzymatic catalysis, because water molecules are essential for maintaining enzymes active in non-aqueous environments (see Figure 3) (*10*). As regards the anion, their polar character decreases as a function of the size/delocalization of the negative charge (*e.g.* $Cl>NO_2>NO_3>BF_4> NTf_2>PF_6$), while in the case of cations, the polarity is mainly determined by the length of the alkyl chain groups. ILs are immiscible with most hydrophophic organic solvents, thus providing a non-aqueous, polar alternative for two-phase systems that has been widely applied to extracting products from reaction mixtures. However, among the goals of green chemistry is the search to reduce the use of substances hazardous to human health and the environment, and so an alternative strategy for recovering products from IL systems without breaking the greenness of processes was found by using SCFs. Studies of ILs-$scCO_2$ phase behaviour indicated that such systems are unusual biphasic systems, although the high solubility of $scCO_2$ in ILs permits dissolved solutes to be recovered easily (*11*).

Enzymatic Reactions in $scCO_2$

Lipases and esterases are the most widely used enzymes applied for biotransformations using $scCO_2$ as reaction medium in anhydrous conditions, because of the excellence of this fluid for dissolving and transporting hydrophobic compounds. The synthesis of aliphatic esters of different alkyl chain lengths (*e.g.* from isoamyl acetate to oleyl oleate, terpenic esters, etc.) is the most popular enzymatic process in $scCO_2$. In this respect, transesterification (*e.g.* by alcoholysis, acidolysis or interesterification) approaches have also been applied to the modification and/or valorization of oils and fats (*i.e.* isolation of PUFAs, formation of structured TAG as nutraceuticals; formation of MAG, saccharide-FA esters, etc.). Currently, the use of lipases for the asymmetric synthesis of esters is one of the most important tools for organic chemists. The unique properties of $scCO_2$, combined with the catalytic excellence of lipases, have led to the successful chiral resolution of a large number of racemates (*i.e.* 1-phenylethanol, glycidol, ibuprofen, etc.). Other kinds of reactions on polymeric substrates, where the high diffusivity of $scCO_2$ is the key parameter, such as lipase-catalyzed polymerizations (*e.g.* polyester synthesis) or depolymerization (*e.g.* production of ε-caprolatone from polycaprolactone) in $scCO_2$, as well as, hydrolytic reactions catalyzed by polysaccharide hydrolases (*e.g.* α-amylase-catalyzed corn starch hydrolysis) in H_2O-$scCO_2$ biphasic systems, have also been demonstrated (*8*).

Several types of enzymatic reactor (see Figure 4), such as, stirred-tank, continuous flow or membrane reactors have been applied with SCFs, and have been used with many kinds of enzymatic preparation (*e.g.* free, immobilized, PEGylated, lipid coated, encapsulated etc.). The appropriate design of SCF bioreactors is key feature, where mass-transfer limitations, environmental conditions (pressure and temperature) and product recovery need to be easily controlled. For example, Marty *et al.* (*12*) developed a recycling packed bed enzyme-reactor at pilot scale for Lipozyme®-catalyzed ethyl oleate synthesis by esterification from oleic acid and ethanol in $scCO_2$ (see Figure 1). The proposed system was coupled with a series of four high-pressure separator vessels, where a pressure cascade was produced by back-pressure valves, allowing continuous recovery of the liquid product at the bottom of each separator, and then recycling unreacted substrates. Furthermore, membrane reactors constitute an attempt to integrate catalytic conversion, product separation and/or concentration and catalyst recovery into a single operation. Thus, enzymatic dynamic membranes, formed by depositing water-soluble polymers (*e.g.* polyethyleneimine, etc) on a ceramic porous support, have exhibited excellent properties for continuous synthetic processes in $scCO_2$, together with a high operational stability for reuse (*13*).

Downloaded by CORNELL UNIV on June 22, 2012 | http://pubs.acs.org
Publication Date (Web): April 28, 2010 | doi: 10.1021/bk-2010-1038.ch015

Downloaded by CORNELL UNIV on June 22, 2012 | http://pubs.acs.org
Publication Date (Web): April 28, 2010 | doi: 10.1021/bk-2010-1038.ch015

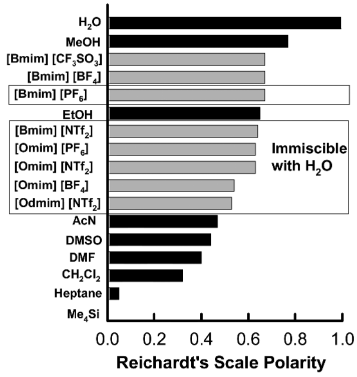

Figure 3. Polarity of some ILs and organic solvents according to the Reichardt scale (24). Water-immiscible ILs are inside the box.

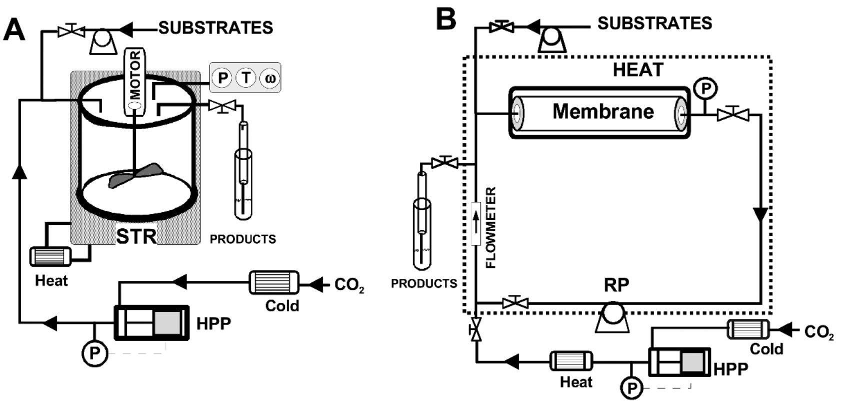

Figure 4. High-pressure stirred tank reactor (A) and membrane reactor with recirculation (B) for enzyme-catalyzed transformations in scCO₂. HPP, High pressure pump; RP, recirculation pump (13).

Pressure, temperature and water content are the most important environmental factors affecting enzymatic catalysis in SCFs, especially their activity, enantioselectivity and stability (*14*). SCFs are compressible fluids, and so changes in pressure and/or temperature are accompanied by a dramatic changes in density and transport properties, including their partition coefficient, viscosity, diffusivity and thermal conductivity, all parameters that indirectly modulate enzyme activity. Pressure and temperature may also directly affect enzyme activity by changing the rate-limiting steps or modulating the selectivity of the enzyme. As an example, in the synthesis of butyl butyrate catalyzed by Novozyme, the synthetic activity was exponentially increased by the decrease in $scCO_2$ density accompanying different combinations of pressure and temperature (*13*). In the same way, in the lipase-catalyzed esterification of *rac*-citronellol with oleic acid in $scCO_2$, an ester product of ee >99.9 % can be obtained simply by manipulating pressure and temperature around the critical point (*15*). In the same context, when lipid-coated lipase was employed in $scCHF_3$, the enzyme activity could be switched on and off by adjusting pressure or temperature (*16*).

Temperature influences enzyme activity much more than pressure, not only due to the usual increment in reaction rates at higher temperatures, but also as a result of enzyme deactivation processes. The optimal temperature of enzymatic processes in SCFs is related with pressure because both control solvent properties. However, the strong influence that temperature has on the deactivation has been related with changes in the hydration level of the enzyme. As happens with enzymes in organic solvents, water concentration in the supercritical reaction system is a key factor that influences enzyme activity and stability. Enzymes require a specific amount of bound water molecules to be active, and it should be noted that $scCO_2$ may dissolve up 0.3-0.5 % w/w water, depending on the temperature and pressure (*17*). On the other hand, if the water content in the supercritical medium is too high or if the water is a product of the reaction, the increased humidity may lead to enzyme deactivation. In other words, when immobilized enzymes are used, the support plays a key role in partitioning water molecules between the enzyme microenvironment and the supercritical medium, which affects the enzyme stability. The actual amount of water needed is specific to each SCF-substrate-enzyme system, and must be maintained constant throughout the process (*8*, *18*).

The excellence of SCFs for extracting, dissolving and transporting chemicals is only tarnished by the denaturative effect it has on enzymes. In the case of $scCO_2$, several adverse effects on enzyme activity and stability have been described due to, for example, local changes in the pH of the hydration layer, or the conformational changes produced during the pressurization/depressurization steps, as well as the ability of CO_2 to strip the water molecules from enzymes and to form carbamates with free amine groups on the protein surface, resulting in changes in the secondary structure, all of which reduces their activity. In this context, the review published in 1999 by Beckmann and Russel´s group states: "*...the advantages of replacing conventional organic solvents with supercritical fluids have not been fully demonstrated yet*" (*19*). Since 2000, several strategies have been developed to protect enzymes against these adverse effects of $scCO_2$, the best results being obtained when the biocatalyst was applied in suspension or coated with another green solvent, such as ionic liquids (ILs).

Enzymatic Catalysis in Ionic Liquids

The use of ILs as non-aqueous solvents for enzyme-catalyzed reactions was started in 2000 with two publications, this number having increased exponentially (more than 400 published papers to date), covering a variety of categories including research, review, opinion, etc (*20*). The unique solvent properties of ILs, especially as regards their polar character (which depends on the nature of the involved ions) have opened an alternative door for using organic solvents in

Downloaded by CORNELL UNIV on June 22, 2012 | http://pubs.acs.org
Publication Date (Web): April 28, 2010 | doi: 10.1021/bk-2010-1038.ch015

Downloaded by CORNELL UNIV on June 22, 2012 | http://pubs.acs.org
Publication Date (Web): April 28, 2010 | doi: 10.1021/bk-2010-1038.ch015

enzymatic catalysis in non-aqueous liquid environments (*21*). Thus, research on enzymatic catalysis in ILs first focused on the potential of these neoteric solvents as reaction media, then on understanding the exceptional behavior of enzymes in some kinds of IL, and finally on the development of integrated biotransformation/separation systems made possible by the unique properties of ILs. The relationships between the chemical structures of ILs and the activity, enantioselectivity and/or stability displayed by enzymes are still not clearly understood.

The great ability of ILs to dissolve both polar and non-polar compounds is responsible for the large number of enzymes (*e.g.* lipases, proteases, peroxidases, dehydrogenases, glycosidases, etc.) and reactions (*e.g.* esterification, kinetic resolution, reductions, oxidations, hydrolysis, etc.) that have been tested (see Table 1). As mentioned above, the behavior of enzymes in non-aqueous media is strictly related with the degree of hydration of the protein, and the importance of this parameter in ILs is crucial. Based on the miscibility of ILs with water, two types of enzymatic reaction system may be considered: aqueous solutions of ILs and ILs in nearly anhydrous conditions (*21*, *22*).

Aqueous solutions of ILs have been used to increase the solubility of polar substrates and products with hydrophobic moieties (*e.g.* amino acids derivatives). For such reaction media, the IL and the assayed concentration are key criteria because of the high ability of water-miscible ILs to deactivate enzymes. For example, in the case of the subtilisin (Alcalase from Novo)-catalyzed resolution of N-acetyl amino acid esters in aqueous solution of [EtPy][TFA], the best enzyme activity and enantioselectivity was obtained at 10 % v/v IL concentration, while both fall drastically at higher concentrations (see Figure 5) (*23*).

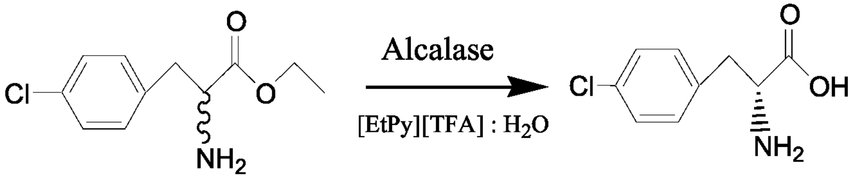

Figure 5. Subtilisin-catalyzed resolution of 4-chlorophenylalanine ethyl ester using a 15 % v/v [EtPy][TFA] solution in water as reaction medium (23).

Table 1. Some of enzymes, ILs and enzyme-catalyzed reactions in ILs (*21*)

Enzyme	*Ionic Liquid*	*Reaction*
Proteases	[Bmim][PF_6]	Acylation of allylic alcohols
Thermolysin	[Hmim][PF_6]	Acylation of levoglucosan
α-Chymotrypsin	[Omim][PF_6]	Hydrolysis of β-methylstyrene oxide

Continued on next page.

Table 1. (Continued). Some of enzymes, ILs and enzyme-catalyzed reactions in ILs (*21*)

Enzyme	***Ionic Liquid***	***Reaction***
Alcalase	[Bmpy][PF_6]	Oxidation of syringaldazyne
Papain	[Emim][NTf_2]	Production of biodiesel
Lipases from	[Bmim][NTf_2]	Reduction of *rac*-2-octanone
C. antarctica	[Btma][NTf_2]	Resolution of *rac*-1-phenylethanol
M. Miehei	[Htma][NTf_2]	Resolution of amino acid esters
P. cepacia	[Toma][NTf_2]	Resolution of Indinavir
C. rugosa	[Emim][BF_4]	Resolution of N-Ac-amino acid esters
Porcine pancreas	[Bmim][BF_4]	Resolution of *rac*-2-pentanol
Other enzymes	[Bdmim][BF_4]	Resolution of *rac*-glycidol
Peroxidase,	[Hmim][BF_4]	Resolution of *rac*-ibuprofen
Laccase C	[Omim][BF_4]	Resolution of *rac*-methyl mandelate
Cytochrome-C	[Bmpy][BF_4]	Resolution of *sec*-arylalcohols
Alcohol DHase	[Bpy][BF_4]	Synthesis of aliphatic esters
Morphine DHase	[Bmim][TfO]	Synthesis of ascorbyl palmitate
β-Galactosidase	[Bmim][$EtOSO_4$]	Synthesis of citronellyl esters
Epoxide Hydrolase	[Bmim][$BuSO_4$]	Synthesis of cyanohydrins
Mandelate racemase		Synthesis of N-acetyllactosamine
Cellulase		Synthesis of oxycodone
Glucose oxidase		Synthesis of polyesters
Penicillin G acilase		Synthesis of pyridoxine esters
		Synthesis of Z-aspartame

Downloaded by CORNELL UNIV on June 22, 2012 | http://pubs.acs.org
Publication Date (Web): April 28, 2010 | doi: 10.1021/bk-2010-1038.ch015

Downloaded by CORNELL UNIV on June 22, 2012 | http://pubs.acs.org
Publication Date (Web): April 28, 2010 | doi: 10.1021/bk-2010-1038.ch015

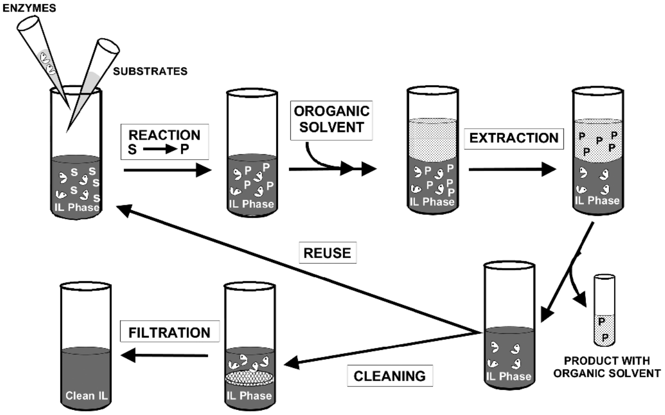
ENZYMES
SUBSTRATES
REACTION
S → P
OROGANIC SOLVENT
EXTRACTION
IL Phase
REUSE
FILTRATION
CLEANING
Clean IL
PRODUCT WITH ORGANIC SOLVENT

Figure 6. Operational strategy for enzymatic reactions in monophasic ILs systems, including recycling, product separation and clean IL recovery steps.

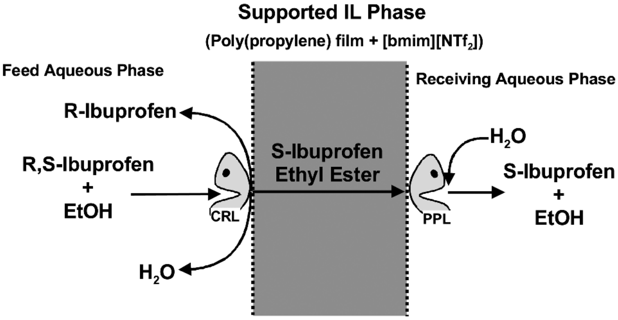
Supported IL Phase
(Poly(propylene) film + [bmim][NTf2])
Feed Aqueous Phase
Receiving Aqueous Phase
R-Ibuprofen
R,S-Ibuprofen + EtOH
H2O
S-Ibuprofen Ethyl Ester
CRL
PPL
H2O
S-Ibuprofen + EtOH

Figure 7. Schematic diagram of enantioselective transport of S-ibuprofen through a lipase-facilitated supported IL membrane. CRL, Candida rugosa lipase; PPL, porcine pancreas lipase (Miyako et al. (30)).

In the same way, the cleavage of mandelonitrile catalysed by a hydroxynitrile lyase from *Prunus* proceeded more rapidly in aqueous media containing (alkyl)mim BF_4 at 2–6% (v/v), while concentrations higher than 10% v/v halved the residual activity (*24*). A similar behavior was observed for other enzymes such as chloroperoxidase, formate dehydrogenase, β-galactosidase, etc., which was attributed to the ability of ions from water-miscible ILs to strongly interact with proteins, producing deactivation by unfolding of the 3-D structure. However, the kosmotropic or chaotropic character of ions related with the Hofmeister series does not seem a solid basis for predicting the compatibility of enzymes and water-miscible ILs in aqueous solution (*21*).

The remarkable results obtained for enzymatic reactions in water-immiscible ILs in nearly anhydrous conditions have underlined the suitability of these solvents as a clear alternative to molecular organic solvents. The typical

Downloaded by CORNELL UNIV on June 22, 2012 | http://pubs.acs.org
Publication Date (Web): April 28, 2010 | doi: 10.1021/bk-2010-1038.ch015

operational strategy applied for enzymatic processes in ILs is described in Figure 6. At low water content (< 2% v/v), all the assayed water-immiscible ILs (*e.g.* [Bmim][PF_6], [Btma][NTf_2], etc.) were shown to be suitable reaction media for biocatalytic reactions (*21*, *22*). The enzymes displayed a high level of activity and stereoselectivity for synthesizing many different compounds, *e.g.* aspartame, aliphatic and aromatic esters, amino acid esters, chiral esters by (dynamic) kinetic resolution of racemic alcohols, carbohydrate esters, polymers, terpene esters, etc. Furthermore, free enzyme molecules suspended in these media behave as anchored or immobilized biocatalysts because they cannot be separated by liquid-liquid extraction (*e.g.* with buffer or aqueous solutions) (*25*, *26*). ILs can be easily cleaned of protein molecules by filtering the enzyme-IL solution through ultrafiltration membranes with a cut-off lower than the molecular weight of the enzyme (*27*). ILs form a strong ionic matrix and the added enzyme molecules could be considered as being included rather than dissolved in the media, meaning that ILs should be regarded as liquid enzyme immobilization supports, rather than reaction media, since they enable the enzyme-IL system to be reused in consecutive operation cycles (*25*, *28*). Finally, after an enzymatic transformation process in ILs, products can usually be recovered by liquid-liquid extraction, although the organic solvents used in this step represent a clear breakdown point for the integral green design of any chemical process. To overcome this problem, alternative strategies for product recovery by coupling $scCO_2$, membranes or vacuum systems have successfully been applied (*29*). For example, the kinetic resolution of *rac*-ibuprofen has been carried out by coupling two lipase reactions with a membrane containing supported ILs. As supported liquid membranes based on ILs permits the selective transport of organic molecules, the system provides for the easy and selective permeation of *S*-ibuprofen through the membrane, allowing successful resolution of the racemic mixture (Figure 7) (*30*).

The excellent stability displayed by enzymes in water-immiscible ILs for reuse and under high temperatures has been widely described (*21*, *22*, *25*, *26*). In the case of free enzyme, the ability of these neoteric solvents to maintain the secondary structure and the native conformation of the protein towards the usual unfolding that occurs in non-aqueous environments has been demonstrated by spectroscopic techniques (e.g. fluorescence, circular dichroism, FT-IR, etc) (*21*, *31*, *32*).

To understand the structure-function relationships of enzymes in water immiscible ILs, it is necessary to consider the molecular characteristics of these neoteric solvents. The structural organization of imidazolium ILs in solid and liquid phases has been described as an extended network of cations and anions connected by hydrogen bonds (*33*). The monomeric unit always consists of one imidazolium cation surrounded by at least three anions and, in turn, each anion is surrounded by at least three imidazolium cations, where the strongest hydrogen bond always involves the most acidic H2 of the imidazolium ring. The three dimensional structure of these ILs are formed by chains of the imidazolium ring and, in some cases, there are typical π–π stacking interactions among rings, resulting in a liquid phase, as revealed by Raman studies. The incorporation of other molecules and macromolecules into the IL network involves changes in the physical properties of these materials and can cause, in some cases (e.g. water), the formation of polar and non-polar regions (*9*). Wet ILs are nano-structured materials which allow neutral molecules to reside in less polar regions and ionic or polar species to undergo faster diffusion in the more polar or wet regions. In this context, enzymes in water immiscible ILs should also be considered as being included in the hydrophilic gaps of the network, where the observed stabilization of enzymes could be attributed to the maintenance of this strong net around the protein. In fact, the protein unfolding process that occurs in water as temperature increases could also be regarded as a loss of its three-dimensional structure, which produces the disruption of the medium structure because of the heat-induced increase in the kinetic energy of water molecules. The extremely ordered supramolecular structure of ILs in liquid phase might be able to act as a mould, maintaining an active three-dimensional structure of the enzyme in aqueous nano-environments, and avoiding the classical thermal unfolding. These facts imply that free enzyme suspended in ILs systems can be considered as carrier-free-immobilized enzyme derivatives (*25*, *32*).

Downloaded by CORNELL UNIV on June 22, 2012 | http://pubs.acs.org
Publication Date (Web): April 28, 2010 | doi: 10.1021/bk-2010-1038.ch015

Green Enzymatic Processes in IL/scCO$_2$ Biphasic Systems

In 1999, Brennecke's group demonstrated the exceptional ability of scCO$_2$ to extract naphthalene from certain ILs based on the 1-butyl-3-methylimidazolium (Bmim) cation. This was due to the fact that, although scCO$_2$ is highly soluble in the IL phase, the same IL is not measurably soluble in the scCO$_2$ phase (*34*).

The phase behavior of IL/scCO$_2$ systems has been studied for several ILs and supercritical conditions, as well as, in the presence of solutes dissolved into the IL phase. A knowledge of this phase behavior is essential for any process development because it determines the contact between scCO$_2$ and solute, and also reduces the viscosity of the IL phase, which enhances the mass-transfer rate of any the reaction system. In this context, CO$_2$ has even been used to extract a wide variety of solutes from ILs, as well as a "switch" to separate ILs from organic solvents or water. Because of the unique properties of IL/scCO$_2$ biphasic systems, a solute dissolved in an IL can be easily recovered with scCO$_2$ without any cross contamination. The lack of solubility of ILs in the scCO$_2$ phase has been attributed to both the extremely low vapor pressure of IL, and the inability of CO$_2$ molecules to adequately solvate ions into the supercritical phase (*8*, *35*).

In this context, a new concept for continuous biphasic biocatalysis, where a homogeneous enzyme solution is immobilized in a liquid phase (working phase), while substrates and products reside largely in a supercritical phase (extractive phase), has been proposed as the first approach to integral green bioprocesses in non-aqueous media, directly providing products (see Figure 8). The system was tested for two different enzymatic reactions: the synthesis of butyl butyrate from vinyl butyrate and 1-butanol, and the kinetic resolution of *rac*-1-phenylethanol at 150 bar and in a range of temperatures (40-100 °C). In both cases, an exceptional level of activity, enantioselectivity (ee> 99.9) and operational stability was obtained even after 11 cycles of 4 h of work. These excellent results were corroborated in extreme conditions: 100 bar and 150 °C. Furthermore, for these

$IL/scCO_2$ systems, the substrates must be transported from the supercritical to the enzyme-IL phase, and vice versa in the case of products, their solubility in this liquid phase being the key parameter for controlling the efficiency of the reaction system (*36–38*).

Biphasic systems based on IL and $scCO_2$ have also been used for the enzymatic synthesis of octyl acetate in batch processes, with the IL acting as a solvent rather than as protective agent of the enzyme (*8*). The kinetic resolutions of both *rac*-2-octanol (*39*) and rac-2-phenyl-1-propanol (*40*) catalyzed by lipase and cutinase, respectively, as well as the dynamic kinetic resolution of rac-1-phenylethanol (by coupling the enzymatic step with a chemical catalytic step in the IL phase) (*41*), are additional examples of how $IL/scCO_2$ biphasic systems can be successfully used to develop continuous green enzymatic processes for the synthesis of fine chemicals.

However, some ILs have been described as being not fully green solvents, because of their low biodegradability and high (eco)toxicological properties (*21*). In this context, a further step towards reducing the amount of IL used in the enzymatic processes in $IL/scCO_2$ biphasic systems has resulted from the development of monolithic solid supports containing a covalently attached IL phase (*42*). The adsorption of a lipase onto this linked IL phase provides excellent immobilized biocatalysts with enhanced activity and increased operational stability for the synthesis of citronellyl butyrate in $scCO_2$, compared with the original strategy based on enzymes coated with ILs.

Downloaded by CORNELL UNIV on June 22, 2012 | http://pubs.acs.org
Publication Date (Web): April 28, 2010 | doi: 10.1021/bk-2010-1038.ch015

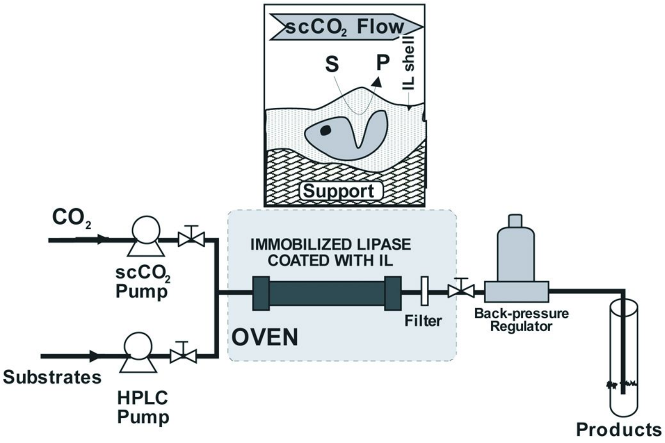

Figure 8. Experimental set-up of the continuous green enzyme reactor working in $ILs/scCO_2$ biphasic medium

Downloaded by CORNELL UNIV on June 22, 2012 | http://pubs.acs.org
Publication Date (Web): April 28, 2010 | doi: 10.1021/bk-2010-1038.ch015

Future Trends

Enzymes are increasingly used in organic synthesis and their advantages in SCFs are manifold, because these green media allow rapid reaction rates, simplify product recovery and permit the reuse of solvent. The weakness of biocatalysts working in these non-conventional media is overcome by the use of ILs supporting enzymes. The exceptional ability of water-immiscible ILs to stabilize enzymes and maintain their native and active conformation even under extremely harsh supercritical conditions seems to be related with their unique structure, which has been described as a supramacromolecular dynamic network. Fundamental studies on enzyme catalysis in IL/SCF biphasic systems should be carried out to establish clear criteria for specifically pairing the most appropriate ILs/SCFs with the corresponding enzymes or bioprocesses. Furthermore, the enormous potential of multi-enzymatic and/or multi-chemoenzymatic processes in ILs/SCFs for synthesizing pharmaceuticals drugs has only just been realized. The road leading to clean green chemical industry passes through enzymatic processes.

Acknowledgments

This work was partially supported by the CICYT (CTQ2005-01571-PPQ), SENECA Foundation (02910/PI/05), and CARM (BIO-BMC 06/01-0002) grants We like to thanks Mr. R. Martínez from Novo España, S.A. the gift of Novozym.

References

1. Anastas, P. T.; Warner, J. C. *Green Chemistry: Theory and Practice*; Oxford University Press: Oxford, U.K., 1998.
2. Reetz, M. T. *Adv. Catal.* **2006**, *49*, 1–69.
3. Klibanov, A. M. *Nature* **2001**, *409*, 241–246.
4. Hudson, E. P.; Eppler, R. K.; Clark, D. S. *Curr. Opin. Biotechnol.* **2005**, *16*, 637–643.
5. Lozano, P.; De Diego, T.; Iborra, J. L. *Chem. Today* **2007**, *25*, 76–79.
6. Capello, C.; Fisher, U.; Hungerbühler, K. *Green Chem.* **2007**, *9*, 927–934.
7. Jessop, P. J., Leitner, W., Eds.; *Chemical Synthesis Using Supercritical Fluids*; Wiley-VCH: Weinheim, Germany, 1999.
8. Hobbs, H. R.; Thomas, N. R. *Chem. Rev.* **2007**, *107*, 2786–2820.
9. Dupont, J.; de Souza, R. F.; Suarez, P. A. Z. *Chem. Rev.* **2002**, *102*, 3667–3691.
10. Poole, C. F. *J. Chromatogr., A* **2004**, *1037*, 49–82.
11. Keskin, S.; Kayrak-Talay, D.; Akman, U.; Hortaçsu, O. *J. Supercrit. Fluids* **2007**, *43*, 150–180.
12. Marty, A.; Combes, D.; Condoret, J. S. *Biotechnol. Bioeng.* **1994**, *43*, 497–504.

13. Lozano, P.; Villora, G.; Gómez, D.; Gayo, A. B.; Sánchez-Conesa, J. A.; Rubio, M.; Iborra, J. L. *J. Supercrit. Fluids* **2004**, *29*, 121–128.
14. Rezaei, K.; Temelli, F.; Jenab, E. *Biotechnol. Adv.* **2007**, *25*, 272–280.
15. Mori, T.; Li, M.; Kobayashi, A.; Okahata, Y. *J. Am. Chem. Soc.* **2002**, *124*, 1188–1189.
16. Mori, T.; Funasaki, M.; Kobayashi, A.; Okahata, Y. *Chem. Commun* **2001**, 1832–1833.
17. Knez, Z.; Habulin, M.; Primozic, M. *Biochem. Eng. J.* **2005**, *27*, 120–126.
18. Lozano, P.; Avellaneda, A.; Pascual, R.; Iborra, J. L. *Biotechnol. Lett.* **1996**, *18*, 1345–1350.
19. Mesiano, A. J.; Beckman, E. J.; Russel, A. J. *Chem. Rev.* **1999**, *99*, 623–633.
20. Search in ISI Web of Knowledge, Topic: (ionic liquids AND biocatal*) OR (ionic liquids AND enzym*).
21. van Rantwijk, F.; Sheldon, R. A. *Chem. Rev.* **2007**, *107*, 2757–2785.
22. Yang, Z.; Pan, W. *Enz. Microb. Technol.* **2005**, *37*, 19–28.
23. Zhao, H.; Malhotra, S. V. *Biotechnol Lett.* **2002**, *24*, 1257–1260.
24. Lou, W. Y.; Xu, R.; Zong, M. H. *Biotechnol. Lett.* **2005**, *27*, 1387–1390.
25. Lozano, P.; De Diego, T.; Carrié, D.; Vaultier, M.; Iborra, J. L. *Biotechnol. Lett.* **2001**, *23*, 1529–1533.
26. Lozano, P.; De Diego, T.; Guegan, J. P.; Vaultier, M.; Iborra, J. L. *Biotechnol. Bioeng.* **2001**, *75*, 563–569.
27. Kaftzkik, N.; Wasserscheid, P.; Kragl, U. *Org. Proc. Res. Dev.* **2002**, *6*, 553–557.
28. Lozano, P.; De Diego, T.; Gmöuh, S.; Vaultier, M.; , J. L.Iborra *Biocatal. Biotransform.* **2005**, *23*, 169–176.
29. Gubicza, L.; Nemestothy, N.; Frater, T.; Belafi-Bako, K. *Green Chem.* **2003**, *5*, 236–239.
30. Miyako, E.; Maruyama, T.; Kamiya, N.; Goto, N. M. *Chem. Commun.* **2003**, 2926–2927.
31. De Diego, T.; Lozano, P.; Gmouh, S.; Vaultier, M.; Iborra, J. L. *Biotechnol. Bioeng.* **2004**, *88*, 916–924.
32. De Diego, T.; Lozano, P.; Gmouh, S.; Vaultier, M.; Iborra, J. L. *Biomacromolecules* **2005**, *6*, 1457–1464.
33. Dupont, J. *J. Braz. Chem. Soc.* **2004**, *15*, 341–350.
34. Blanchard, L. A.; Hancu, D.; Beckman, E. J.; Brennecke, J. F. *Nature* **1999**, *399*, 28–29.
35. Scurto, A. M.; Aki, S. N. V. K.; Brennecke, J. F. *Chem. Commun* **2003**, 572–573.
36. Lozano, P.; De Diego, T.; Carrié, D.; Vaultier, M.; Iborra, J. L. *Chem. Commum.* **2002**, 692–693.
37. Lozano, P.; De Diego, T.; Carrié, D.; Vaultier, M.; Iborra, J. L. *Biotechnol. Prog.* **2003**, *19*, 380–382.
38. Lozano, P.; De Diego, T.; Gmouh, S.; Vaultier, M.; Iborra, J. L. *Biotechnol. Prog.* **2004**, *20*, 661–669.
39. Reetz, M. T.; Wiesenhofer, W.; Francio, G.; Leitner, W. *Adv. Synth. Catal.* **2003**, *345*, 1221–1228.

Downloaded by CORNELL UNIV on June 22, 2012 | http://pubs.acs.org
Publication Date (Web): April 28, 2010 | doi: 10.1021/bk-2010-1038.ch015

40. Garcia, S.; Lourenco, N. M. T.; Lousa, D.; Sequeira, A. F.; Mimoso, P.; Cabral, J. M. S.; Afonso, C. A. M.; Barreiros, S. *Green Chem.* **2004**, *6*, 466–470.
41. Lozano, P.; De Diego, T.; Larnicol, M.; Vaultier, M.; Iborra, J. L. *Biotechnol. Lett.* **2006**, *28*, 1559–1565.
42. Lozano, P.; Garcia-Verdugo, E.; Piamtongkam, R.; Karbass, N.; De Diego, T.; Burguete, M. I.; Luis, S. V.; Iborra, J. L. *Adv. Synth. Catal.* **2007**, *349*, 1077–1084.

Downloaded by CORNELL UNIV on June 22, 2012 | http://pubs.acs.org
Publication Date (Web): April 28, 2010 | doi: 10.1021/bk-2010-1038.ch015

Downloaded by UNIV OF DELAWARE MORRIS LIB on June 22, 2012 | http://pubs.acs.org
Publication Date (Web): April 28, 2010 | doi: 10.1021/bk-2010-1038.ch016

Chapter 16

On the Merge of Fungal Activity with Ionic Liquids towards the Development of New Biotechnological Processes

M. Petkovic,[1] J. Ferguson,[2] A. Bohn,[1] J. R. Trindade,[1] I. Martins,[1] C. Leitão,[1] M. B. Carvalho,[1] C. Rodrigues,[1] H. Garcia,[1] R. Ferreira,[1] K. R. Seddon,[1,2] L. P. N. Rebelo,[1] and C. Silva Pereira[1,*]

[1]Instituto de Tecnologia Química e Biológica (ITQB) - Universidade Nova de Lisboa and Instituto de Biologia Experimental e Tecnológica (IBET), Oeiras, Portugal
[2]Queen's University Ionic Liquid Laboratories, QUILL, Queen's University of Belfast, United Kingdom
[*]Corresponding author: spereira@itqb.unl.pt

In this work we present the toxicological assessment of sixteen ionic liquids (ILs), containing either an imidazolium, or a pyridinium ring, or a cholinium function, to filamentous fungi (*Penicillium* sp.) as eukaryotic model organisms. It is shown that among this family there are members which show much higher tolerance towards ILs than any other microorganism studied so far. Furthermore, guided by the paradigm that the choice of an ionic liquid as catalyst can alter the outcome of a given chemical reaction, we investigated the ability of ILs to alter the metabolic profile in fungi. The metabolic footprinting, using ESI-MS, revealed that fungal cultures respond to specific liquid salts by changing the cell biochemistry, resulting in a different pattern of secondary metabolites.

Introduction

In the last two decades, ionic liquids (ILs) attracted a lot of scientific and commercial interest, demonstrated in numerous publications and patents. They are, by definition, salts that are liquid at, or near, room temperature, completely

In Ionic Liquid Applications: Pharmaceuticals, Therapeutics, and Biotechnology; Malhotra, S.;
ACS Symposium Series; American Chemical Society: Washington, DC, 0.

composed of ions (usually a large organic cation and a small inorganic anion) (*1*). Their negligible vapour pressure (*2*) and usual non-flammability are the basis for their classification as "green" solvents. In addition, ILs can be, by design, chemically and thermally stable, recyclable, and with tunable physical and chemical properties. This, together with their outstanding solvation ability opened doors for numerous industrial applications as a replacement for conventional organic solvents. After remarkable advances in chemistry, thermodynamics, electrochemistry, material science and separation processes, ILs are offering unexpected opportunities on the interface with the life sciences, e.g. as solvents in enzymatic catalysis (*3*) and whole-cell biocatalysis - the latter is mainly exploiting water immiscible ILs (*4*). In order to move ILs beyond being an academic curiosity, their environmental, health, and safety impact must be fully determined. Significant efforts were made on obtaining ecotoxicological data (for review see (*5*)) and on designing ILs composed of naturally-derived materials for reduced toxicity and increased biodegradability (*6*). The most recent challenge in customizing ILs for specific applications, under the flag of "the third evolution of ionic liquids", was towards their use as active pharmaceutical ingredients (API) (*7*).

Filamentous fungi are significant members of the Mycota kingdom, widespread in nature, especially in soil. They play an important role in the carbon cycle on Earth, food spoilage, and as pathogens. On the other hand, due to the enormous diversity of species and their rich enzymatic systems, resulting in a broad range of secondary metabolites, they are widely used in biotechnological processes for production of chemicals, pharmaceuticals, food ingredients, and enzymes. Many secondary metabolites of filamentous fungi have found application as therapeuticals and bioactive compounds (antibiotics, cholesterol-lowering agents, antitumour agents and immunosuppresors (*8*, *9*)). Their ability to adapt to extreme environmental conditions and to degrade some of the most recalcitrant materials (as lignin and aromatic xenobiotics (*10*)) makes them a very attractive model for screening the toxicity of chemicals owning an unknown risk factor. In this work, for the first time, filamentous fungi were used as eukaryotic model organisms to access the possible impact of ILs whenever they are released into the environment.

Metabolic profiling using Mass spectroscopy (MS) became one of the most important methodologies in different areas of research, going from diagnostic tools, to functional genomics (*11*), to taxonomy of filamentous fungi (*12*), or even as part of a screening strategy for the search of new compounds with biological activity. Within this approach, metabolic footprinting is focused on qualitative scanning of extracellular metabolites secreted by the cells. Components of substrate that were transformed by the organism are also a part of the footprint (*11*).

The cell chemodiversity strongly depends on inherited phylogenetic information (genome), as well as, on environmental conditions. We propose a relationship between phylogenetic origin of fungal species, their specific response to the presence of ILs, and the alteration of the metabolic profile caused by it.

Downloaded by UNIV OF DELAWARE MORRIS LIB on June 22, 2012 | http://pubs.acs.org
Publication Date (Web): April 28, 2010 | doi: 10.1021/bk-2010-1038.ch016

Experimental

Chemicals

All ionic liquids tested were received from QUILL (Queen´s University Ionic Liquids Laboratory, Belfast, UK), except [*Ch*]Cl (Sigma, Germany), [C_2*mim*][SCN] (Fluka, Switzerland) and [C_2*mim*][*Et*SO_4] (Solvent Innovation, UK). D (+) glucose, K_2HPO_4, $ZnSO_4x7H_2O$, $CuSO_4x5H_2O$, $FeSO_4x7H_2O$, KCl and ethyl acetate were purchased from Sigma Aldrich (Germany). $MgSO_4x7H_2O$, $NaNO_3$, methylimidazole and pyridine were purchased from Fluka (Switzerland). NaCl was purchased from Panreac (Spain), acetonitrile from Merck (Germany) and CsCl from Fluka (Switzerland).

Fungal Isolates

The following fungal isolates were used: *Penicillium brevicompactum, P. olsonii, P. janczewskii, P. glandicola, P. corylophilum, P. glabrum, P. restrictum, P. adametzii, P. variabile, P. diversum*, all belonging to the Instituto de Biologia Experimental e Tecnológica (IBET) culture collection and had been previously isolated from cork samples purchased from several Portuguese cork industries (*13*, *14*).

Toxicity Tests

The toxic effect of ILs on filamentous fungi was determined by measuring the culture medium optical density (OD) at 600 nm.

Minimal growth medium containing: 1.0 $g \cdot L^{-1}$ glucose, 1.0 $g \cdot L^{-1}$ K_2HPO_4, 3 $g \cdot L^{-1}$ $NaNO_3$, 0.01 $g \cdot L^{-1}$ $ZnSO_4x7H_2O$, 0.005 $g \cdot L^{-1}$ $CuSO_4x5H_2O$, 0.5 $g \cdot L^{-1}$ $MgSO_4x7H_2O$, 0.01 $g \cdot L^{-1}$ $FeSO_4x7H_2O$, 0.5 $g \cdot L^{-1}$ KCl, dissolved in distilled H_2O and autoclaved was supplemented with ILs in order to obtain a final concentration of 50 mM (corresponding to 7-20 $g \cdot L^{-1}$, depending on the molecular weight of the IL).

Two milliliters of each liquid medium was inoculated with a fungal spore suspension, prepared as previously described (*15*), in order to obtain the final concentration of 10^5/mL of spores, and spread in 8 wells (250 µL each) of 96-wells plate. Cultures were incubated at 25 °C, in the dark.

The control samples (inoculated) and the blanks (non-inoculated) were produced and incubated under the same conditions: negative control (IL free medium), osmotic stress controls (medium supplemented with either 50 mM of NaCl, or 50 mM of CsCl: high-charge density and low polarizability, or low-charge density and high polarizability, respectively), organic function controls (medium with 50 mM of methylimidazole or pyridine), and blank samples (medium with addition of the selected substances).

Fungal growth (or lack thereof) was followed daily by measuring the absorbance (600 nm) of the medium. Increase of absorbance was taken as

Downloaded by UNIV OF DELAWARE MORRIS LIB on June 22, 2012 | http://pubs.acs.org
Publication Date (Web): April 28, 2010 | doi: 10.1021/bk-2010-1038.ch016

Downloaded by UNIV OF DELAWARE MORRIS LIB on June 22, 2012 | http://pubs.acs.org
Publication Date (Web): April 28, 2010 | doi: 10.1021/bk-2010-1038.ch016

indication of growth, while spore formation (annotated by eye observation) and/or reaching a constant value of absorbance indicated that the culture entered stationary growth phase. Culture supernatant was separated from mycelium by centrifugation (4 °C) and filtration (0.2 μm nylon membrane) and stored at -20 °C until further analysis.

Toxicity Data Analysis

The toxicity data were analysed using the R language, version 2.7.1 (R Development Core Team 2008). The hierarchical cluster analysis of the data was done using average linking based on the Manhattan distance between the toxicity profiles of the species. Given the binary nature of the data (growth or its inhibition), distance measure between species is equivalent to the number of different cases between two fungal species.

Metabolite Extraction

Fungal secondary metabolites (fSM, IL free) were extracted from fungal culture extracts. 1 mL of the extract was lyophilized (freeze-dried) in order to remove water and 1 mL of ethyl acetate was added to the residue. Extraction with ethyl acetate was repeated twice. The choice of organic solvent was due to its common use for extraction of fSM and due to its limited miscibility with the tested ILs (IL solubility tests in ethyl acetate were done). Extracts were evaporated in a vacuum concentrator and residue was dissolved in 400 μL of acetonitrile and ultrasonicated for 10 min. The same procedure was applied on blank samples previously prepared (see Toxicity tests).

ESI-MS Analysis

The electrospray mass spectra were recorded on a Bruker, Esquire 3000 plus ion trap mass spectrometer in the positive and negative polarity modes (Bruker Daltonics, Billerica, MA). The samples (fSM in acetonitrile) were injected at a rate of 100 μL h^{-1} into the electrospray ionization (ESI) probe. The capillary temperature was set to 250 °C. All spectra acquisitions were done using the Esquire Control Programme (Bruker Daltonics, Billerica, MA) and then converted to the *ascii* file format for computational interpretation.

Computational Interpretation of MS Data

Data were analyzed using the R language, version 2.7.1 (R Development Core Team 2008). After binning to unit m/z values, mass spectra were reprocessed and the m/z values were detected and aligned using the msProcess package. Peak intensities were normalized by the sum of intensities, and values below 0.001 were set to zero. Peaks of the sample spectra were compared with the spectra from solvents and blanks, and coinciding peaks were eliminated from the peak matrix. To eliminate IL cations or anions with z=1, only m/z values between 150 and 1100 were considered in the analysis. IL solubility in ethyl acetate (metabolite extraction) is very limited but its ion nature may lead to an intense m/z peak even at a neglectful concentration.

The resulting binary matrices, containing the peaks originating in the sample spectrum only, were analyzed by hierarchical cluster analysis using average linking based on the Manhattan distance, being equivalent to the number of differences in peak presence.

Downloaded by UNIV OF DELAWARE MORRIS LIB on June 22, 2012 | http://pubs.acs.org
Publication Date (Web): April 28, 2010 | doi: 10.1021/bk-2010-1038.ch016

Results and Discussion

Toxicological Assessment

In this work we present an examination of toxicity of ILs to filamentous fungi, belonging to *Penicillium* genus. The selection of 16 ILs as test compounds was made by combining seven different cations from five common cation classes (methylimidazolium, pyridinium, cholinium, pyrrolidinium, piperidinium) and six different anions (chloride, ethylsulfate, thyocianate, acetate, lactate, bis((trifluoromethyl)sulfonyl)imide) (chemical structures and abbreviations are presented in Figure 1). This approach enabled us to investigate mainly the toxic effect of the head group in the cation. Focusing on Cl^-, acetate and lactate anions, we assessed the additional toxic effect of the anion.

In order to prove that the ILs are not solely causing a toxic effect due to osmotic stress, the effect of NaCl and CsCl was tested. The latter imitates ILs low-charge density and high polarizability. The addition of CsCl to the growth medium have inhibited fungal growth (except for the case of P. *adametzii*), therefore causing a stronger growth inhibitory effect than all the tested ILs. This data were not used in the hierarchical clusters presented, but its inclusion does not alter the clusters profile (data not shown). Methylimidazole and pyridine, as commonly used building blocks in ionic liquid chemistry, were also tested to assess if these aromatic head groups have a deciding role in the antifungal activity of the ILs.

The hierarchical cluster analysis of the inhibitory effect of 20 selected compounds, using a molar concentration of 50 mM, to the growth of ten *Penicillium* species is illustrated in Figure 2.

The IL growth inhibitory effect was simplified to a binary matrix of fungal growth, inhibition or no inhibition.

It becomes evident that the chemical nature of the head group in cation influences the IL overall toxicity: This has been demonstrated in numerous studies (*16–20*).

The [C_2*mim*] cation, with various anions, has the highest toxicity ranking with an average of 3 toxic cases. Comparison of [C_2*mim*]Cl and [C_4*mim*]Cl showed the expected tendency of increased toxicity with the augment of the

Downloaded by UNIV OF DELAWARE MORRIS LIB on June 22, 2012 | http://pubs.acs.org
Publication Date (Web): April 28, 2010 | doi: 10.1021/bk-2010-1038.ch016

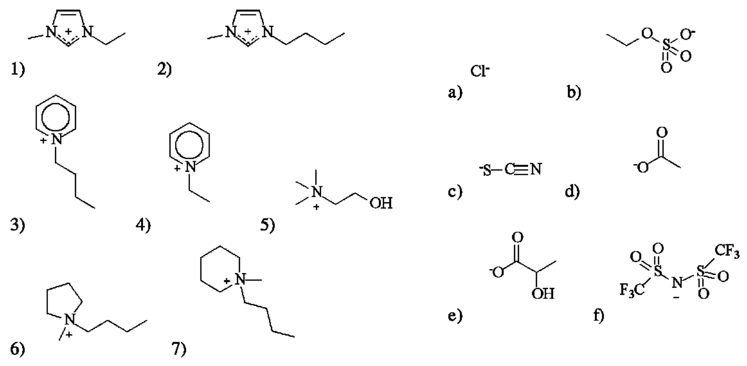

Figure 1. Chemical structures of all ILs used (cations and anions, numbers and letters, respectively). (1a) 1-ethyl-3-methylimidazolium chloride ([C$_2$mim]Cl); (1b) 1-ethyl-3-methylimidazolium ethylsulfate [C$_2$mim][EtSO$_4$]); (1c) 1-ethyl-3-methylimidazolium thyocianate ([C$_2$mim][SCN]); (1d) 1-ethyl-3-methylimidazolium acetate ([C$_2$mim][OAc]); (1e) 1-ethyl-3-methylimidazolium lactate ([C$_2$mim][Lac]); (2a) 1-butyl-3-methylimidazolium chloride ([C$_4$mim]Cl); (3a) N-butylpyridinium chloride ([C$_4$Py]Cl); (4d) N-ethylpyridinium acetate ([C$_2$Py][OAc]); (4e) N-ethylpyridinium lactate ([C$_2$Py][Lac]); (5a) cholinium chloride ([Ch]Cl); (5d) cholinium acetate ([Ch][OAc]); (5e) cholinium lactate ([Ch][Lac]); (5f) cholinium bis((trifluoromethyl)sulfonyl)imide ([Ch][NTf$_2$]); (6a) N-butyl-N-methylpyrrolidinium chloride ([C$_4$mpyrr]Cl); (6e) N-butyl-N-methylpyrrolidinium lactate ([C$_4$mpyrr][Lac]); (7d) N-butyl-N-methylpiperidinium acetate ([C$_4$mpip][OAc])

alkyl side chain (*19*). The [*Ch*] cation elicited the lowest toxic effect. Moreover, [*Ch*]Cl hasn´t inhibited growth in any of the fungal species. The behaviour of the ILs containing pyridinium, pyrrolidinium or piperidinium head group in the cation was between these two extremes mentioned above. The only exception was [C$_2$*Py*][*Lac*] showing no toxic effect.

The corresponding control compounds, methylimidazole and pyridine, proved to be highly toxic, inhibiting growth in 100% and 60% of the cases, respectively, thus impacting on fungi in a completely distinct manner as compared with imidazolium and pyridinium based ILs.

Within the two groups of ILs containing [C$_2$*mim*] and [*Ch*] combined with Cl, O*Ac* and *Lac*, the acetate anion was the most toxic. In the remaining ILs no correlation could be observed between the structure of selected anions and toxicity. Therefore, it seems that both the cation and the anion account for the overall IL antifungal activity. This is in agreement with previous observations, where the toxic effect of some anions was compared to the augmented toxicity in an IL due to an increased length of the alkyl side chain (*18*).

To the best of our knowledge, this is the first time that filamentous fungi were used in toxicological study on ILs. The most significant observation is the very high tolerance of *Penicillium* species towards the ILs. Only in 20% of ILs/species cases, complete inhibition of growth was noted. The concentration of ILs that was tested in this report (50 mM) is much higher (several orders of magnitude) than in any other testing system reported so far (*16*, *20*). In addition, we have observed that fungi can tolerate in some cases even higher IL concentrations, for e.g. *P. olsonii* growth was detected in the presence of 375 mM of [C_2*mim*]Cl (data not shown).

The hierarchical cluster analysis of growth behavioral profiles (Figure 2) revealed three groups: two groups of fungal species highly clustered together, showing the highest IL susceptibility, and the third one, sub-divided into two sub-clusters, of intermediate susceptibility. The sub-clusters comprise three distinct fungal species each, being two more closely related. *P. adametzii* and *P. glandicola* are therefore, relatively dissociated from their sub-clusters. Comparison was made with the clusters in phylogenetic study on *Penicillium* species of Wang *et al.* (2007), based on calmodulin gene partial sequences (about 600 nucleotides) (*21*). The study distinguishes 11 clusters and covers all the species featured in our work, except *P. diversum* and *P. olsonii*. High degree of correlation between the phylogenetic background of the species and their response to an IL-environment could be observed. The distinct clusters obtained, set by order of IL highest susceptibility - (*P. diversum, P. variabile*) > (*P. restrictum, P. corylophilum*) > *{*(*P. janczewskii*) > (*P. brevicompactum, P. glandicola, P. olsonii*) > (*P. glabrum*)} - correlate well, with the exception of *P. adametzii*, with groups XI, VIII, I and II, respectively, by Wang.

This indication of high correlation between the genetic proximity of the species and their susceptibility to different environmental conditions can be used in the rationalization of toxicological studies and in the prediction of behaviour of different species. Testing a vast number of ILs and organisms is rather time consuming and costly. The aforementioned cluster strategy, along with the concept of QSAR (quantitative structure-activity relationship), which refers to estimation of the hazard potential of ILs based on structure, simplifies the risk evaluation of these liquid salts.

Downloaded by UNIV OF DELAWARE MORRIS LIB on June 22, 2012 | http://pubs.acs.org
Publication Date (Web): April 28, 2010 | doi: 10.1021/bk-2010-1038.ch016

Metabolic Footprinting

In order to assess the ability of ILs to alter metabolic footprinting of fungi, fungal culture extracts (fSM extracts, IL free) were analyzed by ESI-MS. The spectra interpretation was solely performed from a qualitative perspective, i.e. binary matrix of peak presence or absence.

Selection of samples (combinations of fungal species and ILs) was made based on the analysis of toxicological data, presented above. The following species: *P. variabile, P. adametzii, P. janczewskii, P. brevicompactum, P. glandicola, P. restrictum* and *P. corylophilum* were used, taking one, or more, representatives from each cluster. Selected ILs: [C_2*mim*]Cl, [C_2*mim*][*Lac*], [C_4*Py*]Cl, [C_2*Py*][*Lac*], [*Ch*]Cl and [*Ch*][*Lac*] comprised all cation groups which have shown distinct effects, imidazolium and choline, as the most and the least toxic, respectively, and pyridinium based ILs, with intermediate toxic effect. Negative controls and NaCl controls were included.

Downloaded by UNIV OF DELAWARE MORRIS LIB on June 22, 2012 | http://pubs.acs.org
Publication Date (Web): April 28, 2010 | doi: 10.1021/bk-2010-1038.ch016

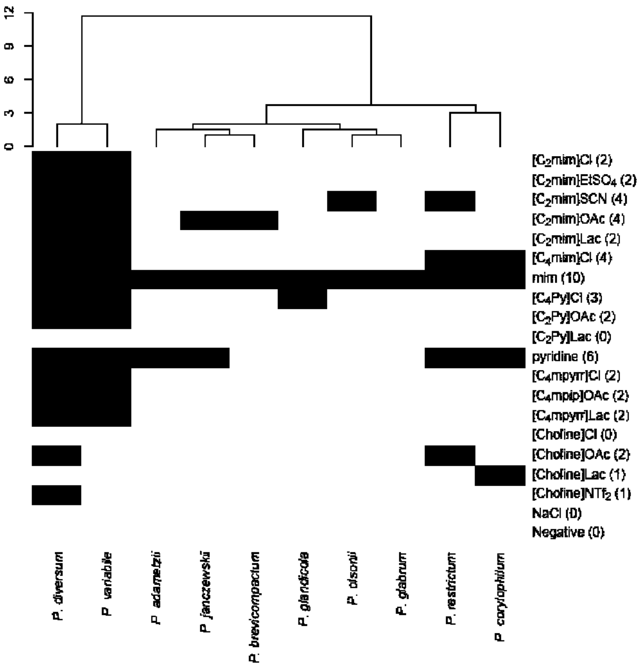

Figure 2. Cluster analysis of Penicillium species growth behaviour in an IL containing medium. Data were analysed by hierarchical cluster analysis using average linking based on the Manhattan distance between the toxicity profiles (equivalent to the number of different cases between two fungal species). Black fields show cases of IL growth inhibition, names on the right indicate the tested ILs (align by common cation group) and the number in brackets corresponds to the IL toxicity ranking (from 0 to 10).

The cluster analysis of metabolic footprint for each individual species, after growth under IL specific influence, positive and negative mode separately, have not shown any obvious pattern identically observable in all cases (data not shown). However, the fSM induced by [C_2*mim*]Cl and [C_2*mim*][*Lac*] were clustered together for all fungal species, except for *P. glabrum* and *P. brevicompactum*, and more distant from the fSM profile induced by the other ILs.

The integrated assessment of the joint peak lists, uniting all individual peak matrices of positive and negative mode, is presented in Figure 3. Two clusters could be observed; one formed by the fSM induced by the imidazolium ILs, and the second one showing the similarity between controls. The fSM induced by pyridinium and choline based ILs remain unassociated to either of these two clusters and to themselves.

Furthermore, the correlation of the number of detectable mass species in extracts and toxicity of corresponding ILs is apparent. [C_2*mim*]Cl and [C_2*mim*][*Lac*] are causing the highest and the most diverse number of mass species, significantly different from the controls. The remaining ILs have also caused obvious alterations in the metabolic footprint of fungi. In fact, [C_2*Py*][*Lac*]

Downloaded by UNIV OF DELAWARE MORRIS LIB on June 22, 2012 | http://pubs.acs.org
Publication Date (Web): April 28, 2010 | doi: 10.1021/bk-2010-1038.ch016

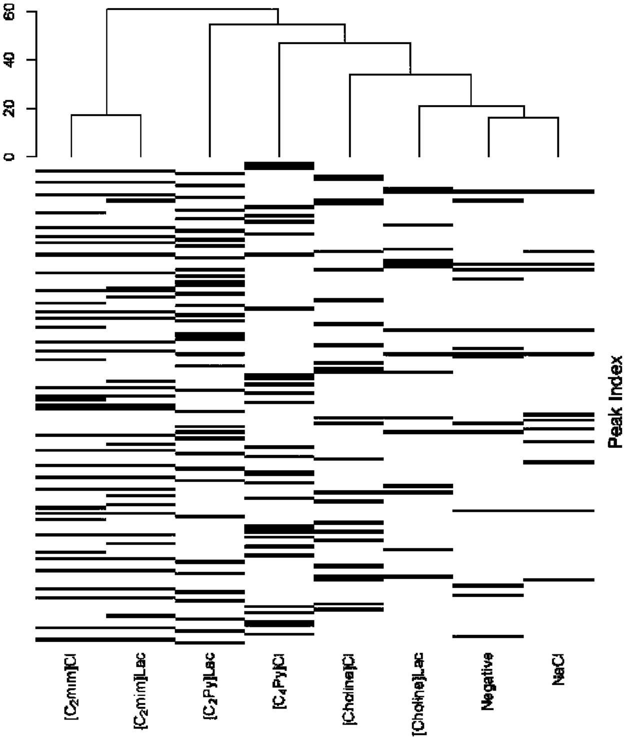

Figure 3. Cluster analysis of the joint peak lists, uniting all individual peak matrices of positive and negative mode, detected by ESI-MS after fungal growth in an IL containing medium. Data were analysed by hierarchical cluster analysis using average linking based on the Manhattan distance, being equivalent to the number of differences in peak presence. Black fields show distinct m/z values.

and [*Ch*]Cl have not inhibited, in any case, fungal growth, but both have provoked notable metabolic alterations.

Our data significantly states that IL induced effects onto the fungal metabolism cannot be solely explained by the IL toxicity. Moreover, IL induced fSM are not correlated with the ones induced by a common salt, such as NaCl. Likewise, even CsCl, in the specific case of *P. adametzii*, clustered closer to the controls than to the ILs (data not shown). This observation was also supported by preliminary data on the fungal secretome (bidimensional electrophoresis analysis) induced by the different ILs (unpublished data). Results suggested that the ILs, for e.g. [*Ch*]Cl and [C_4*mpyrr*]Cl, have induced the expression of a distinct set of fungal extracellular proteins, that could be grouped into IL responsive, IL specific or non-specific, and salt responsive proteins.

In order to provide a more complete picture of the specific events in the metabolic network (both, species and IL dependent), quantitative analysis should be attempted in the future.

The behaviour of fungi and any other organism is highly linked to different omes′ (genome, transcriptome, proteome and metabolome) and influenced by environmental conditions. Recently, transcriptional profiling and proteomic analysis are becoming routine techniques, and joined with metabolite analysis, could build a platform applicable in many areas. Going further from ecotoxicological studies, describing the effect of toxics on living cells, it could be useful in discovery of novel natural compounds and in the development of efficient and environmentally friendly bioprocesses.

The test system described in this work can be highly promising, especially considering that filamentous fungi have the ability of producing biologically active secondary metabolites. Further studies are necessary to prove if ILs have the ability to induce a desired metabolic alteration. In future, this can stand for a great breakthrough in whole-cell biocatalysis, creating a new concept: an ionic liquid controlled bio-tool for designing particular end products.

Downloaded by UNIV OF DELAWARE MORRIS LIB on June 22, 2012 | http://pubs.acs.org
Publication Date (Web): April 28, 2010 | doi: 10.1021/bk-2010-1038.ch016

Acknowledgments

M. Petkovic is grateful to FC&T for the fellowship SFRH/BD/31451/2006. The work was partially supported by a grant from Iceland, Liechtenstein and Norway through the EEA financial mechanism (Project PT015) and by FC&T (Project REDE/1504/REM/2005). The authors wish to acknowledge Dr. Ana V. Coelho and M^{a} Conceição Almeida for providing data from the Mass Spectrometry Laboratory at ITQB-UNL, Oeiras, Portugal and Dr. Jorg Becker for his valuable contribution in data analysis and discussion.

References

1. Deetlefs, M.; Seddon, K. R.; Shara, M. *Phys. Chem. Chem. Phys.* **2005**, *8* (5), 642–649.
2. Earle, M. J.; Esperanca, J.; Gilea, M. A.; Lopes, J. N. C.; Rebelo, L. P. N.; Magee, J. W. *Nature* **2006**, *439* (7078), 831–834.
3. van Rantwijk, F.; Sheldon, R. A. *Chem. Rev.* **2007**, *107* (6), 2757–2785.
4. Pfruender, H.; Jones, R.; Weuster-Botz, D. *J. Biotechnol.* **2006**, *124* (1), 182–190.
5. Ranke, J.; Stolte, S.; Stormann, R.; Arning, J.; Jastorff, B. *Chem. Rev.* **2007**, *107* (6), 2183–2206.
6. Fukaya, Y.; Iizuka, Y.; Sekikawa, K.; Ohno, H. *Green Chem.* **2007**, *9*, 1155–1157.
7. Hough, W. L.; Smiglak, M.; Rodriguez, H.; Swatloski, R. P.; Spear, S. K.; Daly, D. T. *New J. Chem.* **2007**, *31* (8), 1429–1436.
8. Newman, D. J.; Cragg, G. M.; Snader, K. M. *J. Nat. Prod.* **2003**, *66* (7), 1022–1037.
9. Newman, D. J.; Cragg, G. M. *J. Nat. Prod.* **2007**, *70* (3), 461–477.
10. Rabinovich, M. L.; Bolobova, A. V.; Vasil’chenko, L. G. *Appl. Biochem. Microbiol.* **2004**, *40* (1), 1–17.

11. Villas-Boas, S. G.; Mas, S.; Akesson, M.; Smedsgaard, J.; Nielsen, J. *Mass Spectrom. Rev.* **2005**, *24* (5), 613–646.
12. Frisvad, J. C.; Smedsgaard, J.; Larsen, T. O.; Samson, R. A. *Stud. Mycol.* **2004** (49), 201–241.
13. Danesh, P.; Velez Caldas, F.; Figueiredo Marques, J.; San Romao, M. *J. Appl. Microbiol.* **1997**, *82* (6), 689–94.
14. Oliveira, A.; Peres, C.; Correia Pires, J.; Silva Pereira, C.; Vitorino, S.; Figueiredo Marques, J. *Microbiol. Res.* **2003**, *158* (2), 117–24.
15. Silva Pereira, C.; Pires, A.; Valle, M.; Vilas-Boas, L.; Figueiredo Marques, J.; San Romão, M. *J. Ind. Microbiol. Biotechnol.* **2000** (24), 256–261.
16. Pernak, J.; Sobaszkiewicz, K.; Mirska, I. *Green Chem.* **2003**, *5* (1), 52–56.
17. Cieniecka-Roslonkiewicz, A.; Pernak, J.; Kubis-Feder, J.; Ramani, A.; Robertson, A. J.; Seddon, K. R. *Green Chem.* **2005**, *7* (12), 855–862.
18. Stolte, S.; Arning, J.; Bottin-Weber, U.; Matzke, M.; Stock, F.; Thiele, K. *Green Chem.* **2006**, *8* (7), 621–629.
19. Stolte, S.; Arning, J.; Bottin-Weber, U.; Muller, A.; Pitner, W. R.; Welz-Biermann, U. *Green Chem.* **2007**, *9* (7), 760–767.
20. Garcia-Lorenzo, A.; Tojo, E.; Tojo, J.; Teijeira, M.; Rodriguez-Berrocal, F. J.; Gonzalez, M. P. *Green Chem.* **2008**, *10* (5), 508–516.
21. Wang, L.; Zhuang, W. Y. *Biosystems* **2007**, *88* (1−2), 113–126.

Downloaded by UNIV OF DELAWARE MORRIS LIB on June 22, 2012 | http://pubs.acs.org
Publication Date (Web): April 28, 2010 | doi: 10.1021/bk-2010-1038.ch016

Subject Index

A

- Acesulfame anion, 137, 138*t*
- Acetate anion, toxicity effect, 201, 202
- Acetophenone asymmetric reduction, using IL coated-*Geotrichum candidum* dried cells, 162, 163*t*
- Acid, synthesis from enone with
  - (5*R*,6*S*)-isomer epoxy aldehyde
    - aldol reaction, 57, 57*s*
  - (5*S*,6*R*)-epoxide condensation, 57, 57*s*
- 1,6-Ahydro-β-D-glucofuranose, 148
  - structure of, 149*f*
  - yield and selectivity in ionic liquids, 149, 150*t*
- Alanine composition, in (S)-[CHTA]$^+$ [Tf2N]$^-$ IL *versus* enantiomeric compositions, 41*f*, 46
- Aldol reaction, between (5*R*,6*S*)-isomer epoxy aldehyde and enone for acid synthesis, 57, 57*s*
- Alkaloids, as later term for first nitrogen-containing bases, 1
- 1-Alkanols, *rac*-ketoprofen esterification with, catalyzed with CALB, scheme of, 27*f*
- 1-Alky-2,3-dimethyllimidazolium salt ionic liquid, structure of, 64*f*
- Alkyl chain length
  - cation polarity as function of, 184
  - and concentration ratio, influence on CALB-catalyzed esterification of *rac*-ketoprofen, 31*f*
- 1-Alky-3-methyllimidazolium salt ionic liquid, structure of, 64*f*
- Amino acid
  - of aqueous dispersed [MIm][Cl]-IO-NPs, photographs of, 109*f*
  - chemistry, with ionic liquids, 13
  - derivatives, enzymatic and chemical transformations of, 14
  - for lipase PS activation with BDMIM-PEG, 156, 157, 158*f*
- 6-Aminopenicillanic acid
  - comparison of yields in MILWS and BAWS, 87*f*, 88
  - IEP in MILWS, 83*f*, 85
- Ammonium-based ionic liquids
  - antitumor activity, 101
- Ammonium salts
  - as components for DES's with H bond donors, 172*s*, 173, 176
- 1,6-Anhydro-β-D-glucopyranose, 148
  - structure of, 149*f*
  - yield and selectivity in ionic liquids, 149, 150, 150*t*, 151*f*
- Anhydrosugars
  - from carbohydrates as glucose, cellulose, and cellobiose, 150
    - conversions of, 150, 151*f*
    - reaction scheme of, 147*f*
  - effect of chloride ion on formation of, 151, 151*t*
  - from glucose in TMPA-TFSI, 148
    - 1,6-anhydro-β-D-glucofuranose, 148
    - 1,6-anhydro-β-D-glucopyranose, 148
    - cation effect, 149
    - temperature effect in, 148
  - as hyperbranched polysaccharides, applications of, 152
  - from polysaccharides in ionic liquids by microwave irradiation, 145
- Anions
  - acesulfame, 137, 138*t*
  - bis(trifluoromethanesulfonyl)imide, 137, 138*t*
  - dicyanoamide, 137, 138*t*
  - exchange

Downloaded by 89.163.35.42 on June 22, 2012 | http://pubs.acs.org
Publication Date (Web): April 28, 2010 | doi: 10.1021/bk-2010-1038.ix002

Downloaded by 89.163.35.42 on June 22, 2012 | http://pubs.acs.org
Publication Date (Web): April 28, 2010 | doi: 10.1021/bk-2010-1038.ix002

        on [MIm][Cl]-Au-NPs change of hydrophobicity, 108*s*
        on [MIm][Cl]-IO-NPs, equilibrium of, 109*s*
    hexafluorophosphate, 137, 138*t*
    N-cyanobenzenesulfonamide, 137, 138*t*
    N-cyanomethanesulfonamide, 137, 138*t*
    polarity as function of negative charge size/delocalization, 184
    saccharin, 137, 138*t*
    structures of, 183, 184*f*
    tetrafluoroborate, 137, 138*t*
    toxicity effect, 201, 202
        acetate, 201, 202
        chloride, 201, 202
        lactate, 201, 202
Anti S_N2' allylation
    of picolinoates with RMgBr/CuBr, of, 57, 57*s*
    selective, with heteroaromatic coppers, 60*s*, 61
Atenolol
    composition in (S)-$[CHTA]^+$ $[Tf2N]^-$ IL *versus* enantiomeric compositions, 40*f*, 45
    solutions and pure S-$[CHTA]^+$ $[Tf2N]^-$, NIR spectra of, 38*f*, 44
    structures, 36*s*, 46

B

Bases, pharmaceutical salts as first nitrogen-containing, 1
BDMIM-PEG. *See* [1-Butyl-2,3-dimethylimidazolium][cetyl-PEG10-sulfate]
Biomedical application, of biopolymer-based materials, from ionic liquids, 115
Biomolecules. *See* Deoxyribonucleic acid
Biopolymer-based materials
    for biomedical application, 115
    preparation using ionic liquids, 124
    fibers, 124, 125, 126
    film, coating and membrane, 124
    with heparin/cellulose, schematic representation for, 123*f*
    by spinning, 130*t*
Biopolymers
    blood compatibility, 125
        effect of heparin on, 125
    composites, blood compatible, 125
    dissolution of, using ionic liquids, 119
    solubility in ionic liquids, 122*t*
Biotechnological processes, from fungal activity with ionic liquids, 197
Bis(trifluoromethanesulfonyl)imide anion, 137, 138*t*
Blood compatibility, of biopolymers, 125
    effect of heparin on, 125
Breast cancer, panel of human tumor cell lines, 93, 98*t*
Burkholderia cepacia lipase
    by chiral pyrrolidine-substituted imidazolium salt, 159
    by imidazolium salt coating, 159, 160*f*
    using amino acid with BDMIM-PEG, 156, 157, 158*f*
2-Butanol, used for ethyl valerate iCALB-catalyzed transesterification in DES's, 173, 174, 174*s*, 175*t*, 176
Butyl acetate/water system
    6-APA in, comparison of yield in MILWS, 87*f*, 88
    enzymatic activity and stability in, 85
        influence of pH, 84*f*, 85
[1-Butyl-2,3-dimethylimidazolium][cetyl-PEG10-sulfate]
    chiral pyrrolidine-substituted, design of, 158*f*, 159
    for lipase PS activation with amino acid, 156, 157, 158*f*
Butyl-methylimidazolium bis(trifluoromethanesulfonyl)imide
    cation effect on glucose, 149

Downloaded by 89.163.35.42 on June 22, 2012 | http://pubs.acs.org
Publication Date (Web): April 28, 2010 | doi: 10.1021/bk-2010-1038.ix002

  - yield and selectivity in ionic liquids, 149, 150*t*
- 1-Butyl-3-methylimidazolium hexafluorophosphate, 66
  - with [C$_4$mim]BF$_4$/water system, phase diagram of, 67, 68*f*
  - micrograph pictures, 68, 69*f*
  - ratio with [C$_4$mim]BF$_4$ *versus* ln K, 72, 73*f*
- 1-Butyl-3-methylimidazolium tetrafluoroborate, 66
  - with 1-butyl-3-methylimidazolium hexafluorophosphate
    - mole ratio effect in penicillin/PAA partition ratios in MILWS, 81, 82, 82*f*
  - with [C$_4$mim]PF$_6$/water system, phase diagram of, 67, 68*f*
  - concentration difference in relation to ln K, 70, 70*f*
  - micrograph pictures, 68, 69*f*
  - ratio with [C$_4$mim]PF$_6$ *versus* ln K, 72, 73*f*

C

- CaCo-2 colon carcinoma cell lines
  - relative viability after treatment with
    - [Aliquat] [NTf$_2$], [Aliquat] [DCA], [Aliquat] [Saccharin] and [Aliquat] [Acesulfame], 141, 141*f*
    - [C$_{10}$MIM] [BF$_4$] and [C$_{10}$CO$_2$HMIM] [BF$_4$], 139, 139*f*
    - [DMG] [NTf$_2$], [DMG] [DCA], [DMG] [PF$_6$] and [P66614] [NTf$_2$], 142, 142*f*
  - toxicological assays performed on, 136
- *Candida antarctica* lipase B
  - catalyzed reactions, in deep eutectic solvents, 169, 173, 174*s*
    - perhydrolysis of octanoic acid with cyclohexene oxidation, 174*s*, 176, 177, 177*t*
    - ring-opening polymerization of ε-caprolactone, 174*s*, 176
    - side reactions of, 176, 178*s*
    - stability of, 173
    - transesterification of ethyl valerate with 2-butanol, 174*s*, 175*t*, 176
  - on esterification of *rac*-ketoprofen with 1-alkanols, 29
    - scheme of, 27*f*
- Cation
  - choline, 137, 138*t*, 143
  - dimethylguanidinium, 137, 138*t*
  - effect on glucose in ionic liquids, 149
    - Bmim-TFSI(T), 149
    - DEME-TFSI, 149
    - TMPA-TFSI, 149
  - headgroups, toxicity effect, 201, 202
    - [Ch], 201, 202
    - [C$_2$mim], 201, 202
  - methylimidazolium, 137, 138*t*
  - polarity as function of alkyl chain length, 184
  - structures of, 183, 184*f*
  - tri-*n*-hexyl-tetra-*n*-decylphosphonium, 137, 138*t*, 142
  - tri-*n*-octyl-methylammonium, 137, 138*t*, 141
- Cell death, and [MIm][Cl]-IO-NPs aggregation, observation of, 112*t*
- Cell viability, MTT assay determination of, 137
- Cellobiose, anhydrosugars from carbohydrates, 150
- Cellulose
  - anhydrosugars from carbohydrates, 150
  - fibers, used as biopolymer-based materials, 126
    - FESEM images of, 128, 128*f*
  - solubility in ionic liquids, 120*t*
- Central nervous system cancer, panel of human tumor cell lines, 93, 98*t*

Cesium chloride, addition to IL
  growth inhibitory effect to *Penicillium* species, 201
Chemistry, with ionic liquids of
  amino acids, 13
  peptides, 13
  pharmaceutical compounds, 13
Chiral
  analysis, 36
  imidazolium salts, synthesis of, 57, 58*s*
    from imidazoles conversion, 61, 61*s*
  ionic liquids, 39, 41, 43, 44, 47, 51
  oxaziridine
    enantioselective oxidation in CCl_4 and [bmim][PF_6], 17, 18*t*, 20*f*
    versus hydroperoxyamine, 21*f*, 22
  sulfoxides, in modafinil, 17, 20*f*
Chirality transfer
  definition of, 58
  results with Ph-M/CuBr, 58, 60*t*
Chitin fibers
  used as biopolymer-based materials, 124
    solubility in ionic liquids, 122*t*
  See also Chitosan
Chitosan fibers
  used as biopolymer-based materials, 126
    solubility in ionic liquids, 122*t*
  See also Chitin fibers
Chloride anion, toxicity effect, 201, 202
Chloride ion, effect on anhydrosugars formation, 151, 151*t*
4-Chlorophenylalanine ethyl ester, subtilisin-catalyzed resolution of, in aqueous solution of [EtPy][TFA], 188, 188*f*
Choline cation, 137, 138*t*, 143
Cholinium cation, headgroups, toxicity effect, 201, 202
Colon carcinoma
  toxicological assays performed on, 136
    CaCo-2 cell lines, 136
    HT-29 cell lines, 136
Coupling agents, for peptide synthesis in ionic liquids, 15, 16*f*
Cyclohexene, oxidation of, 174*s*, 176, 177*t*
Cyclopeptides, synthesis and deprotection of
  octapeptide Z-(Gly-(R)-MPG)$_4$-OMe, 15, 19*f*
  tetrapeptide Z-(Gly-(R)-MPG)$_2$-OMe, 15, 17*f*, 18*f*
Cytostatic, active compound parameter, 99, 100, 101*t*
Cytotoxic, active compound parameter, 99, 100, 101*t*

D

Deep eutectic solvents
  components, from mixtures of ammonium salts and H bond donor, 172*s*, 173
  iCALB-catalyzed reactions in, 169, 173, 174*s*
    side reactions of, 176, 178*s*
  influenced by viscosity, 177
Deoxyribonucleic acid, interaction with [MIm][Cl]-IO-NPs, 112
DES's. *See* Deep eutectic solvents
Dicyanoamide anion, 137, 138*t*
Dimethylguanidinium cation, 137, 138*t*
3-(4,5-Dimethylthiazolyl-2)-2,5-diphenyltetrazolium bromide, determination of cell viability, 137
Dispersibility, of [MIm][Cl]-IO-NPs, 109
DNA. *See* Deoxyribonucleic acid
Drugs
  acetylcholinesterase inhibitor, 5*t*
  for antiarrhythmic agent, 5*t*
  for anticholinergic, 5*t*
  for anti-dementia, 5*t*
  for antifbrillatory, 5*t*
  for antimuscarinic, 5*t*
  for antiseptic, 5*t*

Downloaded by 89.163.35.42 on June 22, 2012 | http://pubs.acs.org
Publication Date (Web): April 28, 2010 | doi: 10.1021/bk-2010-1038.ix002

Downloaded by 89.163.35.42 on June 22, 2012 | http://pubs.acs.org
Publication Date (Web): April 28, 2010 | doi: 10.1021/bk-2010-1038.ix002

- for antispasmodic, 5*t*
- for CNS, 5*t*
- components, 3, 5*t*
  - anionic, 7*t*
  - cationic, 7*t*
- development, 2
- for disinfectant, 5*t*
- for functional gastrointestinal disorders, 5*t*
- herbicides, 5*t*
- molecules, 2
- properties, 2
- salt formation for, 2

Dry-jet wet spinning, using ionic liquids, 126

E

Electrospinning, using ionic liquids, 123*f*, 127
- polymer fibers prepared from, 130*t*

Electrospray ionization mass spectroscopy, for fungi metabolic footprinting, 203
- cluster analysis of joint peak lists, 204, 205*f*

Enantiomeric compositions
- *versus* actual composition in (S)-$[CHTA]^+$ $[Tf2N]^-$ IL of
  - atenolol, 40*f*, 41*f*, 45, 46
  - ibuprofen; phenylalanine; alanine, 41*f*, 46
  - naproxen and warfarin, 48, 50*f*
  - propranolol, 44*f*, 47
- determination of pharmaceutical products by IL based method, 35

Enantioselective oxidation, in ionic liquids, 17
- with chiral oxaziridine, 17, 18*t*, 20*f*
- goals of, 17
- of thioanisole, 17, 18*t*, 20*t*, 21

Enantioselectivity, of iCALB-catalyzed transesterification of ethyl valerate with 2-butanol in DES's, 174, 175*t*, 177

Enone
- preparation of, 56, 56*s*, 57
- with (5*R*,6*S*)-isomer epoxy aldehyde aldol reaction, 57, 57*s*
- with (5*S*,6*R*)-epoxide condensation, 57, 57*s*

Enzymatic catalysis
- dynamics of, 88
- in green non-aqueous reaction media, 181, 183
  - advantages of, 182
  - hydrolytic enzymes for, 182
- in IL/$scCO_2$ biphasic systems, 192, 193
  - continuous green enzyme reactor, experimental set-up of, 192, 193*f*
- in ionic liquids, 181, 182, 187
  - of aqueous solutions, 188
  - monophasic, operational strategy for, 190, 190*f*
  - of nearly anhydrous conditions, 188, 190
- role of water in, with different enzyme environments, schema of, 182, 184*f*
- in supercritical CO_2, 181, 182, 183, 185

Enzymatic hydrolysis, of penicillin
- by integrated system/process containing IL, 77

Enzymatic membrane reactor
- for ketoprofen in ionic liquids and supercritical carbon dioxide, 25, 32
  - experimental set-up of, 30*f*

Enzymes, 182, 188*t*
- agents for
  - IL type, design of second generation of, 157*f*
  - novel design of, 159
- chiral pyrrolidine-substituted IL mediated, 155
- esterases, 182, 185
- of *Geotrichum candidum* by chiral pyrrolidine-substituted imidazolium salt coating, 162
- glycosidases, 182, 188
- half-life of

        as function of ILs concentration and inorganic salt, 86*f*, 87
    of lipase PS, using amino acid with BDMIM-PEG, 156, 157, 158*f*
    lipases, 182, 185, 188, 188*t*
    proteases, 182, 188, 188*t*
    See also Enzymatic catalysis
5,6-Epoxyisoprostane A_2 phosphorylcholine. *See* Epoxyisoprostane phosphorylcholine
Epoxyisoprostane phosphorylcholine, synthesis of, 55, 56*s*
ε-Caprolactone, iCALB-catalyzed polymerization of, 174*s*, 176
Esterases enzymes, 182, 185
Esterification, of *rac*-ketoprofen with 1-alkanols, catalyzed with CALB, 29
    alkyl chain length and concentration ratio influence on, 31*f*
    different ILs influence on, 31*f*
    scheme of, 27*f*
    time-course of, 30*f*, 33*f*
Ethyl valerate, iCALB-catalyzed transesterification of, with 2-butanol in DES's, 174*s*, 175*t*, 176
    enantioselectivity of, 174, 175*t*, 177
    initial activity of, 173, 175*t*
1-Ethyl-3-methylimidazolium cation, headgroups, toxicity effect, 201, 202

F

Fibers, 126
    biopolymer-based
        alginate, 126
        cellulose, 126
        chitin, 124
        chitosan, 126
        gelatin, 126
Fungal activity, with ionic liquids, towards new biotechnological processes, 197
    See also Penicillium species

G

Geotrichum candidum
    dehydrogenase activation by chiral pyrrolidine-substituted imidazolium salt coating, 162
    dried cells, IL coated used for asymmetric reduction of acetophenone, 162, 163*t*
Glucose
    anhydrosugars from, in ionic liquids, 148
        temperature effect in TMPA-TFSI, 148
Glycine, 156, 158*f*
Glycosidases enzymes, 182, 188
Gold nanoparticles, ionic liquid-modified
    biomedical application of, 103
    change of hydrophobicity via anion exchange, 108*s*
    characterization of, 107
    preparation of, 103, 105*s*
    stimuli response of, 107
Green Chemistry, 181
    goals of, 184
Grignard reagents, RMgBr with CuBr for anti S_N2' allylation of picolinoates, 57, 57*s*

H

Half-life of enzyme, as function of ILs concentration and inorganic salt, 86*f*, 87
HeLa cells, culture wells, added with [MIm][Cl]-IO-NPs dispersion, microscopic images of, 111*f*
Heparin
    with cellulose as mixture
        with activited charcoal, FESEM images of, 123*f*, 125

Downloaded by 89.163.35.42 on June 22, 2012 | http://pubs.acs.org
Publication Date (Web): April 28, 2010 | doi: 10.1021/bk-2010-1038.ix002

Downloaded by 89.163.35.42 on June 22, 2012 | http://pubs.acs.org
Publication Date (Web): April 28, 2010 | doi: 10.1021/bk-2010-1038.ix002

    for preparation of composite materials, schematic representation, 123*f*, 125
  effect on blood compatibility of biopolymers, 125
Hexafluorophosphate anion, 137, 138*t*
HT-29 colon carcinoma cell lines
  relative viability after treatment with
    [Aliquat] [NTf$_2$], 141, 141*f*
    [C$_{10}$MIM] [BF$_4$] and [C$_{10}$CO$_2$HMIM] [BF$_4$], 139, 139*f*
    [DMG] [NTf2], [DMG] [DCA] and [P66614] [NTf2], 142, 142*f*
  toxicological assays performed on, 136
Human tumor cell lines
  antitumor activity on ionic liquids, 91, 94*t*, 95
    ammonium, 101
    phosphonium, 101
  by different panels
    breast cancer, 93, 98*t*
    central nervous, 93, 98*t*
    central nervous system cancer, 93, 98*t*
    leukemia, 93, 98*t*
    lung cancer, 93, 98*t*
    melanoma, 93, 98*t*
    ovarian cancer, 93, 98*t*
    prostate cancer, 93, 98*t*
    renal cancer, 93, 98*t*
  drug response curve of, 98*f*
  one dose mean graph of, 95, 97*f*
Hydrogen bond donors, as components for DES's with ammonium salts, 172*s*, 173, 176
Hydrolytic enzymes. *See* Enzymes
Hydroperoxyamine, *versus* chiral oxaziridine, 21*f*, 22

I

Ibuprofen
  composition in (S)-[CHTA]$^+$ [Tf2N]$^-$ IL *versus* enantiomeric compositions, 41*f*, 46
  structures, 36*s*, 46
iCALB*See Candida antarctica* lipase B
ILATPS. *See* Ionic liquids, aqueous two-phase system
Imidazoles, conversion to imidazolium salts, 61, 61*s*
Imidazolium, based ionic liquids, 95
In vitro assay, of [MIm][Cl]-IO-NPs, 110, 111*f*, 112*t*
In vivo assay, of [MIm][Cl]-IO-NPs, 110
Ion exchange, synthesis of R,S-[CHTA]$^+$ [Tf2N]$^-$, 41
Ionic liquids
  ability to alter fungi metabolic footprinting, 203
  aggregates, characterization, 68
    micrograph pictures, 68, 69*f*
  anhydrosugars from glucose in, 148
    temperature effect in TMPA-TFSI, 148
  antitumor activity on human tumor cell lines, 91, 94*t*, 95
  applications, 2
    asymmetric synthesis, 2
    biocatalytic transformations, 2
    biomaterials, 2
    chromatography, 2
    electrochemistry, 2
    material science, 2
    organic synthesis, 2
    polymers, 2
    transition metal catalysis, 2
  aqueous solution phase diagram, 67
    [C$_4$mim]BF$_4$/[C$_4$mim]PF$_6$/water system, 67, 68*f*
  aqueous two-phase system, 66
    aggregates, micrograph pictures, 68, 69*f*
    based from hydrophilic [C$_4$mim]BF$_4$, 66
    penicillin in, extractive behaviors, 70
    phase diagram in, 67, 68*f*

Downloaded by 89.163.35.42 on June 22, 2012 | http://pubs.acs.org
Publication Date (Web): April 28, 2010 | doi: 10.1021/bk-2010-1038.ix002

    uniform formulation of ln K-Δ[ionic liquids], 74, 74*f*
  based method for pharmaceutical products enantiomeric composition determination, 35
  biopolymer-based materials from, for biomedical application, 115
  biopolymers solubility in, 122*t*
  Bmim-TFSI(T), 149
  from cation and anion combination, 201, 202*f*
  cellulose solubility in, 120*t*
  chemical structures and abbreviations, 201, 202*f*
  chiral, 39, 41, 43, 44, 47, 51
  chiral peptidic, 16, 20*f*
  [$C_n$mim]X and [$C_n$dmim]X, structure of, 64*f*
  concentration difference *versus* ln K, uniform formulation in ILATPS and MILWS, 74, 74*f*
  DEME-TFSI, 149
  dissolution of biopolymers using, 119
  enantioselective oxidation in, 17
    with chiral oxaziridine, 17, 18*t*, 20*f*
    goals of, 17
    of thioanisole, 17, 18*t*, 20*t*, 21
  with fungal activity, towards new biotechnological processes, 197
  as green non-aqueous solvent, 182, 183
    cation and anion based, structures of, 183, 184*f*
    characteristics of, 183
    for enzymatic catalysis, 181, 187, 188*t*
    properties of, polarity, 183, 184, 186*f*, 187
  growth inhibitory effect to *Penicillium* species, 201, 202
    with addition of CsCl, 201
    cluster group analysis, 201, 203, 204*f*
  influence on CALB-catalyzed esterification of *rac*-ketoprofen, 31*f*
  integrated system/process, for penicillin separation and recovery, 63, 65*f*, 66
  ketoprofen in , enzymatic membrane reactor for, 25
  as new opportunities for chemistry of
    amino acids, 13
    peptides, 13
    pharmaceutical compounds, 13
  as pharmaceutical salts, 3
    examples with active drug as component, 5*t*
    historical perspective of, 1
  properties, 2, 35, 36, 39
    absence of flammability, 2
    high variability concerning chemical structure, 2
    negligible vapour pressure, 2
    reduced inhalatory exposure, 2
    tunability, 3
  as reaction media
    for amino acid derivatives transformations, 14
    for peptide synthesis, 14
  R,S-[CHTA]$^+$ [Tf2N]$^-$, 41
  solvent system, recyclable use of D-ProMe-PS in, 161, 161*f*
  synthesis, 35, 36, 39
  TMPA-TFSI, 149
  toxicological assessment to *Penicillium* species, 201, 202, 203
  toxicological evaluation, 135, 143*t*
    with methylimidazolium cation for CaCo-2 and HT-29 cells, 140, 140*t*
  used for
    dry-jet wet spinning, 126
    electrospinning, 127
  used to form anhydrosugars from polysaccharides by microwave irradiation, 145
  yield and selectivity in, 150*t*
Iron oxide nanoparticles, ionic liquid-modified

Downloaded by 89.163.35.42 on June 22, 2012 | http://pubs.acs.org
Publication Date (Web): April 28, 2010 | doi: 10.1021/bk-2010-1038.ix002

- added on culture wells of HeLa cells, microscopic images of, 111*f*
- aggregation, and cell death, observation of, 112*t*
- amino group, aqueous dispersed, photographs of, 109*f*
- anion exchange, equilibrium of, 109*s*
- biomedical application of, 103
- characterization of, 107
- dispersibility of, 109
- interaction with DNA biomolecules, 112
- MR images of, 111, 113*f*
- preparation of, 103, 106*s*
- stimuli response of, 108
- toxicity of, 110
  - by in vitro assay, 110, 111*f*, 112*t*
  - by in vivo assay, 110

Isoelectric point, of 6-APA in MILWS, 83*f*, 85

K

Ketoprofen, in ionic liquids, enzymatic membrane reactor, 25

L

Lactate anion, toxicity effect, 201, 202

Leukemia, panel of human tumor cell lines, 93, 98*t*

Lipase enzymes, 182, 185, 188, 188*t*

Lipase PS*See Burkholderia cepacia* lipase

Lung cancer, panel of human tumor cell lines, 93, 98*t*

M

Magnetic resonance, images of [MIm][Cl]-IO-NPs, 111, 113*f*

Melanoma, panel of human tumor cell lines, 93, 98*t*

Metabolic footprinting, of fungi, altered by ionic liquids, 203
- using ESI-MS analysis, cluster analysis of joint peak lists, 203, 205*f*

Methylimidazolium cation, 137, 138*t*
- class of ionic liquids, toxicity results for CaCo-2 and HT-29 cells, 140, 140*t*
- relative viability in combination with anions
  - treated on CaCo-2 cells, 139, 139*f*, 140
  - treated on HT-29 cells, 139, 139*f*

Methyltrioctylammonium bis(trifluoromethanesulfonyl)imide, yield and selectivity in ionic liquids, 149, 150*t*

Microwave irradiation, of polysaccharides in ionic liquids forming anhydrosugars, 145, 150

MILWS. *See* Mixed ionic liquids/water two phase system

Mixed ionic liquids/water two-phase system, 66
- aggregates, micrograph pictures, 68, 69*f*
- 6-APA in
  - comparison of yield in BAWS, 87*f*, 88
  - IEP of, 83*f*, 85
- based from hydrophobic [C_4mim]PF_6, 66
- enzymatic activity and stability in, 85
  - as function of inorganic salt, 86*f*, 87
  - influence of ILs concentration, 84*f*, 87
  - influence of pH, 84*f*, 85
- partitioning ratios of penicillin and PAA in, 82
  - effect of mole ratio of [C_4mim]PF_6 to [C_4mim]BF_4 in, 82, 82*f*
  - influence of pH in, 83*f*, 84

Downloaded by 89.163.35.42 on June 22, 2012 | http://pubs.acs.org
Publication Date (Web): April 28, 2010 | doi: 10.1021/bk-2010-1038.ix002

- penicillin in, extractive behaviors, 70
- phase diagram in, 67, 68*f*
- uniform formulation of ln K-Δ[ionic liquids], 74, 74*f*

Modafinil, chiral sulfoxides in, 17, 20*f*

N

Naproxen, 49, 51
- composition in (S)-[CHTA]$^+$ [Tf2N]$^-$ IL *versus* enantiomeric compositions, 48, 50*f*
- solutions fluorescence spectra, 46*f*, 48
- structures, 36*s*, 46

N-cyanobenzenesulfonamide anion, 137, 138*t*

N-cyanomethanesulfonamide anion, 137, 138*t*

N,*N*-diethyl-*N*-methyl-*N*-(2-methoxyethyl)ammonium bis(trifluoromethanesulfonyl)imide
- cation effect on glucose, 149
- yield and selectivity in ionic liquids, 149, 150*t*

N,*N*,*N*-trimethyl-*N*-propylammonium bis(trifluoromethylsulfonyl)imide
- cation effect on glucose, 148, 149
- glucose transformation in, temperature effect, 148
  - Arrhenius plot, 149*f*
- yield and selectivity in ionic liquids, 149, 150*t*

Novozym*See Candida antarctica* lipase B

O

Octanoic acid, iCALB-catalyzed perhydrolysis with cyclohexene oxidation in DES's, 174*s*, 176, 177*t*

Octapeptide Z-(Gly-(R)-MPG)$_4$-OMe
- deprotection of, 15, 19*f*
- synthesis of, 15, 19*f*

Ovarian cancer, panel of human tumor cell lines, 93, 98*t*

P

Penicillin
- enzymatic hydrolysis
  - by integrated system/process containing IL, 77, 79*f*, 82*f*
  - schematic process for, 79*f*
- in ILATPS, extractive behavior, 70
  - Flory-Huggins expression, 72
  - ionic liquids species effect, 71, 71*f*
  - salt species effect, 70, 70*f*
- in MILWS, extractive behavior, 72
  - ionic liquids species effect on, 73, 73*f*
  - salt species effect on, 72, 73*f*
- and PAA in MILWS, partitioning ratios of, 82
  - effect of mole ratio of [C_4mim]PF_6 to [C_4mim]BF_4 in, 82, 82*f*
  - influence of pH in, 83*f*, 84
- separation and recovery, in an IL integrated system/process, 63, 65*f*, 66
  - from fermentation broth, 66, 67*f*

Penicillium species
- IL growth inhibitory effect to, 201, 202
  - with addition of CsCl, 201
  - cluster group analysis, 201, 203, 204*f*
- metabolic footprinting, altered by ionic liquids, 203
  - using ESI-MS analysis, cluster analysis of joint peak lists, 203, 205*f*
- phylogenetic origin, correlated to IL response, 203

  and toxicological assessment of IL, 201, 202, 203
Peptides
  chemistry, with ionic liquids, 13
  synthesis, in ionic media, 14
    coupling agents, 15, 16*f*
    cyclisation reaction, 15
    drawbacks of, 14
    enzymatic and chemical, 14
    longer cyclopeptides sequences, 15, 17*f*, 18*f*, 19*f*
    protease-catalyzed, 14
Perhydrolysis, iCALB-catalyzed, of octanoic acid with cyclohexene oxidation in DES's, 174*s*, 176, 177, 177*t*
Pharmaceutical compounds, chemistry, with ionic liquids, 13
Pharmaceutical products
  enantiomeric composition determination by IL based method, 35
  structures
    atenolol, 36*s*, 46
    ibuprofen, 36*s*, 46
    naproxen, 36*s*, 46
    propranolol, 36*s*, 46
    warfarin, 36*s*, 46
Pharmaceutical salts
  examples with active drug as component, 5*t*
    bretylium, 5*t*
    butylscopolamine bromide, 5*t*
    cetylpyridinium chloride, 5*t*
    difenzoquat, 5*t*
    diquat, 5*t*
    domiphen bromide, 5*t*
    edrohonium, 5*t*
    methacholine, 5*t*
    methylscopolamine bromide, 5*t*
    neostigmine, 5*t*
    oxyphenonium bromide, 5*t*
    paraquat, 5*t*
    pipenzolate, 5*t*
    pyridostigmine, 5*t*
    tridihexethyl chloride, 5*t*
  ionic liquids as, 3
    historical perspective of, 1
  overview, 1
    also known as vegetable alkalis, 1
    as first nitrogen-containing bases, 1
    later termed as alkaloids, 1
Phase diagram, of ionic liquids
  aqueous solution, 67
  $[C_4mim]BF_4/[C_4mim]PF_6$/water system, 67, 68*f*
Phenylacetic acid
  and penicillin in MILWS,
    partitioning ratios of, 82
    effect of mole ratio of $[C_4mim]PF_6$ to $[C_4mim]BF_4$ in, 82, 82*f*
    influence of pH in, 83*f*, 84
Phenylalanine composition, in (S)-$[CHTA]^+$ $[Tf2N]^-$ IL *versus* enantiomeric compositions, 41*f*, 46
1-Phenylethanol transesterification
  by free lipase PS or amino acid coated lipase PS, 158*f*
  by glycine free lipase PS or amino acid coated lipase PS, 157
Phosphonium-based ionic liquids
  antitumor activity, 101
Phylogenetic origin, of *Penicillium* species, correlated to IL response, 203
Picolinoates
  anti S_N2' allylation of, with RMgBr/CuBr, 57, 57*s*
  racemic, reaction with PhLi/CuBr·Me2S, results of, 58, 59*t*
Polarity
  anion, as function of negative charge size/delocalization, 184
  cation, as function of alkyl chain length, 184
  of ionic liquid, 184, 186*f*
Polysaccharides
  applications of anhydrosugars, 152
  in ionic liquids forming anhydrosugars by microwave irradiation, 145

Downloaded by 89.163.35.42 on June 22, 2012 | http://pubs.acs.org
Publication Date (Web): April 28, 2010 | doi: 10.1021/bk-2010-1038.ix002

Downloaded by 89.163.35.42 on June 22, 2012 | http://pubs.acs.org
Publication Date (Web): April 28, 2010 | doi: 10.1021/bk-2010-1038.ix002

  - synthesis of hyperbranched, reaction scheme of, 147*f*
  - unimolecular reverse micelle with L-leucine moieties, 152, 153*f*

Propranolol
  - composition in (S)-[CHTA]$^+$ [Tf2N]$^-$ IL *versus* enantiomeric compositions, 44*f*, 47
  - solutions fluorescence spectra, 43*f*
  - structures, 36*s*, 46

Prostate cancer, panel of human tumor cell lines, 93, 98*t*

Protease-catalyzed, peptides synthesis, 14

Proteases enzymes, 182, 188, 188*t*

R

Rac-ketoprofen, esterification with 1-alkanols, catalyzed with CALB, 29, 32
  - alkyl chain length and concentration ratio influence on, 31*f*
  - different ILs influence on, 31*f*
  - scheme of, 27*f*
  - time-course of, 30*f*, 33*f*

Renal cancer
  - drug response curve of, 95, 99*f*
  - panel of human tumor cell lines, 93, 98*t*

(R)-pyrrolidine-substituted imidazolium cetyl-PEG10-sulfate-PS, in IL solvent system, recyclable use of, 161, 161*f*

R,S-(3-chloro-2-hydroxypropyl)trimethylammonium bis(trifluoromethanesulfonyl)-imide
  - enantiomeric compositions *versus* actual composition in
    - of atenolol, 40*f*, 41*f*, 45, 46
    - of ibuprofen; phenylalanine; alanine, 41*f*, 46
    - of naproxen and warfarin, 48, 50*f*
    - of propranolol, 44*f*, 47
  - synthesis by ion exchange, 41
  - *See also* Chiral, ionic liquids

R,S-[CHTA]$^+$ [Tf2N]$^-$. *See* R,S-(3-chloro-2-hydroxypropyl)trimethylammonium bis(trifluoromethanesulfonyl)-imide

(5*R*,6*S*)-isomer epoxy aldehyde, aldol reaction with enone for acid synthesis, 57, 57*s*

S

Saccharin anion, 137, 138*t*

Salt pairs
  - ionic liquid like examples with cation and anion as active component, 7*t*
    - aminophenazone gentisate, 7*t*
    - bamethan nicotinate, 7*t*
    - barbexaclone, 7*t*
    - benzalkonium, 7*t*
    - benzalkonium Colawet, 7*t*
    - benzalkonium sulfacetamide, 7*t*
    - benzydamine salicylate, 7*t*
    - benzylpenicillin clemizole, 7*t*
    - bromhexine camsylate, 7*t*
    - camphophylline, 7*t*
    - chloroquine gentisate, 7*t*
    - chloroquine salicylate, 7*t*
    - choline theophyllinate, 7*t*
    - codeine diclofenac, 7*t*
    - didecyldimethylammoniu, 7*t*
    - dimenhydrinate, 7*t*
    - diprinhydrinate, 7*t*
    - heptaminol thephyllinate, 7*t*
    - lidocaine docusate, 7*t*
    - metescufylline, 7*t*
    - nicotinamide ascorbate, 7*t*
    - niscoscrobine, 7*t*
    - ornithine aspartate, 7*t*
    - papaverine camsylate, 7*t*
    - papaverine nicotinate, 7*t*
    - parathiazine theoclate, 7*t*
    - pasiniazide, 7*t*
    - phenazone gentisate, 7*t*
    - phenazone salicylate, 7*t*
    - phenmetrazine theoclate, 7*t*
    - promethazine theoclate, 7*t*

Downloaded by 89.163.35.42 on June 22, 2012 | http://pubs.acs.org
Publication Date (Web): April 28, 2010 | doi: 10.1021/bk-2010-1038.ix002

- ranitidine docusate, 7*t*
- sparteine theophylline, 7*t*
- xanthinol nicotinate, 7*t*

S-ibuprofen, enantioselective transport through a lipase-facilitated supported IL membrane, schematic diagram of, 190, 190*f*

Silk fibers, used as biopolymer-based materials, 125

Solvents, green non-aqueous, for enzymatic catalysis, 181, 182, 183
- advantages of, 182
- hydrolytic enzymes for, 182
- ionic liquids, 181, 182, 187
- role of water in, schema of, 182, 184*f*
- supercritical CO_2, 181, 182, 183, 185

(5*S*,6*R*)-epoxide, condensation with enone, for acid synthesis, 57, 57*s*

Supercritical carbon dioxide, as green non-aqueous solvent, 182, 183
- denaturative effect, for extracting, dissolving and transporting chemicals, 187
- enzymatic catalysis in, 181, 185
  - environmental factors affecting, 186
  - stirred-tank/membrane reactors for, 185, 186*f*

Supercritical carbon dioxide, enzymatic membrane reactor for, 25, 32

Supercritical fluids, 182, 187
- definition of, 183
- properties, 183
- *See also* Supercritical carbon dioxide

T

Tetrafluoroborate anion, 137, 138*t*

Tetra-*n*-hexyl-dimethylguanidinium cation, 141

Tetrapeptide Z-(Gly-(R)-MPG)$_2$-OMe
- deprotection of, 15, 18*f*
- synthesis of, 15, 17*f*

Thioanisole, enantioselective oxidation in ionic liquids, 17, 18*t*, 20*t*, 21
- as function of solvent polarity, 17, 21*f*

Toxicity
- anions, effect of, 201, 202
- assays performed on HT-29 and CaCo-2 cell lines, 136
- cation headgroups, effect of, 201, 202
- evaluation of ionic liquids, 135, 143*t*
  - with methylimidazolium cation for CaCo-2 and HT-29 cells, 140, 140*t*
  - models used for, 136
- ionic liquids, to *Penicillium* species, 201, 202
  - growth inhibitory effect, 201, 202, 203, 204*f*
- of [MIm][Cl]-IO-NPs, 110
  - by in vitro assay, 110, 111*f*, 112*t*
  - by in vivo assay, 110

Transesterification, iCALB-catalyzed, of ethyl valerate with 2-butanol in DES's, 174*s*, 175*t*, 176
- enantioselectivity of, 174, 175*t*, 177
- initial activity of, 173, 175*t*

Tri-*n*-hexyl-tetra-*n*-decylphosphonium cation, 137, 138*t*, 142
- relative viability in combination with NTf_2
  - treated on CaCo-2 cells, 142, 142*f*
  - treated on HT-29 cells, 142, 142*f*

Tri-*n*-octyl-methylammonium cation, 137, 138*t*, 141
- relative viability in combination with anions
  - treated on CaCo-2 cells, 141, 141*f*
  - treated on HT-29 cells, 141, 141*f*

U

Unimolecular reverse micelle, polysaccharides with L-leucine moieties, 152, 153*f*

V

Vegetable alkalis, as first nitrogen-containing bases, 1
Viscosity, influenced on DES's, 177

W

Warfarin, 49, 51
  composition in (S)-$[CHTA]^+$ $[Tf2N]^-$ IL *versus* enantiomeric compositions, 48, 50*f*
  solutions fluorescence spectra, 49*f*
  structures, 36*s*, 46
Water, role in enzymatic catalysis, 182
  with various enzyme environment, schema of, 184*f*

Z

Zwitter ion, 55

Downloaded by 89.163.35.42 on June 22, 2012 | http://pubs.acs.org
Publication Date (Web): April 28, 2010 | doi: 10.1021/bk-2010-1038.ix002